Storm Damage Reduction Project Design for Wallops Island, Virginia

David B. King Jr., Donald L. Ward
Coastal and Hydraulics Laboratory
U.S. Army Engineer Research and Development Center
3909 Halls Ferry Road
Vicksburg, MS 39180-6199

Greggory G. Williams, and Mark H. Hudgins
U.S. Army Engineer District, Norfolk
803 Front Street
Norfolk, VA 23510-1096

Prepared for:
National Aeronautics and Space Administration
Goddard Space Flight Center
Wallops Flight Facility
Wallops Island, VA 23337

September, 2010

Contents

1 Introduction

The National Aeronautics and Space Administration's (NASA's) Goddard Space Flight Center's Wallops Flight Facility (WFF), located on Virginia's eastern shore, was established in 1945 and is NASA's principal facility for managing and implementing suborbital research programs. The facility is divided into two parts: a main base, located on the Delmarva Peninsula, and Wallops Island, a coastal barrier island that houses a series of launch facilities and support buildings. Almost all the facilities and rocket launch pads on the island occupy a sandy strip of land less than 1000 ft (300 m) from the Atlantic Ocean, with most less than half that distance. The current replacement value of the infrastructure on the island is approximately $800 million. Separating Wallops Island from the mainland is a series of open bays and coastal salt marsh roughly 2 miles (3 kilometers) wide, which is a southern extension of Chincoteague Bay.

The shoreline at Wallops Island has experienced chronic erosion for at least the last 150 years. At present, a rock seawall protects much of the facility. Most of the seawall has no exposed beach fronting it, and several sections of the seawall are in a deteriorated condition.

Study Objectives

The US Army Engineer Research and Development Center's (ERDC) Coastal and Hydraulics Laboratory (CHL) has been working with the US Army Engineer District, Norfolk (CENAO) to develop a comprehensive solution to the shoreline erosion problem that will provide substantial storm damage protection to the infrastructure on Wallops Island and at the same time avoid any significant negative impacts to Assawoman Island, the shoreline immediately south of Wallops Island. This report documents the data collection, numerical modeling, and technical analysis undertaken to support the design of storm damage reduction project alternatives for the site.

2 Description of the Study Area

Location

Wallops Island, Virginia is a barrier island located on the Atlantic coast of the Delmarva Peninsula about 90 km north of the mouth of Chesapeake Bay., as shown in Figures 2-1 and 2-2.

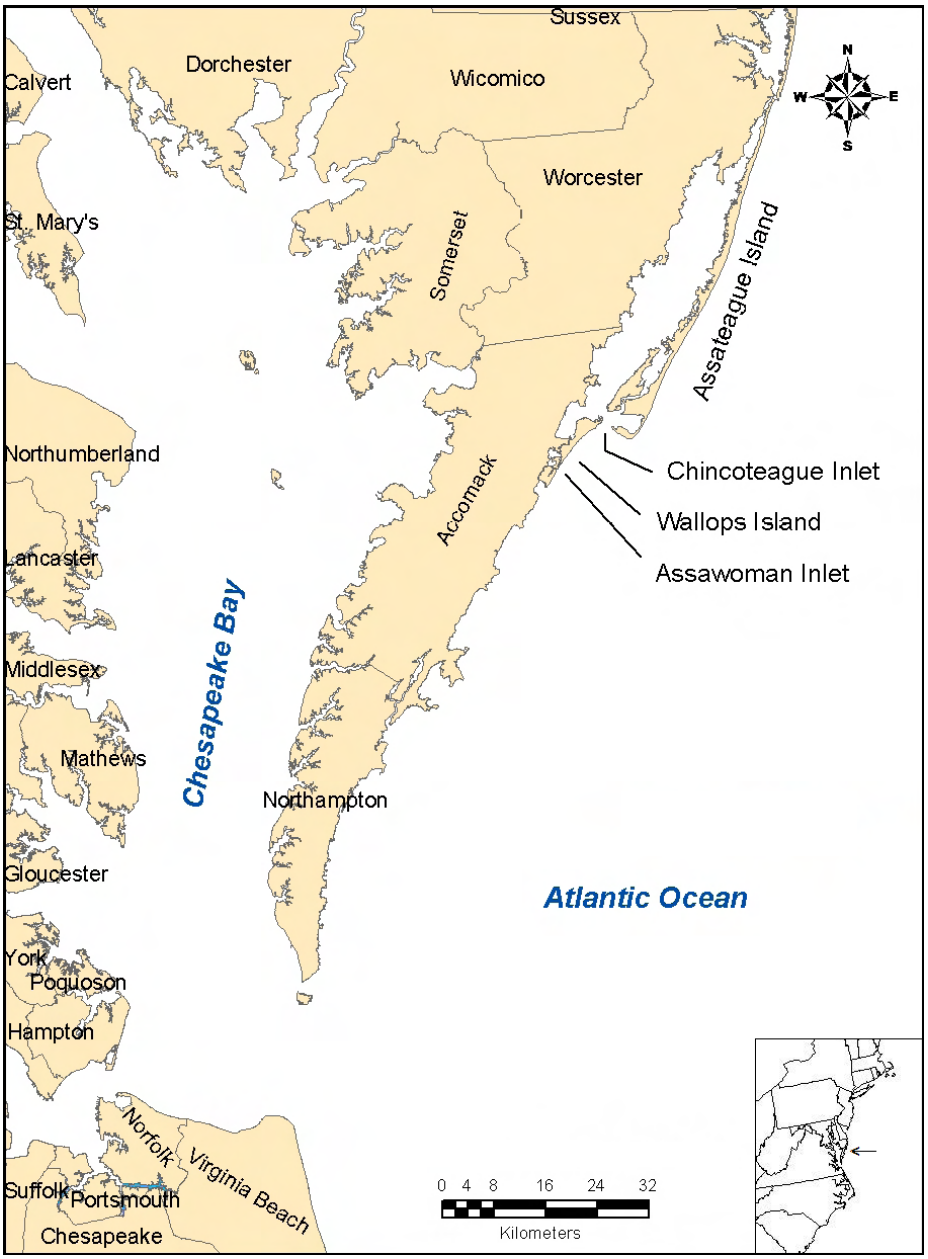

Figure 2-1. Location of Wallops Island on the Virginia eastern shore of the Delmarva Peninsula.

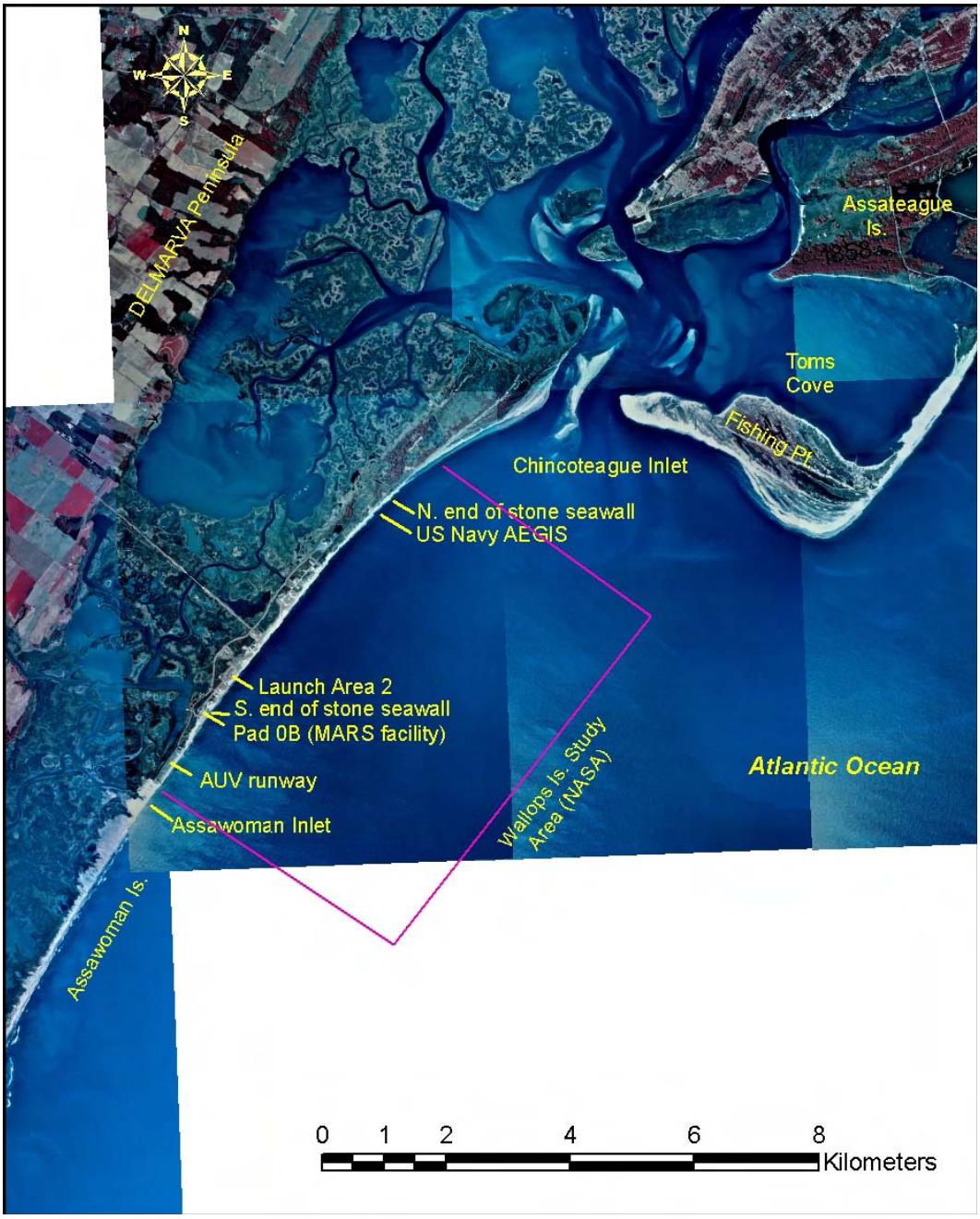

Figure 2-2. Wallops Island, VA study site.

Wallops Island is bounded on the east and southeast by the Atlantic Ocean. To the northeast is Fishing Point, a recurved spit which forms the southern end of Assateague Island. To the north are Chincoteague Inlet, Chincoteague Bay, the town of Chincoteague, VA, and the mainland base for WFF. To the west, Wallops Island is separated from the mainland by a series of marshes and tidal creeks which are a southern extension of Chincoteague Bay. The mainland in the vicinity is comprised mainly of rural farmland. South of Wallops Island is Assawoman Inlet (now closed)

and Assawoman Island, a National Wildlife Refuge managed by the US Fish and Wildlife Service. A string of undeveloped barrier islands extend further south, down the coast to the mouth of Chesapeake Bay. Virginia's Atlantic coast shoreline on the Delmarva Peninsula is one of the longest stretches of undeveloped shoreline on the east coast of the U.S. The only public road access to the entire Virginia shoreline is at the Assateague Island National Seashore located east of the town of Chincoteague.

History of Shoreline Change along Wallops Island

1940's and 1950's

In 1945, the National Advisory Committee on Aeronautics (NACA, the precursor to NASA) began using Wallops Island, VA as a launch site for experimental rocket research. This research mission at Wallops Island continues to the present.

Due to concern about storm damage to facilities being constructed on the island, a seawall was first erected in 1945-1946. The original seawall was made of interlocking 18 ft sections of sheet pile, driven approximately 12 feet into the ground. The Beach Erosion Board of the USACE first studied the problem of beach erosion at Wallops Island in April-May 1946. They documented that the shoreline had receded 500 ft since 1851 and recommended that a groin field be installed when the high water line came within 50 feet of the seawall. Figure 2-3 shows the Wallops Island shoreline in January 1946 looking north. Assawoman Inlet is at the extreme bottom of the photograph.

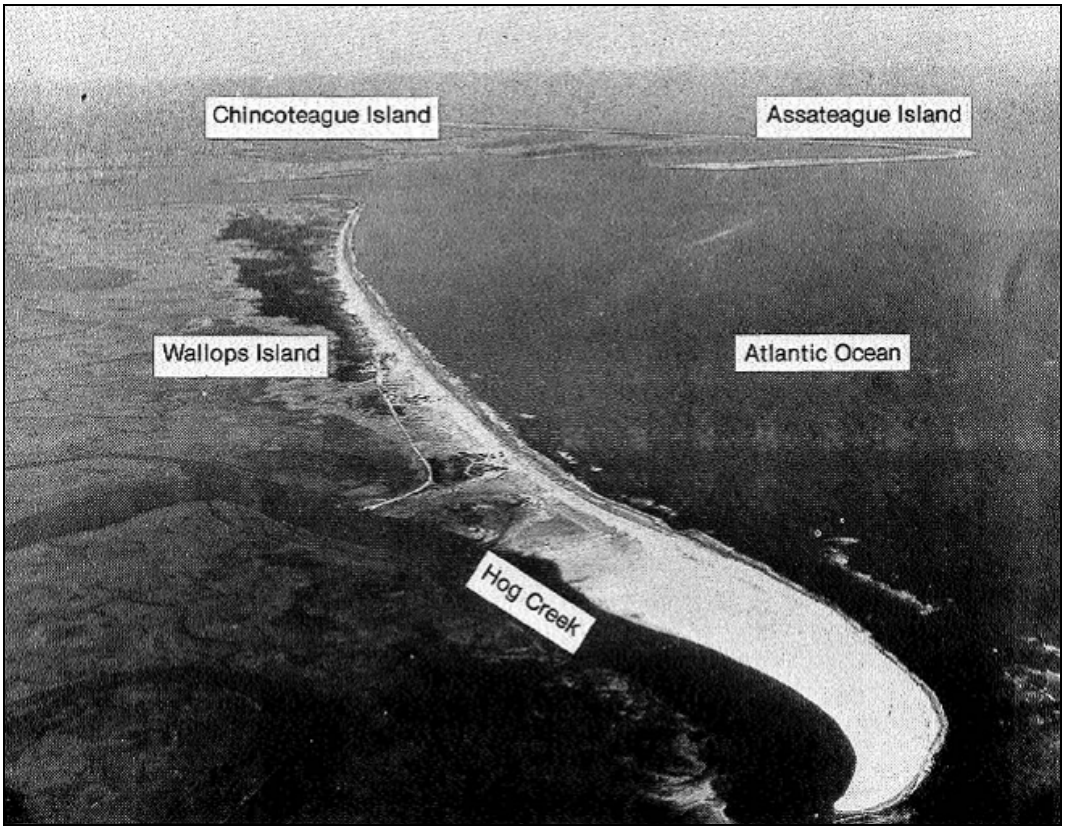

Figure 2-3. Wallops Island shoreline, January 1946.

Figure 2-4 shows the erosion and storm damage to the Wallops Island Association Clubhouse at the north end of the island in May 1949. Figure 2-5, taken in October 1956, shows a portion of the exposed seawall. In May, 1956, the Beach Erosion Board again inspected the beach at Wallops Island and recommended that 8 groins be installed at 400 ft intervals along 2,800 feet of beach. These groins are seen in Figure 2-6, which was taken in December 1959. This figure also shows the causeway connecting Wallops Island to the mainland, which was constructed in 1959. The seawall was extended further to the north in 1960. The above information and Figures 2-3 through 2-7 are from Shortal, 1978.

Figure 2-4. Wallops Island north end erosion damage, May 1949.

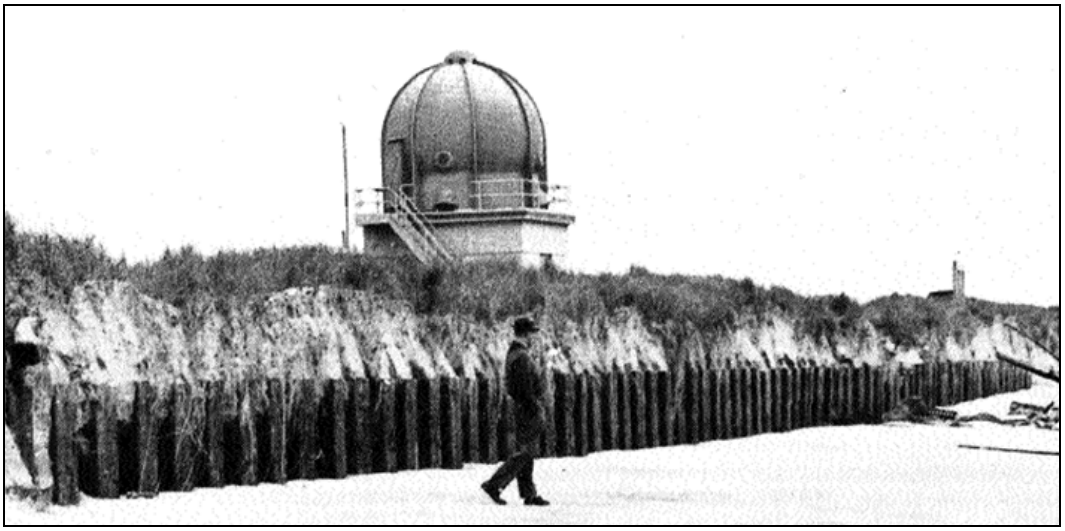

Figure 2-5. Wallops Island seawall, October 1956.

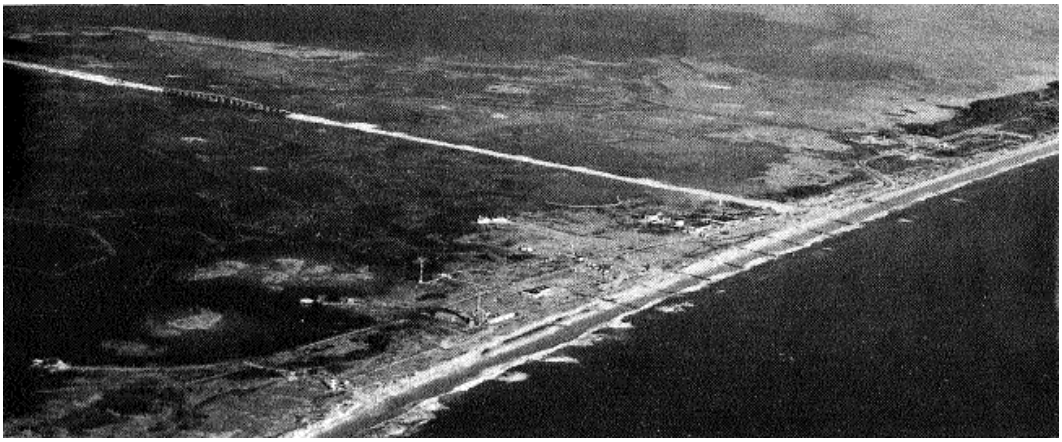

Figure 2-6. Wallops Island, December 1959, showing groin field extending southward from the newly built causeway.

1960's through 1980's

Figure 2-7 shows failed sections of the sheet pile seawall following the Ash Wednesday storm of March 6-8, 1962. This Nor'easter caused extensive damage along the eastern seaboard from New York to North Carolina and is considered one of the ten worst storms in the United States in the 20th century. The damage at Wallops Island was estimated at $1,000,000.

The storm also breached the south end of the island at the location of the present UAV runway and connected Hog Creek (Figure 2-3) directly with the ocean. This breach was mechanically closed with a large rectangular fill as shown in the 1965 photo, Figure 2-8. The southern edge of this fill section is the location of the present day South Camera Stand.

A total of 47 groins had been built along the Wallops Island shoreline by 1972 (Morang, Williams, and Swean, 2006). The groins were constructed of wood as illustrated in the Shore Protection Manual, 1984 and Basco, 2006 (Figure 2-9). Most of the groins ranged in length from 120 ft (30 m) to 400 feet (120 m) and the spacing between them varied from 200 to 650 ft (60 to 200 m) (Table 2 in Moffatt and Nichol, 1986). In the 1960's and early 1970's the groins functioned well, as shown in Figure 2-10, and were considered a success.

The seawall was extended, augmented, and repaired several times in the 1950s through the 1980s (Table 1 in Moffatt and Nichol, 1986). In addition to the steel sheet pile, portions of the seawall were constructed using wooden bulkheads, concrete aprons, and rock rubble mounds. There is little evidence that the groins were regularly maintained, and there is no record of any beach nourishment being placed in the groin field. By the 1980s, the groins showed signs of serious deterioration, as shown in Figure 2-11. Moffatt and Nichol (1998) concluded that the lack of periodic nourishment was the principal reason for the failure of the groins.

Assawoman Inlet was formerly a small, natural inlet at the southern tip of Wallops Island (Slingerland 1983). Most photos and shorelines through the early 1980's show a small, but open, inlet. However, photos and shorelines from the 1990's on show the inlet as closed. Today, the inlet's former location is marked by a series of overwash fans.

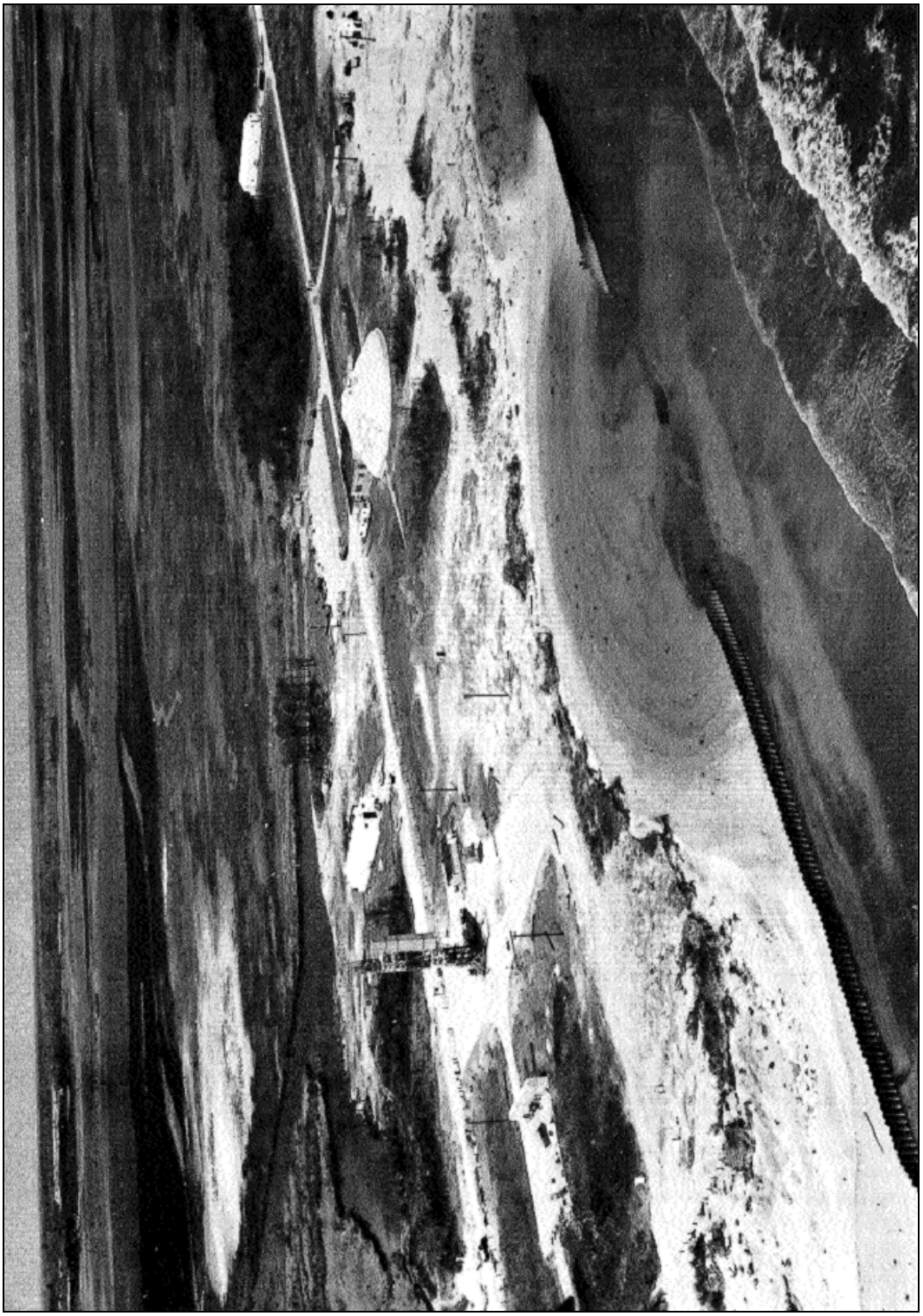

Figure 2-7. Seawall damage from Ash Wednesday Storm of April 1962.

Figure 2-8. Mechanically filled section of the south end of Wallops Island following an Ash Wednesday Storm breach.

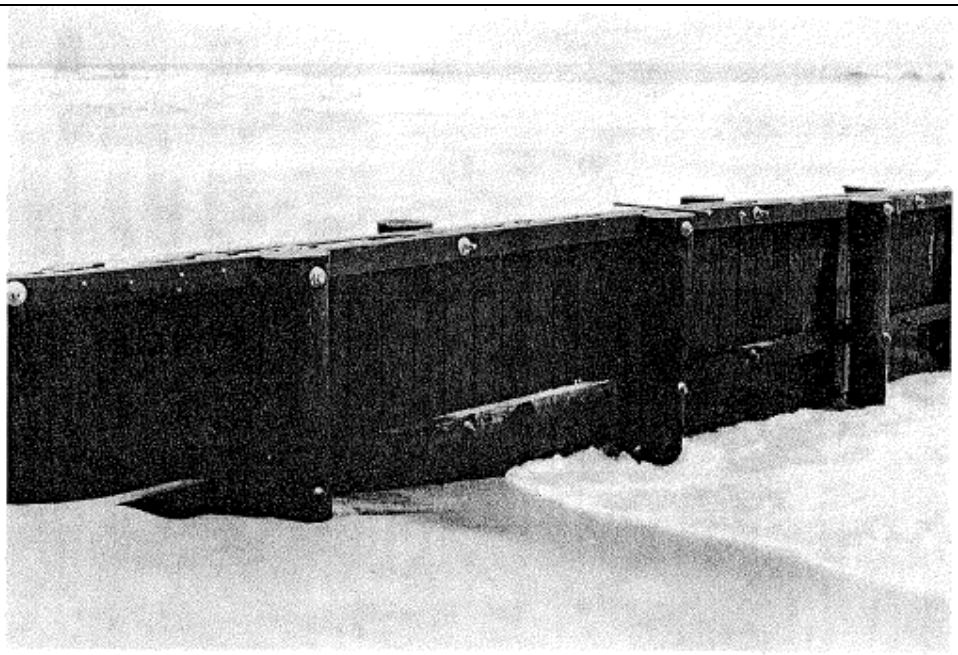

Wallops Island, Virginia (1964)

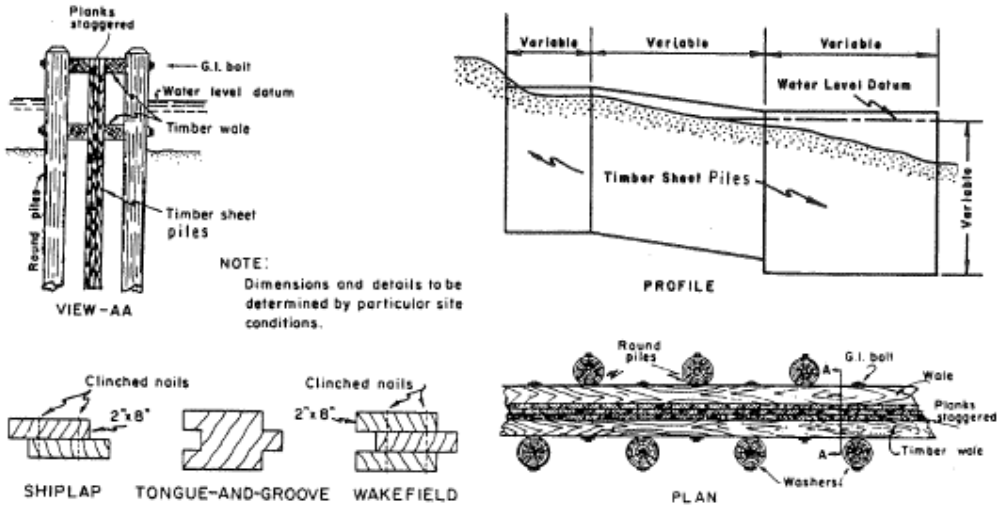

Figure 2-9. Wallops Island wooden groins, from SPM, pg 6-77.

Figure 2-10. Wallops Island groin field in 1969.

Figure 2-11. Condition of groins and seawall in 1983.

WFF attempted several different measures to control the shoreline erosion, including two experimental beach barrier projects, which were initiated in the mid 1980s. Moffatt and Nichol (1989) evaluated these and concluded that both types of experimental shore protection structures failed to provide any significant protection. Figure 2-12 (from Morang, et al, 2006) shows "Beach Prism" sand retention units that are badly misaligned following an April 1988 storm.

Figure 2-12. Experimental beach protection barriers.

1990's to Present

In the mid 1990s NASA built the current rock seawall generally in the same location as the previous seawalls (Figures 2-13 and 2-14). The wooden groins were mostly removed at approximately the same time, though several short sections of wooden pilings still remain in place. Photos from the 1990's generally show a small section of beach remaining in front of the seawall. This rock seawall has substantially halted the shoreline retreat, although the sub-aerial beach has disappeared, except at the northern end. Further, the sub-aqueous beach seaward of the seawall has continued to erode, as discussed in Chapter 6. The rock seawall has suffered damage by undermining and stone displacement. Because the wall is porous, storm waves frequently penetrate it, causing flooding and eroding sand on the landward side. See further discussion of the rock seawall in Chapter 3. Figure 2-15 shows waves from Hurricane Dennis overtopping the rock seawall in September 1999. NASA has made frequent repairs to the seawall since the mid 1990's (Morang, Williams, and Swean, 2006). In 2006, NASA placed a temporary geotextile tube along the beach south of the seawall, as shown in Figures 2-14 and 2-16. Large waves have occasionally damaged portions of this tube. In mid November 2009 a substantial Nor'easter caused island flooding and substantial damage to the geotextile tube (Figure 2-17).

Figure 2-13. Remnants of wooden, steel sheet pile, and concrete seawalls can all be found within and adjacent to the rock seawall in the vicinity of building Y35B.

Figure 2-14. Rock seawall in 2007 looking north along Wallops Island.

Figure 2-15. Rock seawall during Hurricane Dennis, September 1999.

Figure 2-16. 2007 oblique aerial photo looking south from near the south end of Wallops Island, Va. From bottom to top the shoreline shows the geotextile tube and the overwash area that was previously Assawoman Inlet.

Figure 2-17. Damage to the south end of Wallops Island caused by the November 2009 Nor'easter.

Shoreline Change

Like most of the Atlantic coast beaches on the southern Delmarva peninsula (Richardson and McBride, 2007), the beach at Wallops Island has been in a state of chronic erosion for at least the last 150 years, as evidenced by an analysis of a series of measured shorelines. These shorelines are shown in Figure 2-18. The 1849, 1857/1858, 1909/1911, 1933, and 1983 shorelines are taken from the US Coast and Geodetic Survey charts. The 1994 shoreline was digitized from a rectified aerial photograph. The 1996 and 2005 shorelines were obtained from LIDAR surveys.

On Figure 2-18, distances are in miles. The figure has the same orientation and origin as the GENESIS grid discussed in Chapter 5. The origin is located near the Dynamic Balance Facility Building on Wallops Island. In this figure, Wallops Island extends horizontally from -1½ miles to +4 miles. The dominant direction of wave approach for this section of

coastline is from the northeast (left) and sediment transport is generally to the south (right), though a significant transport reversal occurs on Wallops Island (discussed below and in Chapter 5).

Panel A of Figure 2-18 shows the 1849 and 1857/1858 shorelines. At this time the shoreline was much straighter as Fishing Point spit had not formed. The inlet shown in the 1849, which is now called Assateague Channel, has shifted to the southwest in the 1857 shoreline, suggesting that the main direction of longshore sediment transport was to the south.

By 1909/1911, Figure 2-18, Panel B, Fishing Point had started to form. Assateague Channel had shifted further to the southwest. The Wallops Island shoreline had retreated by approximately 75 meters (250 ft). By 1933, Fishing Point had formed a distinct hook, but it had not grown enough to redefine the mouth of Chincoteague Inlet.

By 1983, Figure 2-18, Panel C, substantial changes had occurred. Fishing Point had grown to the extent that the tip of it and the northern shoulder of Wallops Island had started to re-define the location of the throat section of Chincoteague Inlet. Some aerial photographs from the 1980s show the existence of an emergent ebb shoal. However, these points were still well over a mile apart.

The northern end of Wallops Island was now sheltered enough by Fishing Point that it had started to accrete, which was a change from earlier decades as shown in panel C (see also Figure 2-4). Because the mouth of Chincoteague Inlet was still so wide, it is likely that a substantial portion of the accretion at the northern tip of Wallops Island was due to a transport reversal on Wallops Island, caused by Fishing Point blocking waves from the northeast. The rest of Wallops Island and Assawoman Island were still experiencing substantial erosion.

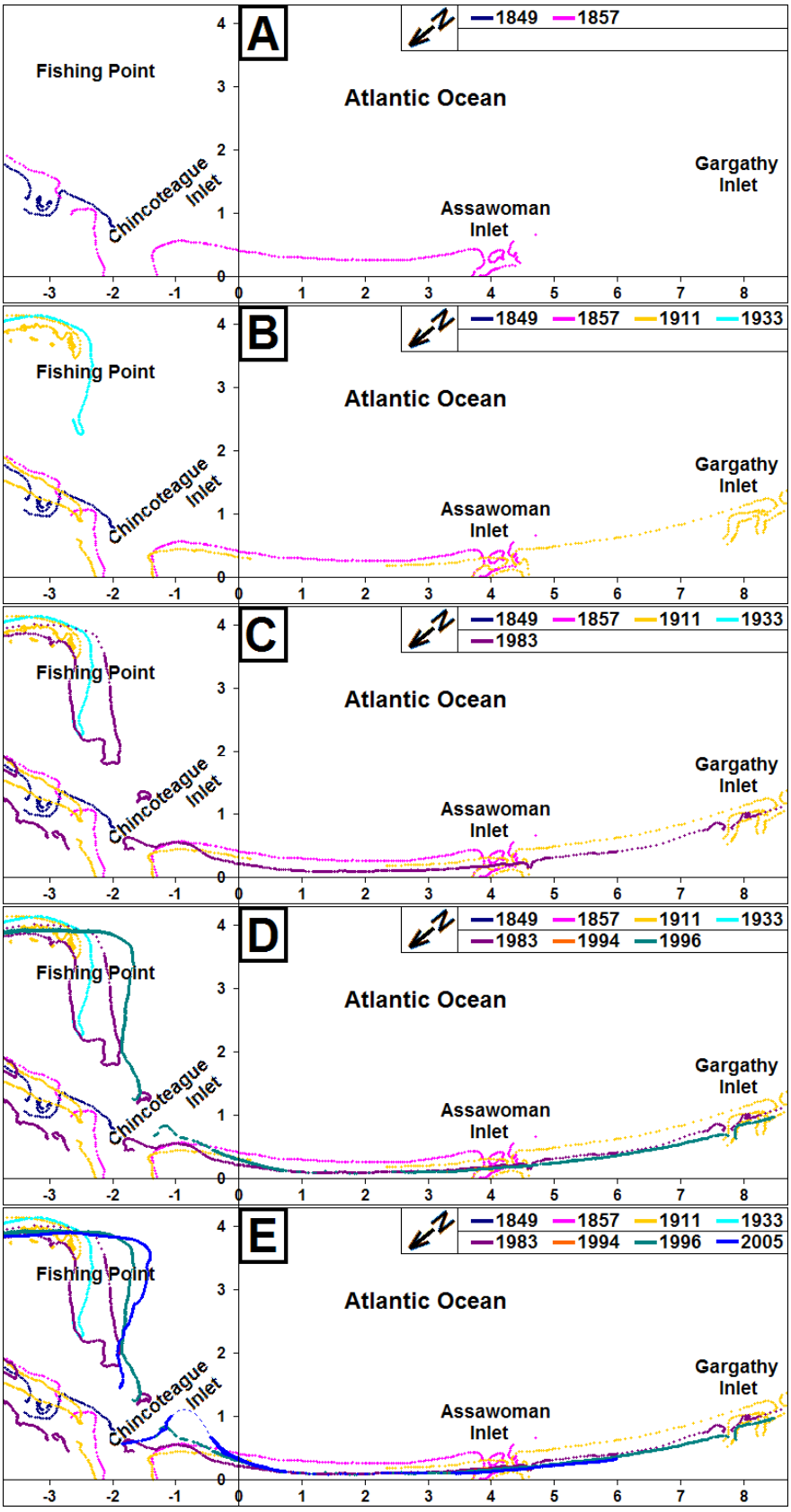

Figure 2-18. Wallops Island shoreline changes between 1849 and 2005.

By 1996, Figure 2-18, Panel D, Fishing Point and the northeastern shoulder of Wallops Island had both grown enough that the mouth of Chincoteague Inlet was less than a half mile wide, and substantial inlet bypassing (from Fishing Point to Wallops Island) had started to occur. This is supported by the fact that CENAO began dredging Chincoteague Inlet in 1995. Subsequent dredging of the inlet channel has been required at intervals ranging from one to three years (Morang, Williams, and Swean, 2006). On Wallops Island, the area of accretion at the northern tip had extended further to the south; though the southern part of the island continued to erode.

Figure 2-18, Panel E shows the 2005 shoreline. The dashed portion of this shoreline at the northern end of Wallops Island was not covered in the LIDAR survey. Instead, this shoreline is inferred from limited GPS readings taken in 2007. The northern end of Wallops Island has continued to strongly accrete, both as a result of sediment bypassing of Chincoteague Inlet and northward net transport along the northern end of the island. Today, the beach at the northern tip of Wallops Island contains a series of trapped shallow sloughs. These are the result of ebb shoal bar bypassing and welding to the inlet's downdrift shoreline. These shoals form in the channel and migrate westward, where they weld onto the northern tip of Wallops Island.

Future Shoreline Trends

The discussion in this section is an extrapolation of present shoreline behavior into the future. It is not intended to be an exact quantitative prediction of rates or timelines for future events, but rather a regional framework which can provide context to help interpret the results of the numerical modeling effort presented in later chapters.

As shown by the growth of Fishing Point in Figure 2-16 and the closure of Assawoman Inlet, the shoreline in the vicinity of Wallops Island is dynamic, and substantial changes will likely continue to occur on decadal time scales, as compared with more typical beaches.

Growth of the Southern Tip of Fishing Point

The development and growth of the cape called Fishing Point over the last 100+ years has captured sand that would have otherwise been available to nourish Wallops Island and the islands further south along the Virginia

eastern shore. This is a dominant reason why these shorelines are all experiencing substantial erosion. The shoreline at Fishing Point is continuing to evolve. Figure 2-19, from the National Parks Service website: http://www.nps.gov/asis/planyourvisit/upload/historicseashore.pdf, shows the growth of the tip of the island through 2002. This growth has not slowed in recent years. The National Park Service has measured the Assateague Island shoreline multiple times yearly since 1997. Figure 2-20 shows their shoreline location data through the spring of 2009 for the very southern tip of Assateague Island and shows that the tip of the island is continuing to grow to the southwest at a rate of approximately 150 ft (50 meters) per year. If this trend continues over the 50-year life of the shore protection project on Wallops Island, the tip will grow to the southwest by about 1.5 miles (2.3 km). This will more strongly shelter the Wallops Island shoreline from ocean waves approaching from the northeast, and will shift the transport divergent nodal point which is currently on the north end of Assawoman Island to the south by roughly that amount. The nodal point and the Wallops Island sediment budget are discussed in Chapter 5.

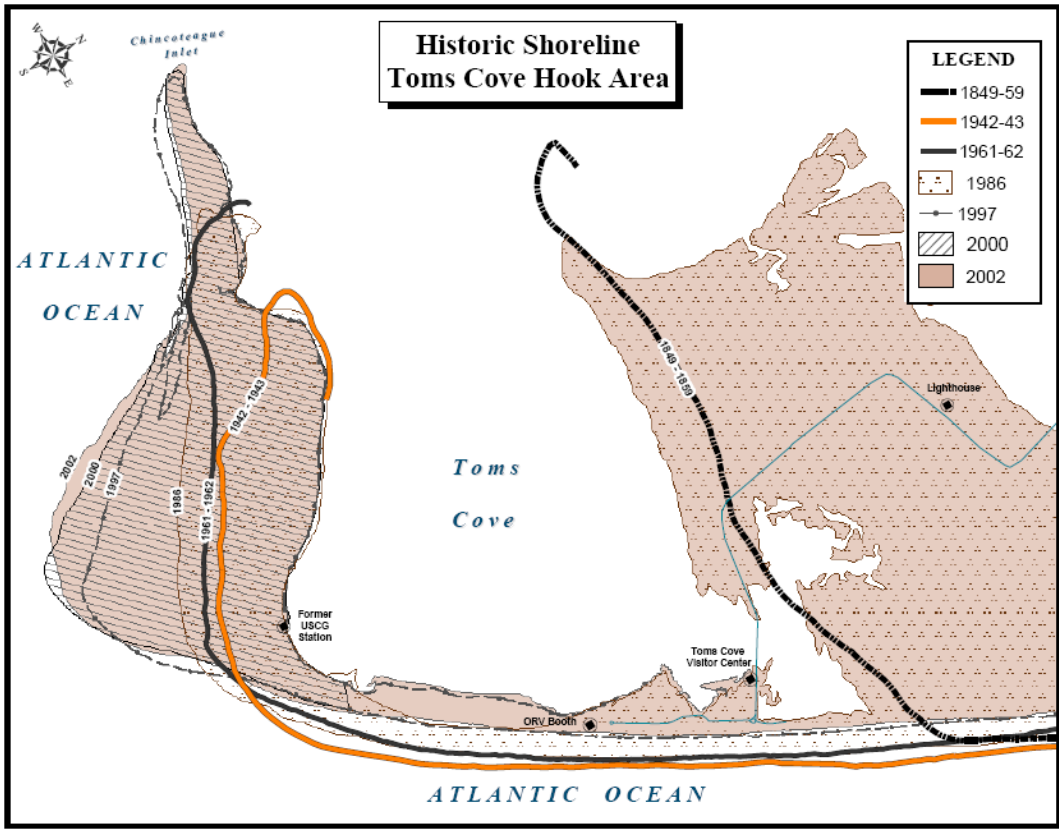

Figure 2-19. Shoreline Changes at the southern end of Assateague Island.

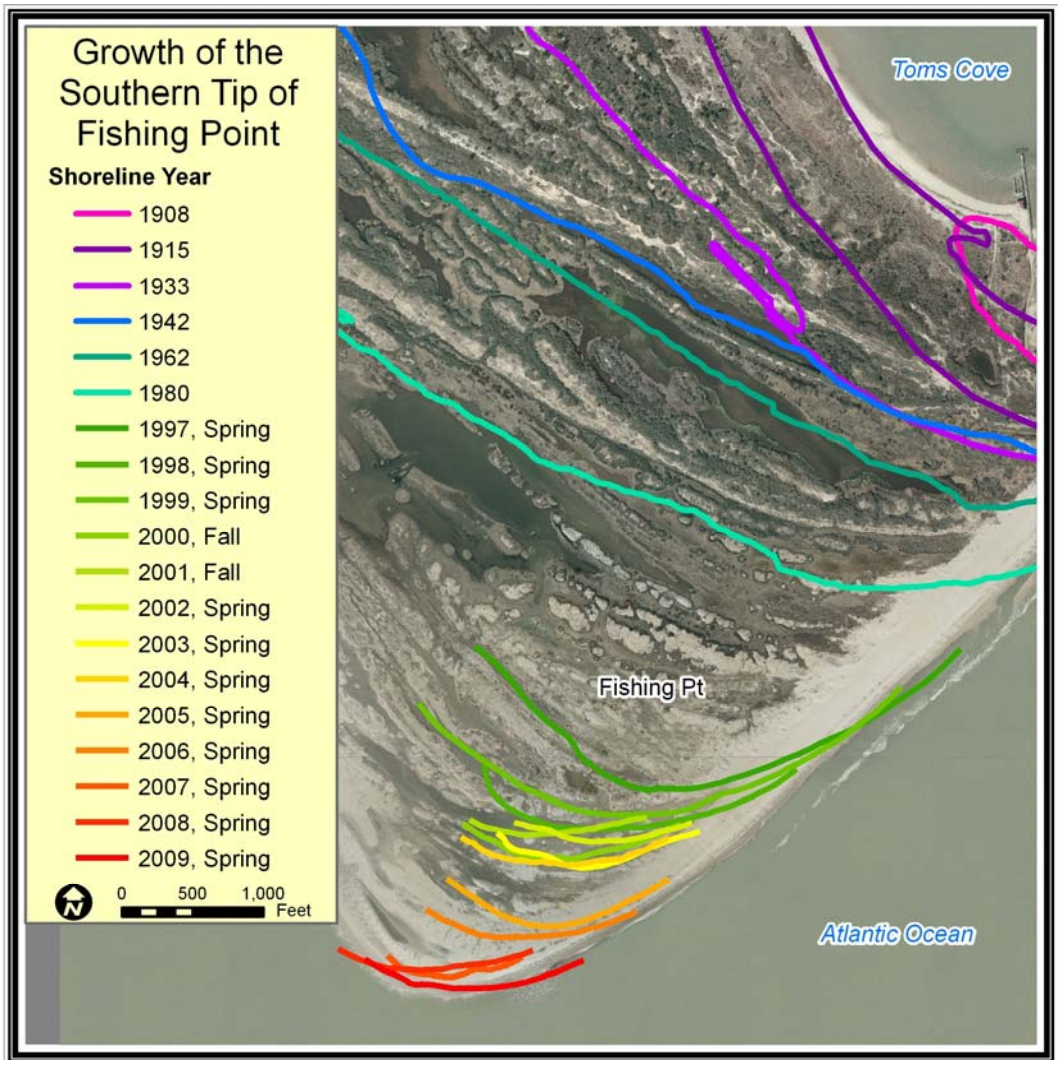

Figure 2-20. Changes in shoreline position at the very southern tip of Assateague Island (Fishing Point) between 1908 and 2009.

Narrowing of the Tom's Cove Isthmus

Another shoreline change feature shown in Figure 2-19 is a narrowing strip of land separating Tom's Cove from the Atlantic. The rate at which the isthmus is narrowing makes it likely that there will be numerous storm-induced breakthroughs between Tom's Cove and the Atlantic during the 50-year lifetime of this project. The first breach in this area occurred as a result of a November 2009 Nor'easter (Figure 2-21). These breaches may close rapidly or they may cause a permanent or semi-permanent inlet(s) to form. Any new inlet would compete with Chincoteague Inlet for the tidal prism of Chincoteague Bay.

The beach fill project on Wallops Island will mine sand offshore of the south end of Assateague Island to obtain fill material. It is critical that this mining operation be done in a way that will have minimal impact on the sediment transport rate along this portion of the Assateague Island shoreline, so that it does not exacerbate the breaching potential. Mining of the offshore shoals is discussed in Chapter 8.

Figure 2-21. Looking south along Assateague Island at breach into Tom's Cove caused by November 2009 Nor'easter.

Sea Level Rise

Sea level rise is currently occurring on a world-wide basis, and current USACE guidance (USACE, 2009a) projects it to continue to occur at an increasing rate, though there is large uncertainty in what future rates will be. By the Bruun rule, (Bruun, 1962) small changes in sea level can be expected to have dramatic effects on shoreline position, with increasing sea levels causing shoreline retreat.

The shoreline at Wallops Island will certainly experience the effects of future sea level rise, and in this report we have followed current USACE policy to account for its impacts. This has primarily been done by

providing an additional sediment volume during each renourishment event that would raise the level of the entire beach fill by an amount necessary to keep pace with the projected rise rate (Chapter 6).

Concerning the shoreline change trends discussed above, sea level rise will work to reduce the rate of southwesterly growth of Fishing Point and the accretion on the north end of Wallops Island (Bruun rule). It will increase the frequency of shoreline breaches in the Tom's Cove area. However, while sea level rise may be the most dominant mechanism affecting shoreline change on many beaches world-wide in the coming decades, at Wallops Island it may not have as great an impact as some of the other effects discussed above.

3 Field Investigations

This section of the report includes a discussion of several recent field investigations in the Wallops Island area that have provided needed data for this study. Most of these investigations were performed in support of the present storm damage reduction project.

Beach Profile Measurements

Beach profile data (wading plus fathometer) were collected for this project by the Norfolk District in 2007. These profiles consisted of 25 long lines and 67 intervening short lines as shown in Figure 3-1.

Profile lines were spaced at 500 foot intervals. For most lines, rod and transect data collection started approximately 100 feet to the west of the existing rock seawall and terminated at the seaward foot of the seawall. Bathymetric data were collected utilizing a survey vessel equipped with an Innerspace Technology depth finder and extended seaward to approximately 1000 feet east of the seawall with every fourth survey line being extended to approximately the 30 foot contour.

Onshore and Nearshore Sediment Survey

Norfolk District personnel collected a total of 170 grab samples from the subaerial and subaqueous portions of the active beach. On the beach at Wallops Island five samples were taken on each of seven transects between the top of the berm and the mean low water elevation. Four transects were taken at the north end of Wallops Island and the remaining three were taken at the south end, near the former Assawoman Inlet. The remaining samples were taken along twenty five hydrographic survey lines that ran perpendicular to the shoreline. Sampling was performed at minus 5, 10, 15, 20, 25, and 30 feet depth where practical. These samples were analyzed, and the native beach composite mean diameter was determined to be between 0.20 and 0.21 mm. A D_{50} value of 0.20 mm was applied to characterize the native beach material in the modeling effort.

Additional sediment samples were obtained from 16 cores taken at the north end of Wallops Island in 2009 (USACE, 2009b) at the locations shown in Figure 3-2. Surface samples were extracted from all 16 cores. In addition, samples were extracted at a 2 ft depth for eight of the cores and

at a 4 ft depth for the remaining eight cores. These were sieved using standard methodology.

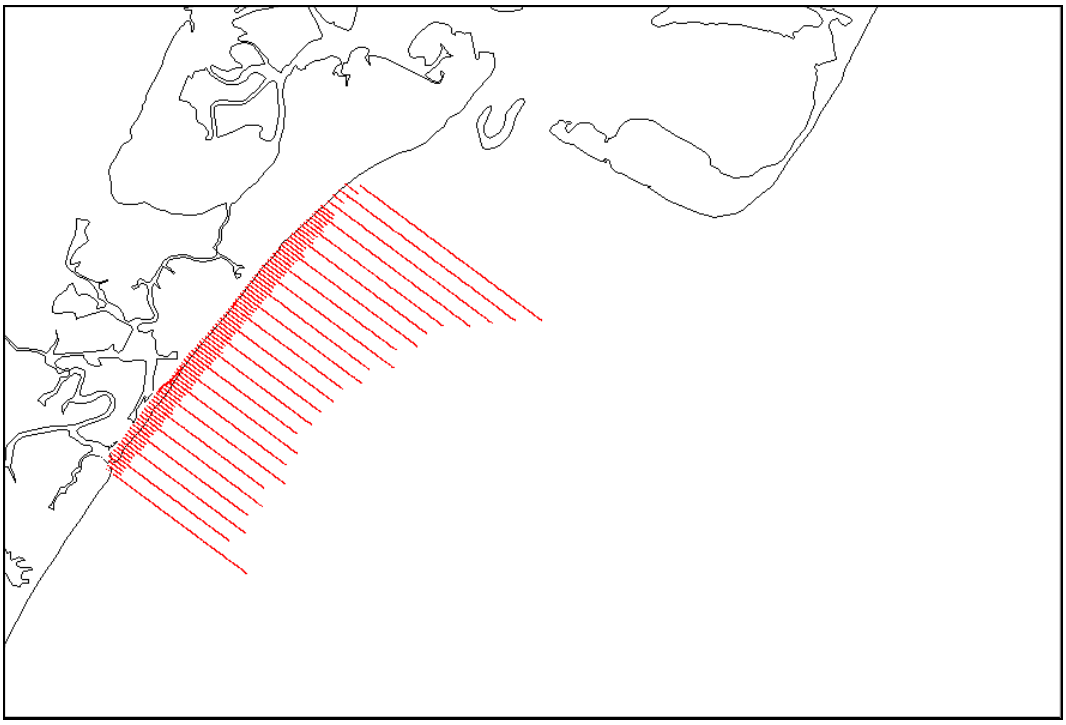

Figure 3-1. Locations of Measured Profiles.

The sieve results were then mathematically combined to obtain average sand distributions at 0, 2, and 4 ft depths, and these were further combined to produce a composite distribution (Figure 3-3). From these distributions, median, mean, and standard deviation values were calculated using the Folk method (Table 3-1). This additional analysis fully supported the characterization of the native sediment material on Wallops Island as having a 0.2 mm median grain size.

Table 3-1. Grain Size Data for Combined Samples, Wallops Island North End

Depth (ft)	Median $D_{(\phi 50)}$	Mean $M_{(\phi 50)}$	Median D_{50}	Mean M_{50}	St Dev σ_ϕ
	Phi units	Phi units	mm	mm	Phi units
0	2.358	2.358	0.195	0.195	0.468
2	2.375	2.375	0.193	0.193	0.529
4	2.266	2.160	0.208	0.224	0.591
Composite	2.342	2.337	0.197	0.198	0.505

Figure 3-2. Locations of 2009 North Wallops Island Sediment Cores.

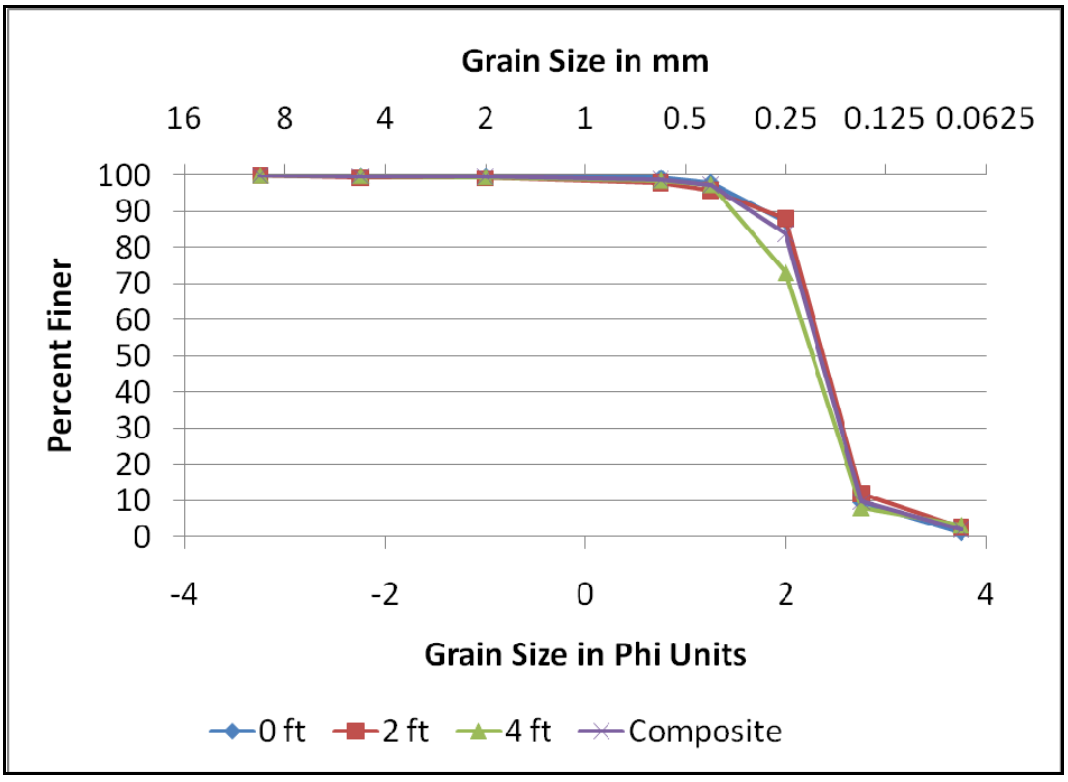

Figure 3-3. Average grain size distributions from 2009 north Wallops Island Sediment Cores.

Offshore Borrow Site Survey and Sediment Characteristics

In May 2007 and December 2007, the Norfolk District supervised subsurface investigations offshore of Wallops Island, Virginia. The purpose of the investigations was to determine if suitable sand size materials were located offshore that could be mined economically and transported to the shoreline on the Wallops Flight Facility. The work was performed in two phases with the first exploration program examining an area covering approximately 230 nautical miles immediately offshore of the project area and possible sites to both the north and south of the project area. The second program was a more detailed examination of potential areas found from the first program attempting to define vertical and lateral extent of potential borrows areas. Details of the surveys and sediment analysis are discussed in Alpine Ocean Seismic Survey (2007 and 2008).

May 2007 Survey

During May 2007, forty vibracores were taken immediately offshore of Wallops Island, Virginia. The purpose of this exploration program was to identify any areas that may contain suitable beach quality materials which may be located near the project area. The program initially concentrated on areas in close proximity to Wallops Island. However, borings collected immediately offshore of the project area generally contained sediments that were unsuitable for beach fill. There was substantial scatter in the median grain size of these sediments, but most had a $D_{50} < 0.20$ mm.

This survey also investigated Porpoise Banks, located southeast of Wallops Island. Six borings performed in this area indicated that this area lacked suitable borrow material.

Four shoals located northeast of Wallops Island off the southern end of Assateague Island were also investigated. These included Chincoteague Shoal, Blackfish Bank, and two unnamed shoals, referred to as Site A and Site B. All four of these shoals were found to contain beach quality sediments.

December 2007 Survey

Chincoteague Shoal lies within the three-nautical-mile jurisdiction of the Commonwealth of Virginia and additional time and cost would be involved

in obtaining permits for the mining of its resources. Since suitable nearby sites were found outside the three-mile limit, Chincoteague shoal was not further investigated in the December 2007 survey. Rather, in December, forty one borings were concentrated on Blackfish Shoal, and on Sites A and B. These potential borrow sites are shown in Figure 3-4.

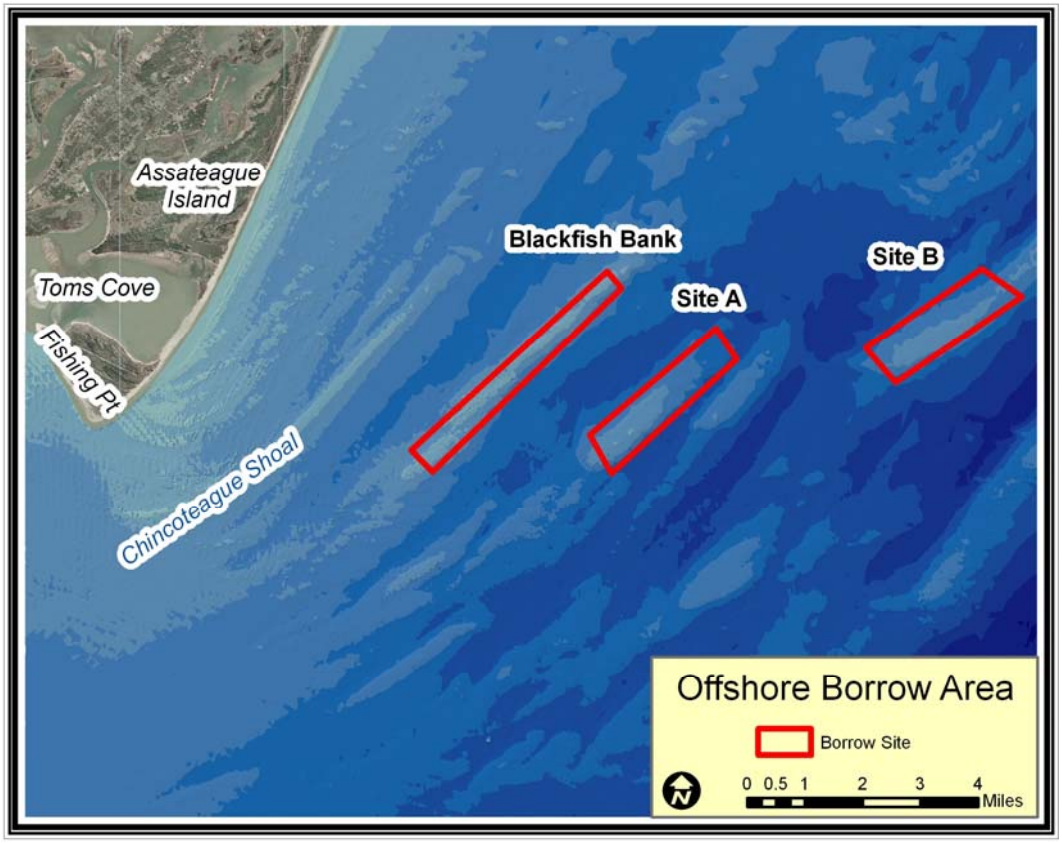

Figure 3-4. Location of potential offshore borrow sites.

Vibracore Sediment Analysis

In the laboratory, the vibracores were split and then photographed, described and the major sandy sediment units were delineated. An example core is shown in Appendix A. The sediments were then analyzed using standard methodology. Two (upper and lower) or three (upper, mid, and lower) sediment samples were obtained from each core. In addition, a composite sediment sample was obtained from the entire length of each core. These samples were sieved with a RoTap type machine and the results were plotted. The plotted sieve results were used to obtain mean, median, and standard deviation values using the Folk method.

Analysis of the vibracores collected at Blackfish Bank indicates that the Bank holds at least 25 million cubic yards of beach quality material having a median sediment diameter of about 0.35 mm. However, there is opposition to the use of this site by local fishermen. In addition, the analysis described in Chapter 8 of this report indicates that mining this shoal would have greater shoreline impacts than mining either Offshore Site A or B. Therefore, this site has been removed from further consideration.

Volumetric analysis indicates that Site A contains approximately 68 million cubic yards, and site B contains approximately 132 million cubic yards of material. These volumes are substantially in excess of the estimated 10 million cubic yards of fill material needed over the lifetime of the project. Mean, median, and standard deviation values of the sediment from the cores obtained at these two sites, along with the locations of these cores, are listed in Appendix A of this report.

The average depth for the upper core sections is 5.5 ft, and for the composite core sections is 12.2 ft. Since the depth to which these shoals might be mined is not known and is expected to vary over the shoal, both the upper and the composite core data were considered in developing a median grain size for the fill material which is a needed parameter in the numerical modeling work. The median grain sizes were ranked from smallest to largest as shown in the histogram (Figure 3-5). This figure shows the data separated by site and depth as well as the four data sets combined. The median values for these curves range from D_{50}= 0.29 mm to 0.34 mm.

In addition, the sieved core results were mathematically combined to produce average upper and average composite curves for Site A and Site B. The statistics for these average curves are given in Table 3-2, and the sediment distribution curves are shown in Figure 3-6.

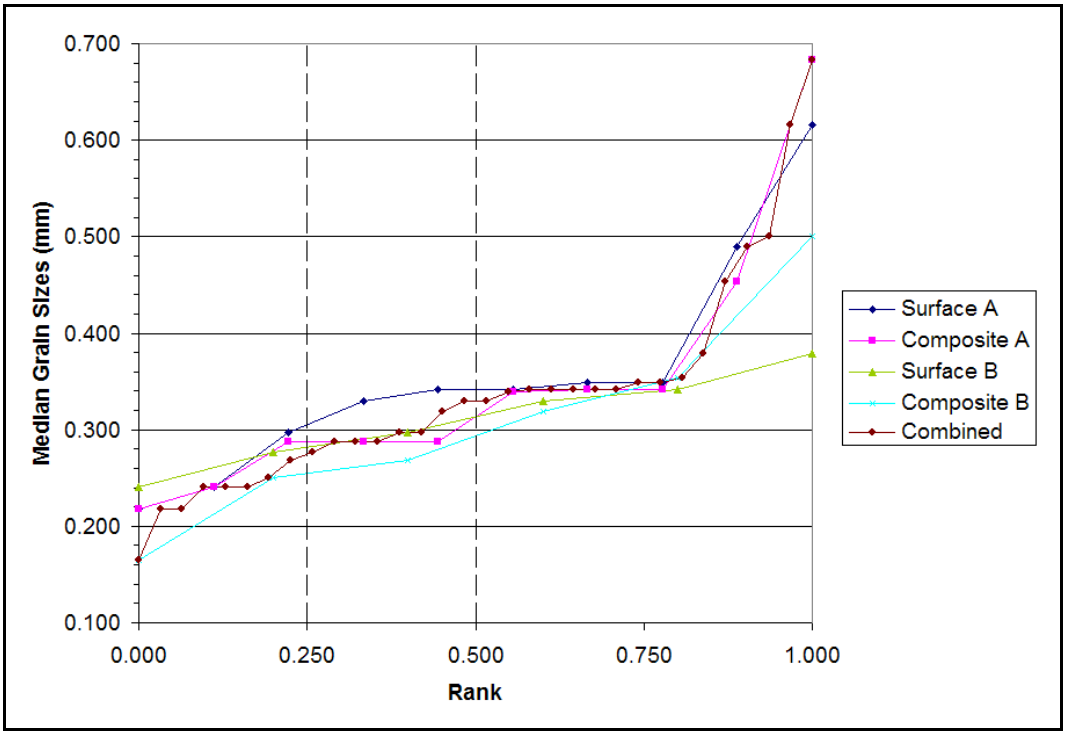

Figure 3-5. Distribution of Median grain sizes from offshore samples.

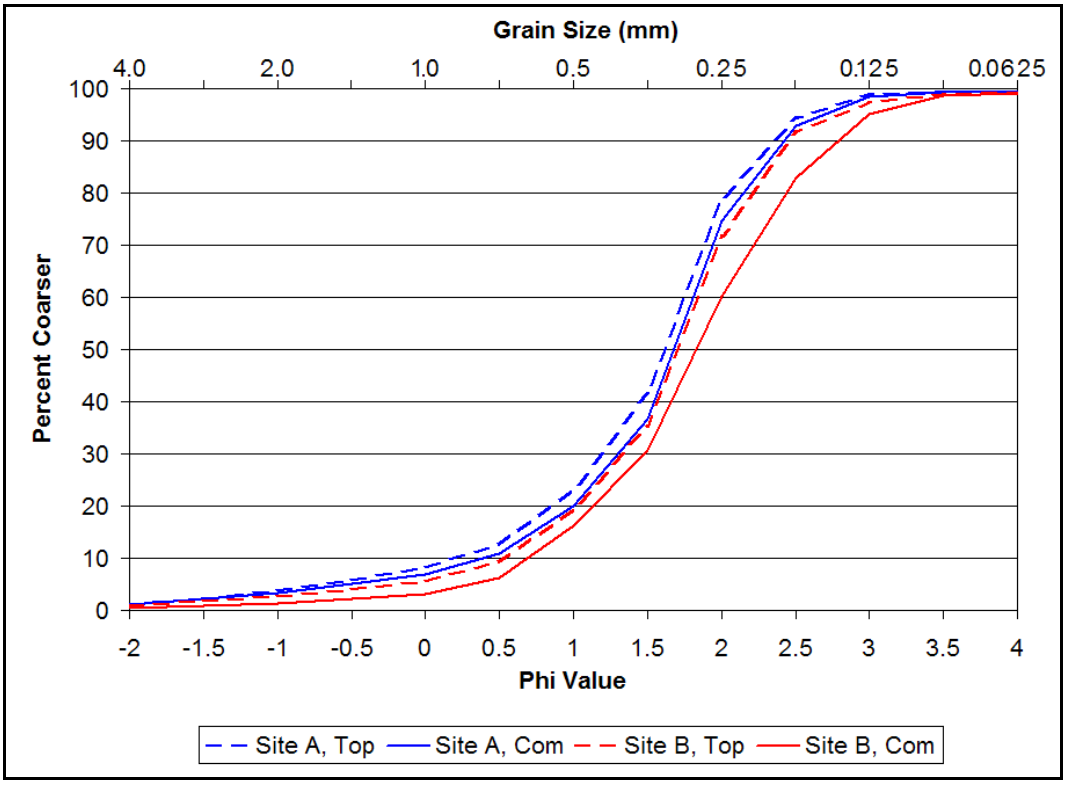

Figure 3-6. Grain Size Distributions of Combined Cores.

Table 3-2. Grain Size Data for Combined Samples, Offshore Borrow Sites

Borrow Location	Depth	Median $D_{(\phi 50)}$	Mean $M_{(\phi 50)}$	Median D_{50}	Mean M_{50}	St Dev σ_ϕ
		Phi units	Phi units	mm	mm	Phi units
Site A	Upper	1.615	1.411	0.326	0.376	0.926
	Composite	1.675	1.517	0.313	0.349	0.903
Site B	Upper	1.703	1.573	0.307	0.336	0.862
	Composite	1.825	1.765	0.282	0.294	0.838

Table 3-2 shows that the average median grain diameter for Site A, the preferred location, is about 0.32 mm. Table A1 lists the median grain diameters for the "upper" and "composite" samples for Site A. These 20 D_{50}'s range from a minimum of 0.218 mm to a maximum of 0.683 mm, and have a mid value of 0.34 mm. Thus, the most likely median grain diameter for the sediment on Unnamed Shoal A is in the range of 0.32 mm to 0.34 mm. However, there are relatively few cores available to characterize the sediment in this two mile^2 area, and an underestimate of this value would lead to an underestimate of the volume of initial fill material needed for the project. The consequences of this are discussed in Chapter 6. Therefore, to be conservative, a smaller median grain diameter, 0.29 mm was chosen for modeling purposes. Fully ¾· of the median grain diameters (Table A1) are this value or larger. The statistical likelihood that the true median grain diameter of the material on Shoal A being less than 0.29 mm decreases rapidly with decreasing grain size. However, an additional margin of safety was incorporated into the Overfill volume (Chapter 6) to allow for the D_{50} of the fill material to be as low as 0.27 mm.

Condition Survey of the Rock Seawall

This section has been extracted from a site visit report to Wallops Island, VA on 28 October, 2008. The purpose of the site visit was to determine if the existing seawall provided sufficient protection to the facility until such time as the nourishment project is completed, to determine if and how the seawall should be included as a component in the storm damage reduction project, and to determine necessary repairs to the seawall. A previous 1999 USACE site visit report is provided in Appendix B of this study.

Geotube™ section at south end of seawall

Although the Geotube™ was partially exposed along its entire length, the Geotube™ section appeared to be in good shape. (See Figures 2-14 and 2-16 for Geotube™ location.) At the extreme southern end the top half of the tube was exposed where there was some flanking around the end, but more typically about 25 percent of the tube was exposed along the southern portion of the tube (Figure 3-7). The amount of exposed Geotube™ increased in the northern portion to one-third to one-half of the tube's height (Figure 3-8). The front face of the bag was exposed down to the scour apron at the northern end of the tube on both the seaside and the landward side (Figure 3-9) but no scouring beneath the apron was observed. A repair to the Geotube™ was evident near the northern end. Here, a second section of Geotube™ was lying adjacent to the main barrier and gave the appearance that the two bags had been stacked and the upper bag pushed off the top to landward (Figure 3-10). There was substantial washout in this section behind the Geotube™, but the tube itself is stable.

Along the crest of the Geotube™ for its entire length, the sand was hard packed (comparable to concrete) without any give. There were several areas where the tube was not completely full leaving a depression in the sand within the tube and the fabric stretched tautly over the top of the depression. These depressions were typically not more than a foot or two across and did not appear to be a problem. No significant rips or tears in the fabric were noted.

Figure 3-7. Looking north from southern portion of Geotube™.

Figure 3-8. Near the middle of the Geotube™ section, looking north.

Figure 3-9. Scour apron exposed on landward side of Geotube™ at northern end of structure.

Figure 3-10. Short Geotube™ behind the north end of main tube.

Seawall Condition

The northern end of the seawall is in an area of sand accretion and is fronted by a wide beach. This portion of the seawall is in good condition. The rest of the seawall is considered to be in a failed condition along much of its length due to reduced crest elevation (Figure 3-11) and/or an overly

steepened seaward face. Point measurements taken during the site visit indicated the crest elevation in the undamaged areas was about 14 ft, with a seaside face estimated to have a slope of 1:2 (vertical: horizontal). Crest elevations in damaged areas were as low as 8 ft, and in some areas the seaward face was steeper than 1:1 (Figure 3-12). By comparison, the seawall designed by Moffatt and Nichol (1998) (referenced in Morang, Williams, and Swean, 2006) had a 14 ft (MSL) crest elevation and a seaside face with 1:3 slope.

Figure 3-11. Area of decreased crest elevation on seawall.

Figure 3-12. Steep seaside face on seawall.

North of radar gun tower Y-110 is a large area of washout behind the seawall. Material has washed out from under a concrete apron causing the concrete to crack with rocks sliding seaward (Figure 3-13).

Figure 3-13. Washout under the concrete apron causing cracking and tilting.

In some areas the remains of earlier seawalls constructed of timber piles (Figure 3-14) or steel sheet pile (Figure 3-15) were seen within or adjacent to the rubble-mound seawall. In sections, wave action moves freely through the seawall causing scour on the landward side (Figure 3-16). Large scour areas behind the seawall were found along approximately 50% of the length of the seawall, with the scour areas as much as 6 ft below the surrounding land area. Some of these scour holes have been filled with rubble, and the rubble repairs are working effectively at halting the localized scour (Figure 3-17).

Figure 3-14. Remnants of concrete apron and timber pile wall.

Figure 3-15. Remnants of concrete apron with steel sheet pile wall.

Figure 3-16. Water flowing through seawall by wave action.

Figure 3-17. Rubble pile behind seawall, presumably to fill scour hole.

Structure Stability

Morang, Williams, and Swean (2006) state that the seawall was constructed with 60 percent 2- to 3-ton stone. If a median stone weight of 2.5 ton is assumed, the Hudson equation (see sample equation in Appendix C for equation and assumptions) indicates a 1:2 slope should be stable against an 8 ft incident wave height or 7 ft wave height if the slope is 1:1.5. The Hudson equation is not intended for slopes steeper than 1:1.5. In places, the seaward face of the seawall is even steeper, appearing to be less than 1:1. It is therefore assumed that waves as small as 6 ft may cause localized damage to the seawall, while waves larger than 8 ft may cause damage along much of the structure. According to the Wave Information Study (WIS) hindcast (available online at http://chl.erdc.usace.army.mil/chl.aspx?p=s&a=DATA;1) for station 179 (37.75 N -75.33 W, depth 18 m), waves greater than 3m (10 ft) have been hindcasted during every year of the data base (1980-1999). The seawall designed by Moffatt and Nichol (1998) called for 3.5-ton stone on a 1:3 slope which should be stable against wave heights of 10 ft.

Structure Runup

Wave runup on a structure is commonly given in terms of either maximum runup (R_{max}) or 2% runup ($Ru_{2\%}$, the elevation that is exceeded by 2 percent of the waves). From a practical standpoint, the two may be used interchangeably. Runup on this seawall is difficult to estimate because the structure has no core or underlayer and water running up the face of the structure will pass through the seawall. Some general comments may be made by making a few assumptions. Looking at the WIS hindcasts for Station 179, most waves of 6- to 8-ft wave height have peak wave period of 7 to 9 sec. Using the example calculation given Appendix C, an 8 ft wave height with an 8 sec peak period will have a 2% runup of 13.2 ft above the swl for a typical seawall. Mean high water is at +2.7 ft. Assuming two feet of storm surge, the seawall would have to have a core elevation of +18 ft to prevent runup from overtopping the seawall during a fairly moderate storm.

Seawall Repair Assessment

An analysis was conducted of the stone requirements for a minimal seawall repair to raise low portions of the wall to +10 ft and to provide a 1:1.5 seaward slope. Additional analyses were undertaken to determine

the stone requirements needed to raise the seawall to +12 and +14 ft and provide a 1:12 seaward slope. Details of the present seawall condition were obtained from a 2005 LIDAR survey of the Wallops Island shoreline collected by the Joint Airborne LIDAR Bathymetry Technical Center of Expertise (http://shoals.sam.usace.army.mil/).

Analysis for +10 ft crest elevation

Two-foot interval contour lines along the seawall were generated from the LIDAR data. Determining areas of low crest elevation was accomplished simply by panning along the image of the structure and visually identifying gaps in the contour lines. Similarly, areas with a steep seaside face were visually identified by noting where the contour lines became close together. Figures 3-18 through 3-26 identify the locations of the areas identified with low crest elevation and the areas with steep seaside face.

Crest elevations over much of the structure were at +14 ft or higher. Areas where the crest was less than +10 ft were identified. Small localized areas of reduced crest elevation were ignored. Although no specific criteria were applied when selecting areas sufficiently long to be of concern, the final areas selected were 30 ft or more along the crest. Table 3-3 lists the areas of reduced crest elevation, identifying the beginning and end of the section where the crest is below + 10 ft. Table 3-3 also lists the length (measured along the crest) of each section and the range of elevations within that section.

Table 3-3. Areas of concern due to low crest elevation.

Area No.	Crest Elev. Range (ft)	Length (ft)	Tons of Rock to Raise Elevation to +10 ft	VA State Plane 4502, meters			
				South End		North End	
				Easting	Northing	Easting	Northing
1	6-10	39	39	3765516.5	1171170.7	3765524.7	1171179.3
2	8-10	30	15	3765675.6	1171364.9	3765681.7	1171371.9
3	8-10	47	23	3765714	1171413.7	3765722.8	1171424.9
4	8-10	107	53	3766849.4	1172853.5	3766869.8	1172878.8
5	6-10	557	552	3767198.1	1173284.5	3767311.5	1173411
Total		780	682				

Normally, raising the crest of an existing structure involves not only raising the crest but recovering the entire seaward and landward sides in order to maintain the desired slopes. Because the areas with the lowest

crest elevation on this seawall were flattened from a higher crest elevation, there is sufficient width on the existing crest that the crest can be raised at least to +10 ft without having to extend the raised crest out to the landside and seaside toes. The amount of stone to raise each of these areas to +10 ft was estimated by assuming the existing crest elevation is the middle of the crest elevation range shown in Table 3-4, using a 10-ft crest width, assuming a unit weight of stone of 165 pounds per cubic foot, and estimating a structure porosity of 40 percent. Total weight required for all five areas is estimated at 680 tons.

Analysis for Steep Seaward Face

There were many areas where the contour lines indicated seaside slopes steeper than 1:1.5. If the seawall were to remain as the primary means of protecting the infrastructure, the seaside slopes should be flattened at least to 1:2. However, guidelines for this analysis were that a new beach fill would act as the primary means of defense in about 3 yrs, and the goal of this analysis was to identify areas that could potentially suffer major damage within the next 3 yrs.

After repeated examination of the contour data, 13 areas were selected as primary "areas of concern." Each area showed a vertical drop of at least 6 ft (4 contour lines) with a slope of 1:1 or steeper over a length of more than 10 ft along the crest. Table 3-4 lists the areas of concern including their length, their upper and lower critical elevations, the width of the steep slope areas, crest length of the area of concern, the front face slope, state plane coordinates of the southern and northern ends of each area, and the volume of rock needed for repair. Because the steepness of the structure face varies along the face of the structure within each area, the slope listed in Table 3-4 is considered representative of the steep areas. In some areas, only portions of the area are excessively steep; Table 3-4 therefore lists the percentage of the length of the area for which the slope is unacceptably steep.

The amount of stone required to improve each section is also included in Table 3-4. The amount of stone listed is considered a minimum, and is intended only to flatten the slope below +10 ft to 1:1.5. The calculations assume the slope will only be flattened to elevation +10 ft, and assume that there is a stone base below the lower contour line on which the flatter slope can be built, rather than extending the slope down to the toe. For example, if Table 3-4 shows a reach where the +12 ft contour line is

separated from the +2 ft contour line by 5 ft (1:0.5 slope), a rock base is assumed at +2 ft sufficient to support a 1:1.5 slope up to +10 ft, and the difference between a 1:0.5 slope and a 1:1.5 slope up to +10 ft is calculated. Stone weight calculations assume a unit weight of 165 pounds per cubic foot and a 40 percent porosity.

Areas 3 and 4 are only 20 and 25 ft in length, respectively, but both areas indicate an 8 ft drop in elevation at a slope of 1:0.5 over the entire length of each area. These appear to be the most critical areas. A portion of Area 5 also shows a slope of 1:0.5, but slope is above +8 ft and therefore of less concern than Areas 3 and 4.

The total weight of stone required for all areas in Table 3-4 is estimated at 285 tons. The total weight of stone required to both adjust the seaward slope and to raise the low crests is 960 tons.

Table 3-4. Areas of concern due to excessively steep seaside slope.

Area No.	Length (ft)	Upper Contour (ft)	Lower Contour (ft)	Slope Width (ft)	Percent of Area	Slope	VA State Plane 4502, meters				Area for 1:1.5 slope to +10	Tons of Rock Needed for Repair
							South End		North End			
							Easting	Northing	Easting	Northing		
1	25	12	2	6	33	0.6	3765313	1170910	3765318	1170916	28.8	11.8
2	14	12	4	5	75	0.63	3765408	1171029	3765410	1171032	15.75	8.2
3	20	12	4	4	100	0.5	3765453	1171085	3765457	1171090	18	17.8
4	25	10	2	4	100	0.5	3765759	1171470	3765764	1171476	32	39.6
5*	290						3766462	1172363	3766516	1172433		
5a		14	4	6	12	0.6					16.2	27.9
5b		14	4	8	12	0.8					12.6	21.7
5c		14	4	6	12	0.6					16.2	27.9
5d		14	8	3	12	0.5					2	3.4
5e		14	8	4	12	0.67					1.67	2.9
6	18	12	4	6	100	0.75	3766550	1172474	3766554	1172477	13.5	12
7	50	12	2	7	50	0.7	3766625	1172571	3766635	1172583	25.6	31.7
8	27	12	4	6	100	0.75	3766671	1172631	3766677	1172637	13.5	18
9	26	12	6	5	25	0.83	3766698	1172663	3766703	1172669	5.33	1.7
10	21	14	6	6	100	0.75	3766765	1172748	3766770	1172753	6	6.2
11	35	12	4	8	100	1	3766785	1172772	3766792	1172780	9	15.6
12	13	12	4	5	100	0.63	3766937	1172966	3766939	1172969	15.75	10.1
13	34	10	2	8	100	1	3766962	1172993	3766968	1173002	16	26.9
Total	598											283.4

Note: Multiple cross-sections were taken of Area 5. Total area of concern was 60 percent of length, evenly divided among cross-sections.

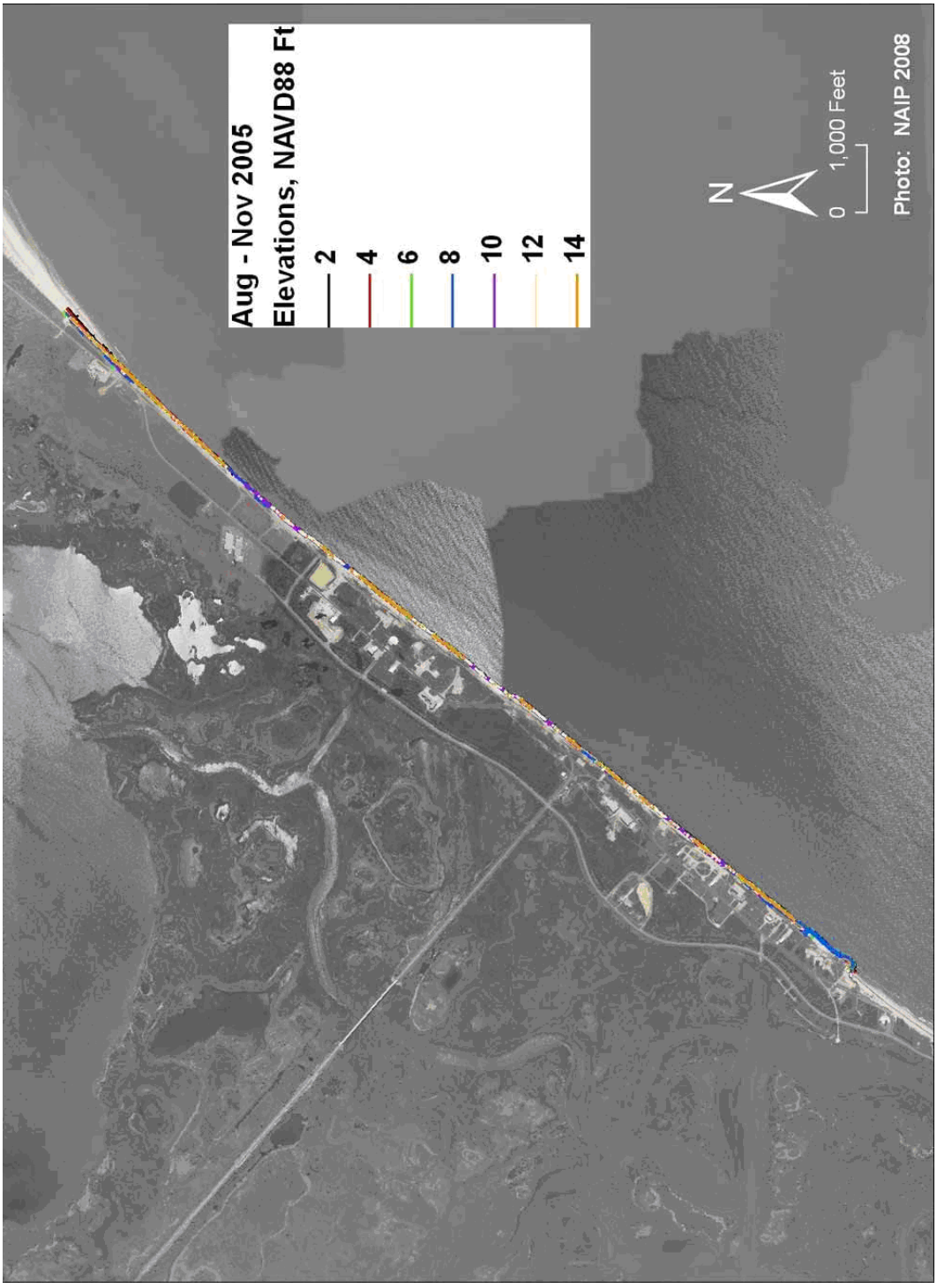

Figure 3-18. Overview of seawall on Wallops Island.

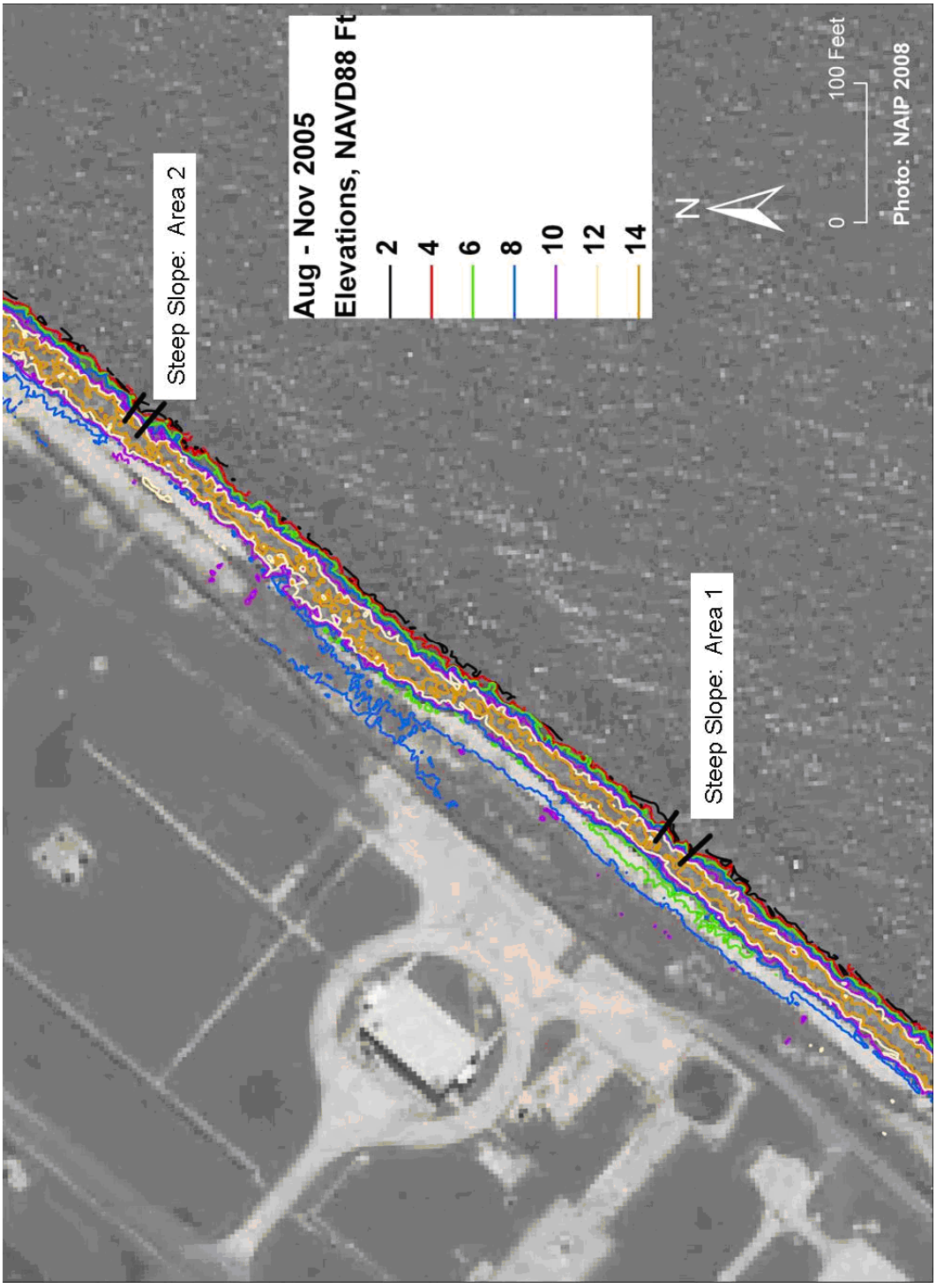

Figure 3-19. Steep slope areas 1 and 2.

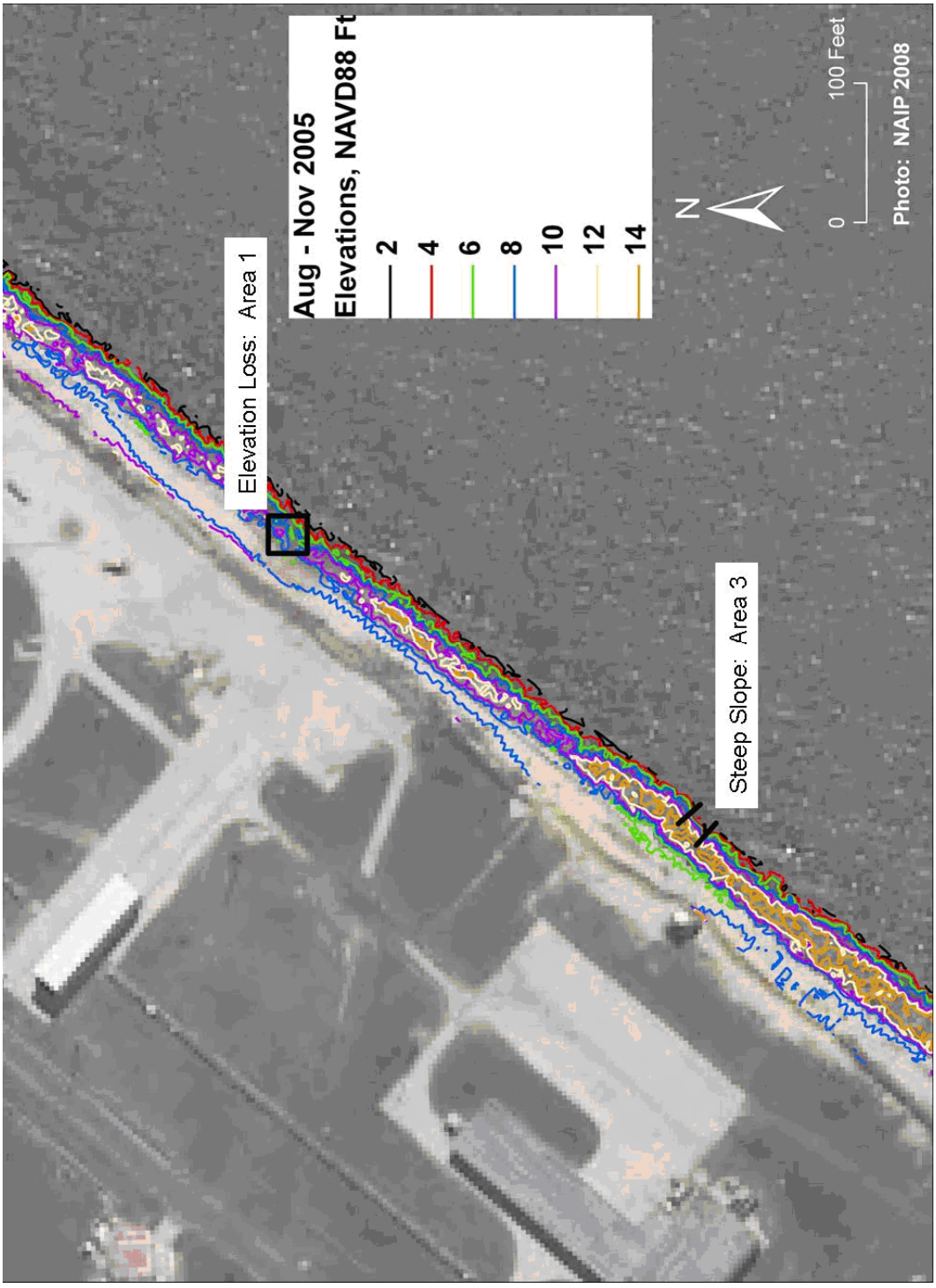

Figure 3-20. Steep slope area 3 and elevation loss area 1.

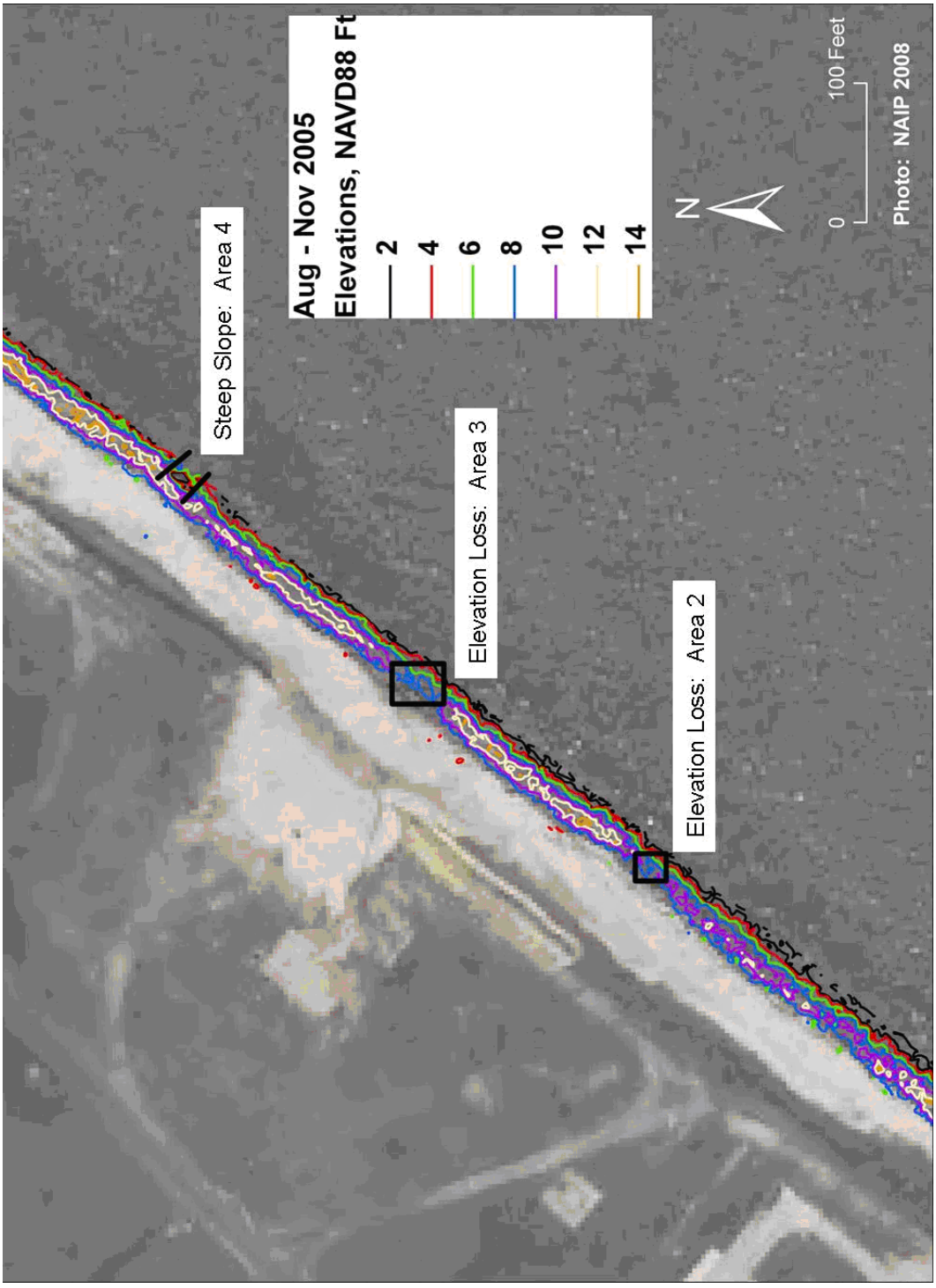

Figure 3-21. Elevation loss areas 2 and 3 and steep slope area 4.

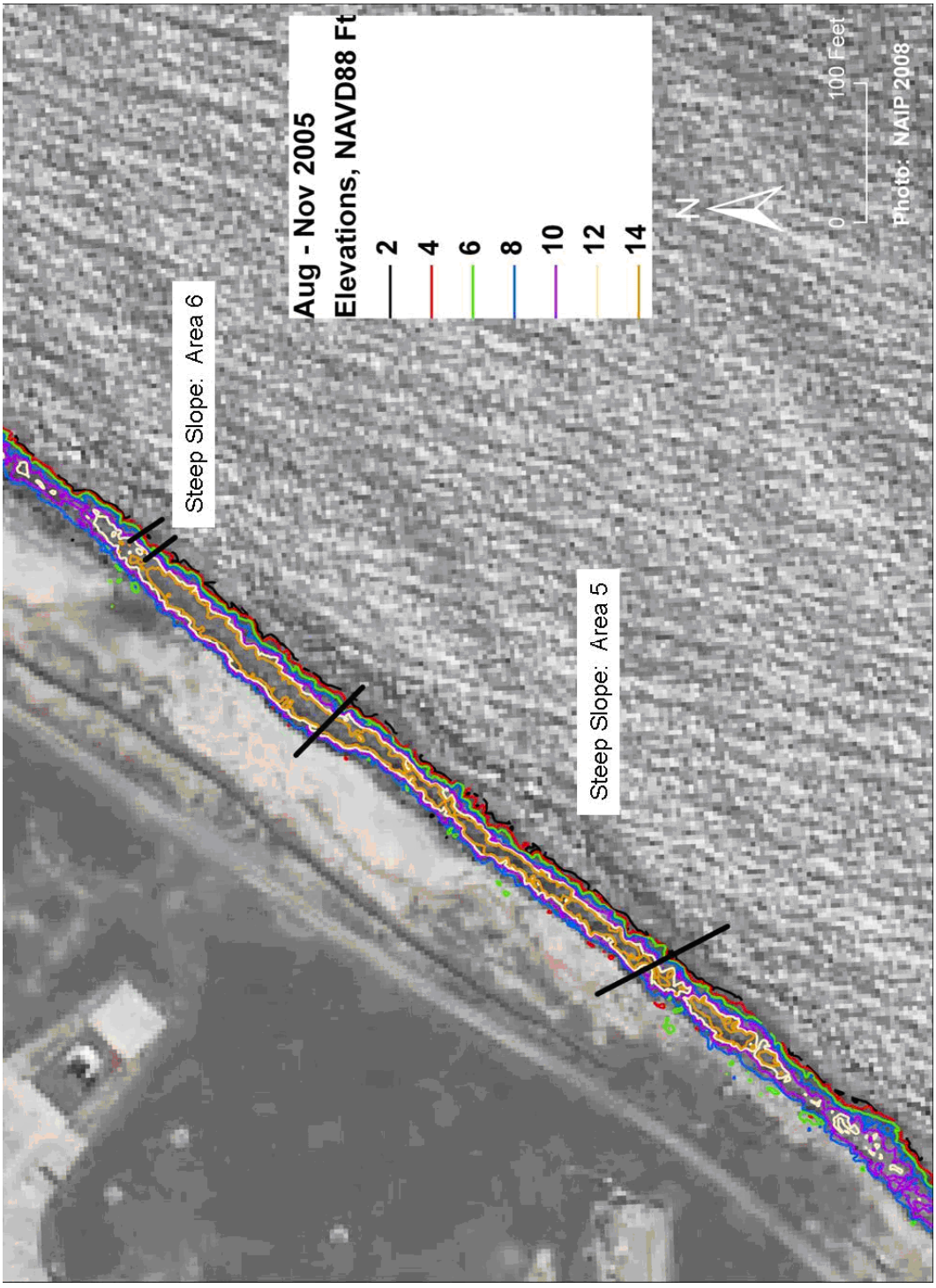

Figure 3-22. Steep slope areas 5 and 6.

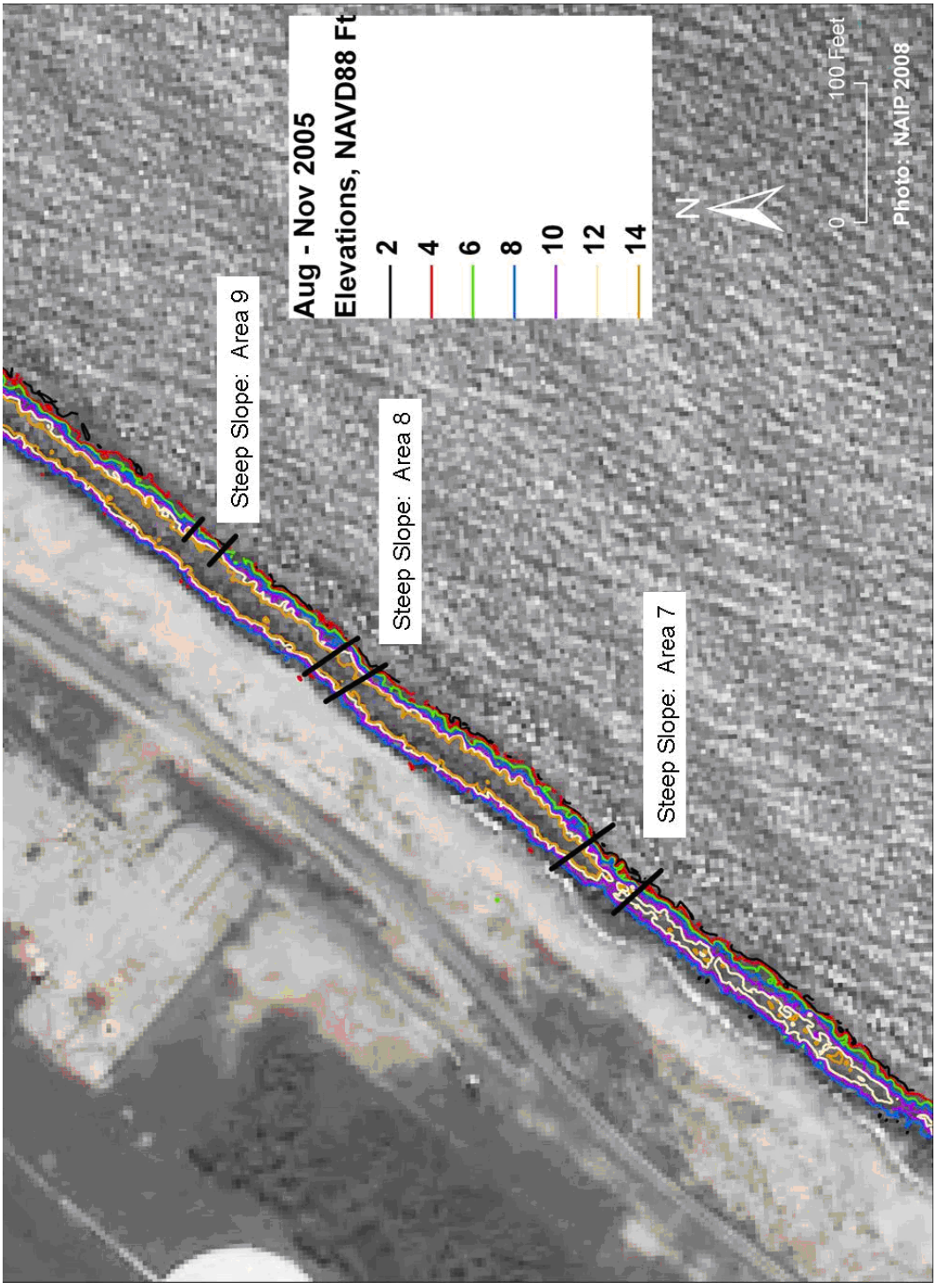

Figure 3-23. Steep slope areas 7, 8, and 9.

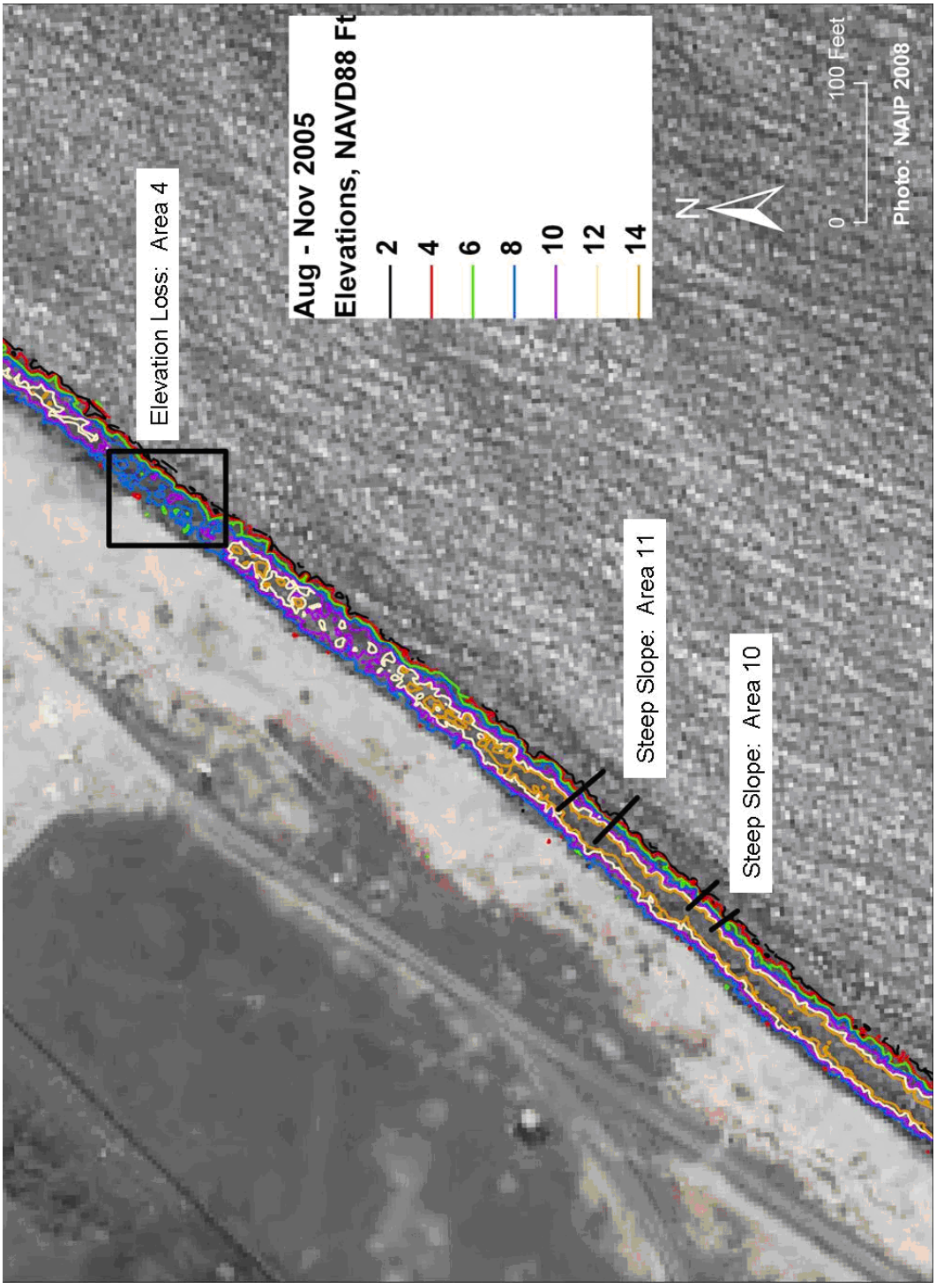

Figure 3-24. Steep slope areas 10 and 11 and elevation loss area 4.

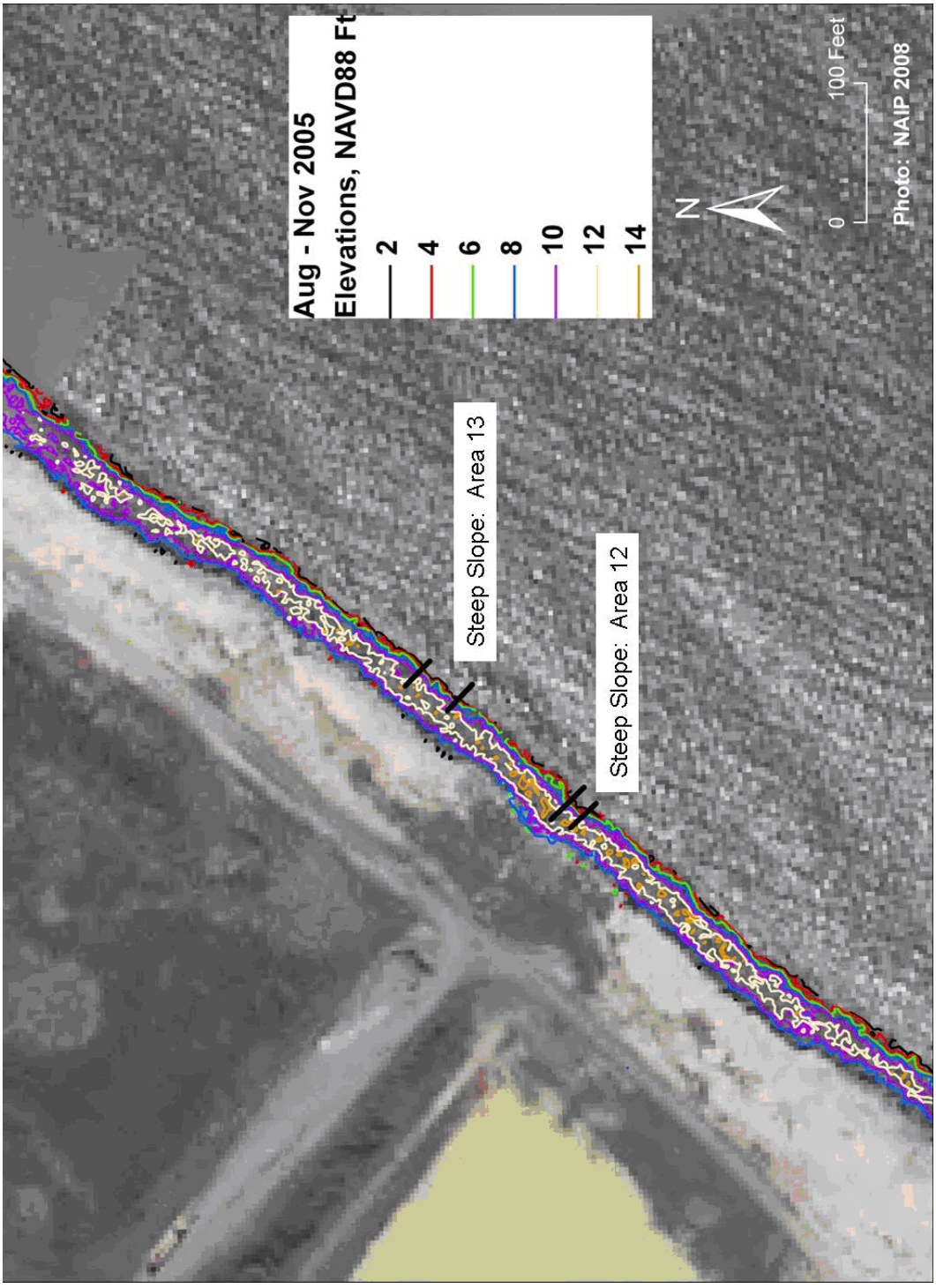

Figure 3-25. Steep slope areas 12 and 13.

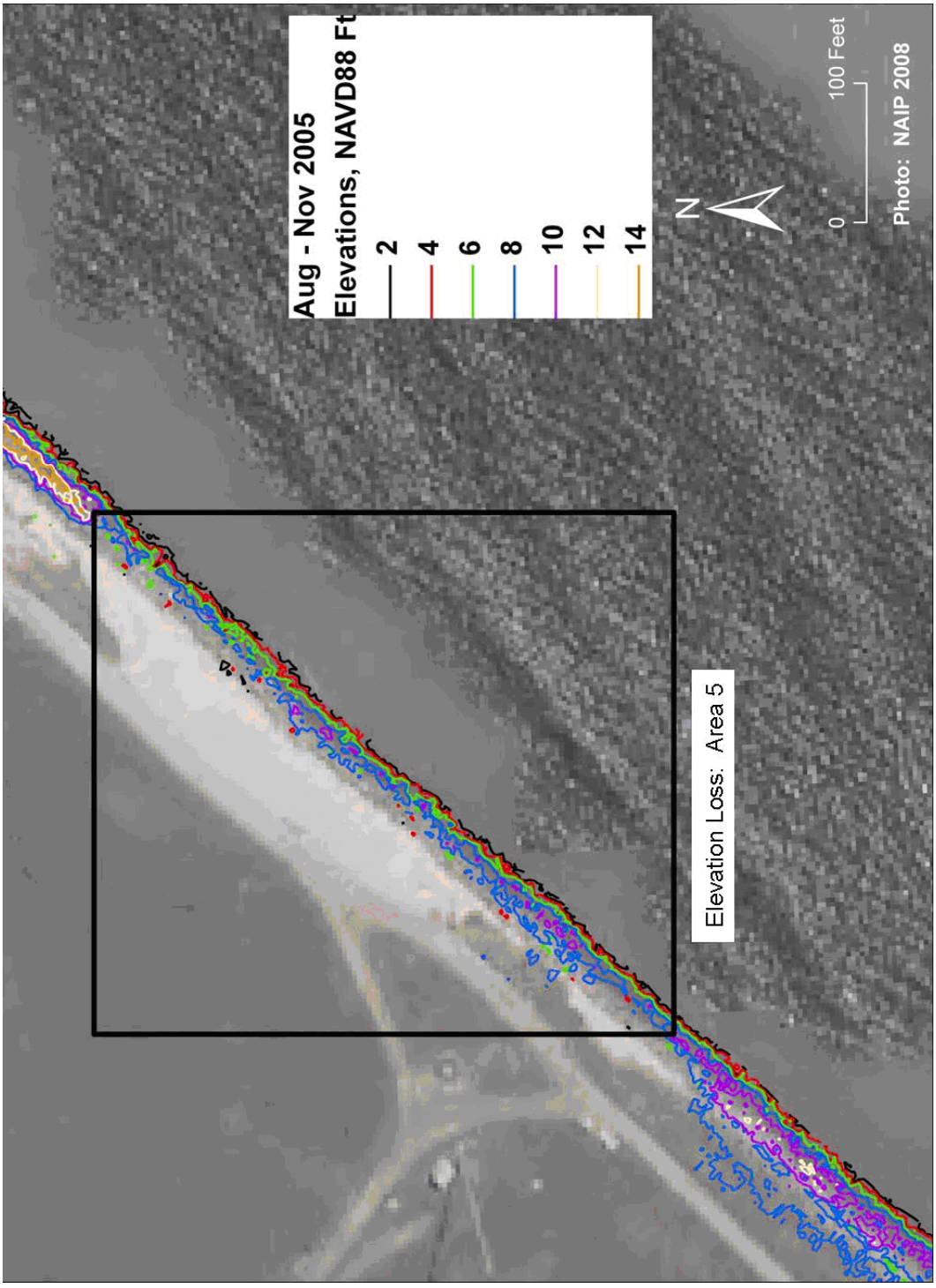

Figure 3-26. Elevation loss area 5

Analysis for +12 ft and + 14 ft crest elevation

Unlike the analysis for a crest elevation of +10 ft, which consisted of simply filling in low areas along the crest, raising the crest to +12 ft or +14 ft would require re-shaping the seawall side slopes to obtain a stable structure. Thus, for the +12 ft and +14 ft crest elevation analyses, the stone requirements were estimated by comparing a design profile to the existing profile at selected cross-sections along the seawall. This type of analysis accounted for both low elevation and steep seaward face seawall repairs.

A design profile for the Wallops Island seawall was selected with crest width of 10 ft at crest elevation either +12 ft or +14 ft. The landward side slope was 1:1.5. On the seaward side, a 1:2 slope was used from the crest down to elevation +6 ft. Normally, the 1:2 slope would continue to the seabed or to a toe berm, or the lower slope might be flattened to 1:2.5 or 1:3. However, because the proposed project will have a sand berm at elevation +6 ft and the lower slope should never be exposed, the design slope was steepened to 1:1.5 below elevation +6 ft.

Sixteen seawall profiles were taken from the LIDAR data at 1,000 ft intervals along the seawall. Locations of these seawall cross-sections are shown in Figure 3-27. The same cross-sections were used for the +12 ft and +14 ft analyses. +12 ft and +14 ft design profiles were overlain on each of these existing cross-sections and the deficits for each were calculated. Where the existing profile exceeded the design profile negative volumes were also calculated.

The +12 ft results indicated that 19,600 cu yds of stone would be needed to raise the existing profile to the +12 ft design profile. However, this analysis also indicated that the seawall currently has 15,600 cu yds of rock that is above the design profile. Assuming stone weight of 165 pcf and a porosity of 40%, yields the results that 26,200 tons of rock are required to raise the existing profile to the design, and 20,900 tons of rock are in the existing profile above the design profile. In other words, the 26,200 tons required to meet the design profile could be met by adding just 5,300 tons new stone and taking the remaining 20,900 tons from the seawall in areas where the existing profile is higher than the design profile. These quantities are shown in Table 3-5.

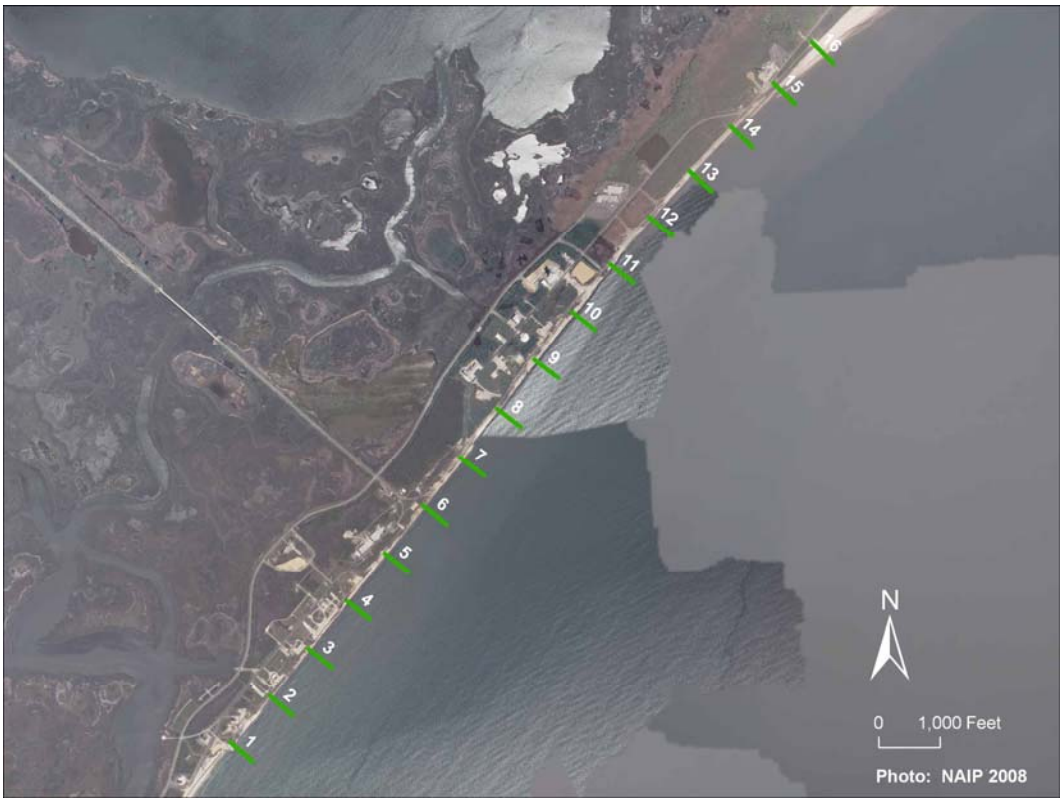

Figure 3-27. Locations of analysis cross-sections for seawall repair to +12 and +14 ft.

The +14 ft analysis showed that 26,300 cu yds of stone would be required to raise the existing profile to the design profile, and there are 3,900 cu yds available where the existing profile is higher than the design profile. Converted to tonnage, that is approximately 35,100 tons of stone required with 5,200 tons on the seawall above the design profile.

Table 3-5. Stone requirements for +12 and +14 ft seawall repair

Crest Elevation (ft)	Stone Required (cu yds)	Stone Available (cu yds)	Difference (cu yds)	Stone Required (tons)	Stone Available (tons)	Difference (tons)
12	19,600	15,600	4,000	26,200	20,900	5,300
14	26,300	3,900	22,400	35,100	5,200	29,900

Experimental Placement of Chincoteague Inlet Dredge Material on Wallops Island Shoreline

The Norfolk District has been dredging Chincoteague Inlet since the mid-1990's, placing the material in an offshore disposal site that is approximately 4,000 feet offshore of Wallops Island. The disposal site, having an area of 1,000 feet by 3,000 feet, is shown in Figure 3-28. The

amount of material dredged is shown in Table 3-6 (Morang, Williams, and Swean 2006).

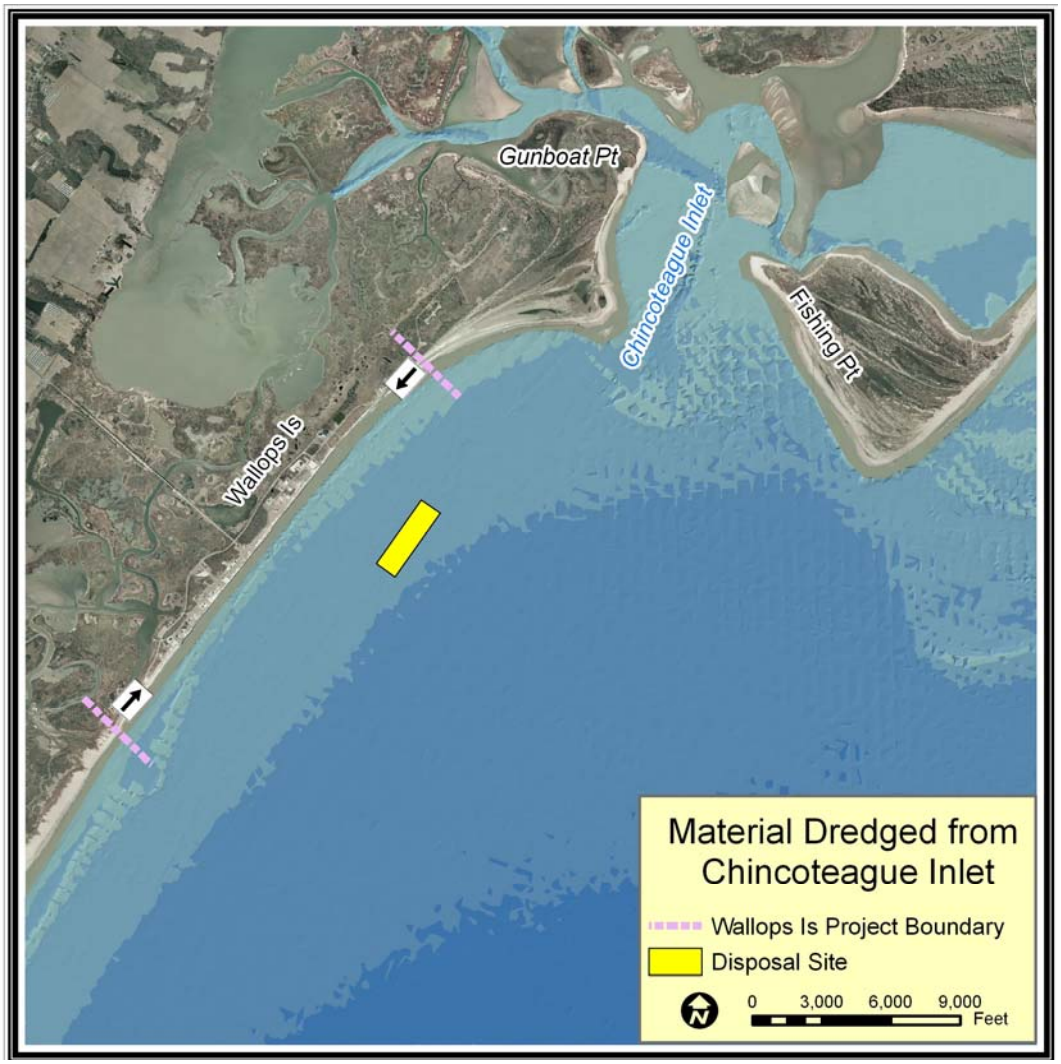

Figure 3-28. Offshore disposal site for Chincoteague Inlet dredge material.

In 2002, the District partnered with NASA to place dredge material from the inlet channel along the Wallops Island shoreline (Figure 3-29.) rather than in the offshore disposal site. The material was taken from the ocean bar portion of the project which lies just south of the westward tip of Assateague Island. The intent was to demonstrate the ability to place material along the shoreline from a hopper dredge, to determine the behavior of the material once placed along the shoreline, and to determine if this placement scenario could be a long term alternative.

Table 3-6. Chincoteague Inlet Dredging History								
Date	Dredge	Dredge Days	Yardage (yd3)	Price Per Yard	Mob and Demob	Beach Work	Total Cost	Total Cost Per Yard
Mar-06	Atchafalaya		70,000	$4.99	$234,817		$584,117	$8.34
Mar-05	Currituck	10	12,455				$102,505	$8.23
Oct-02	Northerly Island	26	91,292	$14.32	$163,260	$592,226	$2,062,787	$22.60
Dec-99	Atchafalaya	13	85,000	$4.50	$210,000		$592,500	$6.97
Aug-98	Mermentau	17	72,592	$3.15	$120,000		$348,665	$4.80
Nov-97	Mermentau	34	122,889	$3.87	$275,000		$750,580	$6.11
Jul-96	Mermentau	30	120,079	$3.58	$150,000		$579,883	$4.83
Apr-95	Mermentau	22	120,835	$3.72	$270,000		$719,506	$5.95
Notes: All operations by hopper dredge.								

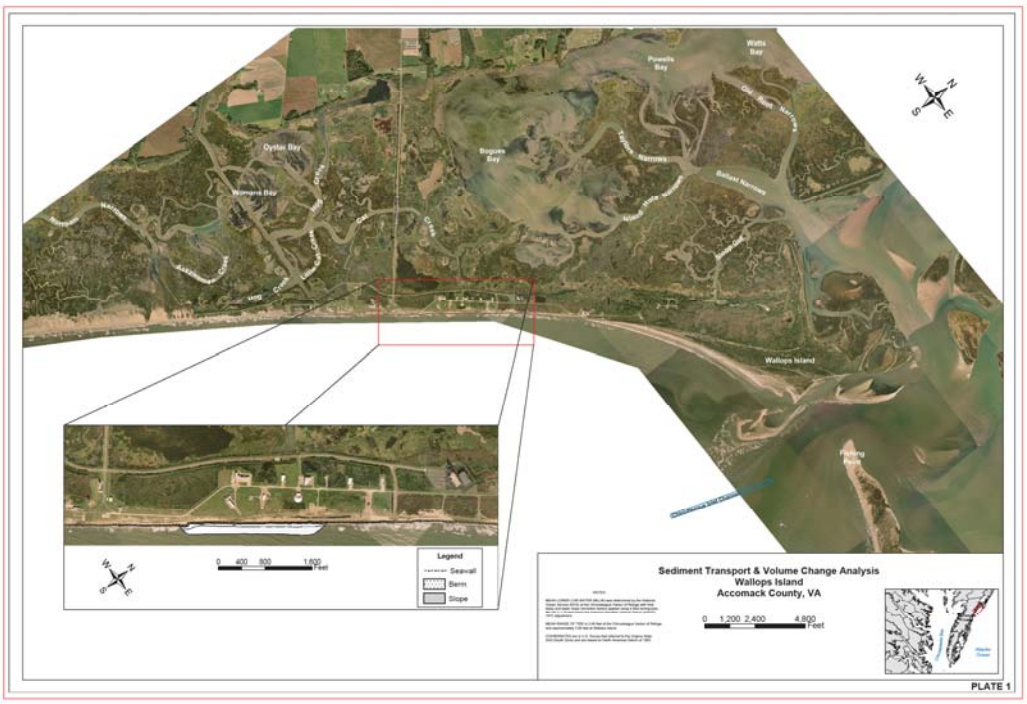

Figure 3-29. Site location map for experimental dredge placement.

For the project, the estimated nodal point along Wallops Island was the outfall for the dredge pipe running from the mooring and pump out buoy. Contract DACW65-02-C-0042 was awarded to B+B Dredging for the maintenance of the project and placement of material along the shoreline. The project was constructed during the period of September 22, 2002 to

October 23, 2002 for a final cost of $2,054,260.44. The volume of material removed, as calculated from bathymetric surveys, was 91,292 cubic yards.

The material from the project consisted mainly of fine sand. The outfall of the dredge pipeline was originally submerged at the start of the project and attached at the estimated nodal point to the toe of the seawall. Surveys and observation showed several feet of scour directly adjacent to the toe of the seawall. During the course of construction, a small beach head was created but not enough dry beach area was created to necessitate movement of the pipe outfall nor was there need for any equipment to spread the material.

Three surveys were performed along the Wallops Island shoreline to detect the placement and movement of material in the area. A before placement survey was performed in September 2002, an after placement survey was performed in November 2002, and a monitoring survey was performed in April 2003.

Comparison of the before placement survey and the after placement surveys generally showed that initial material was distributed along the seawall face and likely filled in a portion of the scour area that had been previously created in front of the seawall out to about 300 ft offshore (Figure 3-30). Comparison of the after placement survey and the monitoring survey (Figure 3-31) generally show that the material had moved away from the seawall face and joined nearshore bars along with generally diffusing throughout the area. Due to the high cost and modest benefits, the process has not been repeated during more recent inlet dredging events.

Figure 3-30. Comparison of pre- and post-placement surveys.

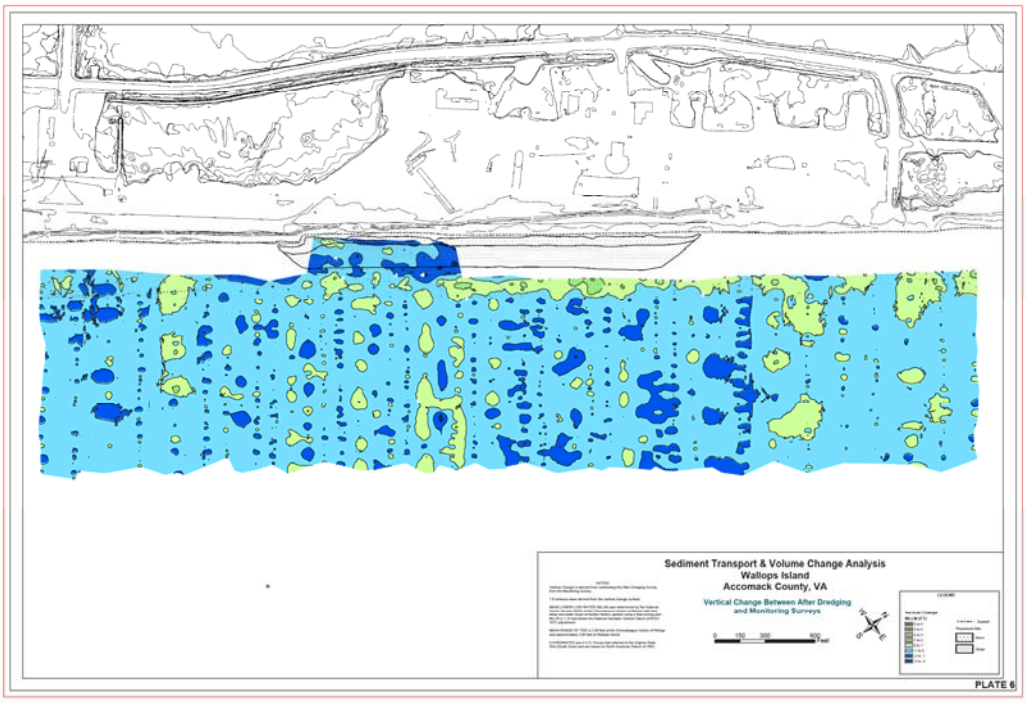

Figure 3-31. Comparison of post-placement surveys.

4 SBEACH / EST Modeling and Levels of Storm Damage Protection

Application of SBEACH and GENESIS Modeling

Following the methodology described in the Coastal Engineering Manual (CEM, Part 5, Chapter 4; Gravens, et al., 2006), the procedure applied in this project has been to develop a target beach profile along the shoreline that would provide an appropriate level of erosion, flooding, and storm damage protection to the facilities on Wallops Island, and then to augment this profile with sufficient advanced nourishment so that, at a minimum, the target profile would be maintained throughout the renourishment cycle. The computer models SBEACH and EST, which are discussed in this chapter, were applied to relate profile characteristics to levels of protection from storm damage. The computer models STWAVE and GENESIS, which are discussed in later chapters, provided estimates of longshore sediment transport rates throughout the study area and determined the volumes of advanced nourishment necessary to maintain the target profile through the end of the renourishment interval.

All SBEACH / EST and the STWAVE / GENESIS modeling work was performed at CHL on PC's using the CEDAS (version 4.03) package of models. A description of this software package can be found at the website: <http://www.veritechinc.com>.

SBEACH Setup

Model Description and Approach

SBEACH (Storm-induced BEAch CHange) is an empirically based numerical model for simulating two-dimensional cross-shore beach change (Larson and Kraus 1989, 1991, 1995; Larson, Kraus, and Byrnes 1990; Wise, Smith, and Larson 1996). The model's intended purpose is for predicting short-term profile response to storms. A fundamental assumption of SBEACH is that profile change is produced solely by cross-shore processes, resulting in a redistribution of sediment across the profile with no lateral gain or loss of material by longshore transport.

When a storm erodes a beach, the sand is usually not lost to the system. Rather, it is moved offshore, frequently into one or more bars. Low wave conditions after the storm will slowly move this material back onshore, rebuilding the berm. The discussion in this chapter addresses the question of how much sand must be placed in a berm and dune to provide adequate protection from storms.

Prior to running the model, input data in the form of representative nourished beach profiles and time series of storm waves and water levels were developed. Other input data included sediment grain size, depth of closure, and default model configuration parameters. The primary SBEACH output was a final (post-storm) profile for each input profile for each storm variant. These profiles are the basis for inputs to EST.

Storm Events

Forty-one hurricanes and tropical storms that impacted the study area between 1856 and 2003 were selected for the historical storm database. Thirty-nine extra-tropical storms (Nor'easters) that occurred between 1954 and 2003 were also included. These storms, listed in Tables 4-1 and 4-2, were culled from a dataset that was developed to analyze shoreline responses to a project in Chesapeake Bay (Melby, et al, 2005). Eleven Hurricanes and four Nor'easters were removed from the Chesapeake Bay dataset because they were found to have negligible impact at Wallops Island.

Table 4-1. Hurricanes and Tropical Storms Database

HURDAT Number	Storm Name	Reference Name	Year	SBEACH Start Date:time	SBEACH End Date:time	Max Wind speed (mph)
0031	unnamed	H-0031_	1856	8/19:0000	8/21:1200	50
0064	unnamed	H-0064_	1861	9/26:1800	9/29:0600	70
0067	unnamed	H-0067_	1861	11/01:1200	11/04:0000	70
0078	unnamed	H-0078_	1863	9/17:0600	9/19:1800	60
0165	unnamed	H-0165_	1876	9/17:0000	9/19:1200	80
0172	unnamed	H-0172_	1877	10/03:0000	10/05:1200	100
0187	unnamed	H-0187_	1878	10/22:0600	10/24:1800	90
0190	unnamed	H-0190_	1879	8/17:1200	8/20:0000	100
0202	unnamed	H-0202_	1880	9/08:0600	9/10:1800	70
0269	unnamed	H-0269_	1888	10/10:1800	10/13:0600	85
0302	unnamed	H-0302_	1893	6/15:1800	6/18:0600	85
0310	unnamed	H-0310_	1893	10/12:1200	10/15:0000	105
0312	unnamed	H-0312_	1893	10/21:1800	10/24:0600	50

0316	unnamed	H-0316_	1894	9/26:1800	9/30:1800	105
0317	unnamed	H-0317_	1894	10/08:1800	10/11:0600	105
0336	unnamed	H-0336_	1897	10/24:0000	10/28:0000	55
0347	unnamed	H-0347_	1899	8/14:1800	8/20:0600	105
0351	unnamed	H-0351_	1899	10/30:0000	11/02:0000	85
0384	unnamed	H-0384_	1904	9/13:1200	9/16:0000	85
0409	unnamed	H-0409_	1908	7/29:1200	8/02:0000	85
0492	unnamed	H-0492_	1923	10/22:0000	10/25:0000	60
0562	unnamed	H-0562_	1933	8/20:1800	8/24:1800	105
0567	unnamed	H-0567_	1933	9/14:1800	9/17:1800	105
0588	unnamed	H-0588_	1935	9/04:1200	9/07:0000	140
0605	unnamed	H-0605_	1936	9/17:0000	9/19:1200	105
0671	unnamed	H-0671_	1944	9/13:0600	9/15:1800	120
0755	BARBARA	H-0755B	1953	8/13:0000	8/16:0000	95
0776	HAZEL	H-0776H	1954	10/14:0600	10/16:1800	120
0780	CONNIE	H-0780C	1955	8/10:0600	8/14:0600	125
0787	IONE	H-0787I	1955	9/18:1200	9/21:0000	105
0830	BRENDA	H-0830B	1960	7/28:1800	7/31:0600	50
0832	DONNA	H-0832D	1960	9/10:1800	9/13:0600	140
0937	DORIA	H-0937D	1971	8/26:1800	8/29:0600	55
1030	BRET	H-1030B	1981	6/29:1200	7/02:0000	60
1070	GLORIA	H-1070G	1985	9/25:1200	9/28:0000	125
1077	CHARLEY	H-1077C	1986	8/15:0000	8/19:0000	70
1175	BERTHA	H-1175B	1996	7/11:1800	7/14:0600	100
1179	FRAN	H-1179F	1996	9/04:1200	9/08:1200	105
1196	BONNIE	H-1196B	1998	8/26:0000	8/30:0000	100
1214	FLOYD	H-1214F	1999	9/15:0000	9/17:1200	135
1264	ISABEL	H-1264I	2003	9/17:0600	9/21:0600	140

Table 4-2. Nor'easters Database

Reference Name	Year	SBEACH Start date:time	SBEACH End Date:time	Maximum Wind speed (m/s)
N540121	1954	1/21:1200	1/24:0000	18.4
N561024	1956	10/24:0600	10/30:1800	14.3
N571002	1957	10/02:0600	10/06:1800	13.7
N581019	1958	10/19:1200	10/22:1200	16.7
N620305	1962	3/05:0600	3/08:1800	16.3
N621126	1962	11/26:0000	12/05:1200	14.5
N660126	1966	1/26:0600	2/01:0600	15.8
N690119	1969	1/19:1800	1/22:1800	12.5
N720524	1972	5/24:0000	5/28:0000	14.0
N721004	1972	10/04:0600	10/08:1800	13.0
N741130	1974	11/30:1800	12/05:0600	14.6
N750628	1975	6/28:1800	7/02:0600	14.8
N771029	1977	10/29:0000	11/03:0000	12.4

N780426	1978	4/26:0000	4/28:1200	14.7
N801226	1980	12/26:1800	12/31:1800	13.2
N810819	1981	8/19:0000	8/23:1200	12.3
N830210	1983	2/10:1800	2/15:1800	13.4
N840328	1984	3/28:1200	3/31:1200	15.8
N840926	1984	9/26:1200	10/03:0000	13.1
N841010	1984	10/10:1200	10/15:0000	14.8
N851028	1985	10/28:1200	11/06:1200	13.6
N861129	1986	11/29:1800	12/04:0600	12.8
N880411	1988	4/11:1200	4/14:1200	14.8
N890307	1989	3/07:0600	3/11:0600	13.6
N910107	1991	1/07:0000	1/12:0000	13.4
N910418	1991	4/18:0000	4/21:1200	14.4
N911028	1991	10/28:0000	11/01:0000	14.6
N911108	1991	11/08:0000	11/10:1200	18.2
N930312	1993	3/12:1200	3/15:1200	13.8
N941012	1994	10/12:0000	10/16:1200	13.1
N961003	1996	10/03:1200	10/10:0000	12.4
N970601	1997	6/01:0000	6/08:0000	12.0
N971014	1997	10/14:0600	10/21:0600	12.1
N980510	1998	5/10:1200	5/15:0000	12.2
N990428	1999	4/28:1200	5/04:1200	12.5
N990829	1999	8/29:1200	9/07:0000	14.2
N000528	2000	5/28:1200	6/01:0000	15.0
N030408	2003	4/08:0000	4/12:1200	12.1
N030908	2003	9/08:0600	9/12:1800	13.9

Characterization of Storm Water Levels

The storm-induced water elevations were calculated with the ADCIRC model as described in Melby et al. (2005). The ADCIRC grid covered the eastern seaboard from North Carolina to New Jersey and included Chesapeake and Delaware Bays. Water elevation data were obtained from the ADCIRC output (node 7566), just offshore of Wallops Island.

The ADCIRC storm surge results included the historical astronomical tide in the water level time series. Since future storms will strike the coast at random times relative to the tide cycle, the historical tide was removed and replaced with 12 different tidal curves to make 12 variants for each storm. The historical astronomical tidal data was obtained from the website: <http://tbone.biol.sc.edu/tide/>.

The 12 tidal variants were generated with a 12 hour period (semi-diurnal) sine wave with three different amplitudes and four phases. Amplitudes were designated S (= spring), I (= intermediate), and N (= neap). Values

applied were a spring amplitude of 0.714 m (2.34 ft), an intermediate amplitude of 0.535 m (1.76 ft), and a neap amplitude of 0.363 m (1.19 ft). See Appendix D for tidal and datum information. Tidal phases were randomized by synchronizing the peak of the tide with the peak of the storm surge and by then shifting the peak of the tide phase by 90, 180, and 270 degrees (designated 1, 2, 3, and 4, respectively).

An example of these tide plus storm surge curves for storm N801226 are shown in Figure 4-1. This figure shows the ADCIRC generated storm surge in panel A with the historical astronomical tide removed. Panels B through E show the four storm surge plus spring tide curve storm variants (S1 through S4, respectively).

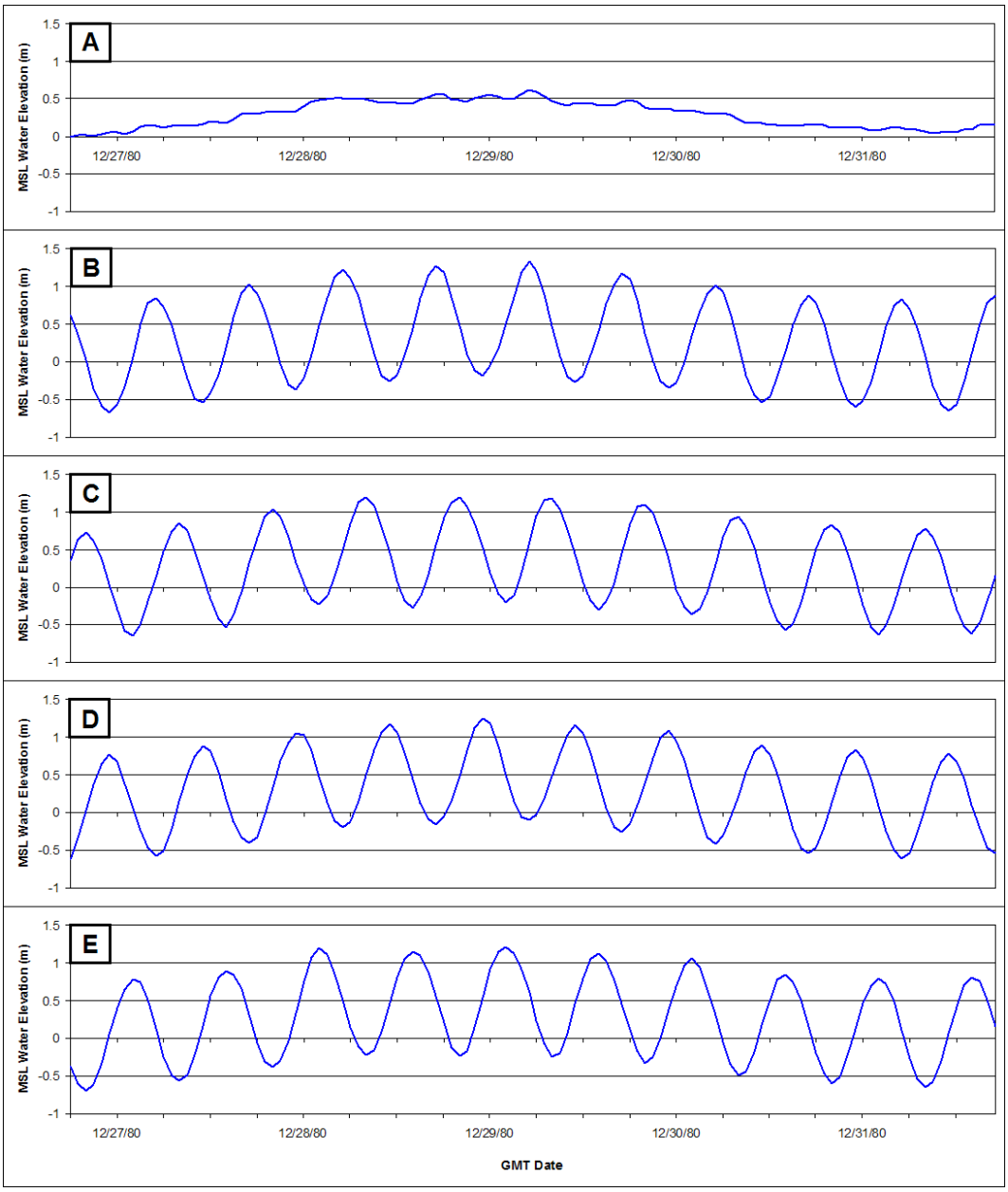

Figure 4-1. Example Spring tide plus surge water level curves for Nor'easter N801226.

Characterization of Storm Waves

Wave data at Wallops Island were available for all storms from 1980-1999 in the form of WIS hindcasts from WIS Atlantic station 178 (see: <http://frf.usace.army.mil/cgi-bin/wis/atl/atl_main.html>). These data were transformed to 6 meters of water depth using the Phase3 transformation routine within CEDAS. Wave data for the other storms used surrogate data from the storm wave data that were available. Wave data were matched to storms having similar maximum water levels and

then time shifted so the maximum wave height occurred at the peak of the storm surge.

An example of the Phase 3 transformed wave height and wave period data for storm N801226 is shown in Figure 4-2. Each of the 12 water level variants for a storm used the same wave data.

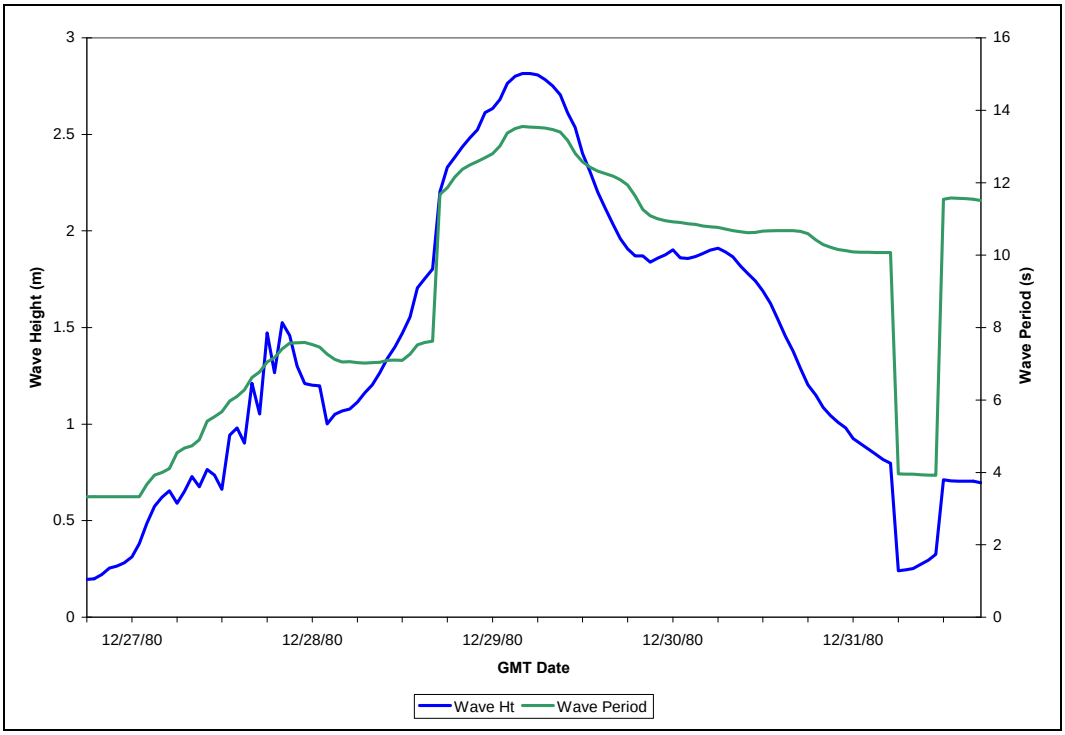

Figure 4-2. Example wave height and wave period for storm N801226.

Characterization of the Beach Profile

There is no exposed beach along much of the seawall (the southern part). However, by comparing profiles north and south of the seawall (primary comparison parameters were berm height, foreshore beach slope, sub-aerial profile volume, and subaqueous profile shape), it was determined that a single idealized profile could represent the nourished profile along the 3.7 mile (6.0 km) length of the project.

The beach profiles described in chapter 3 were analyzed along with initial SBEACH modeling results to develop three idealized "potential" nourished profiles that were used in the SBEACH modeling effort (Figure 4-3). The three profiles differ in the width of the berm and the presence and size of

the dune. The three profile alternatives were designed to be placed adjacent to the seaward face of the rock seawall (the rock seawall extends landward (to the left) from Distance zero in Figure 4-3). However, the rock seawall (non-eroding surface) was not modeled.

- The B030 profile represents a modest project with no dune and a 30 ft berm width. Since this profile lacks a dune, it does not provide flood protection.
- For the B070 profile, the seaward sloping face of the dune rests against the seawall. The distance from the seawall to the seaward shoulder of the berm is 70 ft, of which 40 ft is under the dune and 30 ft is exposed berm width.
- The B100 profile has a 20 ft dune crest plus the seaward sloping dune face. The distance from the seawall to the berm shoulder is 100 ft, of which 60 ft is under the dune and 40 feet is exposed berm width.

For the idealized profiles, the upland elevation (based upon profile data) is set at 7 ft. (All elevations in this discussion are relative to MSL, see Appendix D). The dune elevation of 14 ft is based upon initial modeling results (of storm surge elevations and amount of erosion of dune crest), and is the design elevation of the rock seawall. The dune slope (1:5) is a fairly common choice for a stable engineered dune. The berm height (+6 ft) and foreshore slope (0.073:1=tan(4.17°)) are based upon measured beach profiles. Below MSL an actual long profile from the south end of the project (profile 4) was applied. A full profile is shown in Figure 4-4.

The differences in these three profiles are largely necessitated by differences in the dune. The B030 profile represents a minimal fill project without a dune. The B070 profile has the same amount of exposed berm width (30 ft) as the B030 profile, and represents a minimal fill project that includes a dune. The dune in the B070 profile is only a partial dune (the seaward face of a dune) as it rests against and is supported by the seawall. The B100 profile has a somewhat wider exposed berm (40 ft) in addition to the seaward face and central portion of a dune. However, this B100 dune is still incomplete as it lacks rear slope. Instead, support is supplied by the seawall.

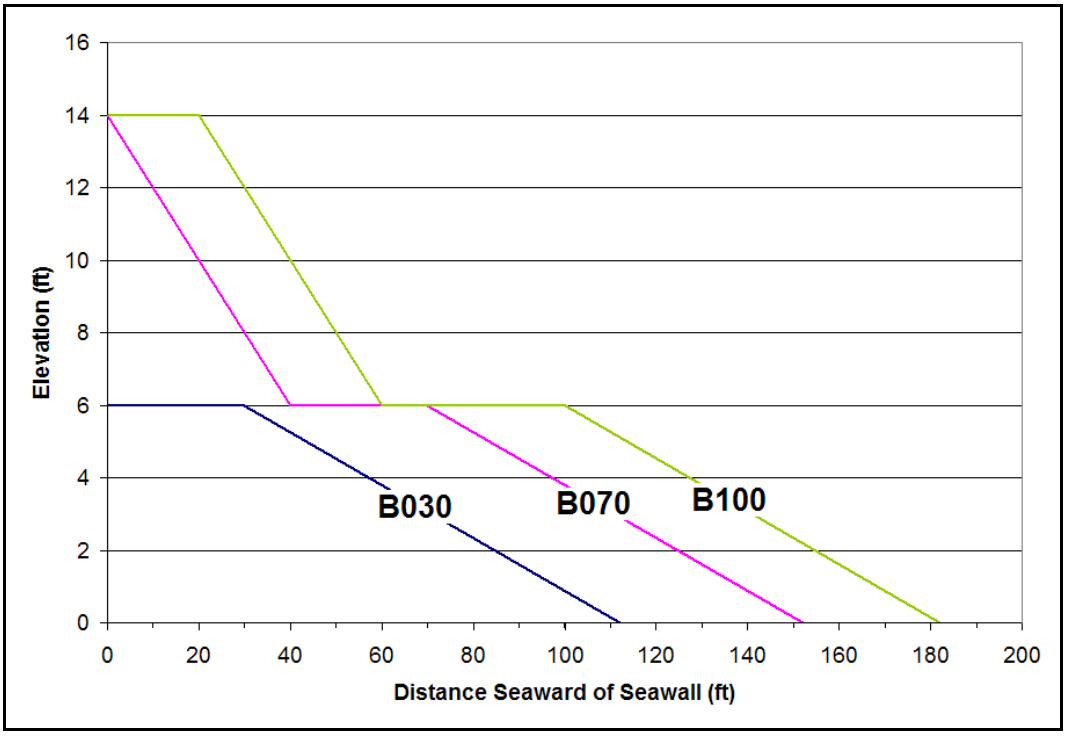

Figure 4-3. Sub-aerial profiles for Alternatives considered.

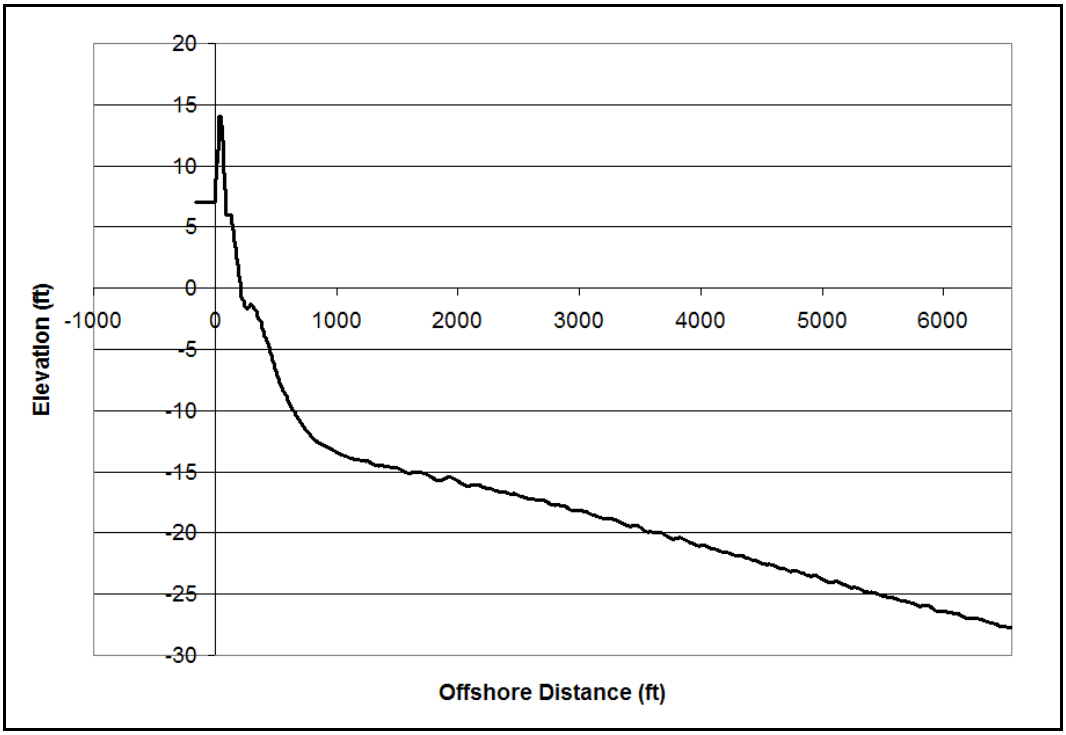

Figure 4-4. Representative Profile.

Characterization of the Depth of Closure

Multiple beach profile datasets were not available to determine a "pinch-out" depth for the depth of closure. Rather, a Closure Depth of 13 ft (4 m) was determined largely upon profile shape information. The profiles all start to become much more nearly flat at this depth and begin to diverge substantially from an equilibrium profile, as shown in Figure 4-5. The GEN Cell 17, 50, and 87 Profiles are representative of the northern, central, and southern portions of the project site. As the Wallops Island shoreline has been experiencing chronic erosion for many decades, a reasonable interpretation for the flatness in the profiles is that this is the depth to which the erosion has cut. In addition, this Depth of Closure value is not greatly different from estimates obtained using the formulas of Hallermeier (1983) or Ahrens (2000). On the 0.29 mm equilibrium profile, this depth of closure is 600 ft (183 m) seaward of the shoreline.

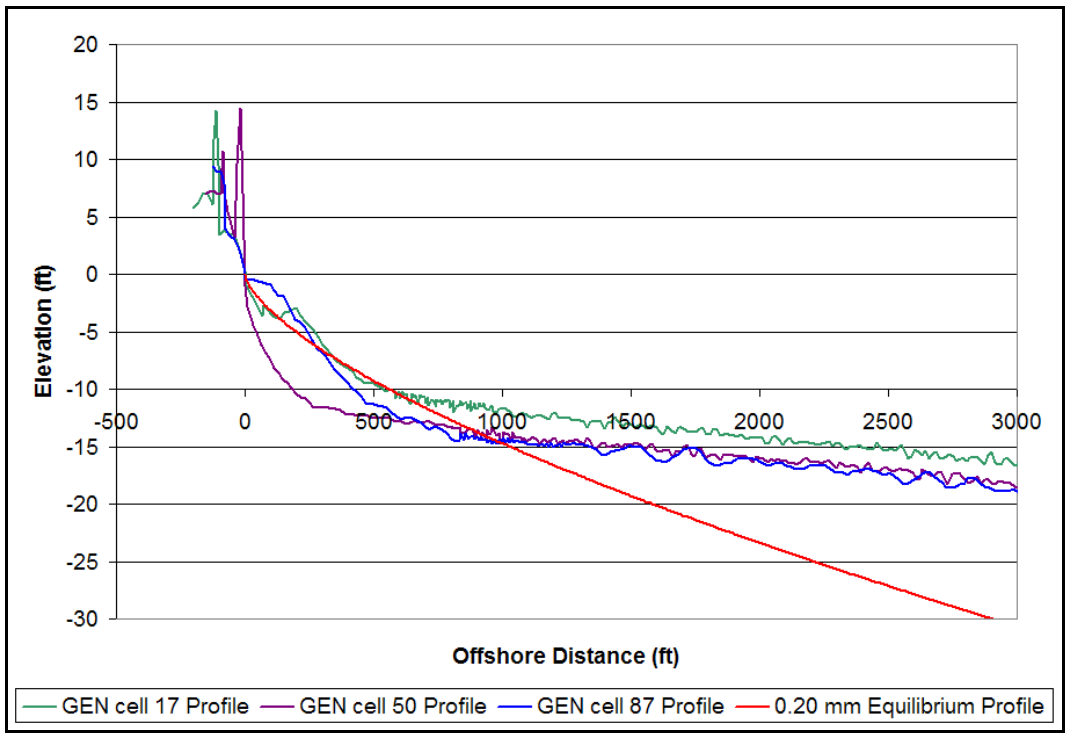

Figure 4.5. Divergence of Wallops Island profiles from an equilibrium profile for depths greater than 4 meters (13 feet).

This depth of closure is substantially less than the value (-28 ft) given in Morang, Williams, and Swean (2006). However, the value given in that report was not calculated for Wallops Island, but taken from the closest site available where the calculation had previously been made, in this case

Sandbridge, VA. In discussions with the senior author of that report, he concurred with the methodology presented here.

While this value appears reasonable, it is recognized that it is shallower than many other U.S. east coast values. An underestimate of this value can lead to an underestimate in the required amount of beach fill material. Uncertainty in this value is discussed in Chapter 6 and additional material is included in the fill estimates specifically to compensate for uncertainties in this and other quantities.

SBEACH Model Runs

The SBEACH model was not calibrated for the Wallops Island site prior to data runs being made, because the appropriate pre- and post-storm profiles were not available for the site. Instead, the default model parameters were applied. This was considered justified as one of the primary sites used to develop the SBEACH default parameters was on Assateague Island, which is immediately north of the project site (Wise, Smith, and Larson, 1996). All of the configuration values for this model are listed in Table E-1 of Appendix E.

Initial model runs indicated that the B070 profile provided optimal storm protection. As discussed below, the beach is only one component of the defenses in this storm damage reduction project (the other two being the rock seawall and interior flood barriers). The philosophy of this tiered approach is that the beach fill alone will provide protection against smaller, more frequent storms, leaving the seawall intact to protect against the largest storms expected over the life of the project.

The B030 profile lacks a dune and initial model results showed that storm waves would impact the seawall at intervals more frequent than the renourishment events. Thus, potential damage to the seawall would be an ongoing issue. The B100 profile provided superior storm damage protection as compared to the B070 profile, but at greater expense, and the additional protection would be, in essence, provided by the rock seawall. At an estimated cost of $10/yd^3$, the B100 design condition would add an additional $5.3 million dollars to the cost of the initial fill placement beyond the cost of the B070 design condition. Based upon this initial screening, only a limited amount of modeling was conducted using the B030 and B100 profiles.

EST Setup

EST (Empirical Simulation Technique) is a statistical numerical analysis procedure designed to simulate multiple life-cycle sequences of a non-deterministic multi-parameter system to determine frequency of occurrence relationships (Borgman, et al, 1992, Scheffner, et al, 1996, Scheffner, et al, 1999). The program generates frequency response information for each output parameter.

The model requires input vectors that describe the process forcing functions (the storms), output vectors that define the parameters to be modeled (the post storm profile responses), and configuration parameters. The following standard nine EST input vectors were developed for each of the 960 storm variants.

1. The peak of the storm surge.
2. The duration of storm surge (length of time the storm surge exceeded 0.3 m).
3. The average value of surge over the storm's duration.
4. The tidal amplitude (spring, average, or neap).
5. The tidal phase at peak surge (high, mid, or low tide).
6. The slope of tide at peak surge.
7. The peak wave height.
8. The duration of storm waves (length of time the wave height exceeded 1 m).
9. The average value of wave height over the storm's duration.

A FORTRAN program extracted a variety of response vectors from the suite of SBEACH post-storm profiles, which were directly imported into EST. EST model configuration parameters are listed in Appendix E.

Profile Responses to Hurricanes and Nor'easters

While there is a great deal of similarity, Nor'easters and Hurricanes can impact the beach profile differently because of differences in these types of storms. Hurricanes that occur at the latitude of Wallops Island are typically fast moving storms, usually producing substantial coastal impacts for something on the order of a day or less. However, because of the low central pressures and high wind speeds, they can generate large storm surges (substantially elevated water levels). In contrast, Nor'easters can cause impacts over longer time scales (several tidal cycles), but usually do

not produce extremely high storm surges. These trends are shown in Figures 4-6 and 4-7, which use data taken from the historical storm sets listed in Tables 4-1 and 4-2. Figure 4-6 shows the storm surge heights (with tides removed) with the data ranked from highest surge height to lowest, for Hurricanes (black) and Nor'easters (red). Figure 4-7 shows the distribution of storm times, as defined by the hours that the surge height exceeded 0.3 m for each of the 12 variants for each storm. The average Hurricane storm time was 23 hours; the average Nor'easter storm time was 48 hours.

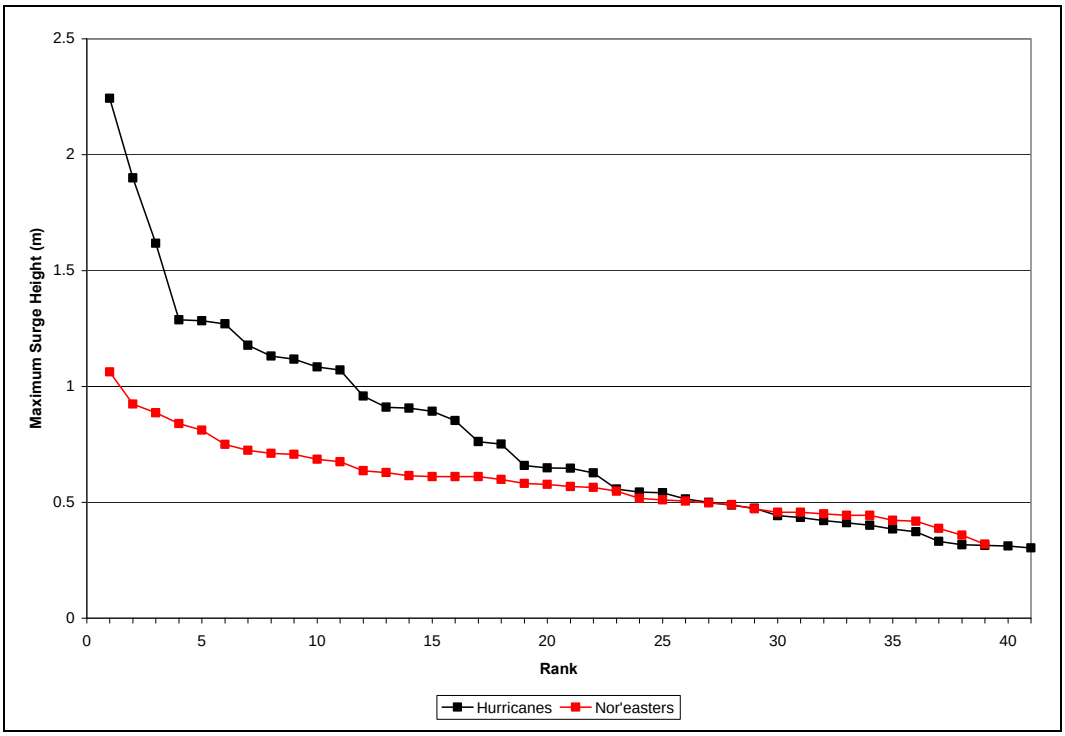

Figure 4-6. Maximum storm surge height for Hurricanes and Nor'easters, ranked from highest to lowest for the storms in the dataset.

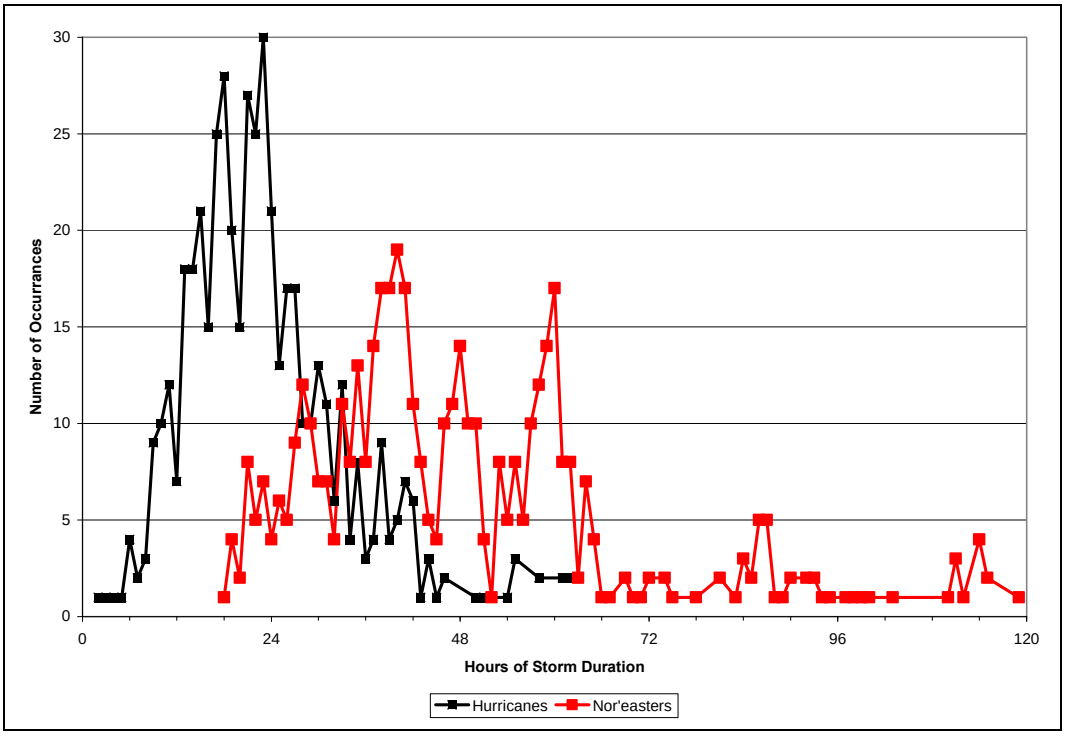

Figure 4-7. Distribution of storm surge durations for Hurricanes and Nor'easters.

These differences affect the way the storms impact the beach profile. Nor'easters, with their lower water levels but longer durations, can produce considerable berm erosion while leaving the dune relatively intact. Conversely, a hurricane can have less impact on the berm, but a greater impact on the dune. Examples of these differences are shown in Figures 4-8 and 4-9. These figures are SBEACH pre (black) and post (red) storm profiles. The pre-storm profiles were model inputs; the post-storm profiles are model predictions. Figure 4-8 shows a Nor'easter that has severely eroded the berm, but has left the dune essentially untouched. Figure 4-9 shows a hurricane that has done less damage to the berm but has started to erode the dune. Where there is no change in the profile only the final (red) profile line is visible.

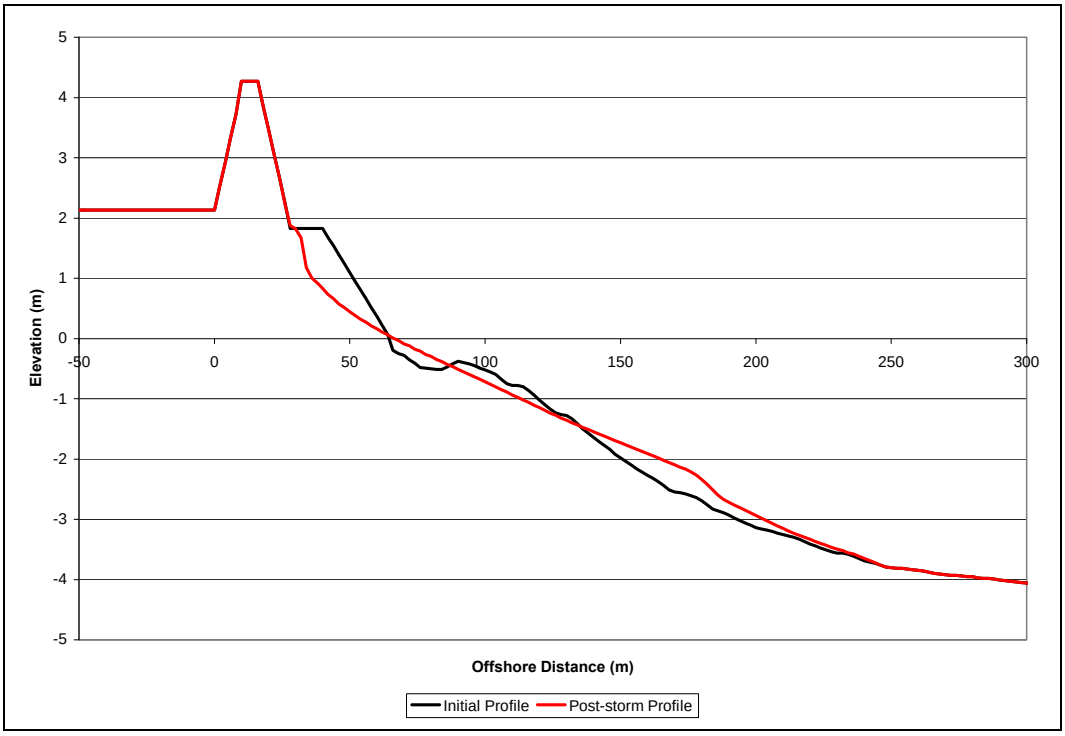

Figure 4-8. SBEACH Profile Response for Storm N621126S3 (Nor'Easter).

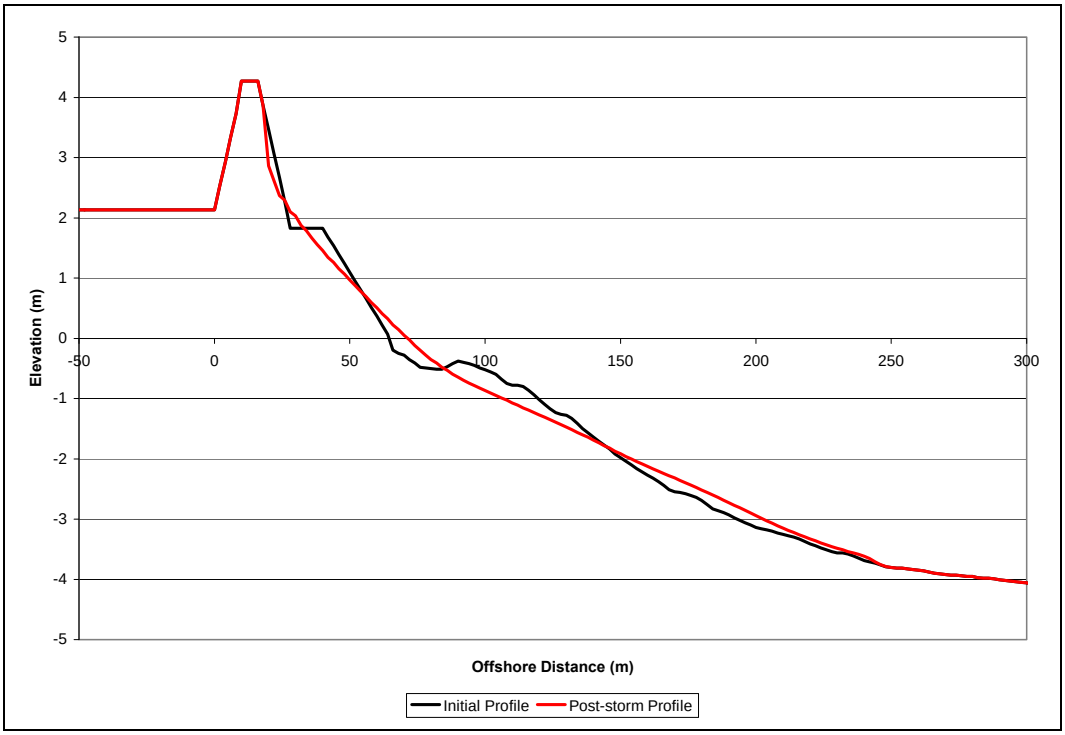

Figure 4-9. SBEACH Profile Response for Storm H-190_S1. (Hurricane).

B070 Profile Response to Storms

Figures 4-10 through 4-14 are EST frequency response plots that show the predicted response of the B070 profile to the suite of storms that are based upon the combined historical data set of Hurricanes and Nor'easters.

Berm Response

Figure 4-10 shows the return period intervals for storm-induced berm recession. This plot shows the landward distance that the berm crest elevation will be reduced by 1 foot. This is equivalent to the recession distance of the 5 ft contour, since the modeled berm crest is flat. This plot shows that a storm that produces 30 ft of berm cutback can be expected to occur with a return period on the order of 8 years. A storm producing 40 ft of horizontal berm erosion has an estimated return period of 40-50 years. The entire seaward face of the berm shows approximately the same behavior. The return period for the recession of the 2 ft contour is shown in Figure 4-11.

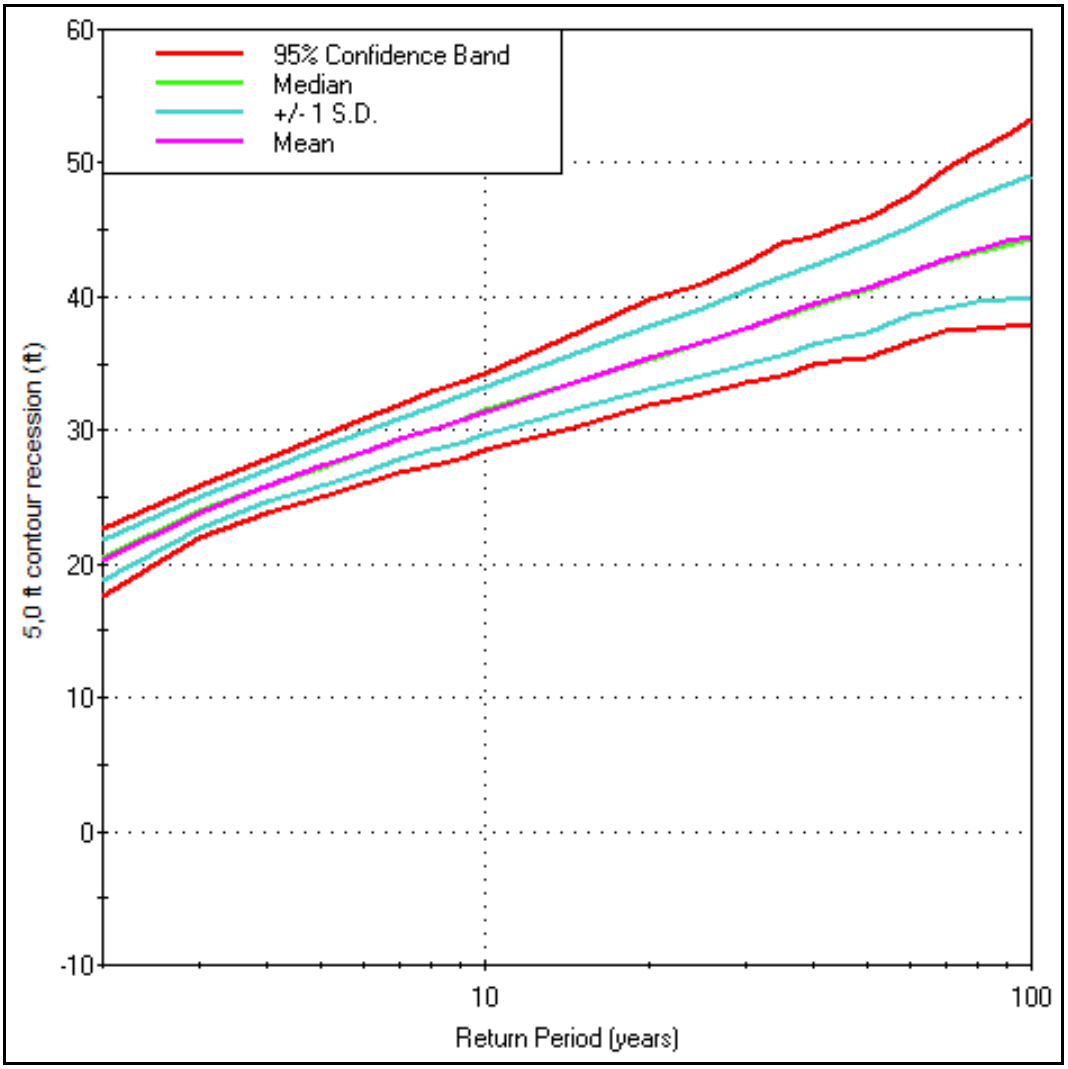

Figure 4-10. Return period of berm recession.

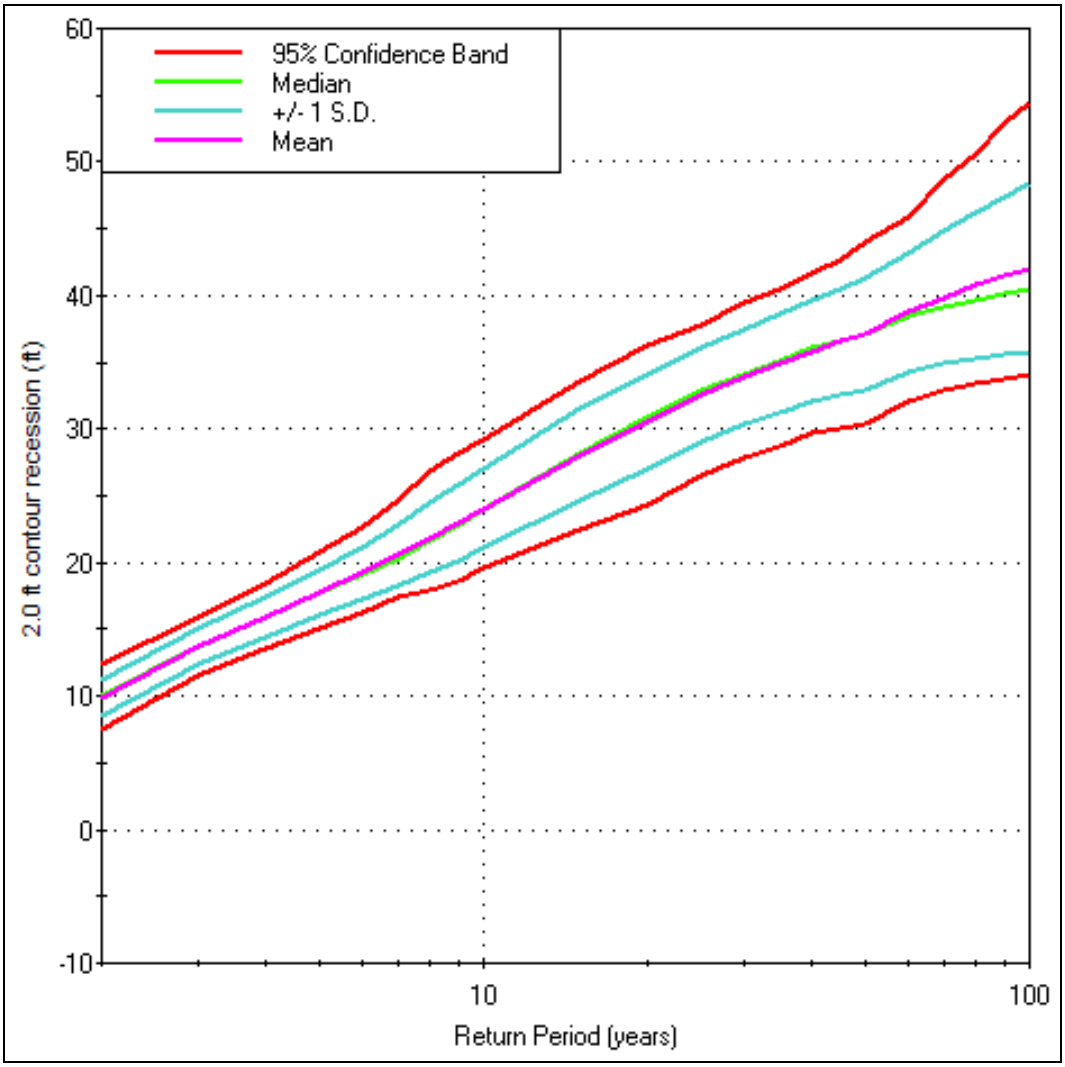

Figure 4-11. Return period for recession of the +2 ft contour.

Dune Response

Figure 4-12 shows the frequency response for dune lowering. This figure shows that storms that are less than 30-40 year return interval events do not impact the +14 ft dune crest.

Unlike a berm, the dune is not expected to recover following storm damage, at least not on the time scales of typical renourishment cycles. Rather it is expected that such damage will require mechanical repair at the time of the next renourishment. Therefore, damage to the dune should be an infrequent event. Figure 4-13 shows the frequency response for recession of the 9 ft contour. This elevation is a little less than half way up

the dune face. Figure 4-13 shows that storms that start to cause dune erosion can be expected to have a 20-30 year return interval.

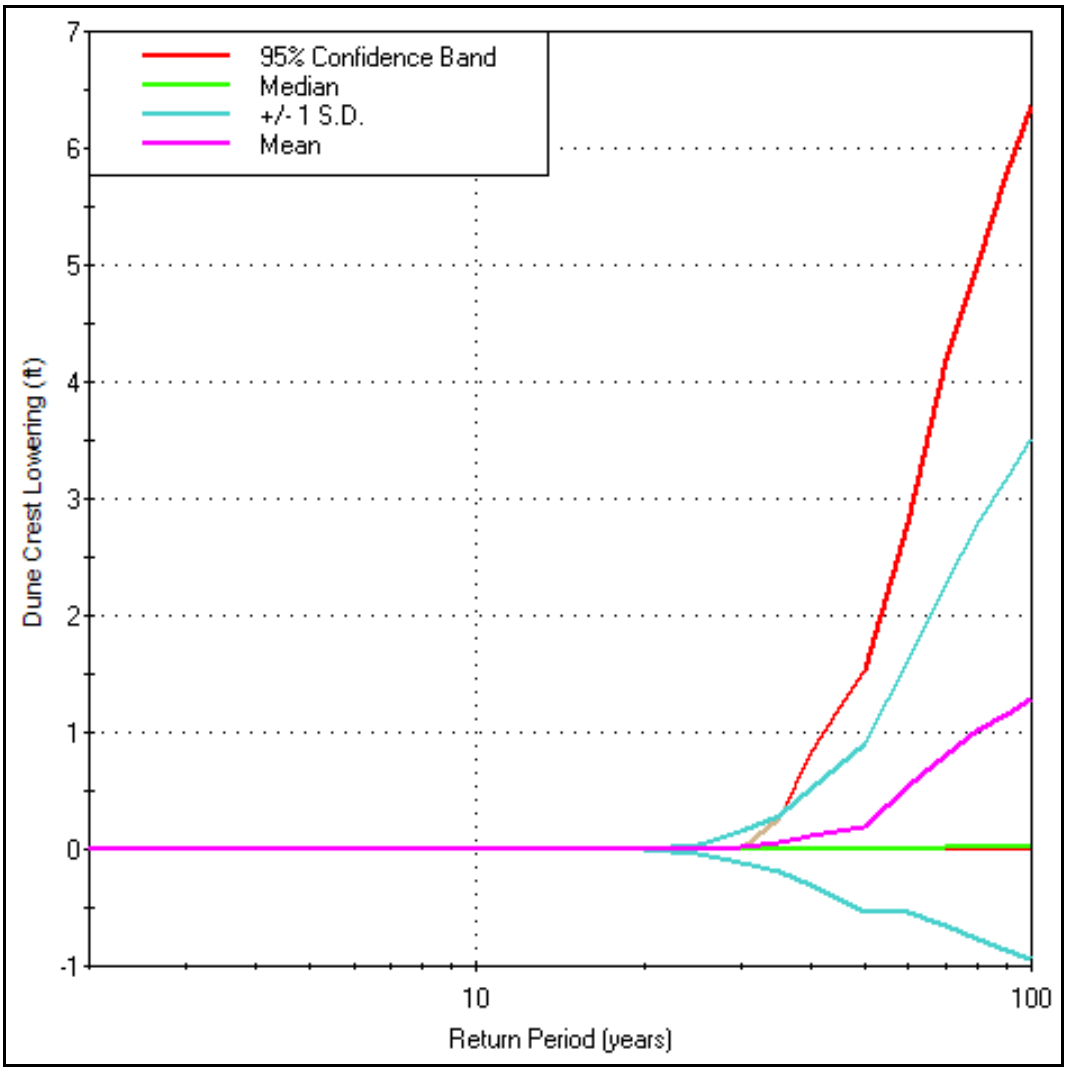

Figure 4-12. Return period for dune crest lowering.

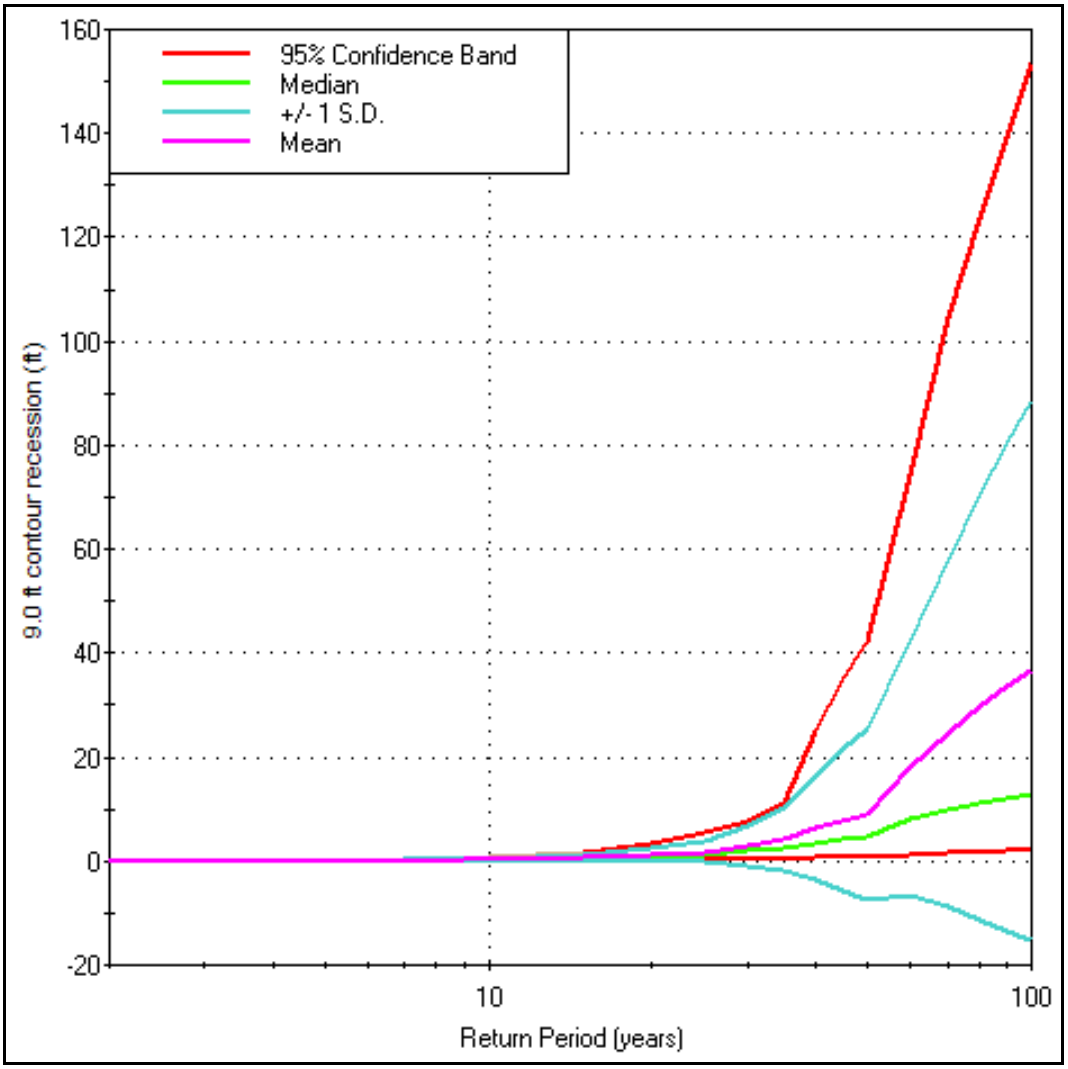

Figure 4-13. Return period for recession of the 9 ft contour.

Storm Surge

Figure 4-14 shows return periods for upland flooding in the absence of a dune. These elevations can be thought of as the mean water elevations at the height of a storm. Wave crest elevations would be on top of these elevations. Assuming that upland elevations at Wallops Island are of the order of +7 ft (MSL), in the absence of a sand dune, storms with return periods on the order of 15 years can be expected to produce flooding. Note that the rock seawall has a design height of +14 ft and can be expected to significantly reduce wave heights; however, it will do little to reduce flooding because of its porosity.

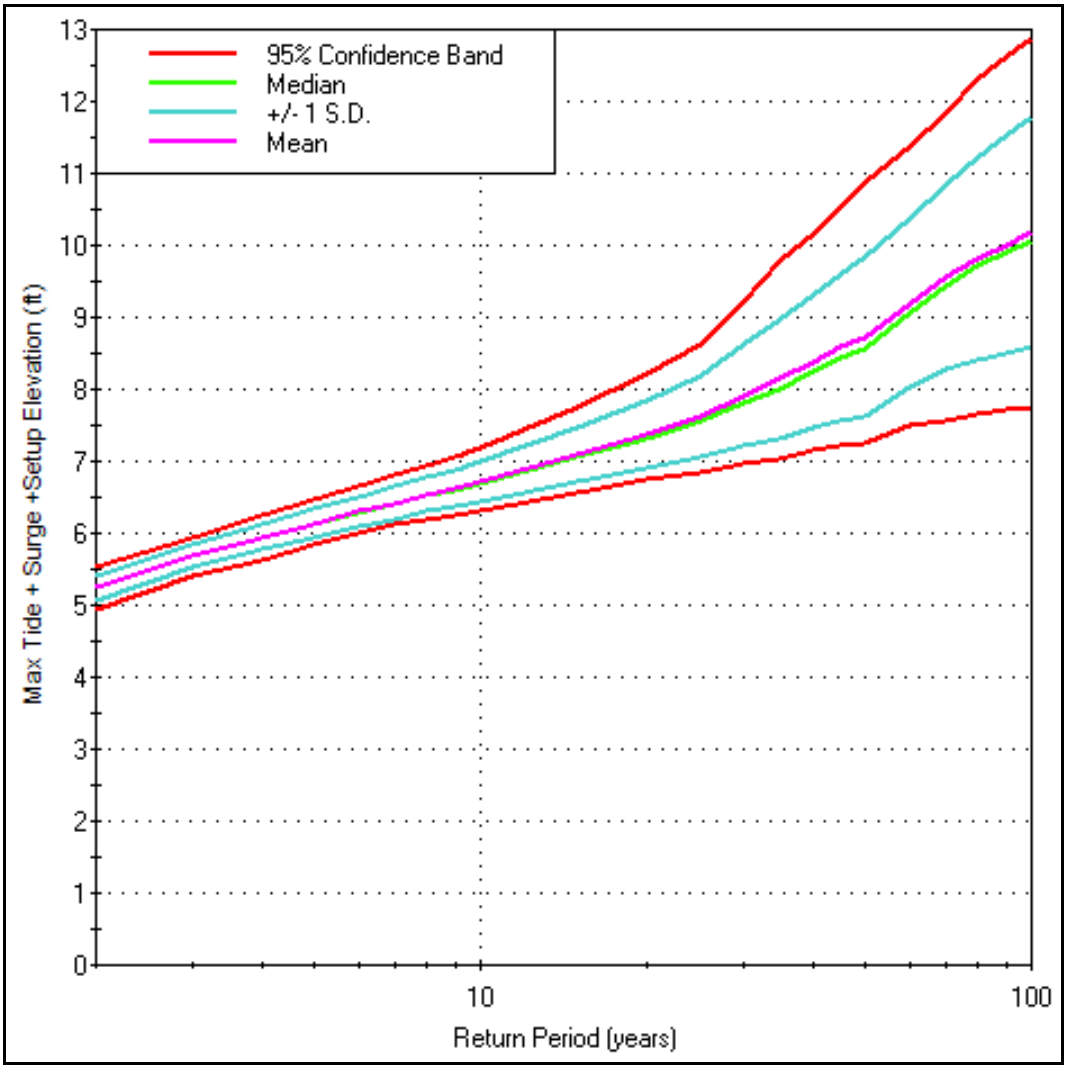

Figure 4-14. Storm surge return period.

Storm Damage Reduction Level of Protection

Following discussions with NASA personnel, a storm damage reduction project that provided significant defense against a design target of a 100-year return interval event was agreed upon. The project consists of three principal components. These include the beach fill project, the rock seawall, and flood barriers and/or other flood protection schemes for individual buildings on the island.

The beachfill project is intended to be the first line of defense. Based upon the analysis presented above, a fill project based upon the B070 profile and a 5-year renourishment interval will, by itself, provide damage

protection from a storm that, on average, is likely to occur only once every 30 years.

Though the dune and berm portion of the beach fill will be substantially degraded during a 100-year return interval storm event, the fill will remain largely in place and provide a shallow water surface for storm waves to break upon, thus reducing wave energy at the seawall. Provided that degraded portions of the rock seawall are repaired with a seaward slope of at least 1 on 1.5, the seawall will be able to withstand waves up to 7 ft in height (see Chapter 3). As a 7-ft wave will typically break in a depth of about 9 ft, the limited depth over the berm will cause waves of that height to first break seaward of the seawall. The seawall should therefore survive a 100 year storm event with minimal damage.

In the presence of a 100-year storm event, the largest incident waves will break offshore, smaller waves will break on the remaining portions of the beach fill, and most of the remaining wave energy will be dissipated at the rock seawall. Although wave runup will carry over the structure, waves generated by the runup will be minimal and the primary potential damage to infrastructure landward of the seawall will be from flooding rather than from direct wave impacts.

As shown by Figure 4-13, during a 100-year storm event, the mean water elevation at the seawall will be approximately +10 ft. Infrastructure is vulnerable to flooding from water coming through the seawall, from water flanking the ends of the project, and from flooding from the bay. Wave heights on the landward side of the seawall are expected to be on the order of a foot. All of the recently constructed facilities on Wallops Island have been designed to accommodate flooding elevations of +12 ft. As part of this project, NASA officials will continue to routinely monitor all structures on the island to make sure that each maintains its +12 ft flood protection strategy.

To protect existing and future proposed facilities on Wallops Island, the length of the project needs to extend from the northern end of the rock seawall (3767988.32 Easting, 1174124.21 Northing) to the south end of the geotextile tube at the south camera stand (3764244.61 Easting, 1169509.68 Northing), a distance of 19680 ft (5998 m).

5 STWAVE/GENESIS Setup and Model Calibration

STWAVE

The longshore sediment transport formula used in GENESIS requires wave height, period, and direction information at the seaward edge of the surf zone (the breaker line.) Wave data for this study were available in the form of WIS hindcasts several miles offshore in nominal 20 meters water depth. The numerical model, STWAVE, (STeady-state spectral WAVE model) was used to transform representative offshore waves to a near-breaking depth, where the shoaled wave data were handed off to GENESIS.

The STWAVE model described in this chapter was applied in conjunction with GENESIS to simulate the sediment transport and shoreline evolution along Wallops Island. STWAVE was also used to evaluate the wave refraction effects of mining offshore shoals to supply sediment for the beach fill. This application is discussed in Chapter 8. The STWAVE grid domain used in this chapter is named the Wallops Island domain. The two STWAVE grid domains used to examine the offshore borrow sites (Chapter 8) are termed the Fishing Point Coarse Grid and the Fishing Point Fine Grid domains.

Model Description

STWAVE is a computationally intense, half plane, steady state spectral wave model that requires a two-dimensional uniform rectilinear grid to transform waves from the offshore region to a near-breaking depth (Resio 1987, 1988a, 1988b; Smith 2001). It solves the complete radiative transfer equation (Jonsson 1990) that includes both propagation effects (refraction, shoaling, diffraction, and wave-current interactions) and source-term effects (wave breaking, wind inputs, and nonlinear wave-wave interactions). As input, the model requires some basic configuration data, a uniform rectilinear bathymetry grid, directional wave spectra at the seaward boundary of the grid, and optionally, wind and current data. Wind and current data were not used in this application.

Model Grid

The required bathymetry data were obtained from the National Ocean Survey (NOS) hydrographic surveys that are available in electronic format from the Geophysical Data System (GEODAS, version 4.0) developed by the National Geophysical Data Center. GEODAS is an interactive database management system for use in the assimilation, storage, and retrieval of geophysical data. Bathymetric surveys collected in the 1960's through the 1990's were used where available, with earlier survey data used to fill gaps in the more recent bathymetry coverage.

The STWAVE grid is shown in Figure 5-1. This figure is oriented so that land (bright green) is at the bottom and offshore is at the top. The elevation scale on the right-hand side of the figure is in meters. The shoreline is the white line running from A to B. C shows the location of Fishing Point and D is at Chincoteague Inlet. (The gap in the shoreline representing Chincoteague Inlet is not modeled.) The black grid running from E to F along Wallops Island shows the location of the GENESIS X-axis within the STWAVE grid. The STWAVE save stations are shown by the light blue line in shallow water offshore of the GENESIS grid. This grid was used to propagate waves from the nominal 20 meter depth to the save stations.

The grid runs for 10 miles (16 km) along shore from about the middle of Tom's Cove in the north (at A) to the middle of Assawoman Island in the south (at B) and runs 12 miles (19 km) offshore to approximately the 20 meter contour. Grid cells were 240 ft (73.152 m) on a side. The bathymetry offshore of Wallops Island varies from being nearly featureless immediately offshore to a complex set of shoals offshore of Fishing Point. These shoals are also shown in Figure 3-2. The STWAVE model domain was extended sufficiently far to the north to insure that these shoals were included in the analysis. Datums for this bathymetry are discussed in Appendix D. The necessary set of bathymetry grid parameters are listed in Appendix E.

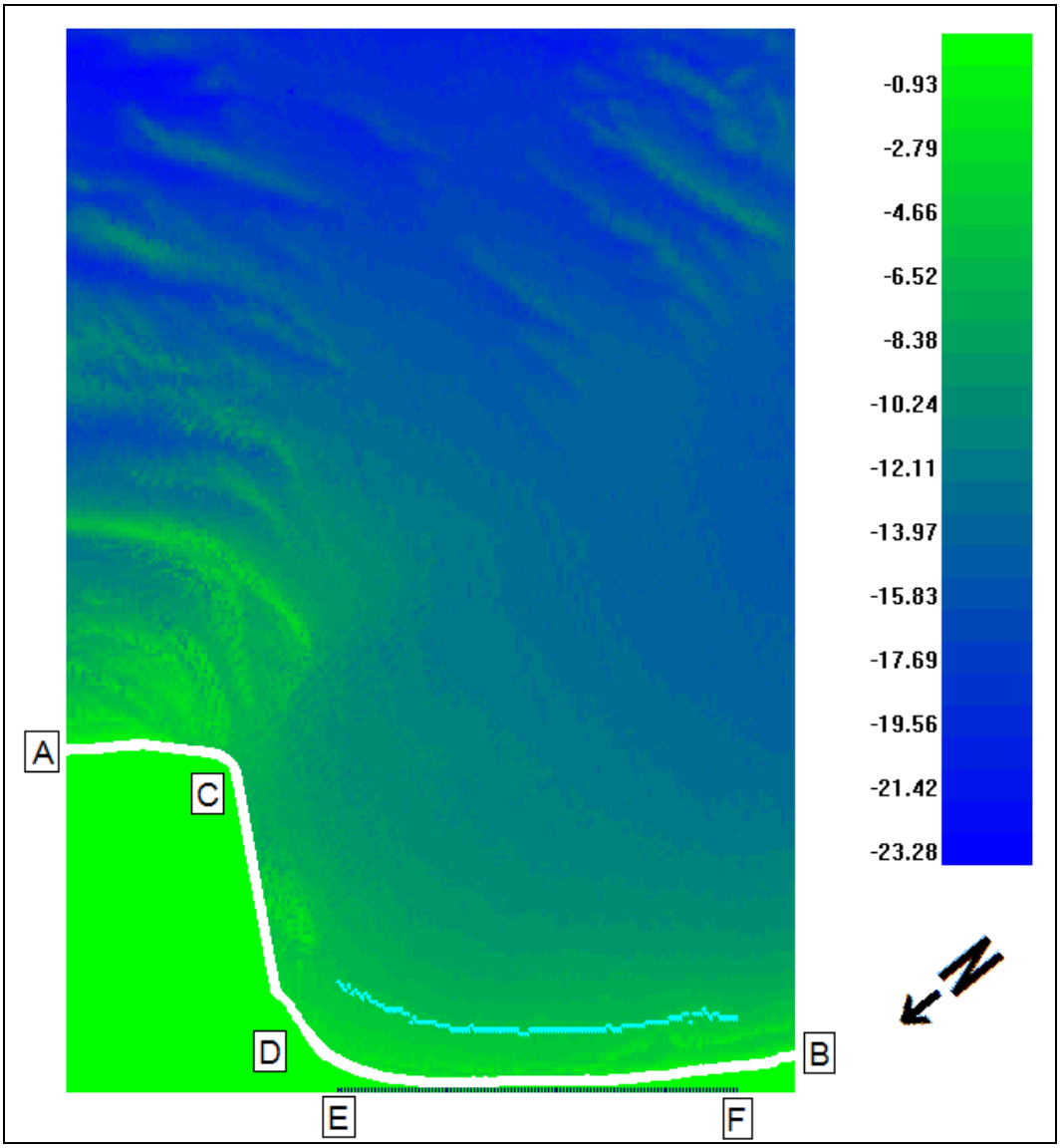

Figure 5-1. STWAVE grid for Wallops Island, VA.

Wave Climatology

Waves are the dominant driving mechanism in longshore sediment transport and are a primary environmental forcing input to STWAVE and GENESIS. A 20-year hourly hindcast (1980-1999) of wave heights, periods, and directions was obtained from <http://frf.usace.army.mil/cgi-bin/wis/atl/atl_main.html> for WIS station 178, located at 37.75° N, 75.25° W, in 20 meters of water depth near the offshore boundary of the STWAVE grid. Comparisons between the WIS hindcast data and measured wave data can be found at the above website and in Tracy (2002) and Tracy and Cialone (2004). Wave direction data from this WIS station were referenced to the local shore normal direction of 129 deg

azimuth as shown in Figure 5-2. Positive wave angles are those approaching the coast from the northeast (from the left for a person standing on the beach looking offshore).

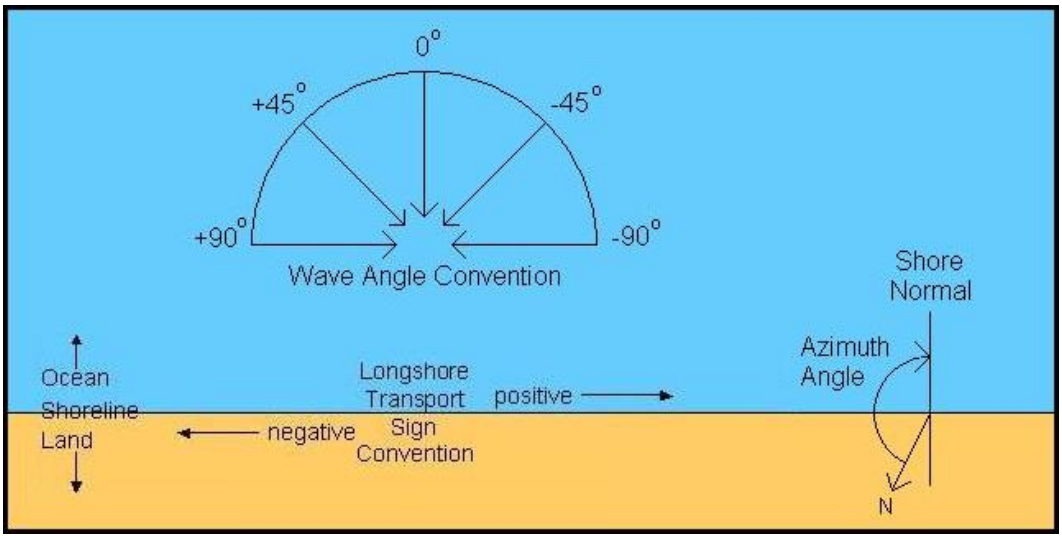

Figure 5-2. Angle and sign convention definition sketch.

Following a phase3 transformation to remove offshore directed wave energy, the 20-year WIS wave hindcast (175,320 hourly wave records) was characterized by binning the data into nine significant wave height bins, eight peak spectral wave period bins, and twelve vector mean wave directions at the peak spectral frequency bins, as shown in Figure 5-3. This figure is a histogram of WIS station 178 wave heights, periods, and directions shown as percent occurrence (the numbers above each bin). The numbers below the bins are the average bin values and the bin boundaries. Bright blue bins indicate those occurring most frequently and gray, least frequently. Figure 5-4 is the corresponding block diagram of wave height versus wave direction. These figures show that average wave heights are around 0.8 meter, average wave periods are 6-7 seconds and the predominant direction of wave approach is from the left of shore normal (from a northeasterly direction).

Of the 864 possible bin combinations (12 wave angles * 8 wave periods * 9 wave heights), the 20-year WIS hindcast populated 661 of the bins with at least an hour of data. STWAVE was run to transform the wave data in these 661 bin combinations from a 20 meter water depth to a near breaking depth. Model wave parameters are listed in Appendix E.

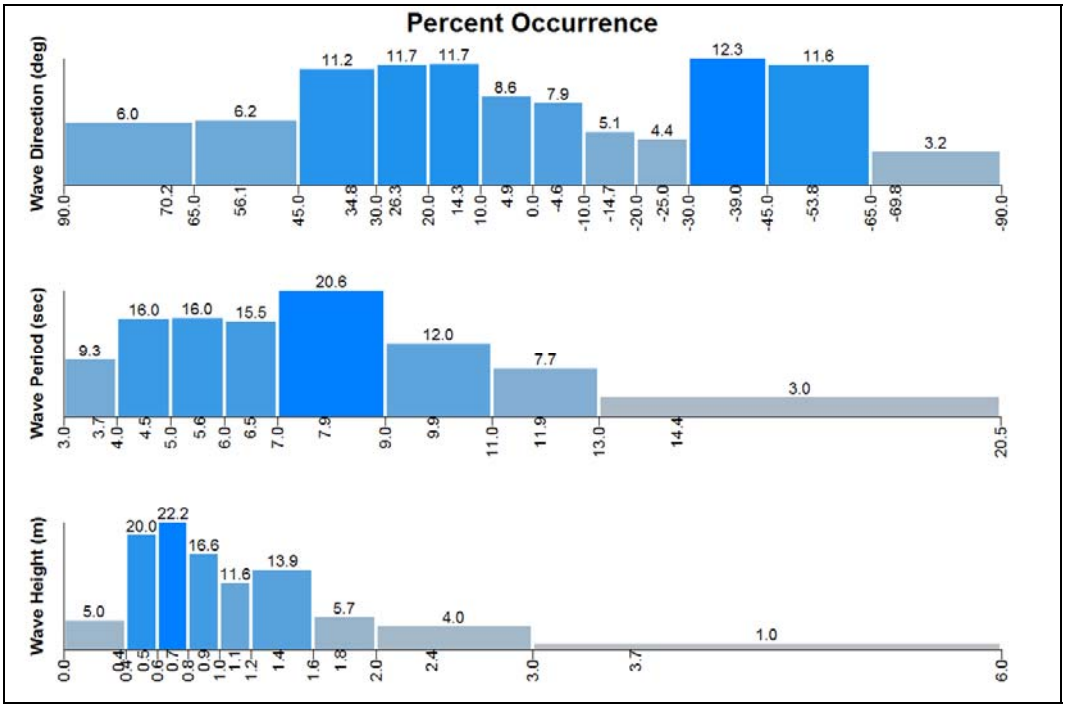

Figure 5-3. STWAVE Wave Height, Period, and Angle bins.

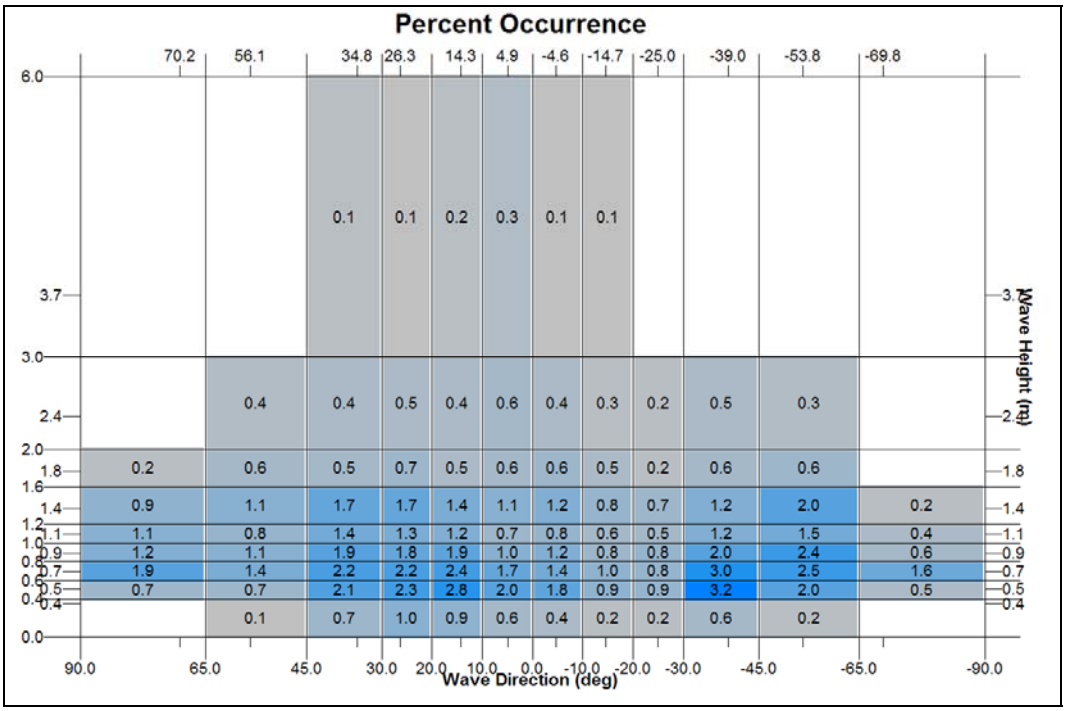

Figure 5-4. STWAVE block diagram of wave height vs. wave angle.

GENESIS

Model Description

GENESIS (GENEralized model for SImulating Shoreline change) is a shoreline change model that simulates longshore sand transport and the resulting change in shoreline position (Hanson 1987; Hanson and Kraus 1989; Gravens, Kraus, and Hanson 1991). One of the GENESIS assumptions is that when erosion or accretion occurs, the entire profile shifts landward or seaward, without changing profile shape, so that only one cross-shore point at each grid cell needs to be tracked. Thus, it belongs to a class of models known as one-line models, and the grid is one-dimensional, running the length of the shoreline in the study area. At each alongshore grid cell, the model applies the transformed wave data supplied by STWAVE to calculate breaking wave heights and angles, and applies this information to calculate the temporally and spatially varying local longshore sediment transport rate. Other inputs include configuration data, shoreline positions, and structure locations. GENESIS can predict shoreline change in a diverse variety of situations involving almost arbitrary numbers, locations, and combinations of groins, jetties, detached breakwaters, seawalls, and beach fills.

Model Grid

A GENESIS grid was laid out as shown in Figure 5-5. For ease of interpretation, Table 5-1 shows the location of several prominent shoreline features referenced to the GENESIS grid. The grid origin is located at 3768396.5200 Easting, 1174969.9500 Northing (in STWAVE cell (264, 83)), which is 3120 feet (951 meters) north of the north end of the rock seawall (and in the front yard of building V50). This location is south of the main shoals of Chincoteague Inlet, though not completely away from the inlet's influence. It is on the accreting part of the beach, to the north of any expected project beach fill or sand retention structure. The grid runs southward along an azimuth of 219° for 29,040 feet (8851.392 meters), ending about a mile (1.6 km) south of Assawoman inlet. This location is south of the expected project construction and far enough south to model project impacts along the north end of Assawoman Island. The grid contains 121 cells, each 240 feet (73.152 m) long; the same cell length as the STWAVE grid. A complete list of grid parameters is given in Appendix E.

Figure 5-5. Layout of GENESIS grid.

Figure 5-6 covers the extent of the grid, and shows the land (green) / water (blue) boundary along with the rock seawall and geotextile tube indicated as hard features (yellow line).

To model the behavior of the detached breakwater, a second finer resolution grid, was set up. Each of the cells in the original grid was divided into four cells, so the fine resolution grid had a total of 484 cells, each 60 ft (18.288 m) long. The smaller cell width necessitated the use of a shorter model time step, so for this grid, a 15 minute, rather than a 1 hour time step was used. The grid origin and orientation remained the same as for the regular grid. These parameters are listed in Appendix E.

Table 5-1. Infrastructure Location along GENESIS baseline

		Approximate location on GENESIS baseline		
Feature	**Building #**	**Cell Wall #**	**feet**	**meters**
GENESIS Grid origin; NASA Dynamic Balance Facility, Center Bldg	V50	1	0	0
NASA Dynamic Balance Facility, South Bldg	V045	3	480	146
Unpaved road access to beach		6	1200	366
North end of Seawall; North end of beach fill project		14	3120	951
Navy Surface Combat Systems Center, SSD Facility	V024	17	3840	1170
Navy Aegis Engineering and Training Complex	V021	31	7200	2195
Water Tower	W055	36	8400	2560
Navy Surface Combat Systems Center WIETC Facility	V003	37	8640	2633
Raised Viewing Stand	W036	39	9120	2780
Blockhouse 3	W020	42	9840	2999
Vehicle Assembly North Building	W065	46	10800	3292
Raised Viewing Stand	W115	49	11520	3511
Tower	X080	50	11760	3584
Flagpole at seaward end of Causeway		56	13200	4023
Camera Stand	X065	57	13440	4097
MRL Launcher Facility	Y039	64	15120	4609
Blockhouse 2	Y030	65	15360	4682
Arc Launcher Facility	Y035B	66	15600	4755
Red and white Tower	Y085	67	15840	4828
Vehicle Assembly South Bldg	Y015	68	16080	4901
Blockhouse	Z065	70	16560	5047
50K Launcher Facility	Z071	72	17040	5194
Prior site of Launch Pad 0A		74	17520	5340
Camera Stand, South End of Rock Seawall	Z040	76	18000	5486
Pad 0B, MARS launch facility		80	18960	5779
UAV Runway		89	21120	6437
South Camera Stand; South End of beach fill project		95	22560	6876
Approx middle of Assawoman Inlet (closed)		100	23760	7242
South end of future possible NASA development on Assawoman Island		104	24720	7535
South end of GENESIS Grid		122	29040	8851

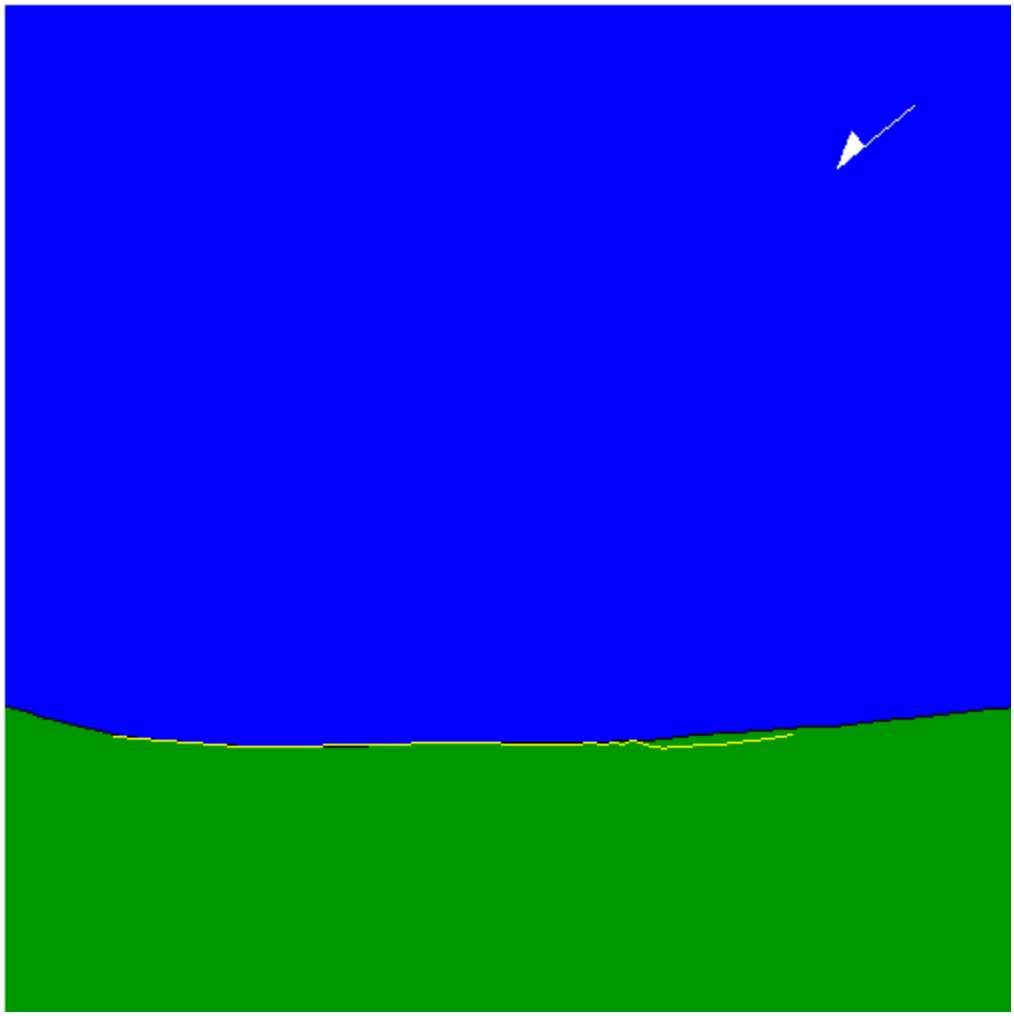

Figure 5-6. GENESIS grid showing Rock Seawall and Geotextile Tube. The 1996 and 2005 shorelines touch most of the seawall but not the geotextile tube.

GENESIS Calibration

Calibration of the GENESIS model consisted of initiating the model with a measured shoreline, and during a run having it evolve the shoreline to approximate a second measured shoreline which was collected at a later date. The 1996 and 2005 measured shorelines were selected for calibration. The results of this calibration are shown graphically in Figure5-7. Note that there is about a 10:1 distortion in offshore to alongshore distance scales which exaggerates the differences in the model comparison, but allows it to be seen. Figure 5-8 shows the difference in the 2005 measured and the final model shoreline (measured minus modeled) and the average yearly difference. The model reproduced the change rate in the 1996 to 2005 shorelines to an accuracy of better than three ft (1 meter) per year at all locations.

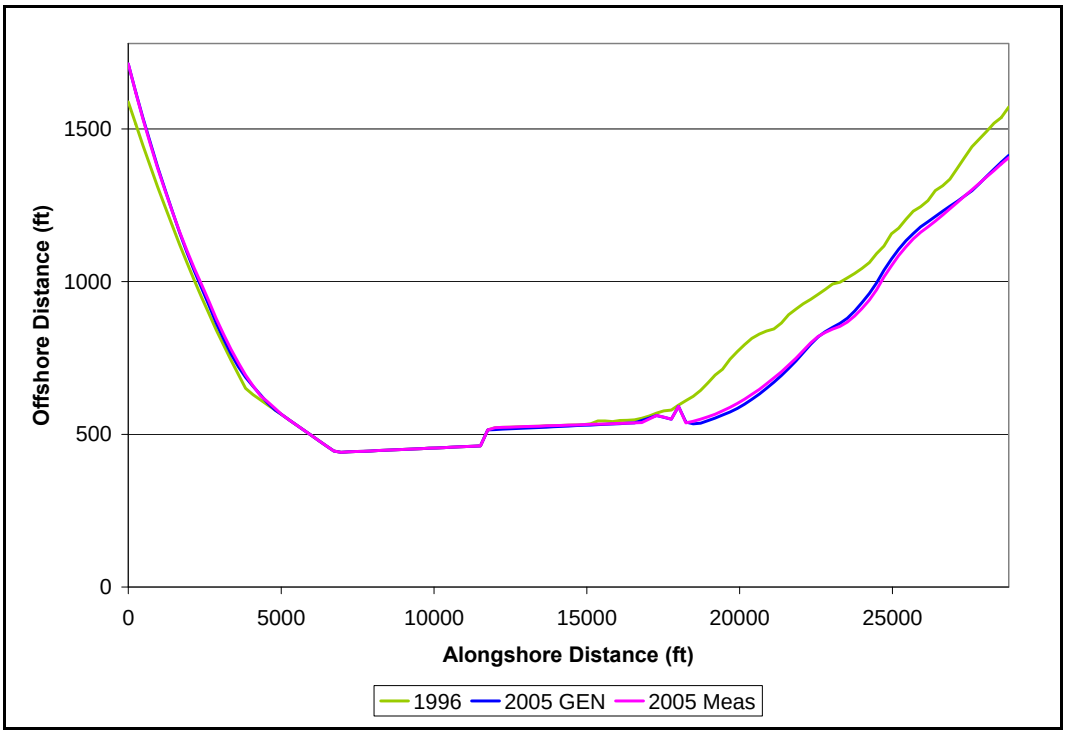

Figure 5-7. GENESIS calibration showing Initial (1996), Final (2005 GENESIS), and Measured (2005) shorelines.

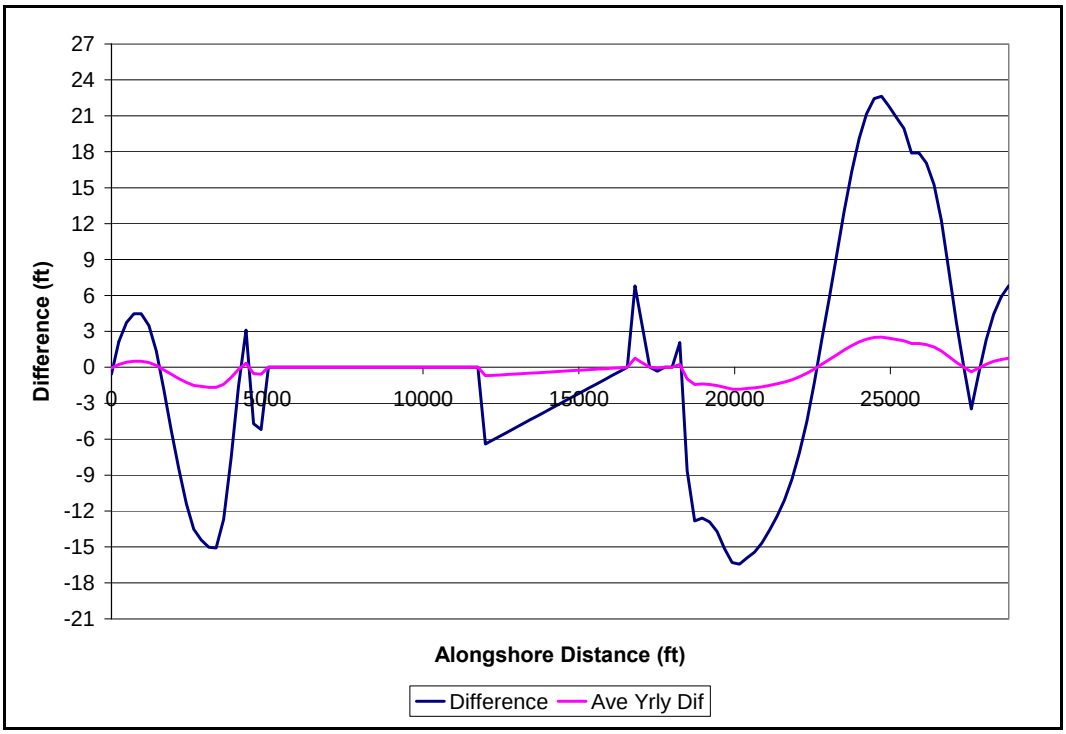

Figure 5-8. Difference in 2005 Measured and GENESIS modeled shoreline.

During calibration, various values for the K1 and K2 constants were tried, however, the default values were found to give satisfactory results and were adopted. Lateral boundary conditions were based upon shoreline change rates obtained from the 1996 and 2005 profiles. For calibration and most model runs, the waves used to drive the model were a 5-year set of average wave conditions. These are described further in the sensitivity section below. The use of a regional contour was found to improve the comparison between the final model and final measured shorelines. Figure 5-9 shows the 5 meter contour obtained from the bathymetry, the 5 meter contour obtained from the beach profiles, the 2005 shoreline (shifted 700 meters seaward) along with the Regional Contour which was applied (shown in blue). This contour was obtained by iteration. It is similar to the other contours shown in Figure 5-9, but is smoother and more flattened on the ends. A complete set of model configuration parameters are given in Appendix E.

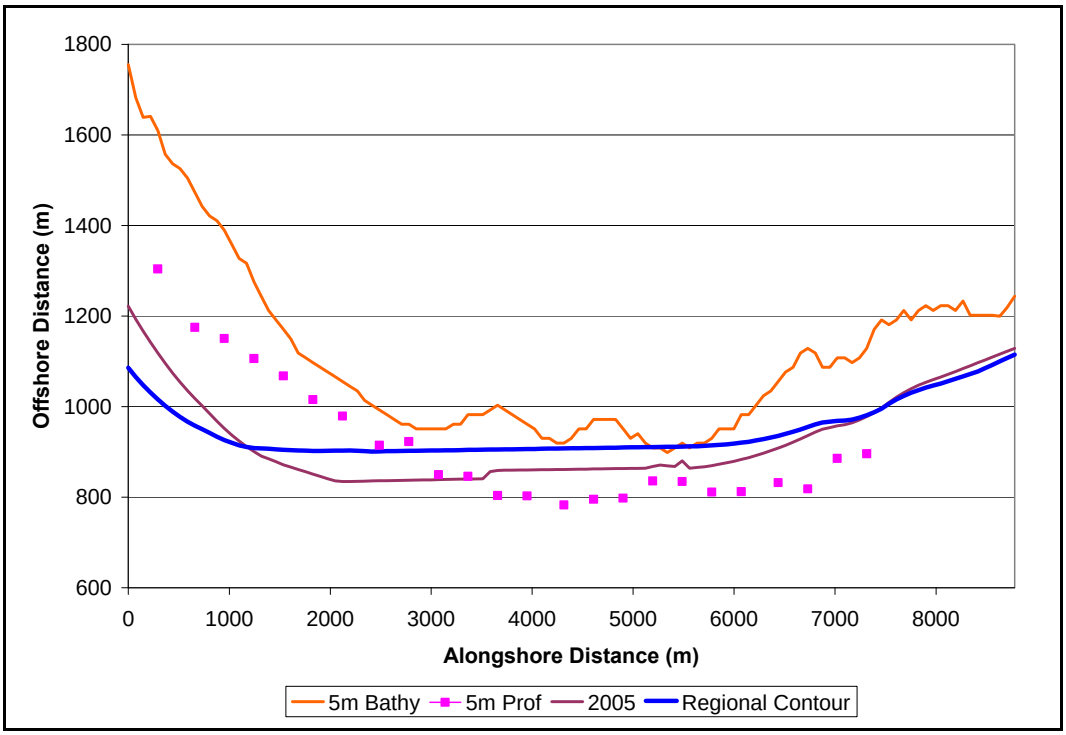

Figure 5-9. Wallops Island Regional Contour. (5:1 vertical to horizontal distortion)

Sensitivity

The 20 years of WIS data for station Atl-178 were analyzed on a year-by-year basis to determine simple sediment transport rates using the method described in Gravens, 1989. Wave data were assembled in 5 year blocks

using the following criteria: Ave - the 5 years whose net sediment transport rates were nearest to the 20 year average net rate. Max - the five years with the maximum gross transport rates. Min - the five years with the minimum gross sediment transport rate, N - the 5 years with the maximum net amounts of northerly transport, and S - the five years with the maximum net amounts of southerly transport. The years selected for each 5-year block are shown in Table 5-2.

These five different wave data blocks were used to drive the GENESIS model. The calibration results presented above (along with much of the modeling discussed below and in the next chapter) were produced using the Ave wave block. GENESIS results using the other four wave blocks, along with the measured 2005 shoreline are shown below in Figure 5-10.

There are not large differences using these different driving conditions. The largest is for the Southward wave set showing additional erosion just south of the seawall. This would not be unexpected. It is noted that the 2005 measured shoreline falls within the envelope of these four modeled shorelines.

Table 5-2.

Year	Ave	Max	Min	N	S
1980					
1981	X				
1982					
1983		X			X*
1984					
1985	X		X		
1986			X		
1987	X		X*		
1988			X*	X*	
1989				X	
1990			X	X*	
1991					X
1992		X*			X*
1993	X				
1994					X
1995	X	X			
1996		X*		X	
1997				X	
1998					
1999		X			X

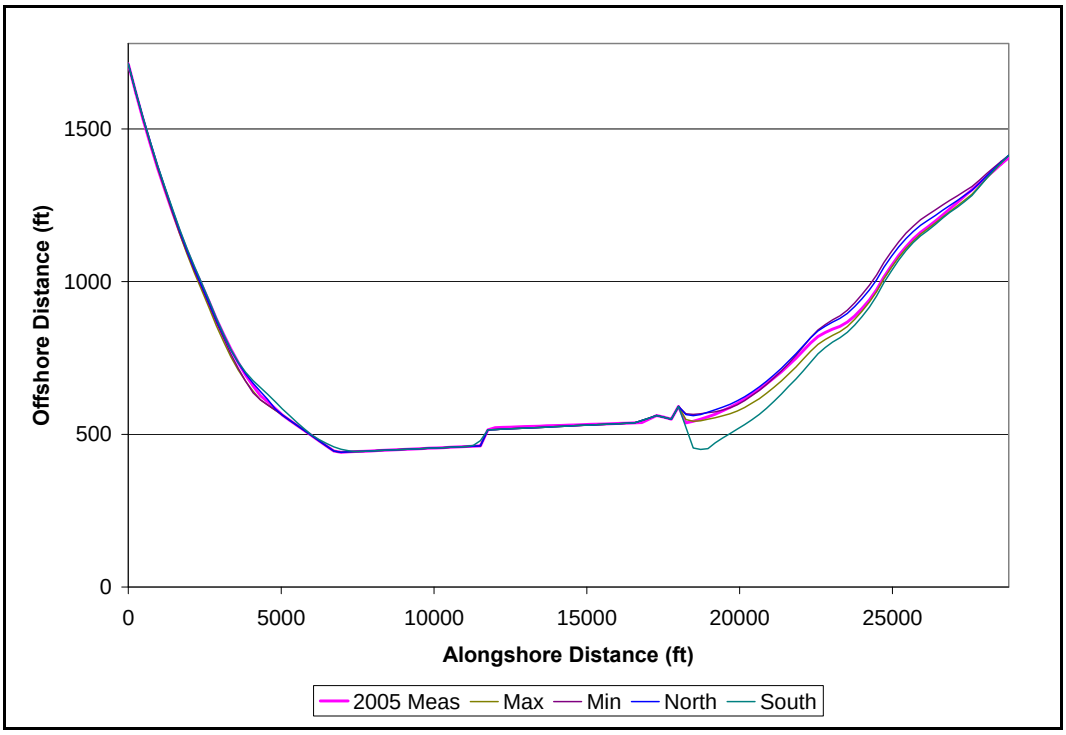

Figure 5-10. Comparison of the 2005 measured shoreline with GENESIS shorelines driven with the Max, Min, North, and South wave blocks.

Verification

Once the GENESIS model was calibrated, it was verified by running the model using a second set of measured profiles. Since the 2007 shoreline was the only other available recent shoreline, for verification, the 2005 shoreline was used as the initial shoreline and the 2007 shoreline was used as the final target shoreline were used for verification. The 2007 shoreline does not extend over the complete GENESIS grid, so the comparison, shown in Figure 5-11 is truncated at both ends. The 2007 measured shoreline (pink) does not agree as well with the 2007 GENESIS verification shoreline (blue) as in the calibration (Figure 5-7). However, the 2007 measured shoreline does fall almost completely within the envelope of the Max, Min, North, and South shorelines that were run using the 2005 shoreline as the initial shoreline. Since these runs were only two years long, two year wave blocks containing the maximum value years were used to drive the model. The years used are shown by asterisks in Table 5-2.

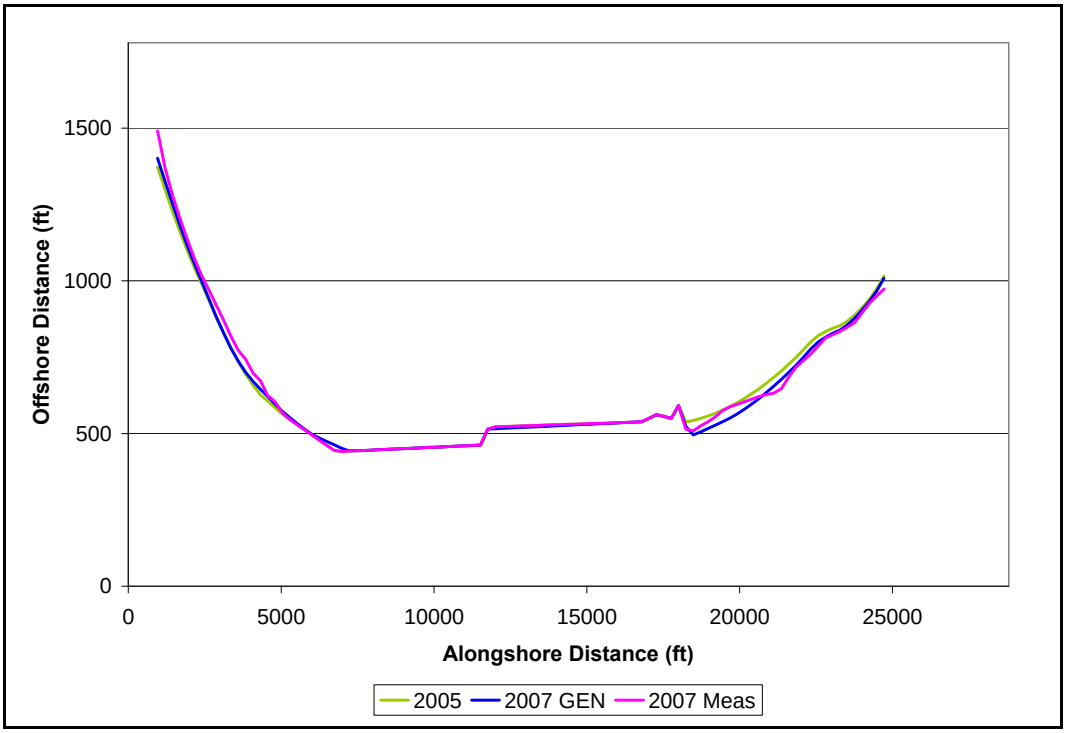

Figure 5-11. Comparison of Initial (2005), Final (GENESIS modeled) and Meas (2007) Shorelines, showing only the portion of the shoreline where there is 2007 data.

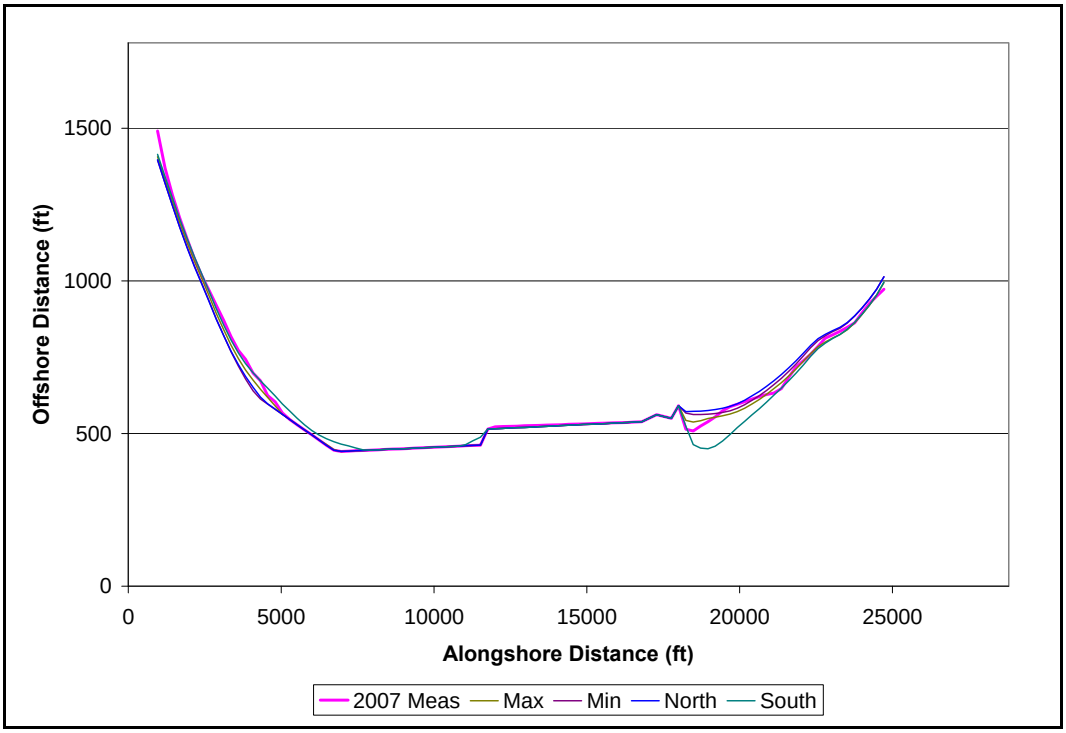

Figure 5-12. Comparison of the 2007 measured shoreline with GENESIS shorelines driven with the Max, Min, North, and South wave blocks.

STWAVE Results

The presence of Fishing Point greatly affects the wave patterns seen on the shore at Wallops Island. Wave energy coming from the northeast is largely blocked by Fishing Point, whereas wave energy coming from the southeast arrives at the beach with little change (see Figures 1-2, 5-1, e.g.). An example of this is shown in the STWAVE output given in Figure 5-13. This figure shows the near breaking wave heights that occur along the beach at Wallops Island for a 4 second, unit height offshore wave that approached the coast from a variety of angles. Positive angles are those coming from left of shore normal (the northeast); negative angles are those coming from the southeast (see Figure 5-2). Waves coming from the southeast have roughly the same height everywhere along the shoreline, but waves coming from the northeast have dramatically decreasing height (and thus energy) the further north they are along the shoreline. This means that they have less ability to transport sand to the south. This wave sheltering from Fishing Point and the offshore shoals is the primary reason that there is a transport reversal on Wallops Island.

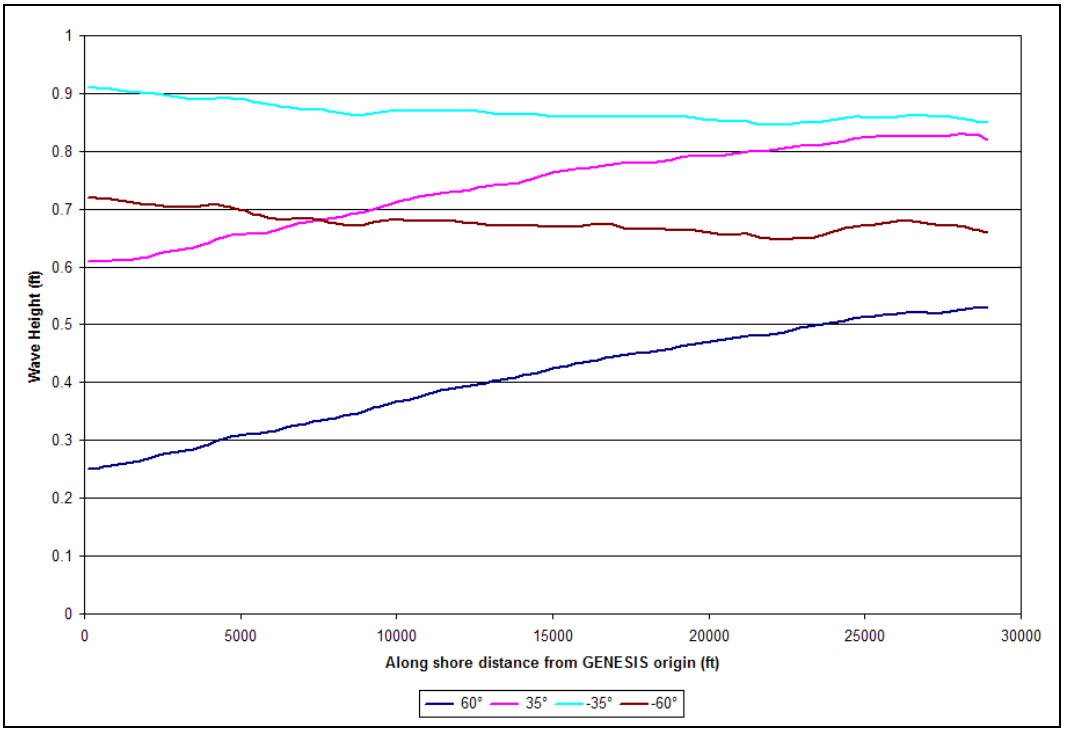

Figure 5-13. Example of nearshore wave heights along the beach at Wallops Island.

The point is further illustrated in Figure 5-14. This figure shows wave heights everywhere within the STWAVE grid for one of the four cases shown in Figure 5-13, the case for a unit high, 4 second, wave having an deep water (pre-refracted) angle of +60°. The offshore direction of this wave is shown by the black insert arrow at the top of the figure. Colors on the figure and scale are referenced to an offshore wave height of 1 unit. The lines on the figure are lines of constant wave height. Seaward of the shoals in the vicinity of Fishing Point, there is little change in wave height. However, near shore along Wallops Island there is a strong gradient in the wave height, with the height decreasing to the north.

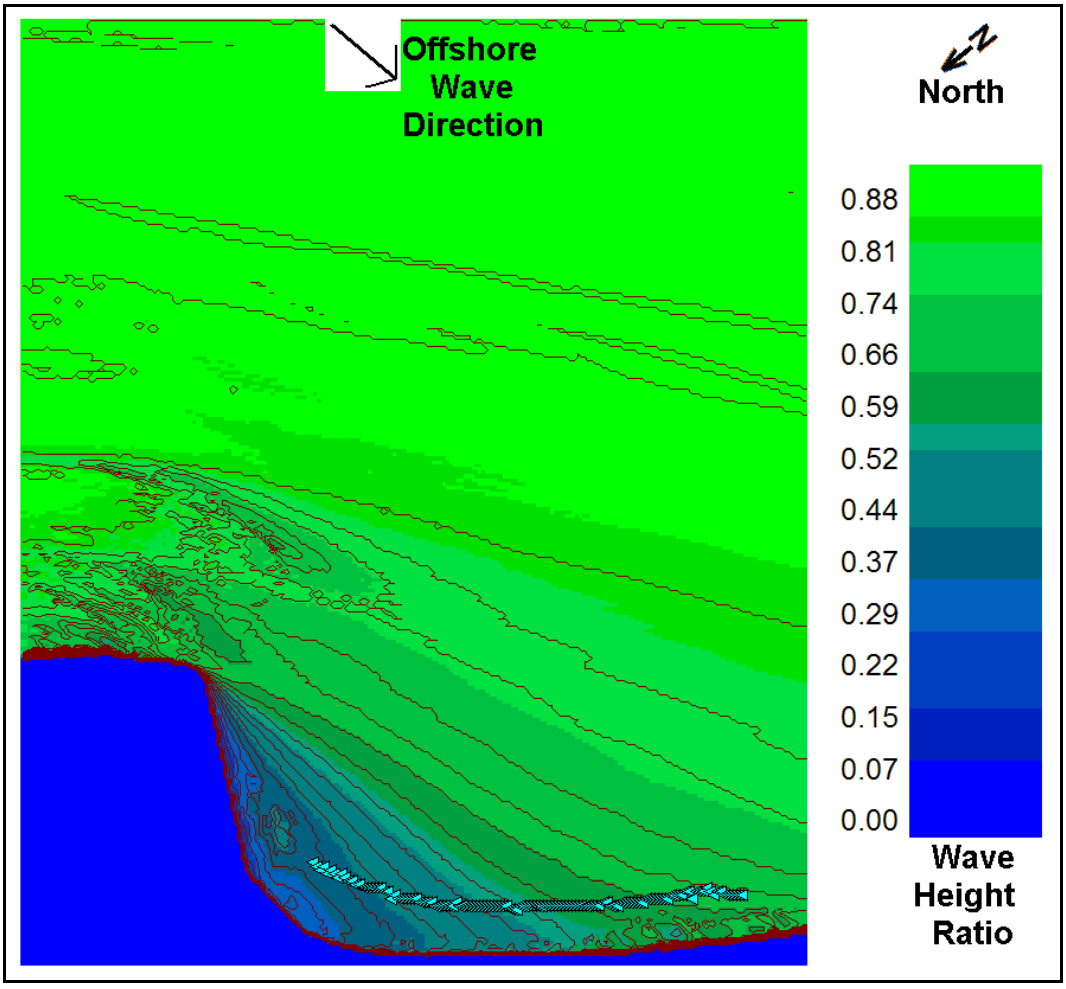

Figure 5-14. Example of wave heights throughout the STWAVE grid.

GENESIS Results -Wallops Island Sediment Budget

Longshore sediment transport rates vary from year to year primarily because of yearly variations in the input wave field. To determine the average transport rate along Wallops Island, the 20-year WIS wave data set was broken into 20 different four-year blocks (1980-1983, 1981-1984, etc.). GENESIS was run using each of these blocks and the model estimated net transport rates during the 4th year were averaged. This average net transport rate is shown in Figure 5-15. The sign convention assigns transport to the right (South) as positive and to the left (North) as negative. This figure indicates that for average transport conditions there is a divergent nodal point on the north end of Assawoman Island, with net southward transport to the south of that point and net northward transport to the north. The 95% confidence limits indicate that for most years the varying wave conditions shift the divergent point along the shoreline within about a 7000 ft window (a mile and a half).

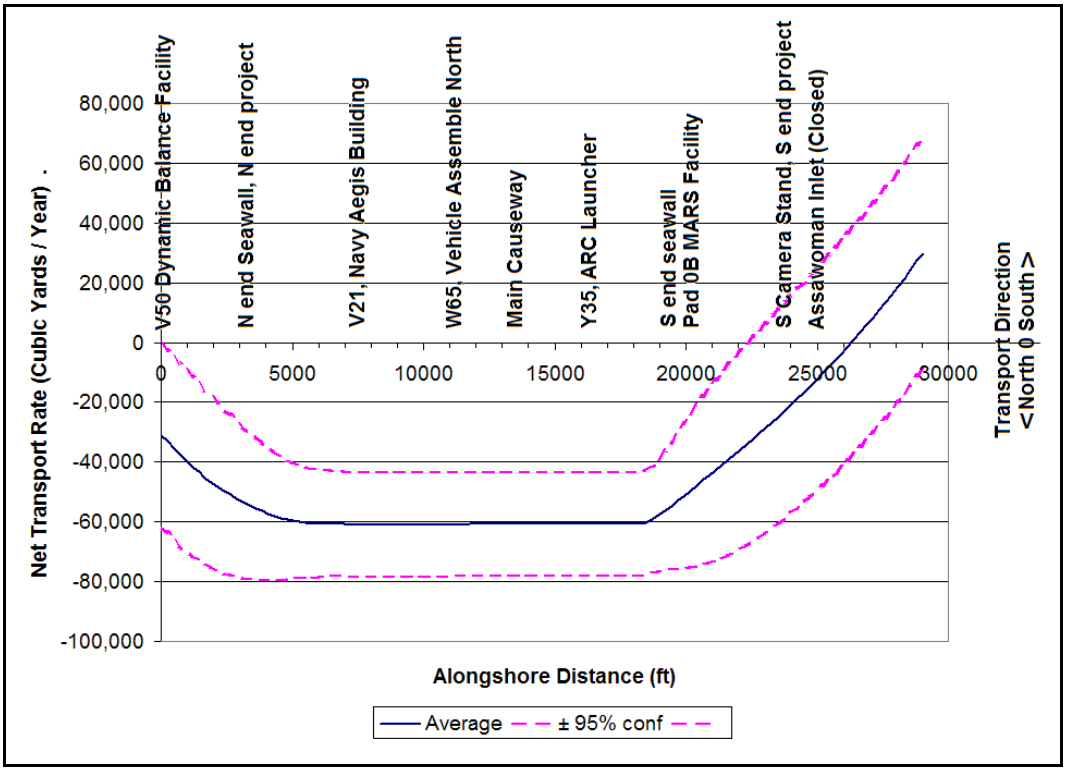

Figure 5-15. Wallops Island Sediment Budget

The GENESIS results presented in Figure 5-15 were used to produce the more typical schematic sediment budget representation shown in Figure

5-16. In this figure, the numbers 20, 40, and 60 represent thousands of cubic yards of transport per year, as per Figure 5-15.

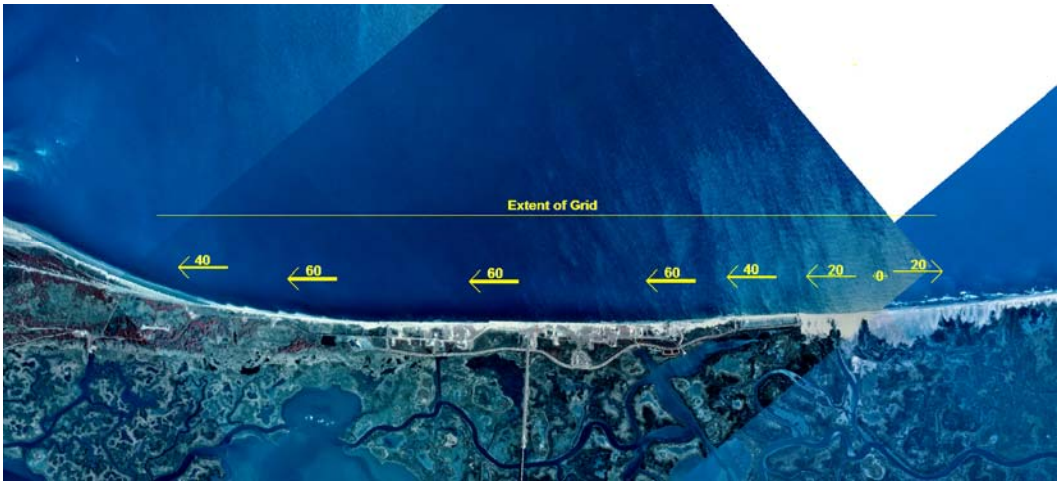

Figure 5-16. Wallops Island Sediment Budget. Numbers are the average net transport rate in thousands of cubic yards per year.

Figure 5-17, shows an example of distinct northward transport within the groin field along Wallops Island. It was taken in 1994 and shows several relatively un-deteriorated groins along the north end of Wallops Island. This is in an area of shoreline accretion.

These results show moderate agreement with the Moffat & Nichol 1986 (M&N 1986) sediment budget, which is discussed in Morang, Williams and Swean (2006). This earlier budget also shows the north end of Wallops Island as accreting and the south end as eroding. In addition, net transport rates are of comparable magnitude. The main difference is that the M&N 1986 budget shows a divergent nodal zone which is north of the causeway, and in addition, a convergent nodal zone near the north end of the seawall. The differences in the budgets can be attributed to the different methodologies used to develop them and to the different time periods on which they are based. Because of the continuing growth of Fishing Point (Figures 2-19 and 2-20) along with the southwestward migration of the offshore shoals (Wikel, 2008) it is to be expected that the divergent nodal zone along Wallops Island should be shifting to the south.

Figure 5-18 shows the average gross transport rate along Wallops Island. This figure shows gross rates of the order of 400,000 yd^3/yr south of the seawall, rates of the order of 100,000 yd^3/yr in front of the seawall, and rates on the order of 350,000 yd^3/yr north of the seawall.

Figure 5-17. Groins field on Wallops Island showing transport direction to the north. Photo taken 20 March 1994.

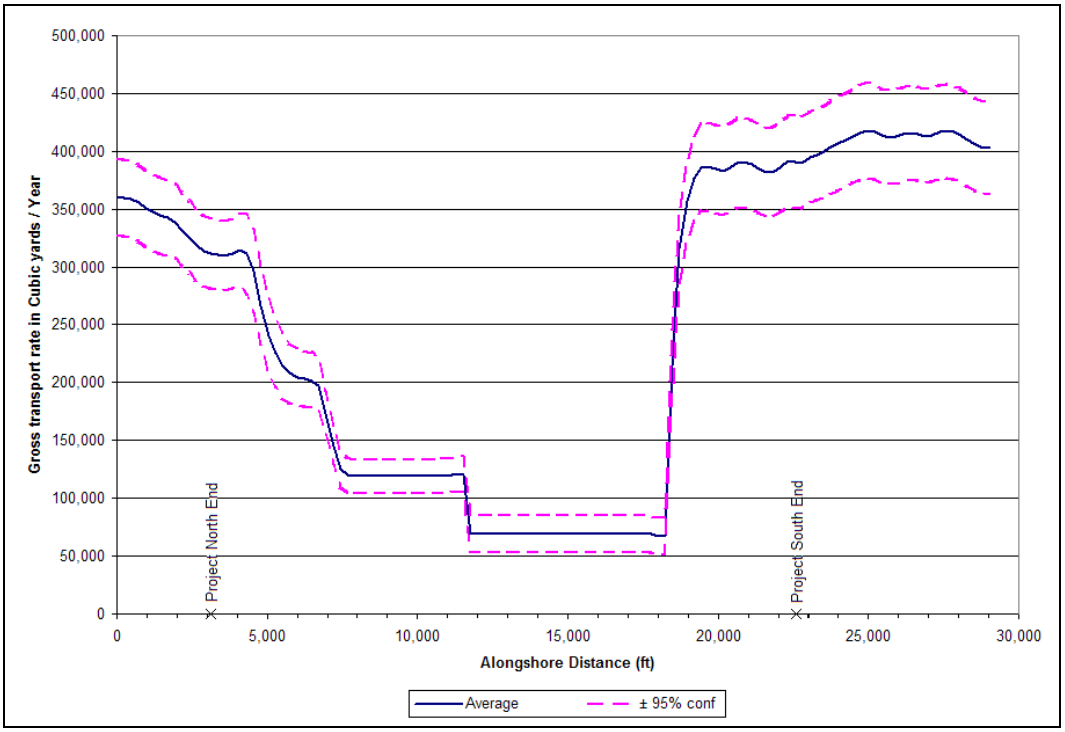

Figure 5-18. Average yearly gross transport rates along Wallops Island.

6 Beach Fill Design Alternatives

The appropriate amount of beach fill is the anticipated minimum amount (the minimum target fill) needed to provide defense from storm damage plus an additional sacrificial amount (the advanced fill) that is expected to be removed by longshore transport between renourishment events. This approach, described in the Coastal Engineering Manual (CEM, Part 5, Chapter 4; Gravens, et al., 2006), strives to ensure that the minimum amount of fill remaining at the project site just before renourishment is still adequate to provide storm damage protection. The volume needed for the minimum target fill is based upon the profile developed in Chapter 4 through SBEACH modeling. The amount of advanced fill is determined by GENESIS modeling of different project designs (alternatives). The derivation of both these volumes is discussed below.

Minimum Target Fill for Storm Damage Protection

The Minimum Target Fill volume was derived by summing several component volumes: the volume needed to bring the shoreline to an equilibrium condition (the Seawall Deficit volume), plus the volume needed to advance the shoreline seaward to achieve the B070 profile described in Chapter 4 (the Berm volume), plus the Dune volume for the B070 profile.

Characterization of the Seawall Deficit Volume

The Rock Seawall has halted the shoreline retreat along its length. However, as is typical, this has come at the cost of removing material below the waterline (steepening the profile) in front of the seawall. Profiles at both ends of the study area do not show this sub-aqueous sediment deficit. Figures 6-1 through 6-3 compare an equilibrium profile (shown in red) that is based upon the native beach grain size (D_{50} = 0.20 mm) to profiles at three locations. Figure 6-1 shows the profile at GENESIS cell 17, which is near the north end of the project site 3840 feet (1170 m) south of the GENESIS origin. The beach in front of the seawall at this location is accreting and is in a healthy condition. Figure 6-2 shows the profile at GENESIS Cell 50, near the center of seawall at a distance 11760 ft (3580 meters) south of the GENESIS origin. This location is 1200 ft (366 m) south of Building W-65. The profile here shows the greatest

sediment deficit. Figure 6-3 shows the profile for GENESIS Cell 87, which is at the south end of the study area near the middle of the geotextile tube and 20640 ft (6290 meters) south of the GENESIS origin. The shoreline here is retreating but there is a sub-aerial beach and the position of the shoreline is not constrained by the geotextile tube. Figures 6-1 and 6-3 show that the native beach equilibrium profile is a reasonable approximation of the profiles north and south of the seawall and that these profiles have no substantial deficit of material. However, there is a substantial deficit of material on the Figure 6-2 profile, as, to a lesser extent, there is along most of the rock seawall.

Figure 6-4 shows these deficits in plan view for all the profile lines. Calculations for these deficits are based upon a D_{50} = 0.29 mm equilibrium profile, the median diameter of the borrow site material. In Figure 6-4, surplus (positive values for profile elevation minus 0.29mm equilibrium profile elevation) are shown in green and deficits (negative values) in red. The scale across the bottom of the figure shows the amount of the differences. The profile lines in this plan view run between the shoreline and the depth of closure. The black line in this figure shows the location of the rock seawall.

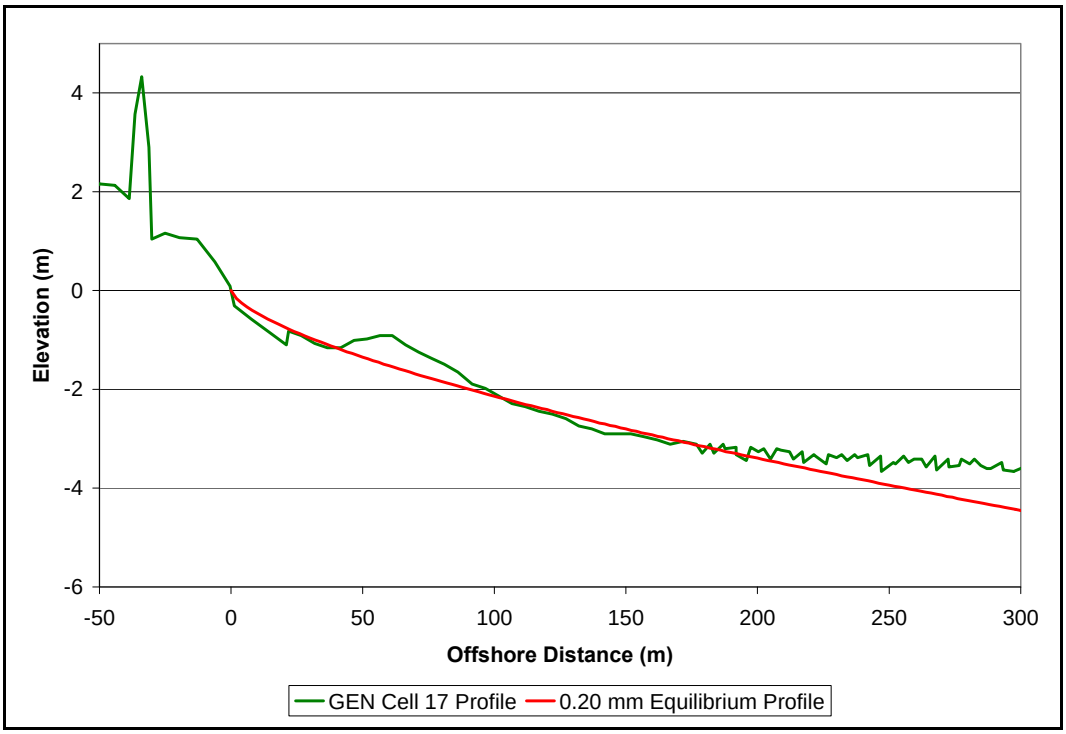

Figure 6-1. Comparison of healthy profile at north end of seawall with 0.20 mm Equilibrium profile.

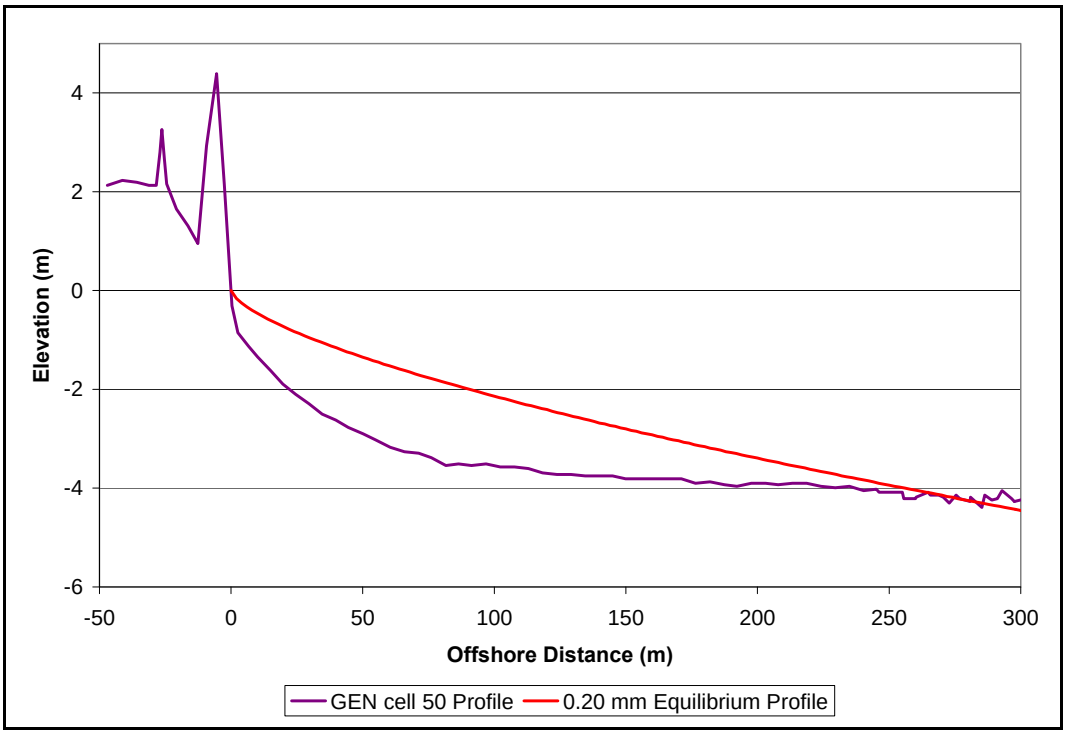

Figure 6-2. Comparison of eroded middle of seawall beach profile with the 0.20 mm Equilibrium profile.

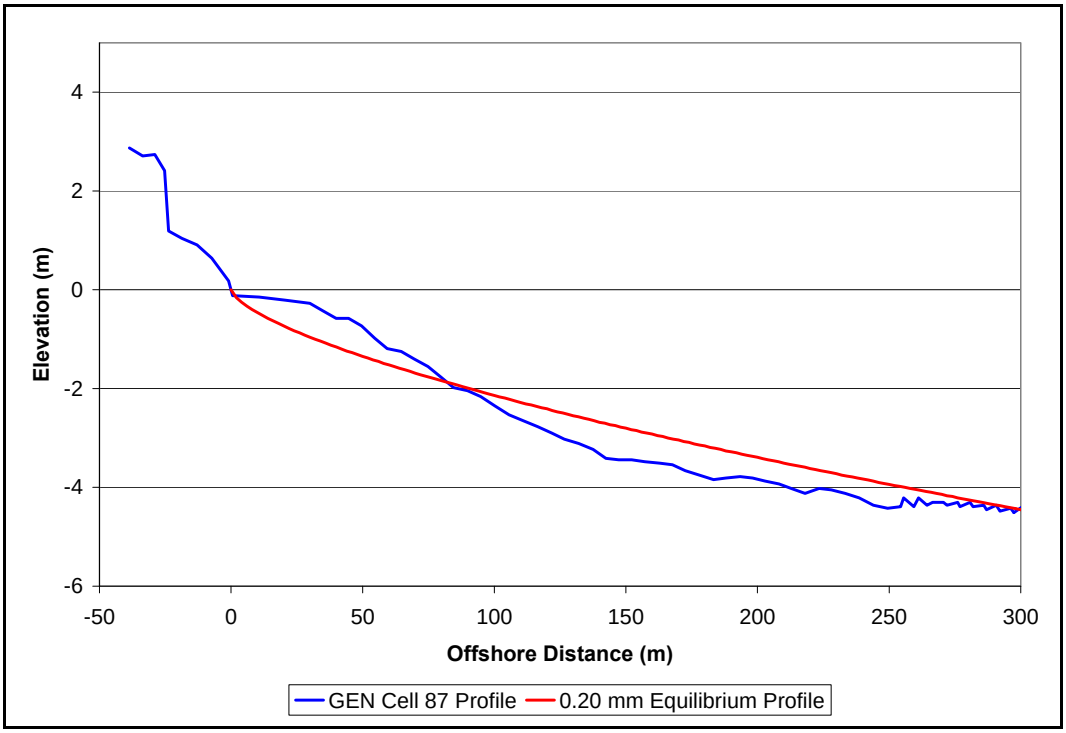

Figure 6-3. Comparison of healthy GENESIS Cell 87 profile with the 0.20 mm Equilibrium profile.

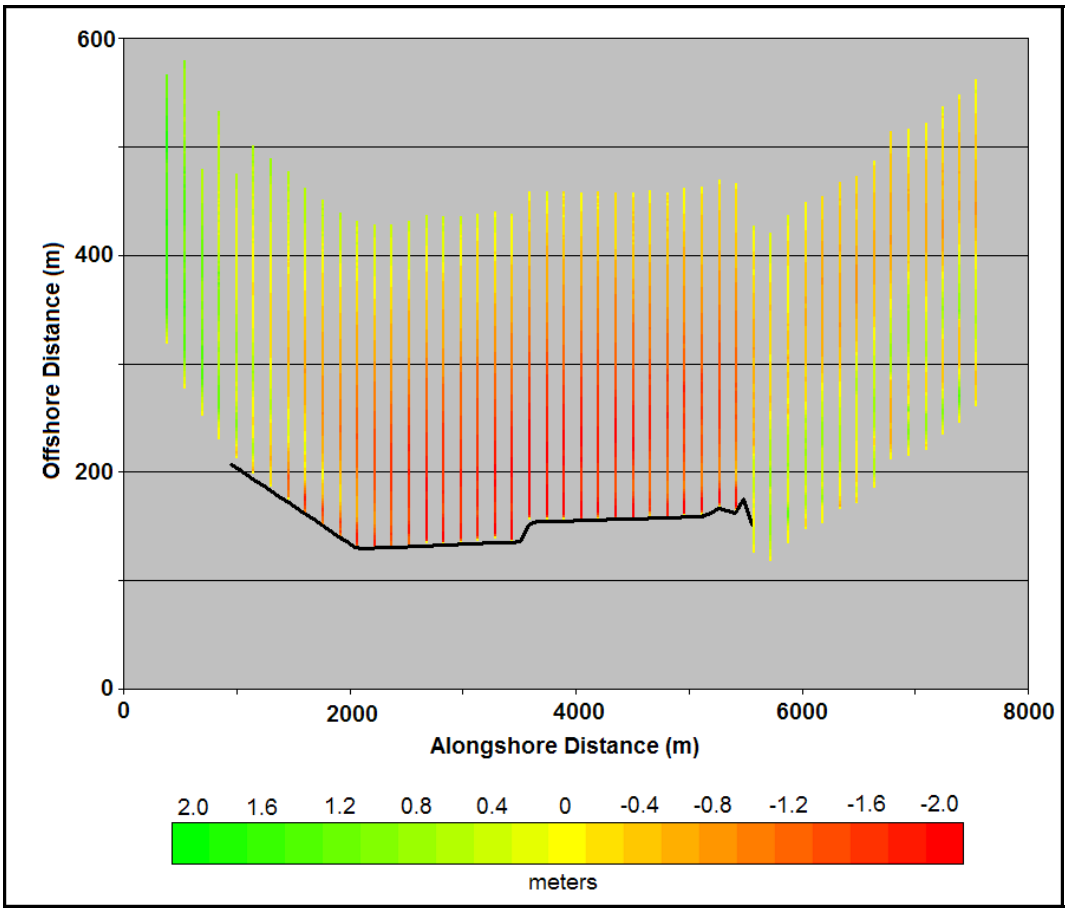

Figure 6-4. Locations of deficits in profile elevations. Note there is approximately a 10:1 distortion in the offshore to alongshore scales.

Before beach nourishment can advance the shoreline seaward, material must be provided to restore the profile to an equilibrium condition along the portions of the seawall where it is needed. In this report, this volume is termed the Seawall Deficit Volume. Volumes were calculated by interpolating the beach profile elevations into each GENESIS cell and comparing those profiles with a D_{50} = 0.29 mm equilibrium profile. Then the volumes needed in each GENESIS cell were summed along the length of the project. Based on the 2005 profiles, the Seawall Deficit Volume for this project is estimated at 684,000 yd^3 (523,000 m^3).

The Seawall Deficit estimate is based upon the beach fill material having a median grain size (D_{50}) of 0.29 mm. If, for any reason, the fill material that is placed on the beach has a finer grain size (for instance, by switching to an alternate borrow site), then additional material will need to be provided to compensate for the change in the underwater portion of the

equilibrium profile. The difference in a 0.29 mm and a 0.20 mm based equilibrium profile is shown in Figure 6-5. The orange area between the two profiles represents the additional needed material. Table 6-1 lists the additional volume of material required if the fill material has a D_{50} less than 0.29 mm.

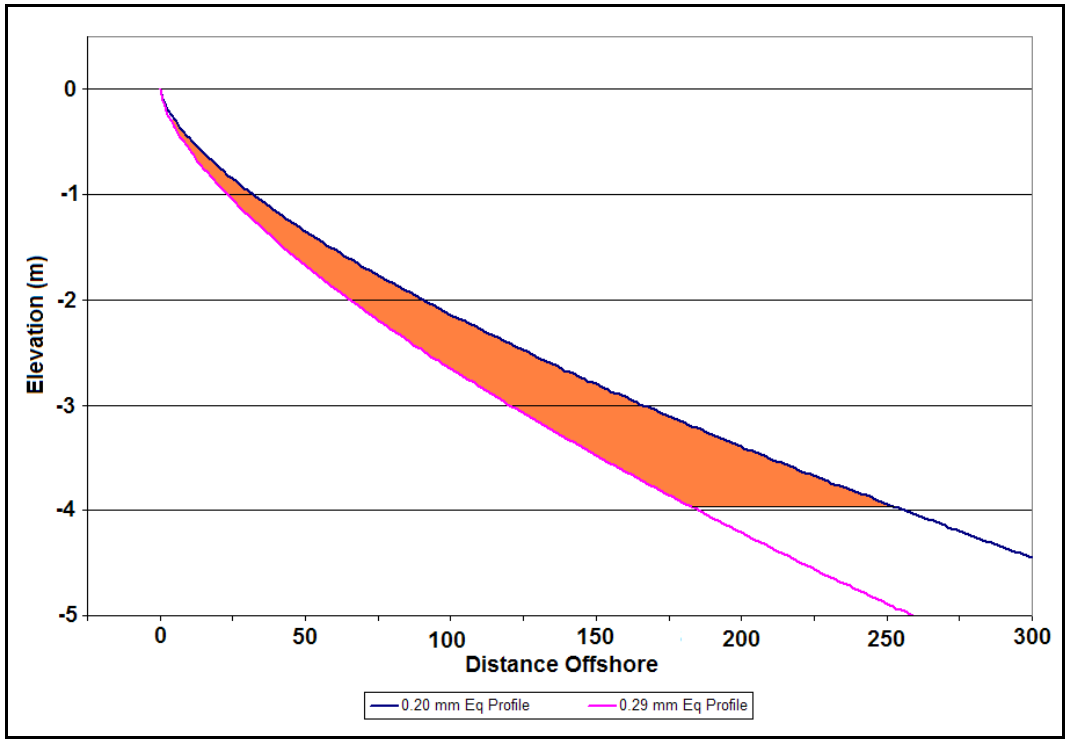

Figure 6-5. Equilibrium profiles for 0.20 mm and 0.29 mm grain sizes.

Table 6-1. Profile Adjustment Volumes based upon Fill Grain Size.

Median grain size (mm)	Profile Adjustment Volume (yds^3)
0.29	0
0.28	62,000
0.27	127,000
0.26	200,000
0.25	292,000
0.24	393,000
0.23	501,000
0.22	619,000
0.21	748,000
0.20	889,000

Characterization of Berm and Dune Volumes

Berm volumes were calculated for each GENESIS cell by multiplying the berm width (determined to be 70 ft (21 m) in Chapter 4) by the height between the berm elevation (+6 ft (1.83m)) and the depth of closure elevation (-13 ft (-3.96m)) by the cell width (240 ft (73.152 m)). These were summed to determine the total berm volume. Dune volumes were also calculated for each GENESIS cell and summed over the project length. Adjustments were made to cells at the south end of the project that did not have a rock seawall. The total berm and dune volumes needed for this project are 964,000 yd^3 and 255,000 yd^3, respectively (737,000 m^3 and 194,000 m^3).

Characterization of Overfill Volumes

The median grain diameter presently on the beach at Wallops Island is in the vicinity of D_{50n} = 0.20 mm = 2.32 ϕ, and the sediments are moderately well sorted with a typical standard deviation of $\sigma_{\phi n}$ = 0.5, where the subscript "n" is applied to the native material. The median grain diameter of the proposed offshore borrow material (subscript "b") is approximately D_{50b} = 0.29 mm = 1.79 ϕ. These sediments have standard deviations of $\sigma_{\phi b}$ = 0.5 to 0.9. As discussed in the CEM (Section V-4-1-e-3-i and Figure V-4-9 on pg V-4-26), this implies that the beach fill sediments will be within the stable region and the appropriate overfill multiplier is 1.0.

There is another issue to address in considering the Overfill Volume. This is the inclusion of a margin of safety in the design to help insure project success. There are two areas of greatest concern. The first is the grain size of the fill material. The project design analysis has been based upon the fill material having a D_{50} of 0.29 mm. This value was derived from sediments obtained from cores taken at the two most likely offshore borrow sites (Site A, and Site B; see Chapters 3 and 8). The average and the median of the D_{50}'s are in fact both coarser than 0.29 mm. However, these statistics are derived from a very limited dataset. Ten cores were obtained from Site A and six cores from Site B. Both sites cover two square miles. As shown in Table 6-1, the consequences of over-estimating the true fill grain size would lead to a significant underestimate of the appropriate under-water volume of fill material needed for the initial nourishment. However, the probability of the true grain size being less than 0.29 decreases rapidly with decreasing grain size.

If the true median grain size at the borrow site is as small as that represented by the smallest ¼ of the core sample D_{50}'s from both shoals, Figure 3-5 shows it would be near 0.27 mm, rather than the 0.29 mm value used for modeling purposes. Applying this value to Table 6-1, an Overfill Volume of 125,000 yds^3 was chosen. The preferred location, Shoal A (Chapter 8) has a larger median grain size than Shoal B. As discussed in Chapter 3, ¾ of the sediment samples from Shoal A had median grain sizes of 0.29 mm or larger.

While an overestimation of the median grain size of the fill material would have a significant impact on the volume of fill material needed on the underwater portion of the profile, there would be fewer impacts to the above water portion of the profile. These would be mostly limited to the portion of the profile between mean sea level and the berm crest (the foreshore slope), and this portion has been modeled in a conservative manner. This portion of the profile is exposed to wave action during the higher portions of the tide cycle and can be expected to reach an equilibrium slope based upon grain size in a manner similar to the underwater (below mean sea level) portion of the profile (steeper slopes for larger grain sizes). However, the Dean Equilibrium Profile Theory, which was applied for the underwater portion, is normally only applied up to an elevation of mean sea level. For this project, the foreshore slope was modeled as a straight line with a slope of tan (4.17°). This value was obtained as an average of foreshore slopes taken from existing profiles measured north and south of the seawall. The native beach material at Wallops Island is about 0.2 mm, and the foreshore slope is naturally adjusted for that grain size. The grain size of the fill material is expected to be substantially larger than this, and thus following nourishment the foreshore slope will likely be steeper than at present. A steeper foreshore slope would require less fill material between the berm crest and the depth of closure than is called for in the present design, and therefore the present design is considered conservative.

The other area of concern was the depth of closure value of 13 ft used in the analysis. Though the methodology used seemed defensible, given the lack of multiple profile data sets, the resulting value is low compared to other east coast sites. If the overfill volume chosen above is not needed to compensate for an overestimation of the fill grain size, it would provide sufficient additional material to adjust the depth of closure to over 15 ft.

Characterization of Sea Level Rise Volumes

The most recent USACE guidance on sea-level rise (SLR) (USACE, 2009a, pg 2, section 6b), which is an update of earlier guidance (USACE, 2000), requires a project assessment using Low, Intermediate, and High rise rates. The Low rate of SLR should be based upon the historic rate, the Intermediate rate upon Curve I of the National Research Council's (NRC) 1987 report *Responding to Changes in Sea Level: Engineering Implications*, and the High rate upon NRC (1987) Curve III.

The total rate of historical SLR (1.12 ft/100 years) at Wallops Island was obtained by taking the average of the rates from three nearby tide gage locations: Lewes, DE, Solomons Island, MD, and Portsmouth, VA. These stations have local trends from long term tide gage records (shown in Table 6-2) as evaluated by Zervas (2001). The locations are about equidistant from Wallops Island and are in widely different compass directions.

Table 6-2. NOAA Tide Stations used to obtain total SLR rate at Wallops Island, VA.

Station Name	Latitude	Longitude	First Year	Year Range	MSL Trend and Standard Error (mm/yr)		Distance from Wallops Island, VA (miles)	Direction from Wallops Island, VA (degrees)
Lewes, DE	38° 46.9' N	75° 07.2' W	1919	81	3.16	0.16	68	16°
Solomons Island, MD	38° 19.0' N	76° 27.1' W	1937	63	3.29	0.17	63	301°
Portsmouth, VA	36° 46.7' N	76° 18.1' W	1935	53	3.76	0.23	86	212°

Following NRC (1987), Knuuti (2002), Rosati and Kraus (2009), and USACE (2009a), the increase in sea level at a future date above the current level can be estimated using the equation:

$$Rise = (e + M)(t_2 - t_1) + b(t_2^2 - t_1^2) \qquad (6\text{-}1)$$

where:

$(e + M)$ is the total historical rise rate
= 0.0112 ft/yr for Wallops Island
t_2 is the future date minus year 1986,
t_1 is the project start date (2010) minus year 1986, and
b is a set of coefficients given in NRC (1987)
$b_{(\text{Historical})} = 0$

$b_{(\text{Curve I})} = 9.2 \times 10^{-5}$ ft/yr^2
$b_{(\text{Curve II})} = 21.7 \times 10^{-5}$ ft/yr^2
$b_{(\text{Curve III})} = 34.5 \times 10^{-5}$ ft/yr^2

Figure 6-6 shows the projected rate of SLR at Wallops Island for the 50-year project life as obtained from Eq. 6-1 for the Historical rate and for the three NRC (1987) curves. This figure shows that the NRC (1987) Curve III predicts a 2.25 ft (0.69 m) SLR at Wallops Island by the end of the project lifetime (2060). This 2060 SLR amount is four times the amount of SLR predicted by the historical (Low) amount (0.56 ft, 0.17 m) and 2.2 times the Curve I (Intermediate) amount (1.01 ft, 0.31 m).

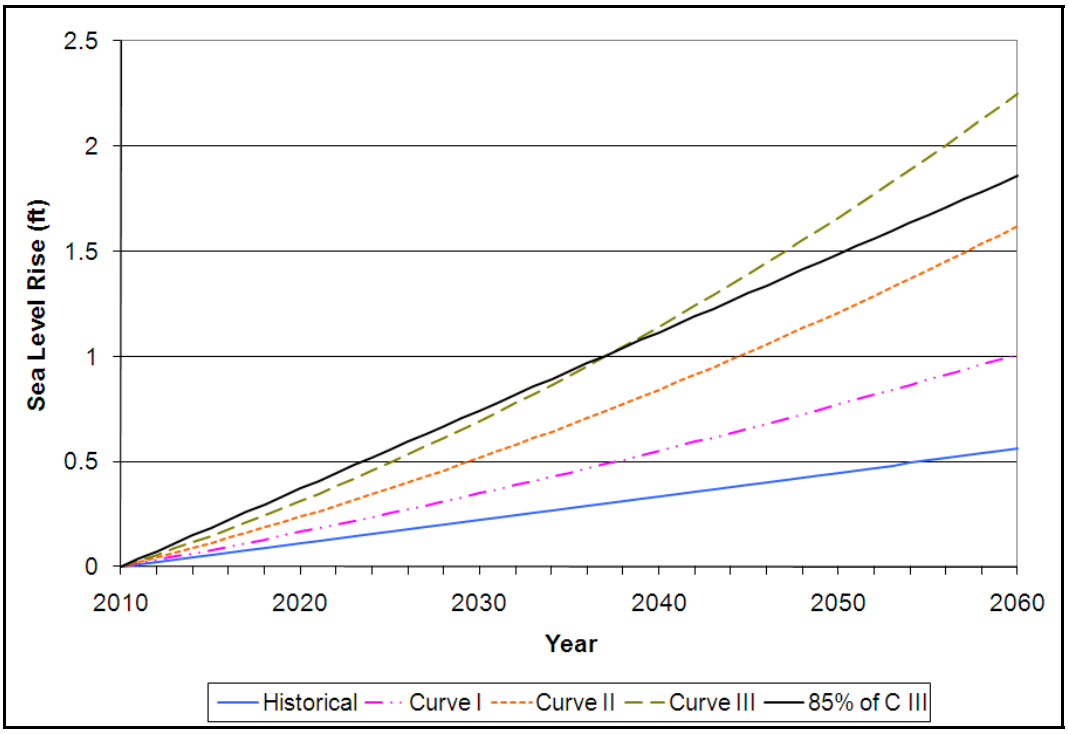

Figure 6-6. Projected Wallops Island, VA SLR, as based upon NRC (1987) curves.

For project planning purposes, it was decided to choose a target fill volume which was based upon 85% of the 2060 Curve III amount, but to add that volume in constant increments (for ease of planning). This equates to a 1.91 ft (0.58 m) of SLR in 2060 calculated as a constant rise rate of 0.037 ft (0.011 m) per year. This target value was chosen because it predicts a year 2060 rise that is about 80% of the difference in the historical and the Curve III amounts and about 70% of the difference in the Curve I and the Curve III amounts. This 85% line is also shown in Figure 6-6.

There is no USACE guidance that mandated the use of 85% (or any other percent) of the 2060 Curve III amount. It was chosen for planning purposes to be greater than that predicted by the Low and Intermediate estimates and a little less than the High estimate. This procedure was considered to conform to USACE guidelines and to be appropriately conserva-tive. However, the guidance is flexible enough that other procedures could have been equally well justified.

In the early years of the project, the amount of fill being added would exceed the amount necessary to match the Curve III amount with the cross over point being about halfway through the project lifetime (in the 28th year, 2038). Because this procedure uses a constant rise rate instead of a parabolic increasing rate (described by Eq. 6-1), this procedure places about 94% as much SLR sand on the beach as would be placed by following Curve III throughout the project lifetime.

The project plan to account for SLR is to add an appropriate additional amount of material at each planned 5-year renourishment interval. This SLR volume is the amount of material needed to elevate the entire profile (from the back of the dune seaward to the depth of closure) by (5 years * 0.037 ft/yr =) 0.186 ft (0.057 m). A schematic representation of this is shown by the blue area in Figure 6-8, below. For the Wallops Island project, the projected SLR volume needed at each 5-year renourishment interval based upon the 85% curve is 112,000 yd^3 (86,000 m^3). The total SLR volumes needed for the nine renourishment events based upon the 85% curve along with the Low, Intermediate, and High curves are given in Table 6-3.

Table 6-3. Wallops Island SLR Volumes.

SLR rate estimate	2060 SLR (ft) above 2010 level	Total volume of fill (yds^3) needed for all renourishments to account for SLR	Percent of the 85% volume planning estimate
Low - based upon historical rate	**0.56**	304,000	30%
Intermediate - based upon NRC (1987) Curve I	**1.01**	507,000	50%
Planning - based upon 85% of Curve III in yr 2060	**1.91**	1,008,000	100%
High - based upon NRC (1987) Curve III	**2.25**	1,067,000	106%

By compensating for SLR at each renourishment interval, the volume of material placed can be adjusted to match the amount of actual SLR, as obtained from the monitoring data, which could be greater or less than the predicted amount. It should be pointed out that the main usefulness of the SLR rate discussed here is to provide one of the component values needed to calculate the total volume of beach nourishment material that is expected to be needed over the project lifetime. It is not intended that this value actually be used at the time each renourishment occurs. Rather, it is intended that the volumes needed at renourishment will be primarily based upon an analysis of the data collected from the on-site project monitoring program.

Summary of Components Common to All Alternatives

Figures 6-7 and 6-8 show a conceptual representation of the components of the initial and renourishment B070 fill profiles, respectively. In these figures, Brown represents existing material (beach and upland sediments and rock seawall), Tan represents the Seawall Deficit Volume, Green represents the Berm Fill Volume, Yellow represents the Dune Volume, Pink represents the Advanced Fill Volume, and Light Blue represents the Sea Level Rise Volume. The amount of initial and renourishment advanced fill varies with the alternative chosen and is discussed below. The rest of the volumes are listed in Table 6-3. In this table, the row titled "Minimum Target Fill Volume for Storm Damage Reduction" is the sum of the "Seawall Deficit", "Berm", "Dune", and "Overfill" volumes.

Table 6-3. Volumes for B070 beach fill components.

Volume Component	yd^3	Ave yd^3/ft
Seawall Deficit	684,000	34.8
Berm	964,000	49.0
Dune	255,000	13.0
Overfill	125,000	6.4
Minimum Target Fill Volume for Storm Damage Reduction	2,028,000	103.2
Sea Level Rise	112,000	5.7

Note: This table does not provide either the total initial or the total renourishment fill volumes. For those volumes, see Table 7-1.

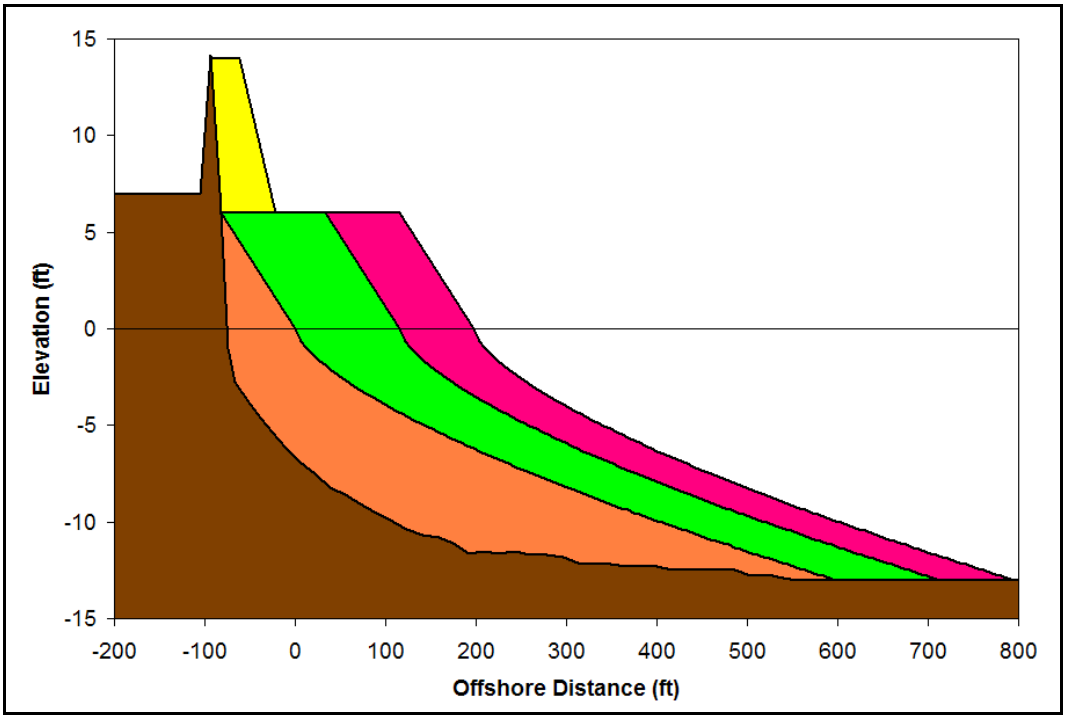

Figure 6-7. Conceptual Schematic of Initial Fill Placement.

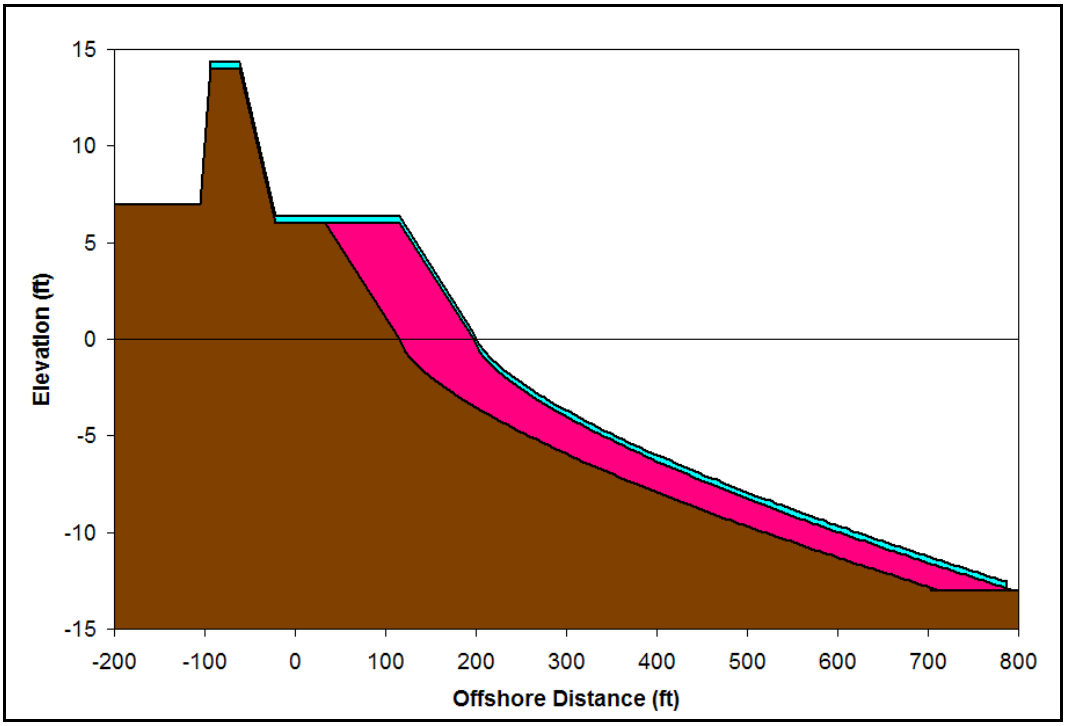

Figure 6-8. Conceptual Schematic of Renourishment Fill Placement.

Beach Fill Alternatives

In consultations among NASA, CENAO, and ERDC personnel, a large list of beach fill alternatives were initially screened. Most of these were removed from further consideration because either they did not provide adequate storm damage protection or they were less cost effective than similar designs. One example of each of three classes of alternative was retained for more complete analysis and optimization. These three alternative classes were:

1. A beach fill with no south end sand retaining structure.
2. A beach fill with a south terminal groin.
3. A beach fill with a south detached breakwater.

In addition to the features listed in Table 6-3, the three alternatives all have the common features listed in Table 6-4. Another important feature that all three alternatives have in common is that they all decrease the rate of erosion on the northern end of Assawoman Island.

Table 6-4. Common features for all alternatives.

Project Length	19,680 ft	6000 m
Project North End	North end of Rock Seawall	
Project South End	South Camera Stand	
Minimum Target Berm Width	70 ft	21.3 m
Minimum Target Width from Seawall to MSL	152 ft	46.3 m
Target Renourishment Interval	5 years	
Project Lifetime	50 years	
Projected Number of Renourishment Cycles in Project Lifetime	9	

Modeling of Advanced Fill Volumes

Following calibration and the modeling of existing conditions, the alternatives were modeled with GENESIS. Specifically, the model was used to address the question of how the shoreline of a particular alternative evolved over the time period between renourishment events. The fill volumes for each of the alternatives protrude different distances seaward of the present shoreline and the general tendency of most fill projects, including this one, is for the longshore sediment transport to move sediment along the coast away from the project site in both directions. The modeling consisted of iteratively including differing amounts of advanced fill to determine the optimal amount so that the volume left at the time of renourishment was sufficient to provide

adequate protection from storm damage. Including a south terminal groin or a south detached breakwater changed the transport patterns, so the optimal designs of these features were obtained through additional iterations. The amount of renourishment advanced fill was determined by calculating the volume needed to return the beach to the initial advanced fill condition. This is a more conservative approach than running GENESIS for a second (and third, etc.) 5-year interval to iteratively determine the renourishment advanced fill volume.

For the modeling effort described above the wave block used to drive the model was generally the average year block described in the Sensitivity Testing section of Chapter 5. Once an acceptable solution was obtained using this wave set, the model was run 20 times using each of the twenty 4-year wave data blocks described in the Sediment Budget section of Chapter 5. This created 20 sets of output (for each model year) that could be averaged and for which 95% confidence intervals could be calculated. The modeling results for each alternative are presented below.

Alternative 1 - No sand retention structures

Alternative 1 has no sand retaining structures and thus requires the greatest initial and renourishment advanced fills. GENESIS modeling yielded an Advanced Initial Fill Volume of 1,939,000 yd^3 and an Advanced Renourishment Fill Volume of 694,000 yd^3 for this alternative.

Figure 6-9 shows the net longshore sediment transport rate during Year 5 (just prior to renourishment) along with 95% confidence limits for this alternative. In comparing this figure to Figure 5-15 (the pre-project condition) it is seen that the divergent nodal point is shifted approximately a mile to the north and that maximum transport rates substantially exceed present conditions.

Figure 6-10 shows how net transport rates vary from year to year. Though it is intended that renourishment should occur at the end of year 5, this analysis was carried out to year 14 without renourishment to help determine if adverse impacts occur to adjacent beaches if renourishment intervals are postponed or cancelled. This figure shows that substantial accretion occurs adjacent to both ends of the project through year 2. At the south end of the project, over time the transport rate asymptotically approaches a constant rate that is in excess of the current conditions

(Figure 5-15). Accretion occurs at the north end of the project though the rate decreases over time.

Figure 6-11 shows the gross longshore sediment transport rate during Year 5 (just prior to renourishment) along with 95% confidence limits for this alternative. In comparing this figure to Figure 5-18 (the pre-project condition) it is seen that Alternative 1 gross rates at both ends (away from the seawall) slightly exceed those of the present condition. Gross rates varied little from year to year.

Figure 6-12 shows the shoreline position at year 5 along with the 95% confidence intervals. This figure shows that the in many places the shoreline has retreated to near the minimum shoreline for storm damage protection, and thus, this is intended to be shortly before renourishment. Figure 6-13 shows shoreline positions for years 2 through 14. By year 12, all of the fill has been removed from the south end of the project; however, by year 14, there is still fill in front of the seawall.

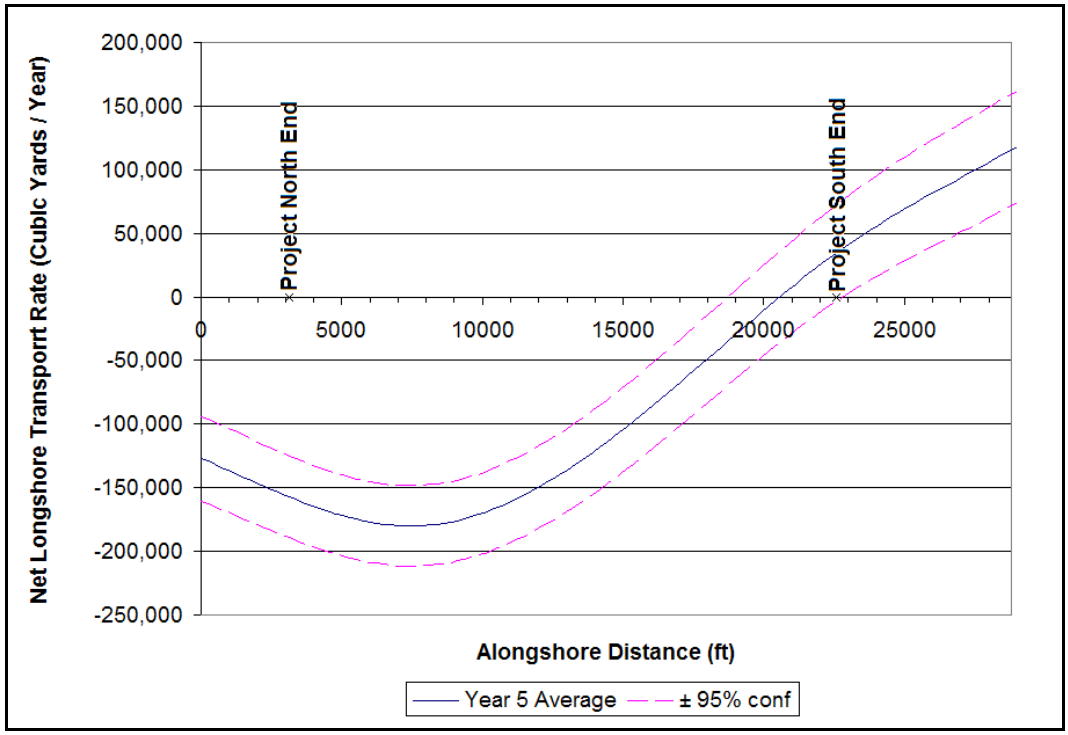

Figure 6-9. Net longshore transport rate for Year 5, Alternative 1.

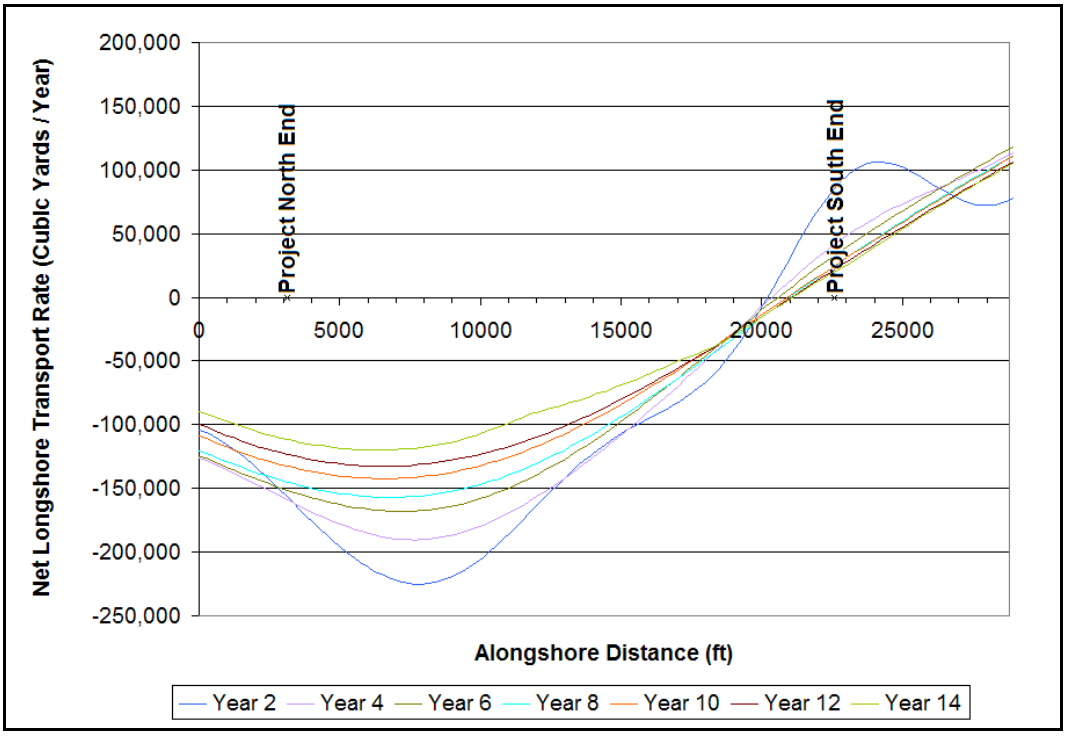

Figure 6-10. Net Transport rates over time for Alternative 1.

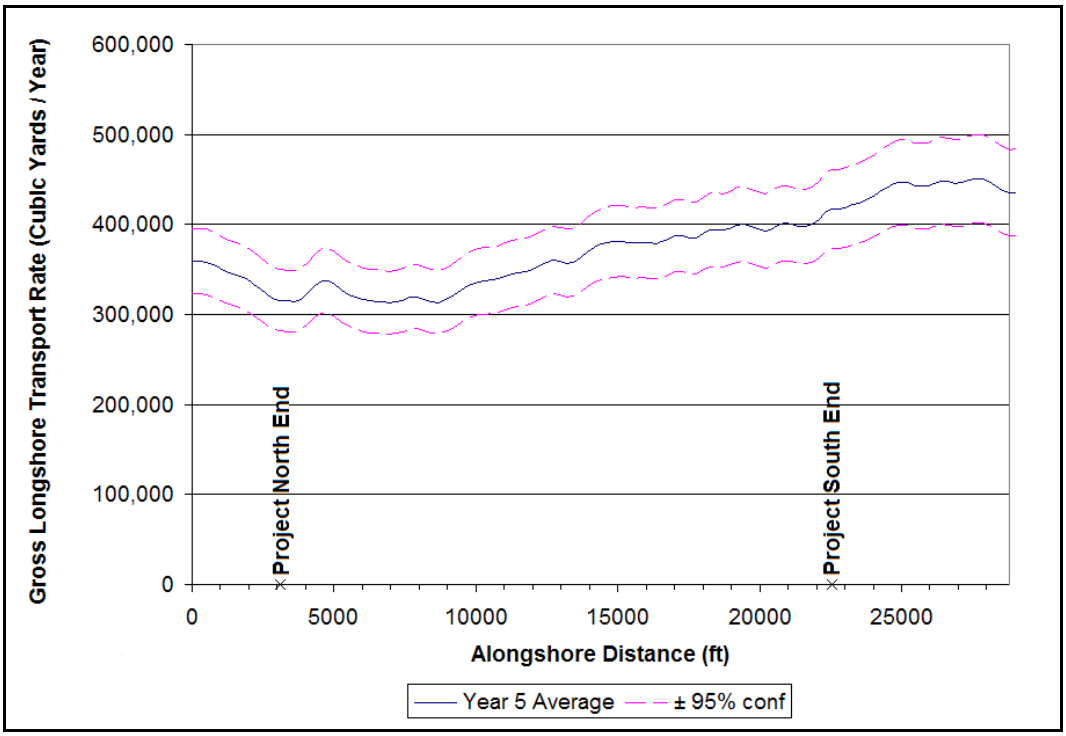

Figure 6-11. Gross Transport rate for Year 5, Alternative 1.

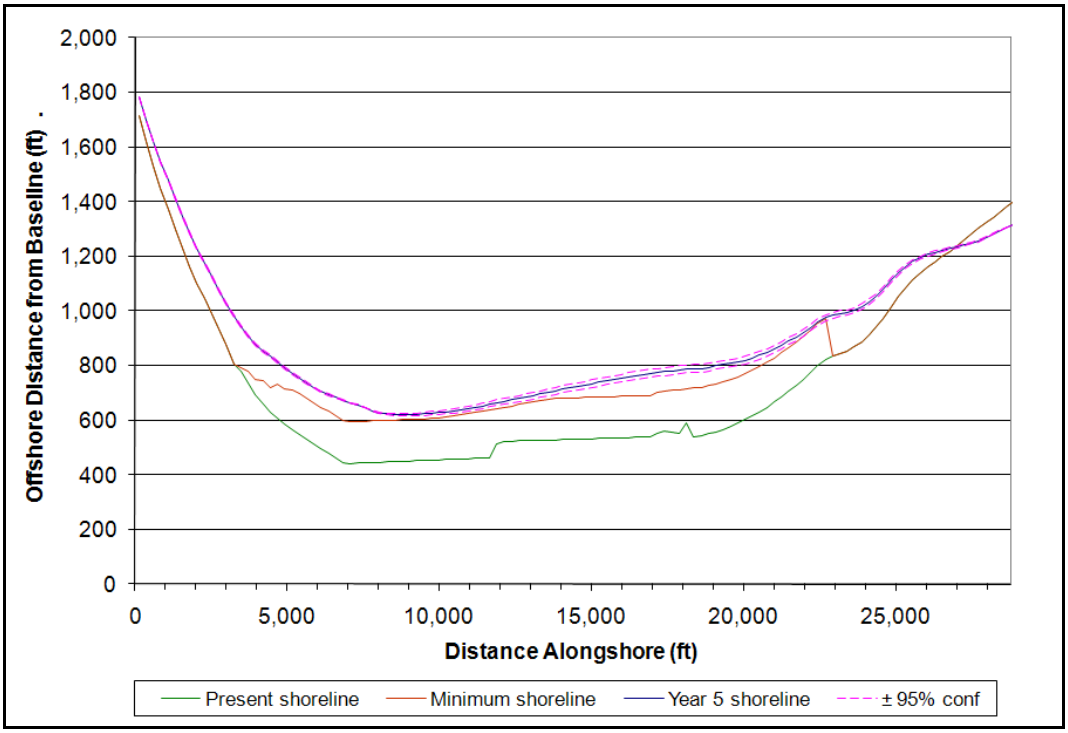

Figure 6-12. Shoreline position for year 5, Alternative 1.

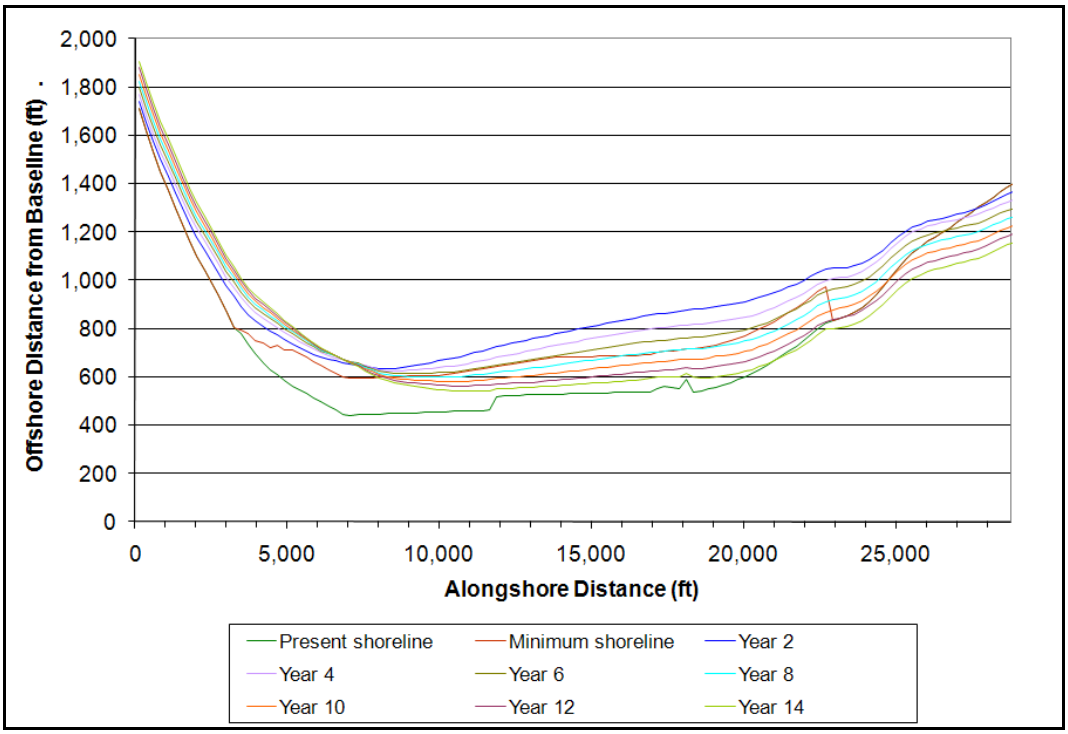

Figure 6-13. Shoreline positions over time for Alternative 1.

Alternative 2 - South terminal groin

Alternative 2 has a south terminal groin as a sand retaining structure. GENESIS modeling yielded an Advanced Initial Fill Volume of 810,000 yd^3 and an Advanced Renourishment Fill Volume of 619,000 yd^3 for this alternative.

The advice and guidance found in ASBPA 2008, Kraus, Hanson and Blomgren 1994, National Research Council 1995, and Basco, D.R. 2002 was followed in the design of the south terminal groin. The groin parameters are given in Table 6-5.

Table 6-5. South Terminal Groin Design

Descriptive Location	South Camera Stand	
Landward Coordinates	3764244 Easting	1169509 Northing
Groin Length seaward of Present Shoreline	431 ft	131 m
Groin Length seaward of Advanced Fill Shoreline	164 ft	50 m
Permeability	0.2	

Figures 6-14 through 6-19, show transport rates and shoreline positions for the south terminal groin alternative (Alternative 2). They are comparable to Figures 6-9 through 6-13 for the no structure alternative.

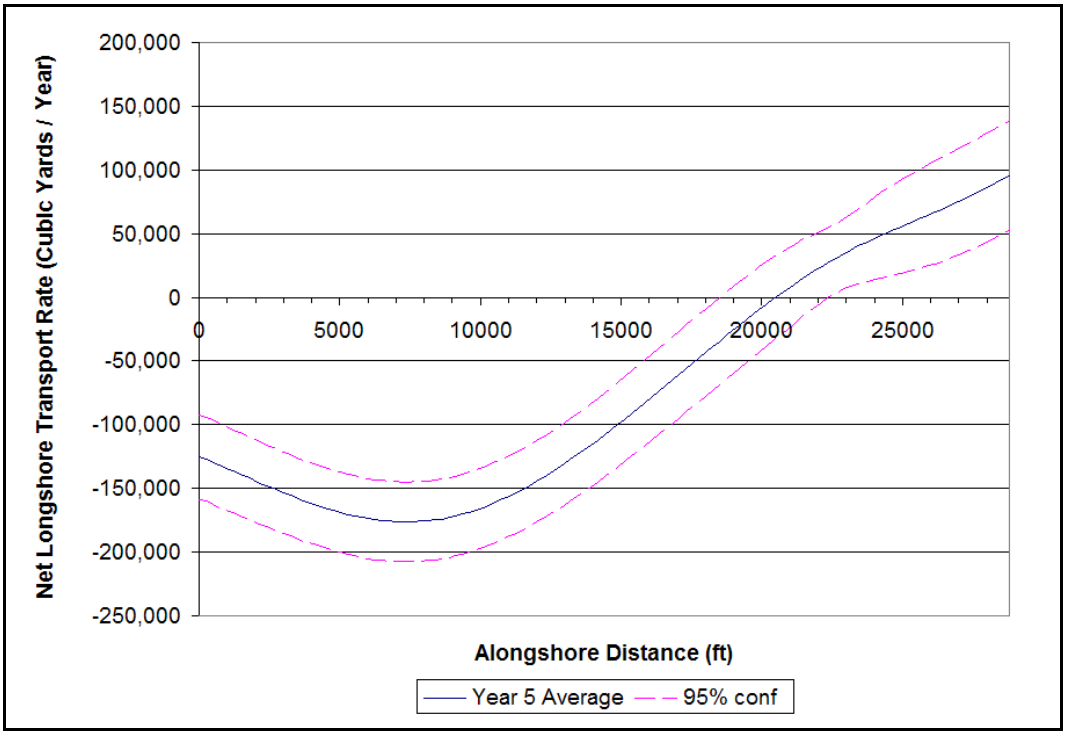

Figure 6-14. Net longshore transport rate for Year 5, Alternative 2.

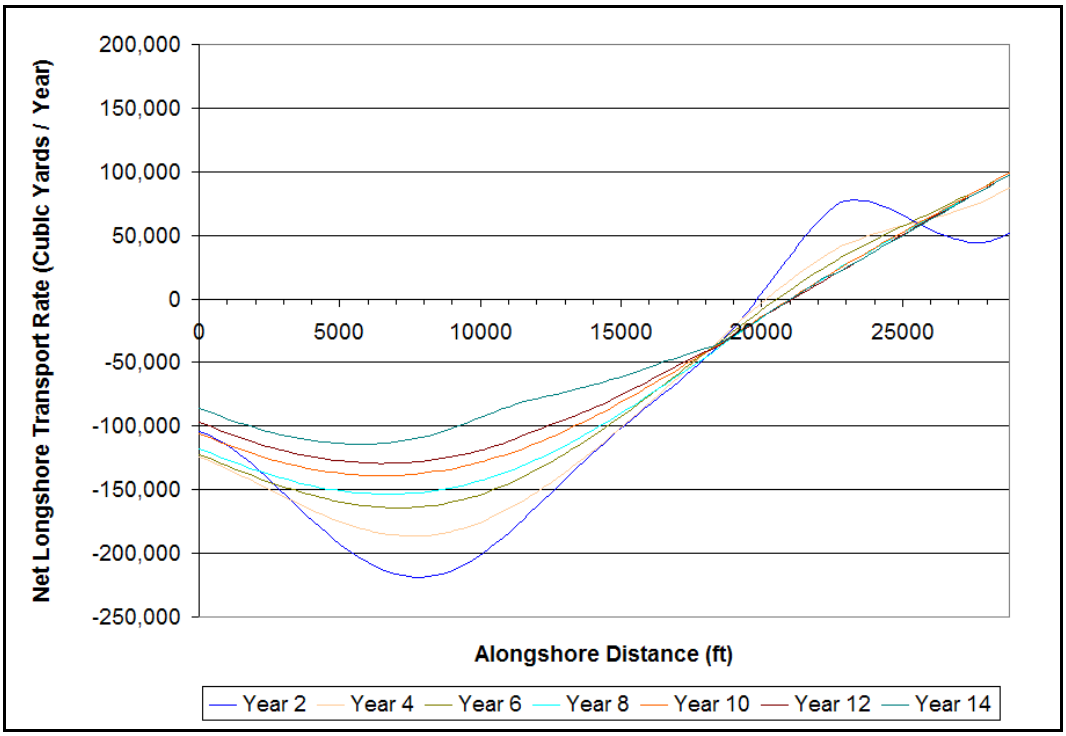

Figure 6-15. Net Transport rates over time for Alternative 2.

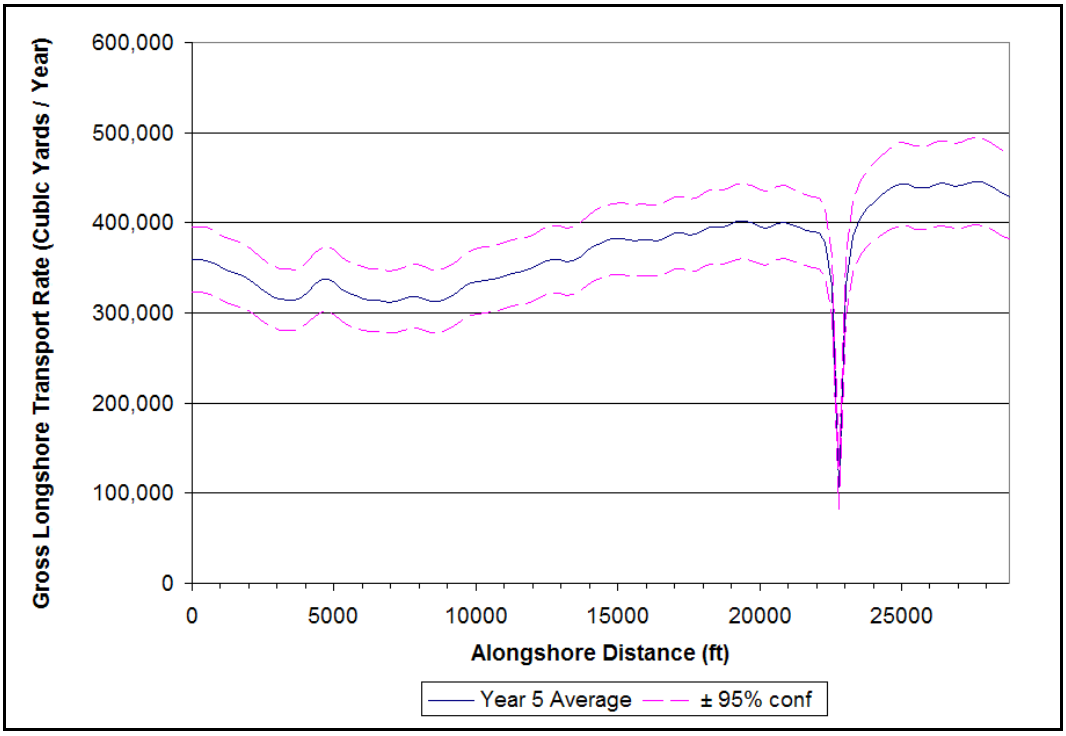

Figure 6-16. Gross Transport rate for Year 5, Alternative 2.

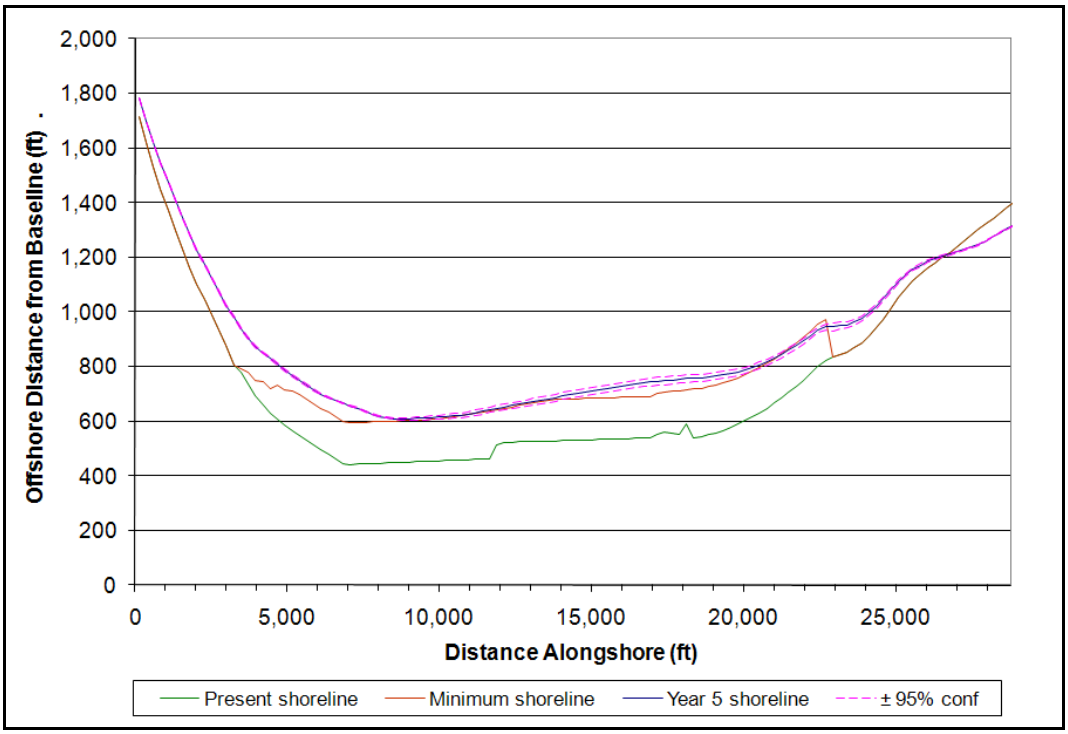

Figure 6-17. Shoreline position for year 5, Alternative 2.

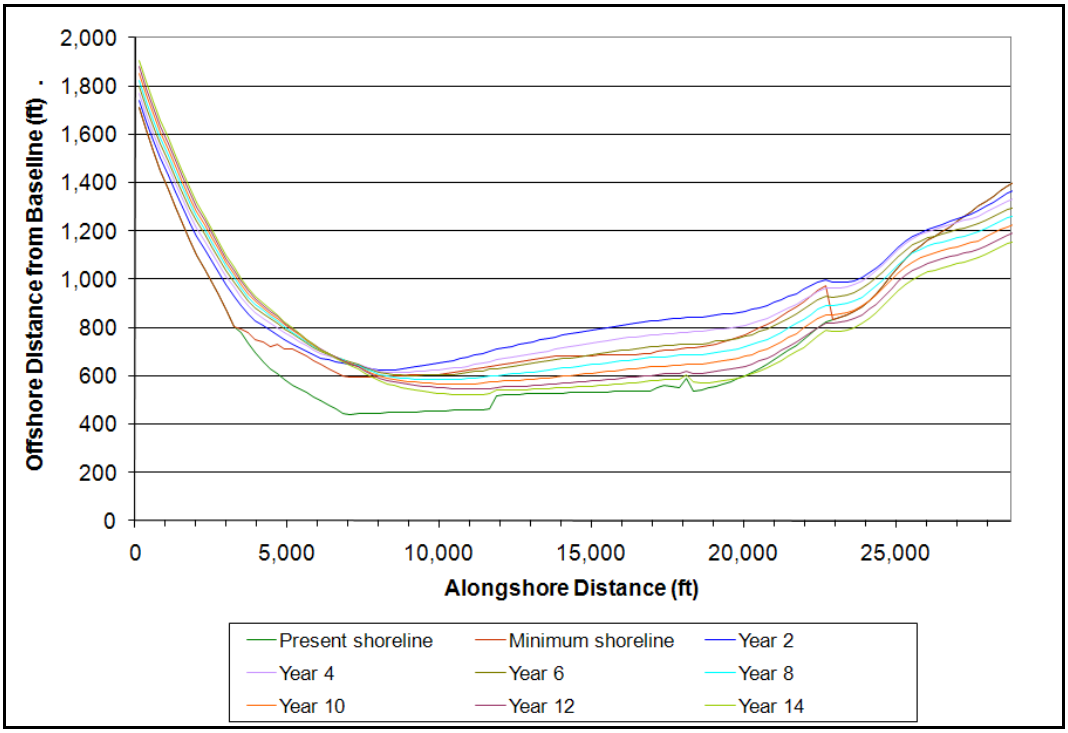

Figure 6-18. Shoreline positions over time for Alternative 2.

Alternative 3 - South detached breakwater

Alternative 3 has a south detached breakwater as a sand retaining structure. The design and modeling of a detached breakwater followed the advice in Chasten, et al. (1993), Basco (2002), Hanson and Kraus (1989), Gravens, Kraus, and Hansen (1991). GENESIS modeling yielded an Advanced Initial Fill Volume of 733,000 yd^3 and an Advanced Renourishment Fill Volume of 561,000 yd^3 for this alternative. The breakwater design parameters are given in Table 6-6.

Table 6-6. South Detached Breakwater Design

Number of Segments	1	
Descriptive Location	Offshore of South Camera Stand	
North End Coordinates	3764531 Easting	1169310 Northing
South End Coordinates	3764477 Easting	1169237 Northing
Breakwater length	300 ft	91 m
Distance Offshore of Advanced Fill shoreline	750 ft	229 m
Distance Offshore of Present shoreline	1014 ft	309 m
Ratio of Breakwater Length to Offshore Distance	0.4	

Figure 6-19 through 6-23 show transport rates and shoreline positions for the detached breakwater alternative (Alternative 3). They are comparable to Figures 6-9 through 6-13 for the no structure alternative and Figures 6-14 through 6-18 for the groin alternative.

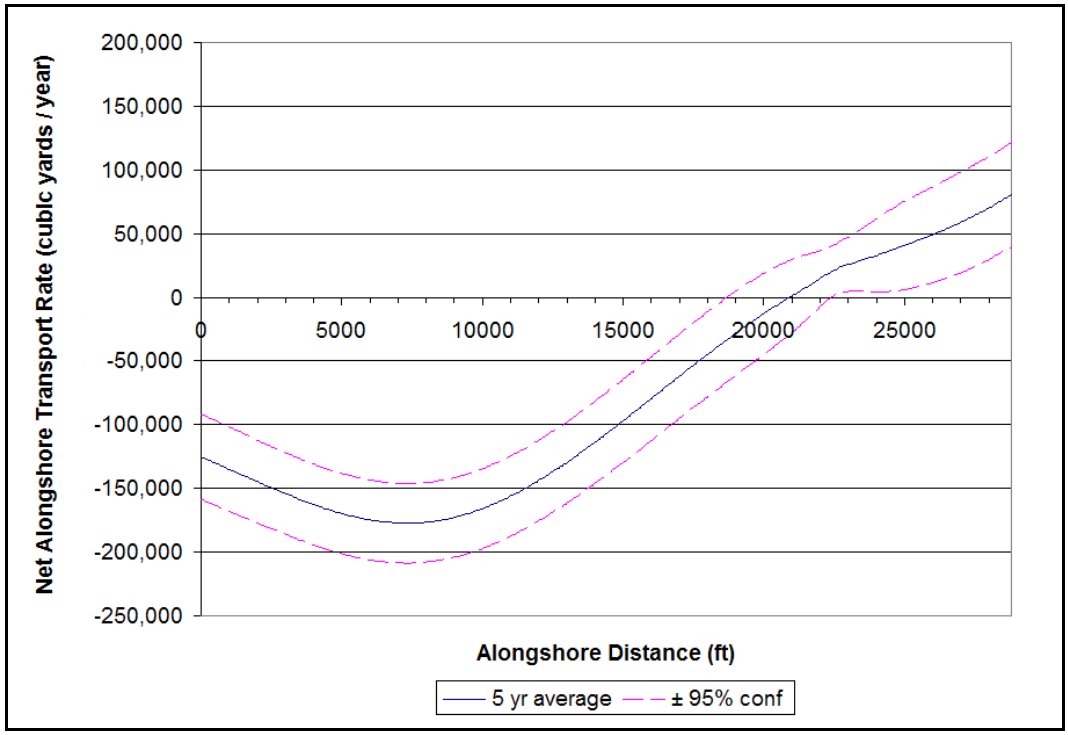

Figure 6-19. Net longshore transport rate for Year 5, Alternative 3.

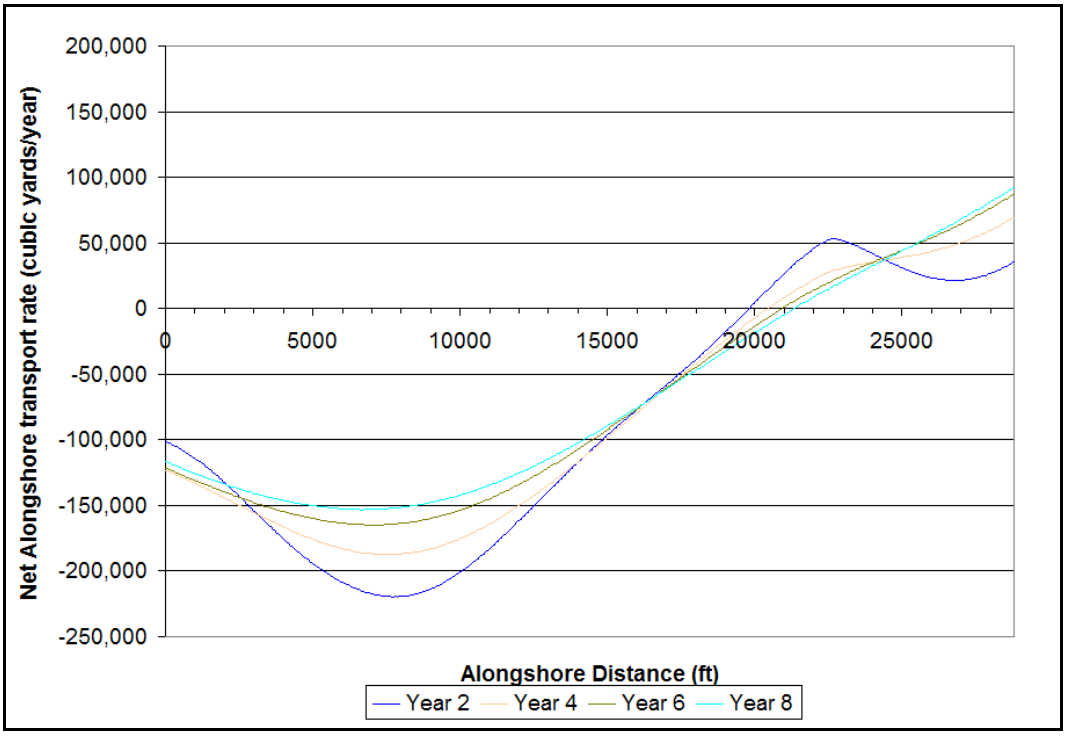

Figure 6-20. Net Transport rates over time for Alternative 3.

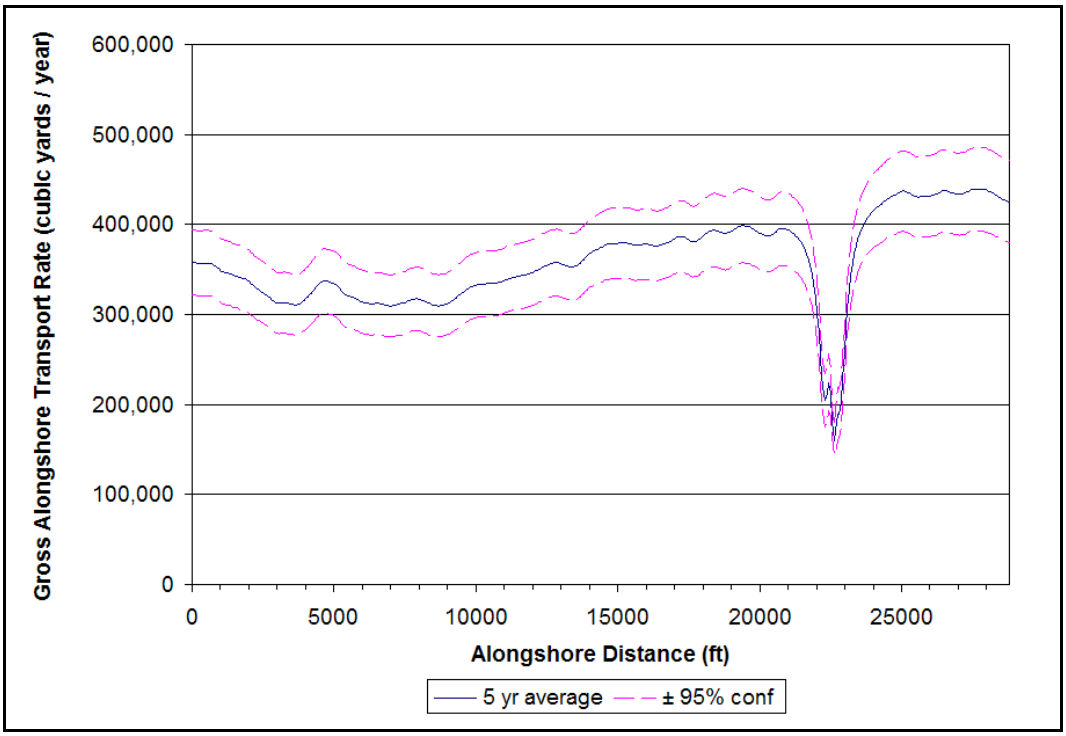

Figure 6-21. Gross Transport rate for Year 5, Alternative 3.

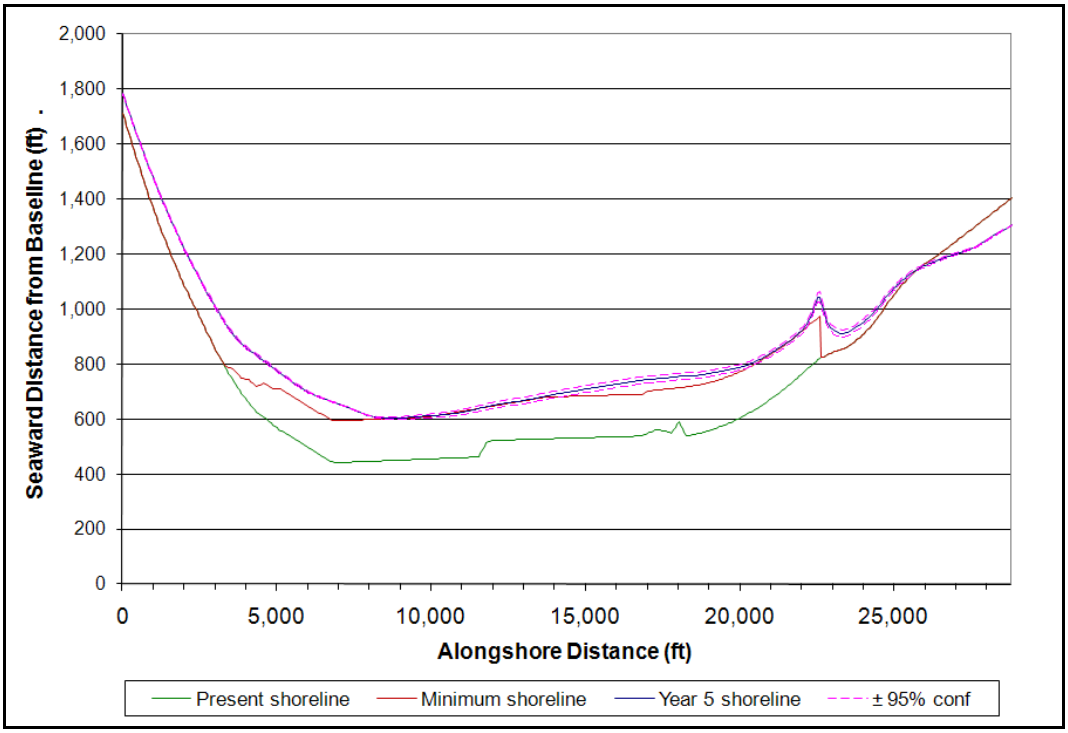

Figure 6-22. Shoreline position for year 5, Alternative 3.

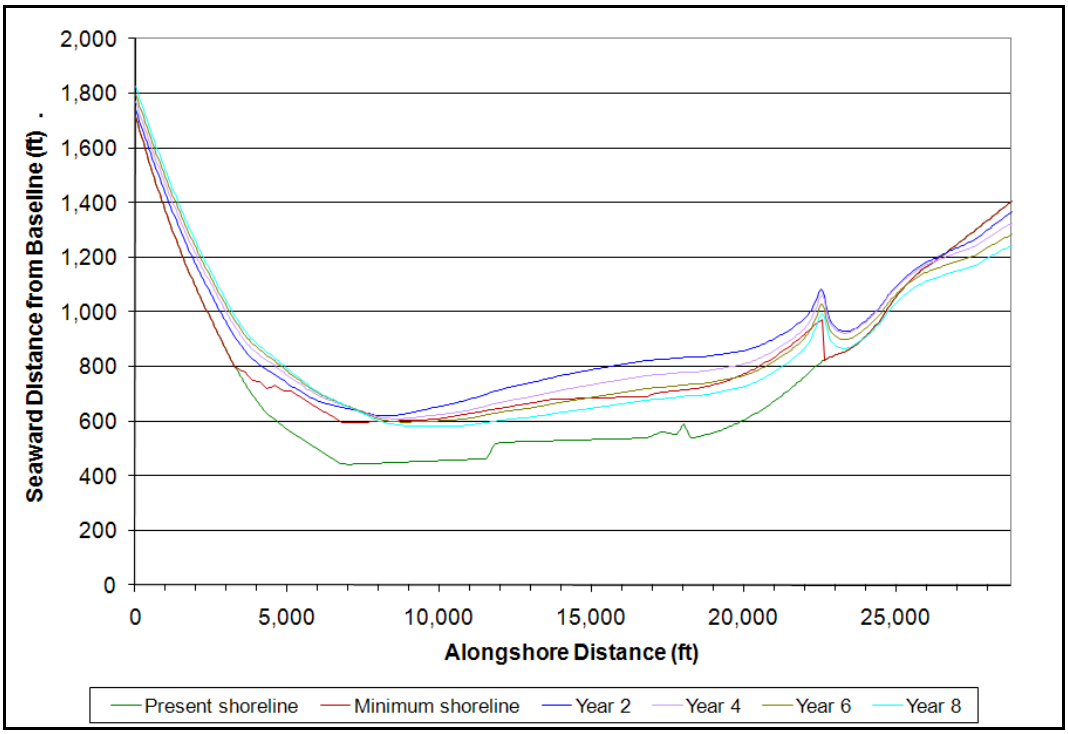

Figure 6-23. Shoreline positions over time for Alternative 3.

7 Wallops Island Storm Damage Reduction Project Design

During the development of this study, the complete storm damage reduction project has evolved to include the following components:

- Rehabilitation of the present rock seawall.
- A southern extension of the rock seawall.
- An initial beach fill along 19,700 feet (6,000 m) of shoreline.
- Depending upon the alternative chosen, the project may include a sand retention structure in the form of a south terminal groin or a detached breakwater or neither.
- A flood damage analysis of the Wallops Island infrastructure.
- A beach fill monitoring program.
- Scheduled beach renourishments at 5-year intervals.

Seawall Maintenance

This topic is covered in Chapter 3 of this report. This task is critically important to the existing rock seawall being able to survive and perform as expected during a target 100-year storm event, as discussed in Chapter 4. Following initial beach fill placement, the seawall is not expected to be exposed to wave attack except during infrequent, large storm events. However, following such events, it is expected that the seawall will be inspected and repaired as necessary.

Seawall Extension

There is significant infrastructure on Wallops Island that is south of the southern end of the rock seawall, primarily Building Z41 and Launch Pad 0B, the MARS facility. The only storm protection these facilities currently have is the geotextile tube and a low riprap wall. The present rock seawall will be extended up to 1400 meters (4600 ft) to the south. This will provide these structures with the same level of protection as the other facilities on the island. The details of the seawall extension design will be provided by USACE personnel at NAO.

Initial Beach Fill

The initial beach fill will provide a minimum beach width that is sufficient to provide storm damage protection along 19,700 feet of beach between the northern end of the rock seawall and the southern end of the present geotextile tube. This fill will be placed so that there will be a 6 ft high berm extending a minimum of 70 ft seaward of the rock seawall with an equilibrium profile that extends seaward to the depth of closure. The profile will also include a 14 ft high dune at the seawall. As discussed below, for budgetary reasons, this initial fill will be partially placed in project year two and completed the following year. Initial fill volumes for each of the three alternatives are given below in Table 7-1.

Sand Retention Structure

Depending upon the alternative chosen, the project may have a south terminal groin or a south detached breakwater. These are discussed in Chapter 6. The sand retention structure will be designed by USACE personnel at NAO.

Flood Vulnerability Analysis

As discussed in Chapter 4, the beach fill project and the rock seawall will provide significant protection to the infrastructure on Wallops Island from the direct impact of wave attack. However, flooding is still expected to pose a problem. NASA has ongoing measures in place to analyze and reduce the flood damage potential for each structure on Wallops Island. NASA intends to maintain this program for existing and future infrastructure.

Beach Monitoring Program

A beach monitoring program will be established to collect data on a regular schedule through the lifetime of the project. These data will be analyzed and relied upon to determine the amount and timing of beach fill renourishments. They will also be used to monitor any negative impacts of the project on Assawoman Island.

Scheduled Beach Renourishments

The storm damage reduction project has a design renourishment interval of 5 years. The design renourishment volume varies depending upon the

alternative chosen and is based upon average longshore transport rates. However, it is intended that the timing and volume of each renourishment should be based upon the analysis results of the monitoring program rather than some predetermined volume and schedule. While it is intended that the initial fill material come from an offshore borrow site, renourishment fill material is expected to be derived from a combination of the offshore borrow site and material on the beach at the north end of Wallops Island that is being backpassed to the project site.

Implementation Schedule

WFF does not expect to receive sufficient funding to implement all of the initial components of the project in a single FY. Instead, the initial components have been staged to be accomplished over a three-year time span. The order in which construction will occur has been carefully considered. If the expected funding in Year-2 or Year-3 is postponed or cancelled, the already constructed portions of the project must be viable projects in themselves that do not have negative shoreline consequences either to Wallops Island or to its neighbors. This, and other issues, have dictated the following sequence for the initial project construction.

By phasing the construction in the manner described, only Year-3 activities will be dependent upon the beach fill alternative chosen. The alternative chosen has no other impacts prior to the time of the first renourishment.

Year-1 Activities

- Rehab and repair of the existing seawall.
- Construction of a 1500 ft southern seawall extension.
- Initiation of the monitoring program.

Year-2 Activities

- Partial initial beach fill (discussed below).
- Continuation of the monitoring program.

Year-3 Activities

- Completion of initial beach fill.

- Construction of the south terminal groin, the detached breakwater, or neither, depending upon the alternative chosen.
- Continuation of the monitoring program.

Discussion of 2-Year Initial Fill Placement

It is understood that requiring two dredging events to place the initial fill will incur additional costs. These include not only the cost of an additional dredge mobilization, but also the cost of the portion of the fill that is transported out of the project site between dredging events. These costs are accepted as being unavoidable due to budget constraints.

It is expected that, in Year-2, funding will be available to place approximately 1.2 million yd^3 of fill material. The volume needed to restore the underwater area in front of the seawall to its equilibrium condition is approximately 914,000 yd^3. The Year-2 fill material will be placed to accomplish this with the remainder of the material (286,000 yd^3) placed mainly in the center of the project site. By placing the majority of the Year-2 fill in the center of the project site, GENESIS modeling has indicated that the one-year end losses of that material are approximately 78,000 yd^3. These calculations were made for average wave conditions, a stormy year would be expected to have higher losses.

There are several consequences to the project in addition to the need to replace this 78,000 yd^3 Staged Placement Loss Volume. The first is that the project site will not obtain the full extent of the storm damage reduction protection until the third year of the project life. However, on the plus side, it is not anticipated that the first renourishment will be required until project year 8.

Initial and Renourishment Fill Volumes

Table 7-1 summarizes the initial and renourishment volumes required for each of the alternatives. As listed in this table, the Minimum Target Fill Volume is the sum of the Seawall Deficit, Berm and Dune volumes listed in Table 6-2. The Advanced Initial Fill Volume varies with alternative and is discussed in Chapter 6. The Staged Placement Loss Volume comes about as a result of not completing the initial fill in a single year, as discussed in the paragraph above. Advanced Renourishment Fill Volumes are discussed with each Alternative in Chapter 6. Sea Level Rise Volume is discussed in Chapter 6 and is listed in Table 6-2.

Table 7-1. Total Initial and Renourishment Volumes for Alternatives			
	Alt 1, No sand retention Structures (yd^3)	Alt 2, South Terminal Groin (yd^3)	Alt 3, South Detached Breakwater (yd^3)
Minimum Target Fill Volume	2,028,000	2,028,000	2,028,000
Advanced Initial Fill Volume	1,093,000	810,000	733,000
Staged Placement Loss Volume	78,000	78,000	78,000
Total Initial Fill Volume	3,199,000	2,916,000	2,839,000
Advanced Renourishment Fill Volume	694,000	610,000	591,000
Sea Level Rise Volume	112,000	112,000	112,000
Total Renourishment Volume	806,000	722,000	703,000
# Renourishment Events	9	9	9
Project Lifetime Volume	10,453,000	9,414,000	9,166,000

Recommended Alternative

The recommended alternative is Alternative 1, the no sand retention structure alternative. The other two alternatives do retain more sand within the project site and, based upon current estimates, have lower overall projected costs, but these benefits are marginal. Because the groin or breakwater would be located in the vicinity of a sediment transport nodal point, they are less effective sand retaining structures than they would otherwise be. The modeling results for the three alternatives (Figures 6-8 through 6-24) do not show substantial differences in project performance.

In the authors' professional judgment, the benefits of Alternatives 2 and 3 do not outweigh the potential risks involved. As has been shown numerous times, sand retention structures placed within the surf zone have the potential for unintended consequences. While best practices have been followed in their design for this project, their behavior cannot be known with certainty. Flaws in the project design, uncertainty in future

funding sources, extreme in weather patterns, or any of other numerous unexpected events all have the potential for causing this project to not perform as expected.

It is recommended that the other two alternatives be considered as adaptive management strategies. After initial project construction and monitoring has occurred, it may be found necessary to modify the project design. These alternatives (2 and 3) should be kept as options in such an eventuality.

8 Impact to Assateague Shoreline of Mining Offshore Shoals for Beach Fill Material

This section of the report assesses the potential impacts that mining of offshore shoals will have on the adjacent beaches. As material is removed from these shoals, the water depth changes. Since wave refraction is a function of the water depth, removal of material can significantly affect the longshore sediment transport on adjacent beaches. (See, for example, Combe and Soileau, 1987.) The analysis presented here closely follows the Minerals Management Service guidelines presented in Kelley, Ramsey, and Byrnes, (2001), referred to as MMS-2001-098 (available on the web at: http://www.mms.gov/itd/pubs/2001/2001-098.pdf).

The procedure used here was to refract offshore waves over the existing bathymetry into near-breaking depths. Then, the same offshore waves were refracted over bathymetry that had been modified by an appropriate increase in the depth in the borrow area(s). Both sets of resulting near-breaking waves were used to drive a sediment transport model, and the two sets of sediment transport results were compared. The amount of difference in the sediment transport for the two conditions was related to natural variation in the wave climate to determine if it was significant.

Deepwater (20+ meter depth) wave information was obtained from WIS data, and the numerical model, STWAVE, was used to transform these waves over the bathymetry to near-breaking depths. As discussed below, this procedure was only a slight modification of that presented in Chapter 5 to investigate the longshore sediment transport at Wallops Island. However, for this application, the full longshore sediment transport modeling capabilities of GENESIS were not required, since the main emphasis was on the differences in the sediment transport rate, rather than the rate itself. This is in accordance with the procedure described in MMS-2001-098. However, the same basic longshore sediment transport relationship that is used in GENESIS (the CERC formula) was also applied here in a simpler context.

Borrow Sites

As introduced in Chapter 3, three offshore sites were proposed as potential locations for obtaining beach fill material. Designated BlackFish Bank, Site A, and Site B, these are located offshore of the south end of Assateague Island in the vicinity of Fishing Point, as shown in Figure 8-1. Their location coordinates are given in Table 8-1. Coring analysis indicated that each of the sites held enough borrow material to satisfy the beach fill requirements of the project over its lifetime as given in Table 7-1.

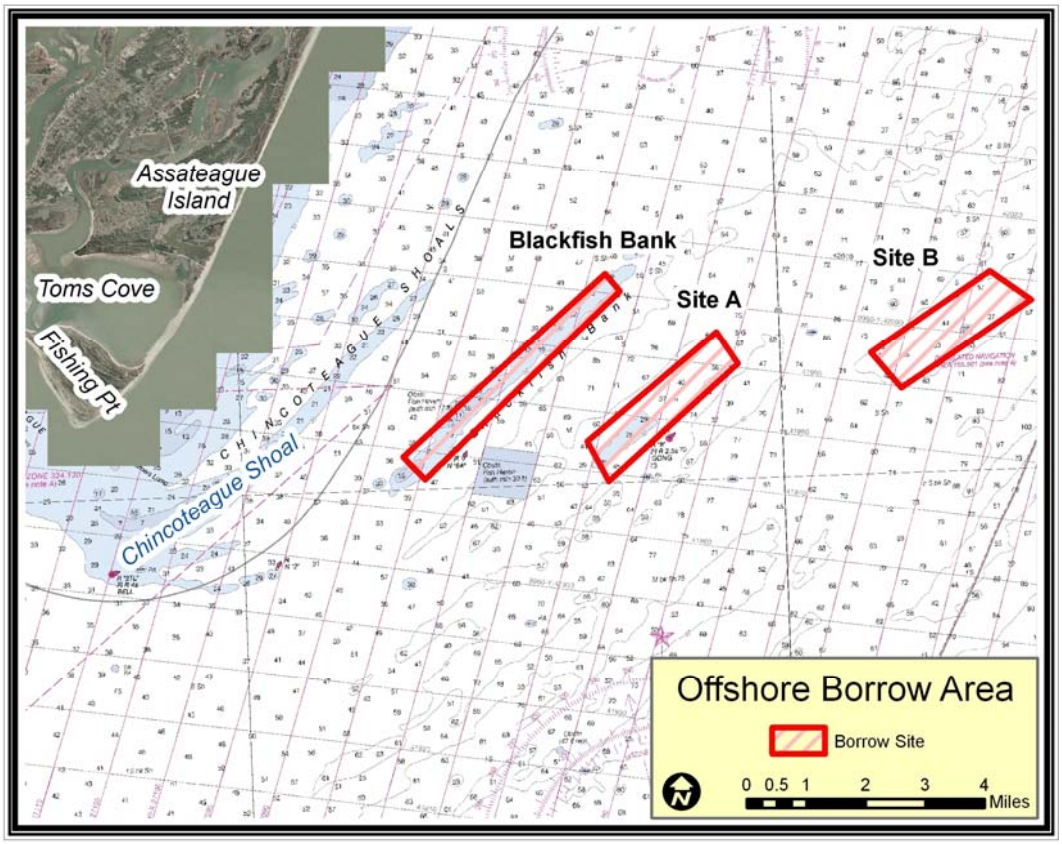

Figure 8-1. Offshore Borrow Site Locations.

The bathymetry offshore of much of the Delmarva Peninsula is extremely complex. McBride and Moslow (1991) indicate that the density of sand ridges in this area is greater than anywhere else in the country. Wikel (2008) discusses the dynamics of these shoals and their southwestward migration. The potential borrow sites are all located on separate sand ridges. Like other ridges in the area, these ridges trend from Northeast to Southwest, and the crests generally get deeper on further offshore ridges. Chincoteague Shoal is another sand ridge complex that is inshore of the three potential borrow sites. Because it is large and shallow, it greatly

modifies the nearshore wave climate, and helps to reduce the shoreline impacts of mining activities that would occur on any of the shoals further offshore.

Table 8-1. Coordinates of the Potential Borrow Sites

BlackFish Bank		Site A		Site B	
Latitude (°N)	Longitude (°W)	Latitude (°N)	Longitude (°W)	Latitude (°N)	Longitude (°W)
37.8414167	75.2835667	37.8437167	75.2268833	37.8631167	75.1387333
37.8845667	75.2196000	37.8693500	75.1859500	37.8819167	75.1012167
37.8802000	75.2152333	37.8614000	75.1796667	37.8746000	75.0887833
37.8358167	75.2771000	37.8338833	75.2205833	37.8541667	75.1297167
Easting	Northing	Easting	Northing	Easting	Northing
3783053.94	1172186.16	3788031.43	1172612.75	3795708.67	1175037.19
3788514.55	1177166.28	3791532.18	1175581.71	3798932.63	1177240.66
3788915.34	1176695.22	3792115.68	1174719.29	3800055.10	1176468.51
3783644.04	1171584.39	3788623.51	1171541.16	3796536.98	1174072.73

The three borrow sites are differently shaped, but are all nearly the same size of 2.0 mi^2 (5.2 km^2). Blackfish Bank is the closest to shore, at a little over 5 miles (8.5 km), and the shallowest, with a minimum depth of -13 ft (-4 m). Site A, on an unnamed shoal is approximately 7.5 miles (12 km) from the nearest shoreline and rises to a depth of -25 ft (-7.6 m). Site B, on another unnamed shoal is the furthest offshore at a distance of over 11 miles (18 km) and the deepest, with a minimum depth of -29 ft (-8.8 m).

STWAVE Model Grids

Coarse and Fine Grids

MMS-2001-098 recommends that a fine grid be used for the beach in the immediate vicinity of the borrow area and a coarser grid be used to look at transport rates on more distant portions of the beach. Since the grid used to model the sediment transport on Wallops Island (Chapter 5) only covered a portion of the needed bathymetry, two new grids, designated the Fishing Point Coarse and Fishing Point Fine Grids, were established for this analysis. The locations of the grids are shown in Figure 8-2; the Coarse grid in green and the Fine grid in pink. In this figure, the Wallops Island grid (in blue, discussed in Chapter 5), the borrow sites (in lime,

orange, and blue green), and two WIS stations (in black) are also shown for reference. The two Fishing Point grids shared the same offshore boundary. The also had the same orientation; the onshore direction is 300° (clockwise from North). This is slightly different than the Wallops Island Grid, whose onshore direction is 309°.

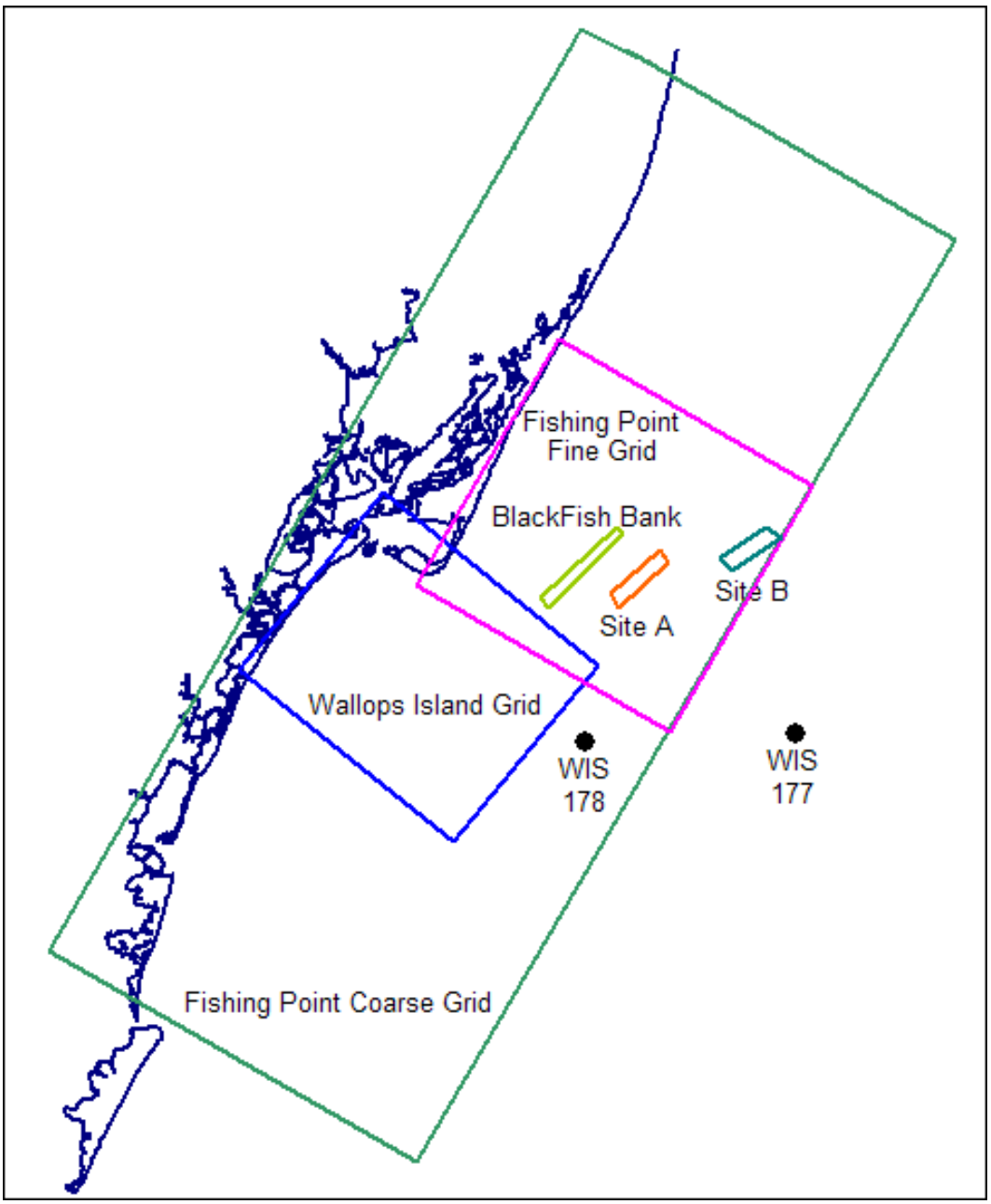

Figure 8-2. Location of STWAVE grids.

Bathymetry data were needed as input to the two STWAVE grids. These data were obtained from the same National Ocean Survey (NOS) source as described in Chapter 5.

Fishing Point Coarse Grid Description

The coarse grid covers 75 km (46.6 miles) of shoreline from Wachapreague Inlet in the south to a location near the Tingles Island Camping Area (part of Assateague Island State Park) which is 17.4 km (10.6 miles) north of the Maryland / Virginia state line. The grid stretches 30 km (18.6 miles) in the offshore direction. The cell size of the coarse grid is 200 m in both the cross-shore and along shore directions. The full grid parameters are listed in Appendix E, Table E-8. The bathymetry covered in this grid is shown in Figure 8-3. In this figure the near-shore save stations are shown in light blue. The color depth scale is given in meters. This grid was used to propagate waves from the nominal 20 meter depth at the right-hand side of the grid to the save stations near the shoreline along the left-hand side.

Fishing Point Fine Grid Description

The fine grid covers the south end of Assateague Island from the south tip at Fishing Point northward for 20 km (12.4 miles) to a point which is 3 km (2 miles) south of the Virginia / Maryland state line. The grid stretches 22.5 km (12.8 miles) in the offshore direction. The cell size of the fine grid is 40 m in both the cross-shore and along shore directions. Measuring in the alongshore direction from the south end of the coarse grid, the fine grid starts at 35,000 m (115,000 ft) and ends at 55,000 m (180,000 ft). The full grid parameters are listed in Appendix E, Table E-9. The bathymetry covered in this grid is shown in Figure 8-4.

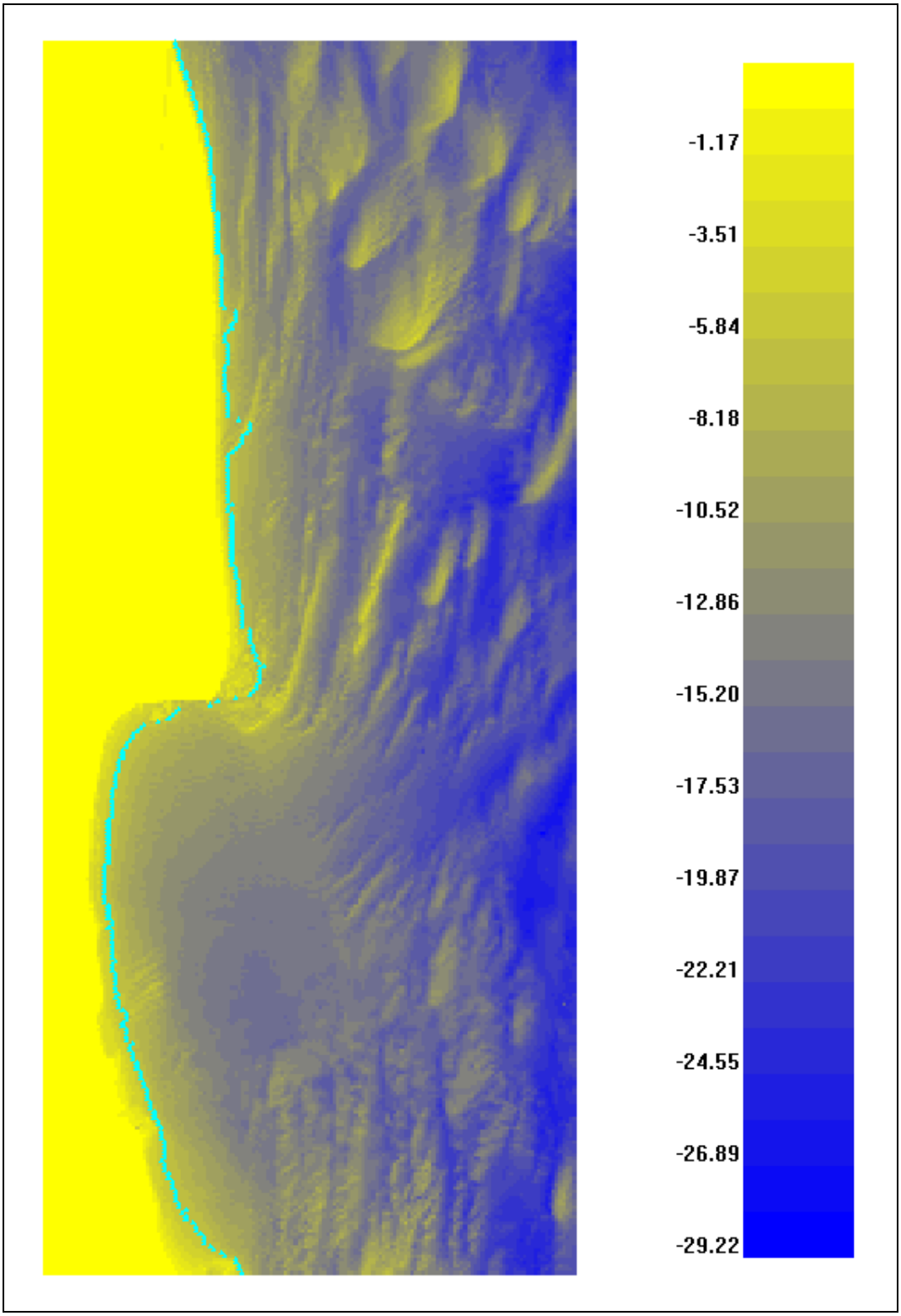

Figure 8-3. Fishing Point Coarse Grid bathymetry.

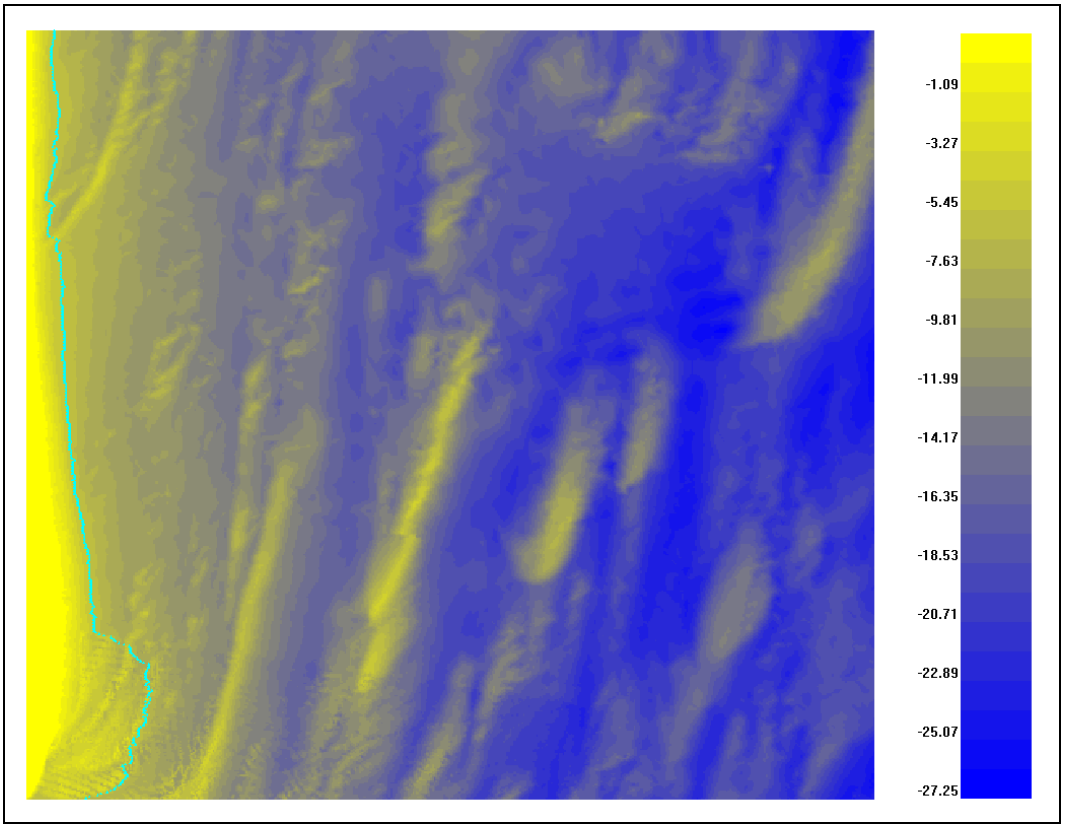

Figure 8-4. Fishing Point Fine Grid Bathymetry.

Cell Distribution within the Borrow Areas

A factor limiting the cell size of the coarse grid was the distribution and minimum number of grid points within the borrow sites. Table 8-2 shows that there were over 100 coarse grid cells within each of the borrow sites. While this is adequate to represent the bathymetry changes, the long slender shape of the BlackFish Bank borrow site was a concern. The distribution of these cells within the borrow sites is shown in Figure 8-5, and it is seen that BlackFish Bank is modeled by a minimum of only three grid cells in the cross-shore direction along several transects. This was considered a minimum number to properly resolve the refraction effects as waves transited the site. Sites A and B, being roughly the same size as BlackFish, but less elongated, had a more generous minimum number of 5 and 7 cells in the cross-shore direction, respectively. Thus, a 200 meter cell spacing was considered the maximum allowable for the coarse grid. This issue was not a concern for the fine grid because, with 40-meter cell spacing, it had a density of grid points that was 25 times as great as the coarse grid.

Table 8-2. Grid points within borrow areas						
Borrow Area	**BlackFish Bank**		**Site A**		**Site B**	
Grid Size	**Coarse**	**Fine**	**Coarse**	**Fine**	**Coarse**	**Fine**
Total points in borrow	134	3372	129	3239	132	3229
Cross-shore min pts	3	16	5	27	7	35
Cross-shore max pts	5	22	7	32	8	36
Along shore min pts	12	58	17	85	13	70
Along shore max pts	14	69	18	89	15	73

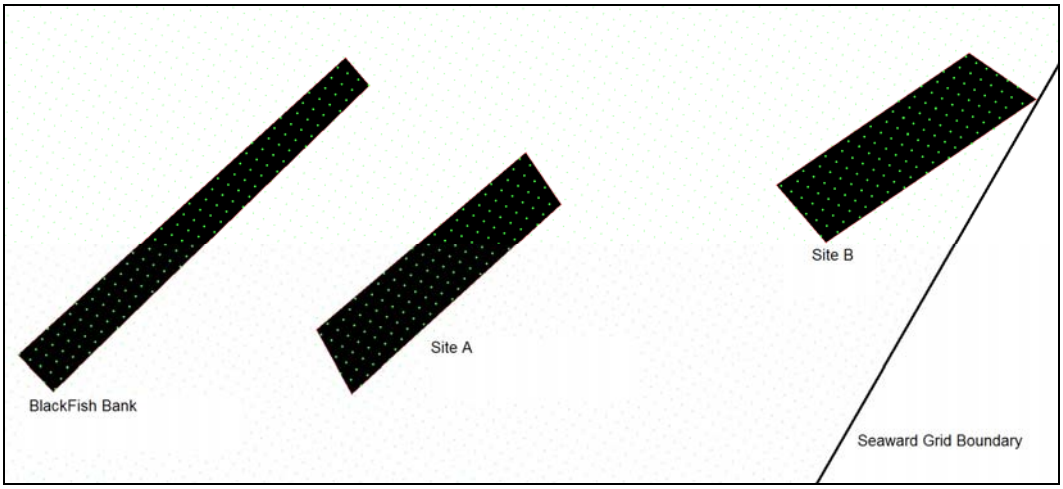

Figure 8-5. Portion of the STWAVE Coarse Grid showing cell locations within the borrow sites.

Dredging Modifications to the Borrow Sites

It is anticipated that a borrow site may be mined several times to supply material for the initial beach nourishment and each of the renourishments. Referring to Table 7-1, the maximum amount of fill material that would be required by the project over its lifetime would be of the order of 10 million cubic yards. The maximum change in wave refraction would occur once the entire volume was removed. Therefore, to determine the maximum impacts, wave refraction over the present bathymetry was modeled, as was wave refraction with 10 million cubic yards removed from each of the borrow sites.

How material would be dredged from the borrow areas is not known ahead of time. For this study, two material removal schemes were modeled. The first method was to remove the highest points within a borrow site down to an elevation that provided an adequate volume of material. This method, termed the Plane Method, would have the effect of turning

rounded hills or ridges into one or more flat mesa tops while leaving lower slopes and adjacent valleys unchanged. The second method, termed the Contour Method, was to remove the same depth of material from all points within the borrow site. This would have the effect of lowering the contour everywhere within the borrow site by a constant amount.

It is not assumed that either of these schemes would be adopted by a dredging contractor. Rather, the first method was assumed to be the one that would have the greatest shoreline impacts, and the second would have more modest shoreline impacts. The actual dredging would likely produce shoreline impacts that fall somewhere between the results for these two scenarios.

The effects of these two methods on each of the borrow sites is shown graphically in Figures 8-6 through 8-8. These figures are histograms that rank all the elevations within the borrow site from highest to lowest for each of the three sites. The blue line represents the present distribution of elevations. The pink line shows the distribution of elevations if the site were Planed, and the lime green line, if the site were Contoured. Table 8-3 lists the highest elevation remaining within the borrow site if the site were Planed and the constant amount the profile would need to be lowered if the site were Contoured. These values were calculated based upon the removal of 10,000,000 yards^3 of material from each borrow site.

Table 8-3. Borrow Area Characteristics

Borrow Area	Blackfish	Site A	Site B
Current Minimum Depth (ft)	13.5	25.0	29.0
Current Maximum Depth (ft)	51.3	70.2	64.5
Plane Depth (ft)	31.5	45.6	46.3
Contour Depth Change (ft)	4.7	4.8	4.9

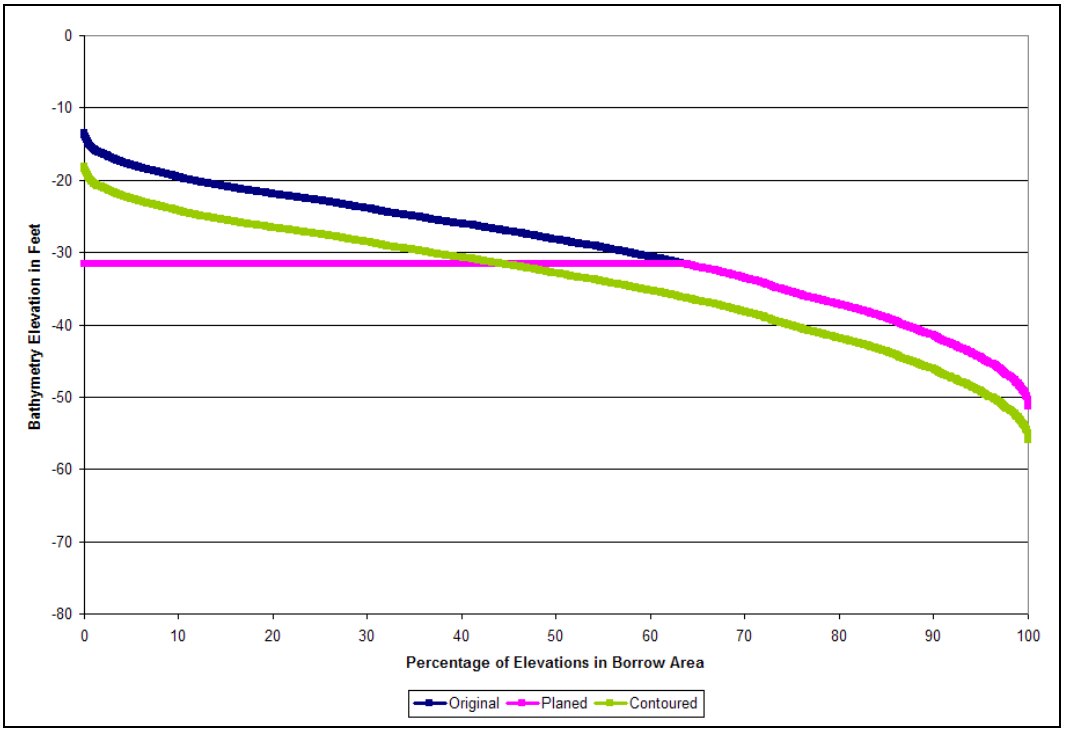

Figure 8-6. Histogram of BlackFish Bank depths for mining alternatives.

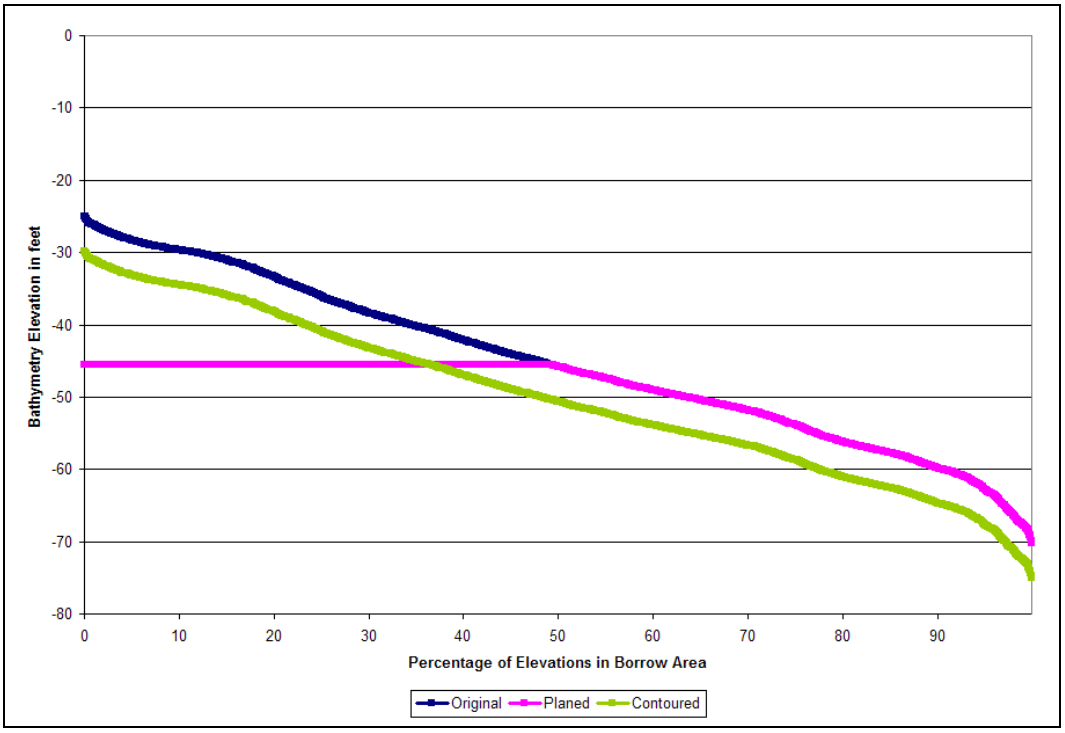

Figure 8-7. Histogram of Site A depths for mining alternatives.

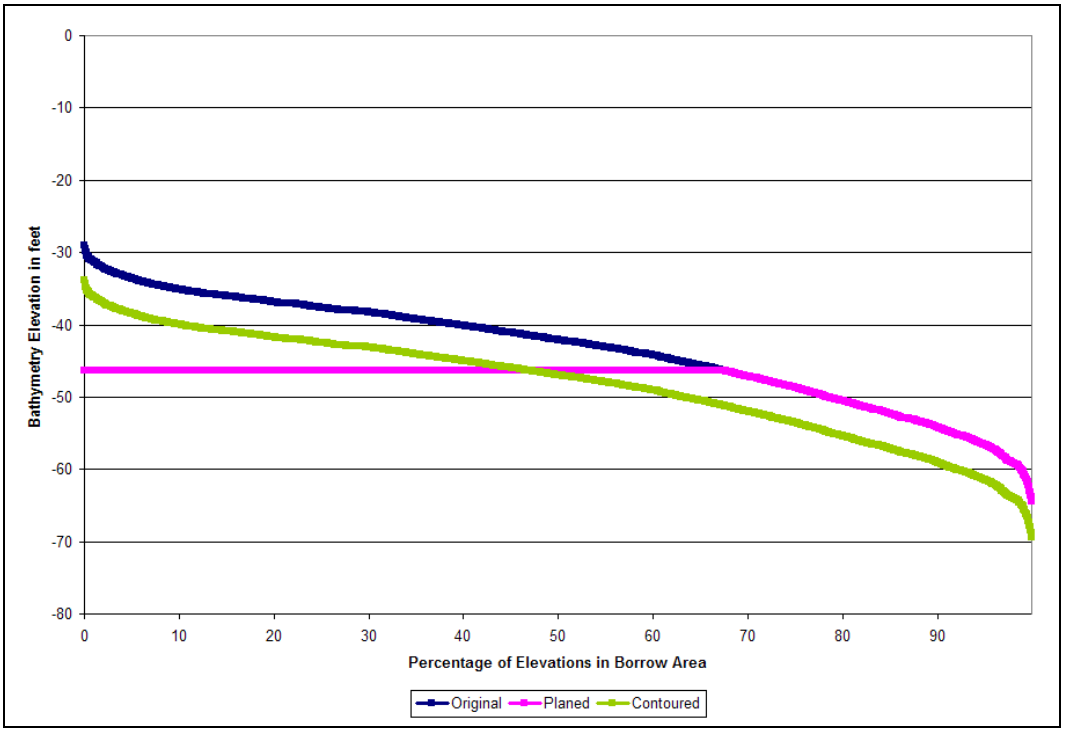

Figure 8-8. Histogram of Site B depths for mining alternatives.

STWAVE Grid Summary

Thus, 14 different bathymetry grids were developed for this analysis, as shown in Table 8-4. STWAVE was run using each of these grids.

Table 8-4. STWAVE Bathymetry Grids

	Coarse Grid	Fine Grid
As Is Bathymetry	X	X
Blackfish, Planed	X	X
Blackfish, Contoured	X	X
Site A, Planed	X	X
Site A, Contoured	X	X
Site B, Planed	X	X
Site B, Contoured	X	X

STWAVE Wave Climatology

For this analysis, wave data were obtained from a 20-year hourly hindcast (1980-1999) of wave heights, periods, and directions from WIS station 177, located at 37.75° N, 75.08° W, in 25 meters of water depth. This station is seaward of WIS station 178 used in the analysis presented in Chapter 5

and seaward of the seaward edge of the two Fishing Point grids, as shown in Figure 8-2.

These wave data were prepared for model use as described in Chapter 5, except as noted. As the grid orientation differed by 9° from the Wallops Island grid (to be better aligned with the shoreline orientation over the whole grid), the shore normal direction was 120°. The 20-year WIS wave climatology (175,320 hourly wave records) was characterized by binning the data into four peak spectral wave period bins, and twelve vector mean wave directions at the peak spectral frequency bins, as shown in Figure 8-9. Figure 8-9 shows the wave heights partitioned into nine bins for ease of comparison with Figure 5-3. However, for this analysis only one wave height bin, which contained all the heights, was used. The 47 period / angle bin combinations that were used are shown in Figure 8-10.

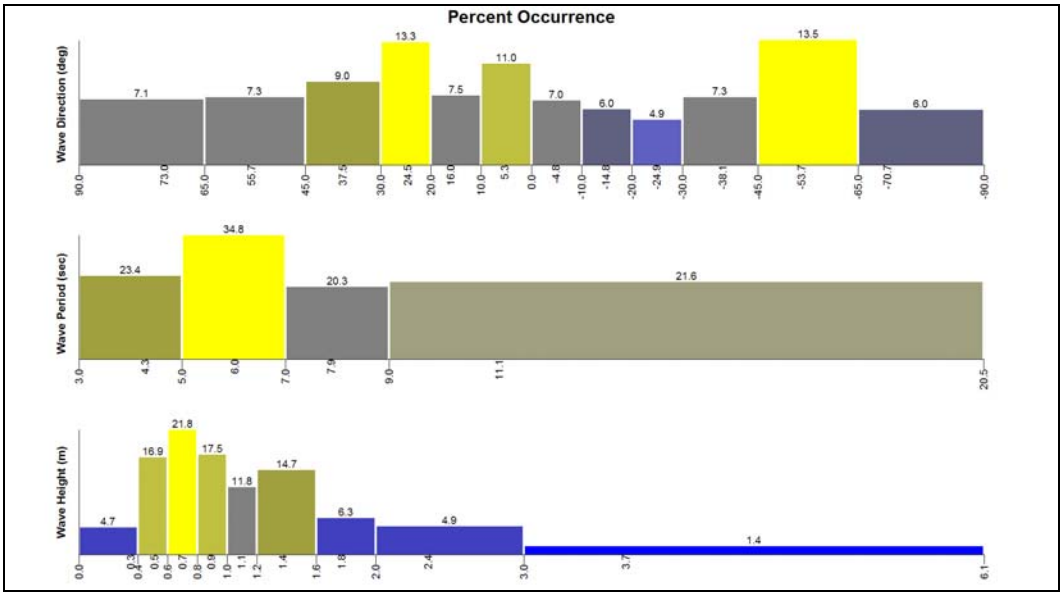

Figure 8-9. STWAVE Wave Height, Period, and Angle bins.

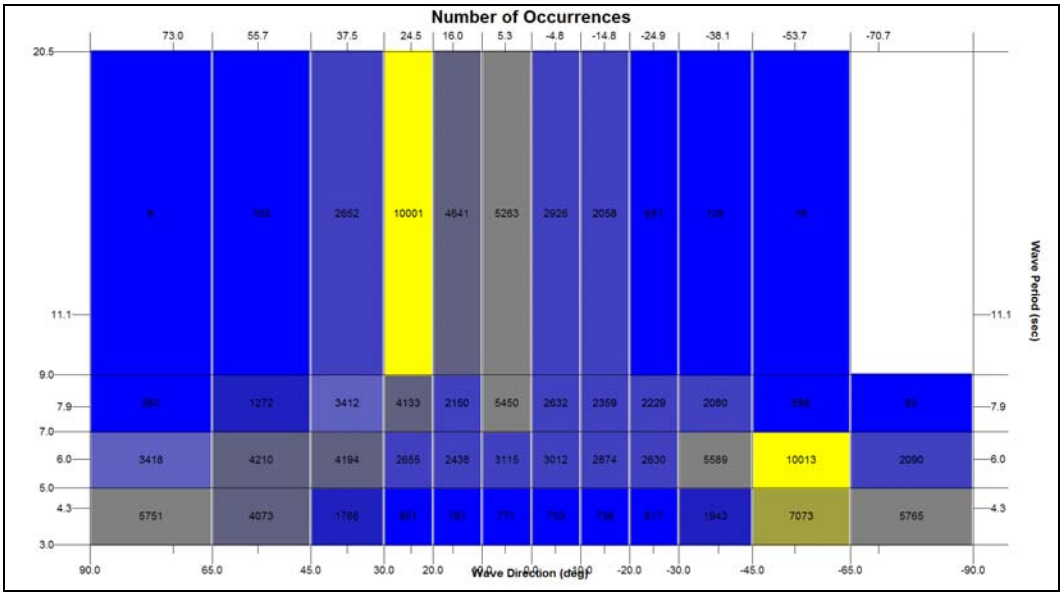

Figure 8-10. STWAVE block diagram of wave height vs. wave angle.

STWAVE was run using each of the 14 grids listed in Table 8-4 for the 47 bin combinations to transform the wave data from the offshore boundary of the grids to a near-breaking depth at the save stations. STWAVE model configuration parameters for these runs are listed in Table E-10 in Appendix E.

Sediment Transport Modeling

Following the STWAVE refraction analysis, sediment transport rates were calculated at each of the alongshore save station locations for each of the 14 grids for each hour in the wave record. Using the appropriate wave bin for each hour, the wave height, period and direction at the save station were obtained. These data were then transformed to breaking depth data using the methodology described in Gravens (1989). Then a longshore sediment transport rate was calculated using the CERC formula (Rosati, Walton, and Bodge, 2006). Repeating this procedure for the 20 years of the WIS data produced 20 yearly sediment transport rates for each shoreline location.

The significance of the offshore borrow site mining was determined using the methodology described in MMS-2001-098. The 20 yearly rates were averaged to obtain an overall average longshore sediment transport for each alongshore location. This was done for each of the 14 grids. For the transport rates calculated using the As Is bathymetry conditions, the yearly transport rates were combined into five 4-year groups and an

average was calculated for each group. The five averages were then used to calculate a 4-year standard deviation (*4Yr St Dev*). If this standard deviation is less than the magnitude of the difference between the average As Is transport rate and the average rate calculated for a mined grid at even a single location (ratio >1 at any location), the MMS guidelines indicate that the shoreline impact is unacceptably large for that offshore shoal mining scenario.

Sediment Transport Rate Results

At each shoreline location, an impact factor was calculated using the formula:

$$Factor = \frac{Abs(A - B_i)}{(4Yr\ St\ Dev)} \tag{8-1}$$

where:

A = the 20-yr average transport rate calculated using the "As Is" conditions, and

B_i = the 20-yr average transport rate derived from one of the altered bathymetries.

Any factors that exceeded 1 would indicate an unacceptably large shoreline impact.

The transport rate analysis results are shown in Figures 8-11 through 8-13 for BlackFish Bank, Site A, and Site B, respectively. The left-hand panel of each figure shows the shoreline, the offshore bathymetry, and the borrow site. The fine grid results are displayed for the area between the pink lines; the coarse grid results are displayed outside of those lines. The center panel of each figure shows the factor number for each shoreline location that is the result of material being Planed from the borrow site. The right hand panel shows the same curve, but based upon the borrow material being removed by Contouring.

The BlackFish Bank Planed analysis yielded three locations where the Factor exceeded one. The Factor did not exceed one in any of the other analyses. (The coarse grid analysis included the region covered by the fine grid. These coarse grid data results are not shown, but in general values

were less than for the fine grid results, and at no location on any coarse grid did the factor exceed one.

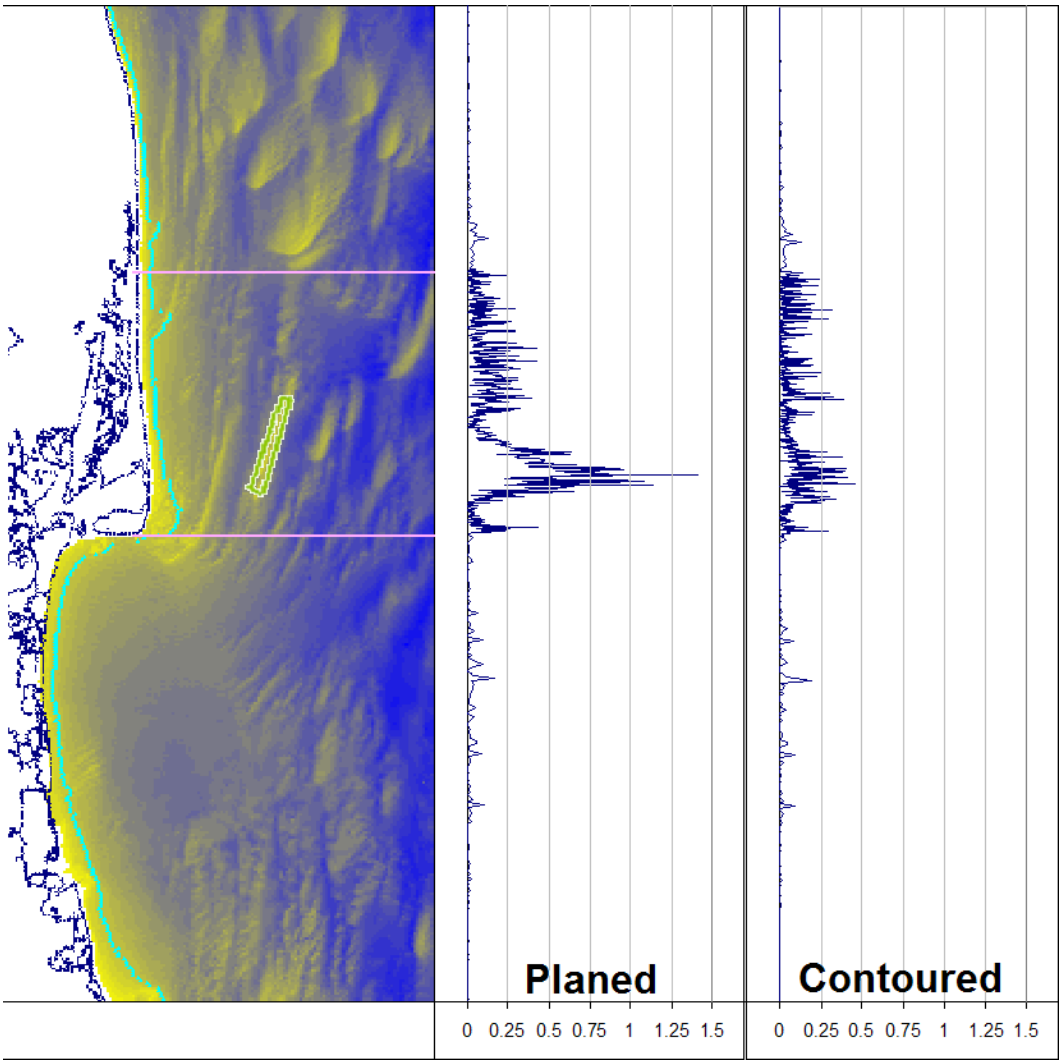

Figure 8-11. Impact Factor Results for BlackFish Bank Borrow Site.

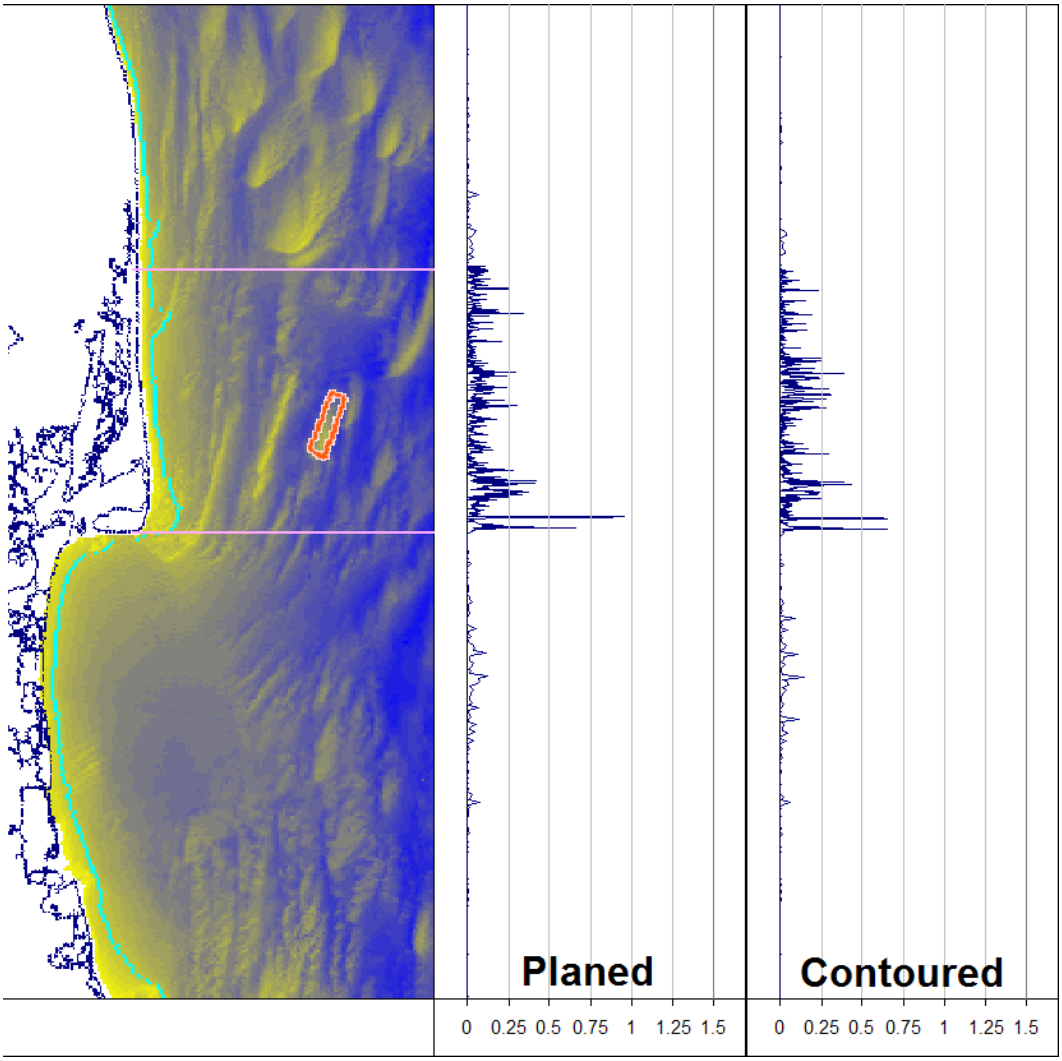

Figure 8-12. Impact Factor Results for Borrow Site A.

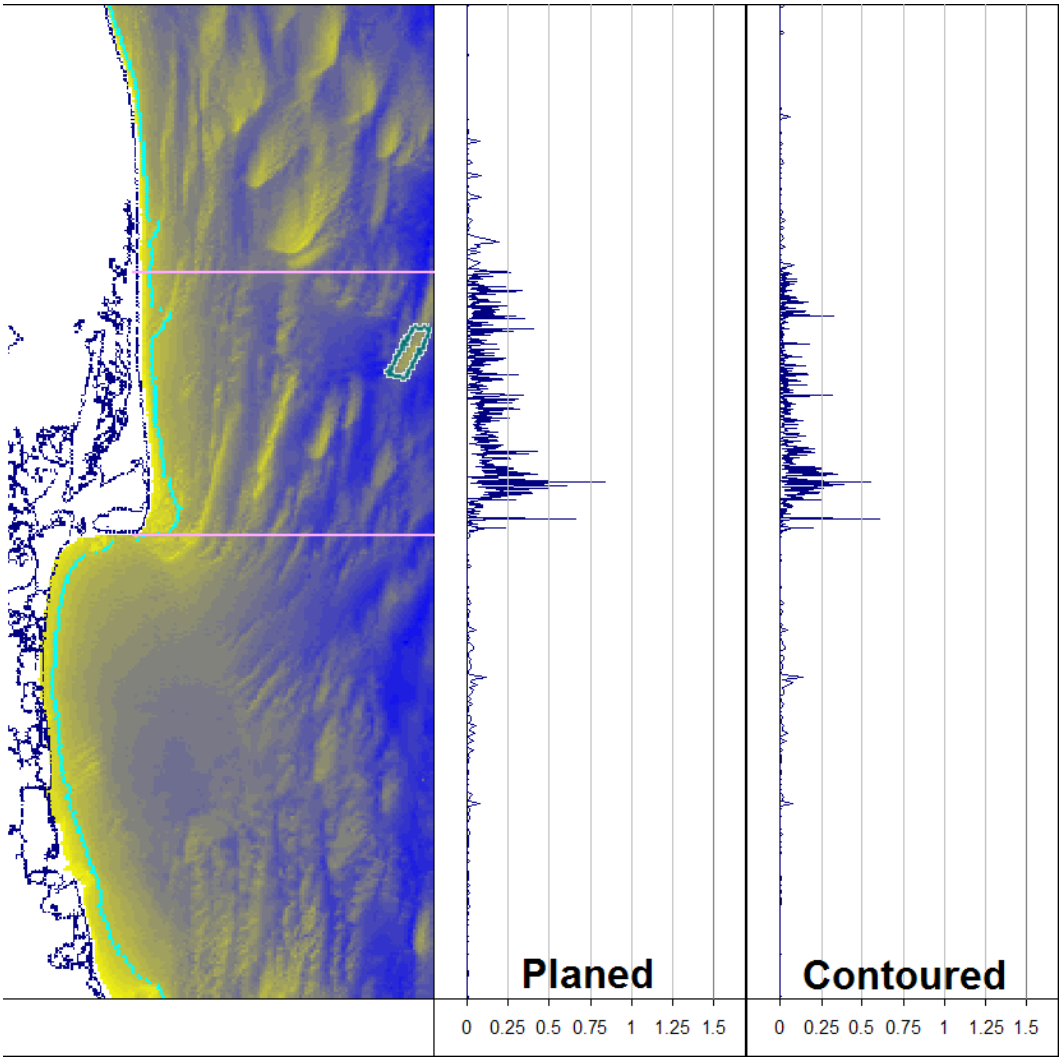

Figure 8-13. Impact Factor Results for Borrow Site B.

Discussion

Removing material from the borrow sites by Planing was included in the analysis not because this was expected to be the methodology used in actual dredging operations, but because it was assumed this would help readily identify less acceptable borrow site locations. By any of several measures, it is clear that the BlackFish borrow site would have a greater shoreline impact than either of the other two borrow sites. This is seen in Table 8-5, which shows the number of locations on the six graphs above where the Factor calculations (equation 8-1) exceed 1.0, 0.75, 0.5, and 0.25.

Table 8-5. Number of Eq 8.1 Exceedence Locations					
		1.0	0.75	0.50	0.25
BlackFish	Plane	3	12	36	111
	Contour	0	0	0	25
Site A	Plane	0	2	3	19
	Contour	0	0	3	15
Site B	Plane	0	1	3	43
	Contour	0	0	2	13

The fact that dredging BlackFish Bank would have a greater shoreline impact than dredging either of the other two shoals is hardly surprising. It is expected that borrow sites in the shallowest water and closest to shore will have the greatest shoreline impacts. Deeper shoals have less ability to refract waves, and greater distances to the shoreline allow the refraction effects to diffuse over a broader area, thus making a less significant impact at any one location. In addition, because Blackfish Bank and particularly Chincoteague Shoals are large shallow nearshore features (Figure 8-1), they exert a significant influence on the wave refraction by causing waves approaching from any direction to tend to align with the bottom contours. Thus, their existence helps to reduce the shoreline impacts that would be caused by mining shoals further offshore.

As discussed in MMS 2001-098, comparing the change in the transport rate caused by dredging to the natural wave variability (as represented by the 4-year Standard Deviation) is a superior method of determining dredge site acceptability when compared to other schemes that have been proposed. However, it is not perfect. Removing offshore borrow site material does not increase the variability in the longshore sediment transport rate so much as it introduces a constant bias in that rate. That is, the quantities in the numerator and denominator of Eq 8-1 are related, but are not the same statistical type. The numerator is the difference of two means, while the denominator is a standard deviation. It is not clear that a value for this factor of < 1 equates to a negligible long term shoreline impact.

The dynamic nature of this area was discussed in Chapter 2 along with the expected continuing occurrence of over-washes and inlet breaches in the Tom's Cove region of Assateague Island during the life of this project. One

of the major goals of the National Park Service's management of Assateague National Seashore is to keep it in as natural a state as possible. Therefore, it is important to minimize any offshore mining effects on the shoreline sediment transport. This modeling effort has shown that the major shoreline impacts from mining any of the proposed borrow sites will be generally in the Tom's Cove area.

Therefore, it is strongly recommended that BlackFish Bank be removed from further consideration as a potential borrow site for this project. It is easily possible that additional modeling could show that a limited amount of material could be removed from that shoal without exceeding MMS guidelines. Indeed, this analysis has shown that the entire 10,000,000 yd^3 could be removed by the reasonable method of Contouring without exceeding MMS guidelines. However, that misses the point that this analysis has shown that this is a marginal site, and that other, more desirable, options are available.

The analysis has shown that Sites A and B are acceptable by MMS guidelines, and that they have fewer potential shoreline impacts than the BlackFish Bank site. In comparing Site A with Site B, this analysis has shown that the overall level of shoreline impact is roughly equivalent for the two sites (Table 8-5). However, comparing Figures 8-12 and 8-13, it is seen that site B produces somewhat larger impacts along the narrow Tom's Cove shoreline than Site A. This fact, in addition to other factors not considered in this chapter (Site A is closer to Wallops Island than Site B and thus has lower transportation costs, Site A sampled grain sizes are a little coarser than Site B (Figure 3-3, and Appendix A), no significant cultural artifacts were found at either site, similar biological organism densities were found at both sites), all support the selection of Site A as the recommended offshore borrow site.

9 On-shore Mining of the North End of Wallops Island for Beach Fill

A partial alternative to the offshore borrow sites exists on the north end of Wallops Island. The beach in this area is rapidly accreting, and the rate is expected to substantially increase as a result of the adjacent fill project. The potential borrow area is shown schematically by the red triangle in Figure 9-1.

Figure 9-1. General area of on-shore borrow site at the north end of Wallops Island.

The exact limits of the borrow area are intentionally undefined at this time as they will undoubtedly vary between mining events in response to: the

volumes and patterns of accretion, the varying suitability of the sediment, Chincoteague Inlet dynamics, changes in vegetative cover, and biological factors, among others.

Sediment Budget

It is not possible to develop a comprehensive sediment budget for the north end of Wallops Island because of the lack of available data. It is clear that the area received sediment from further south on Wallops Island and from Fishing Point. The area also undoubtedly loses material to the interior shoals of Chincoteague Inlet.

GENESIS modeling has shown that, on average, approximately 40,000 yds^3/yr arrives in this area by longshore transport from further south along the Wallops Island shoreline (Chapter 5). Once the beach fill is placed, that volume is expected to increase to 100,000 to 150,000 yds^3/yr for any of the alternatives.

From the pattern of shoreline accretion, it is clear that substantial amounts of beach material cross Chincoteague Inlet from Fishing Point to the north end of Wallops Island. Large ebb shoals migrate westward across the inlet and weld onto the shoreline, causing the very large bulge in the shoreline. However, these are episodic events and their rate is not well documented. Additional material is dredged from the inlet channel and deposited in an offshore disposal site (Chapter 3, Table 3-3).

Since almost all inlets have been shown to be sediment sinks (e.g., Dean and Walton, 1975), it is assumed that Chincoteague Inlet sequesters sand from both adjacent beaches in its flood shoals, however, the rates are not known. What is clear is that the north end of Wallops Island is accreting. Therefore, more sand is being delivered to this area than is leaving.

Site Suitability

Obtaining fill material from this area is an attractive alternative for several reasons:

- There are a very limited number of structures on the island north of the seawall and none of these would be negatively impacted by

mining the beach area. NASA has no plans for new construction in the area.

- The recycling of project fill material is an encouraged USACE policy, where practical, because it will reduce the volume of new fill material needed (and thus the overall disturbance to the environment) over the lifetime of the project.

- Limited analysis (discussed in Chapter 3) has shown that the native material has a D_{50} in the range of 0.25 mm and is suitable as fill.

- Obtaining fill from the site would be cost effective when compared with the costs from offshore sources. This process would most likely be accomplished with large earth moving equipment (pan/scraper) or off road dump trucks in the subaerial (dry) portion of the beach. NOTE: this is just an approximate area not the exact borrow area.

If the initial fill placement is made from offshore sources, the material being transported north to this site will have an expected median grain size of 0.29mm. This will mix with the native material producing a sediment with a D_{50} finer than 0.29mm. The beach fill volume calculations were based upon the fill material having a D_{50} of 0.29mm. The use of finer material will require a one-time additional volume to adjust the beach profile. Assuming the resulting mixture has a D_{50} of 0.25 mm, the one-time profile adjustment volume would be 292,000 yds^3. For other D_{50} sizes, see Table 6-1.

Plan

It is anticipated that the initial fill material will be derived from an offshore borrow site (Chapter 8). The monitoring program will provide detailed information on grain sizes and available volumes on the north end of Wallops Island during renourishment events. Therefore, individual event decisions can be made for whether none, some, or all of the required renourishment volume should be obtained from this adjacent onshore site. For planning purposes, it is reasonable to assume that 50% of the overall needed renourishment volume will be derived from the onshore site.

10 Shoreline Impacts from Seawall Extension

As discussed in Chapter 7, an extension of the southern end of the rock seawall is planned for Year 1 of the project, and the first beach fill placement is planned for Year 2. This section of the report assesses the potential impacts to the shoreline that may occur during the time interval between the construction of the seawall extension and the initial beach fill. The shoreline along the south end of Wallops Island is eroding. The fact that sand would be sequestered behind a seawall extension that would otherwise have eroded will lead to the potential to exacerbate the erosion on the adjacent shoreline.

The extent of this exacerbated erosion during the initial implementation of this project is the focus of this chapter. This is a temporary condition. Once the initial beach fill is in place, the model results presented in Chapter 6 indicate that the shoreline south of the project (south end of Wallops Island and north end of Assawoman Island) will stop eroding and start accreting.

GENESIS Modeling Conditions

The shoreline response was examined by running the GENESIS model described in Chapter 5. For this application, the 2005 shoreline (the most recent complete shoreline available) was used in the model as the initial shoreline. As this modeling effort was intended to represent the time before any sediment placement, no beach fills were included in the model runs. As the preferred alternative has no sand retention structure at the south end of the project, no groin or detached breakwater were included in the modeling.

NASA's current plan is to construct a 1500 ft southern extension onto the end of the current rock seawall. This would provide the MARS launch facility with seawall protection. However, NASA is exploring funding possibilities to extend the seawall further to the south up to 4600 ft, the location of the south camera stand and the southern end of the beach restoration project. To represent various potential designs, seawall extensions of 1500, 3000, and 4600 ft were modeled as shown in Figure

10-1, and shoreline responses for these cases were compared to the zero extension ("as is") condition. Because of model grid spacing and other considerations, the actual seawall extension distances modeled were closer to 1680, 3120, and 4560 ft, respectively, but these distances are referred to by their nominal 1500, 3000, and 4600 ft lengths.

Figure 10-1. Potential seawall extensions modeled in this study.

The results presented below are based upon average shoreline values. These model results were obtained by driving the model with 20 different 4-year wave blocks, and averaging the results, as described in Chapter 5. The 95% confidence intervals were also calculated from the 20 shoreline realizations.

The cross-shore location of the seawall relative to the shoreline has a dominant effect on the extent of the adjacent shoreline impacts. If the seawall is placed far enough landward of the shoreline, erosion will not reach the seawall and the seawall will cause no adjacent shoreline impacts. Initial modeling was done to determine appropriate cross-shore seawall locations. The most significant impacts occur when the seawall is placed along the initial model shoreline. It was determined that only minimal impacts would occur if the seawall were located 10 yards (9.1 m) landward of the shoreline. Therefore, these two cross-shore seawall placements (at shoreline and 10 yards inland) were fully modeled and their results are presented below.

NASA is committed to the project schedule outlined in Chapter 7 with the seawall construction occurring in Year 1 and the initial beach fill in Year 2. However, since federal funding cannot be assured for the out-years of multi-year projects, the modeling also looked at the effect of delays in implementation of the beach fill after a seawall extension was constructed. While any delay is unlikely, if one were to occur, it would most likely mean

that there was a 2-year time period between seawall extension construction and beach fill placement. Longer delays, which seem a remote possibility, were lumped into a generic 10-year period between seawall construction and beach fill placement. Therefore, the modeling looked at
1-year, 2-year, and 10-year shoreline impacts. Except as noted above, the GENESIS modeling parameters are provided in Appendix Tables E5 and E7.

Modeling Results

Shoreline Change

Figure 10-2 shows model predictions of shoreline positions for the portion of the GENESIS grid that is south of the existing seawall, a distance of about 2 miles (see Figure 5-5). Each shoreline is an average of the results of 20 model runs that were driven with the 20 different four-year wave blocks discussed in Chapter 5. This figure is for a 1500 ft extension built at the shoreline. Similar plots for 3000 ft and 4600 ft extensions at the shoreline are shown in Figures 10-3 and 10-4. At this resolution, little difference can be seen in the shoreline position for seawalls built at the shoreline and 10 yds inland.

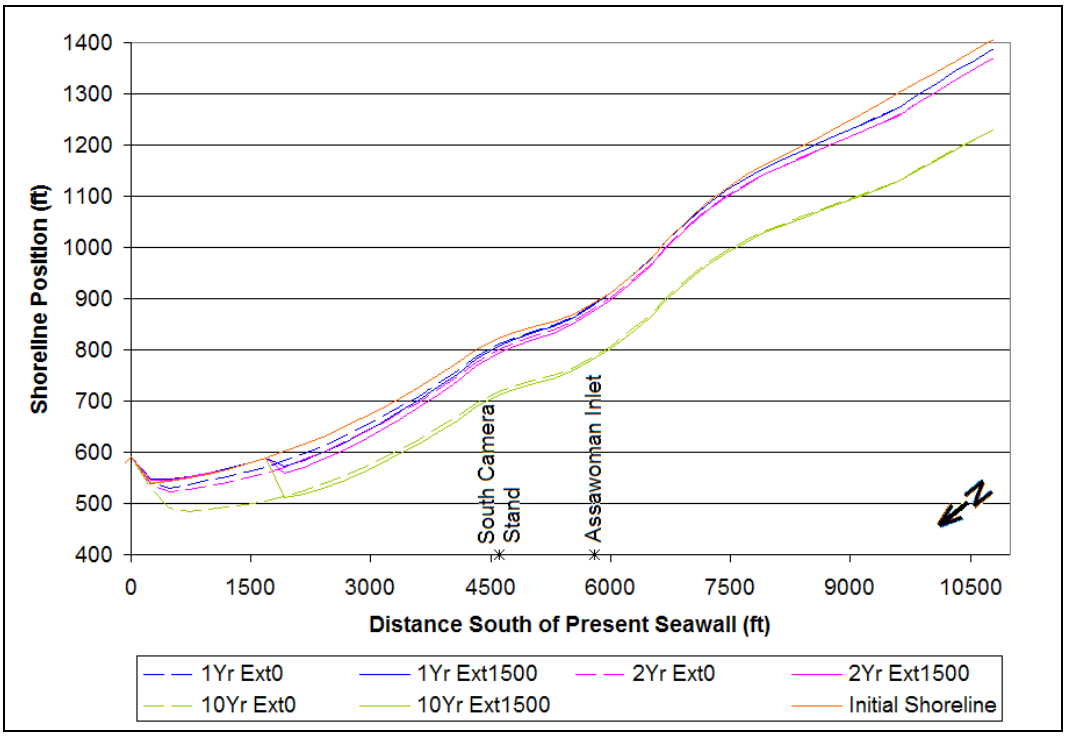

Figure 10-2. Modeled shoreline positions south of the existing seawall at 1, 2, and 10 years comparing the no extension condition to a 1500 ft seawall extension at the shoreline.

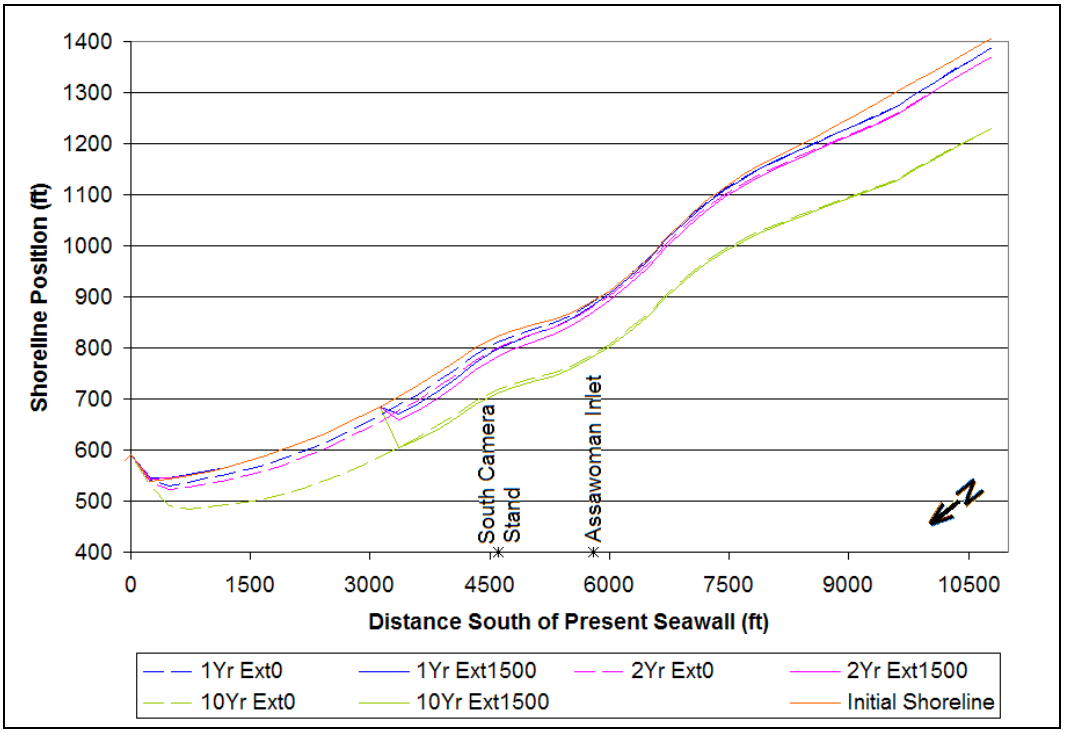

Figure 10-3. Modeled shoreline positions south of the existing seawall at 1, 2, and 10 years comparing the no extension condition to a 3000 ft seawall extension at the shoreline.

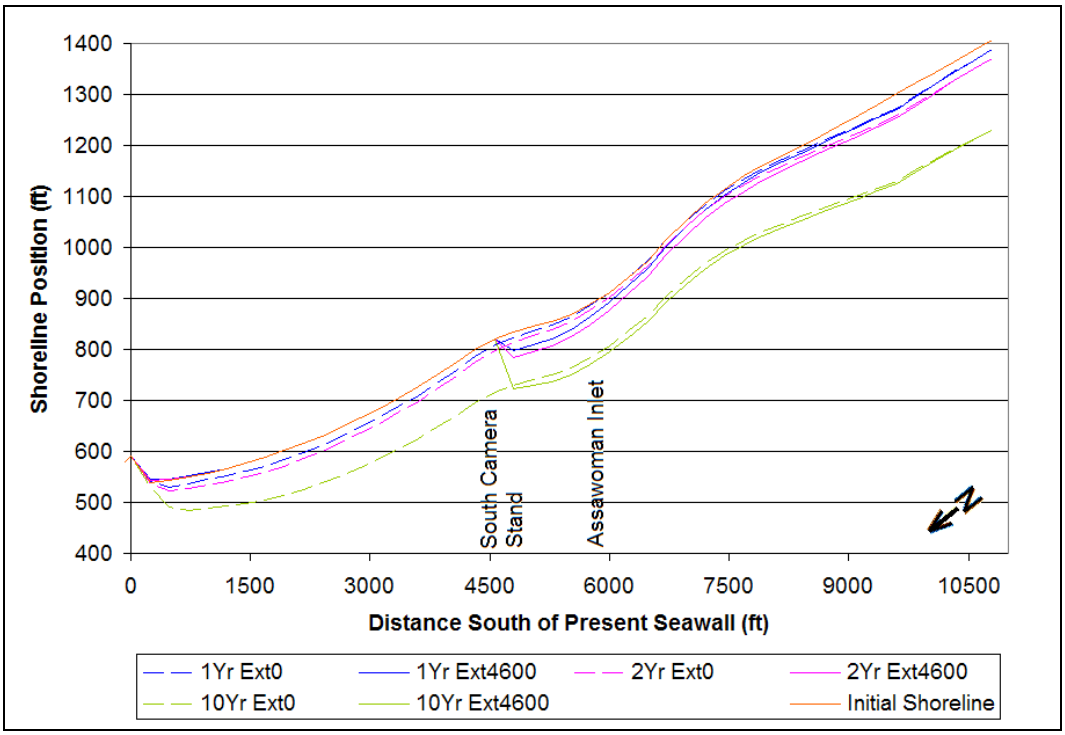

Figure 10-4. Modeled shoreline positions south of the existing seawall at 1, 2, and 10 years comparing the no extension condition to a 4600 ft seawall extension at the shoreline.

To minimize clutter, the 95% confidence interval shorelines are not included in these figures. It should also be noted that there is about a 5 to 1 vertical to horizontal distortion in these figures.

1-Year, 1500 ft Extension

Figure 10-5 covers the same shoreline location south of the existing seawall as Figures 10-2 through 10-4. This figure show the predicted difference in the shoreline position after 1 year for a 1500 ft seawall built at the shoreline. In this figure, the Average (blue) line shows the difference in the two blue lines (dashed and solid) in Figure 10-2. In this figure it can be seen that the greatest increase in the erosion (13.2 ft (4.0 m)) occurs immediately south of the end of the 1500 ft seawall and that the difference asymptotically decreases to zero to the south. Within the first 1500 ft, the seawall has stopped the erosion, so this difference shows up as a positive quantity. However, this positive value should not be interpreted as accretion; it is a decrease in erosion when compared to the no seawall extension condition. This pattern - a decrease in erosion at the seawall extension and a maximum increase in erosion just south of the end of the extension with an asymptotic decrease to zero further to the south - occurs in each of the conditions which were modeled.

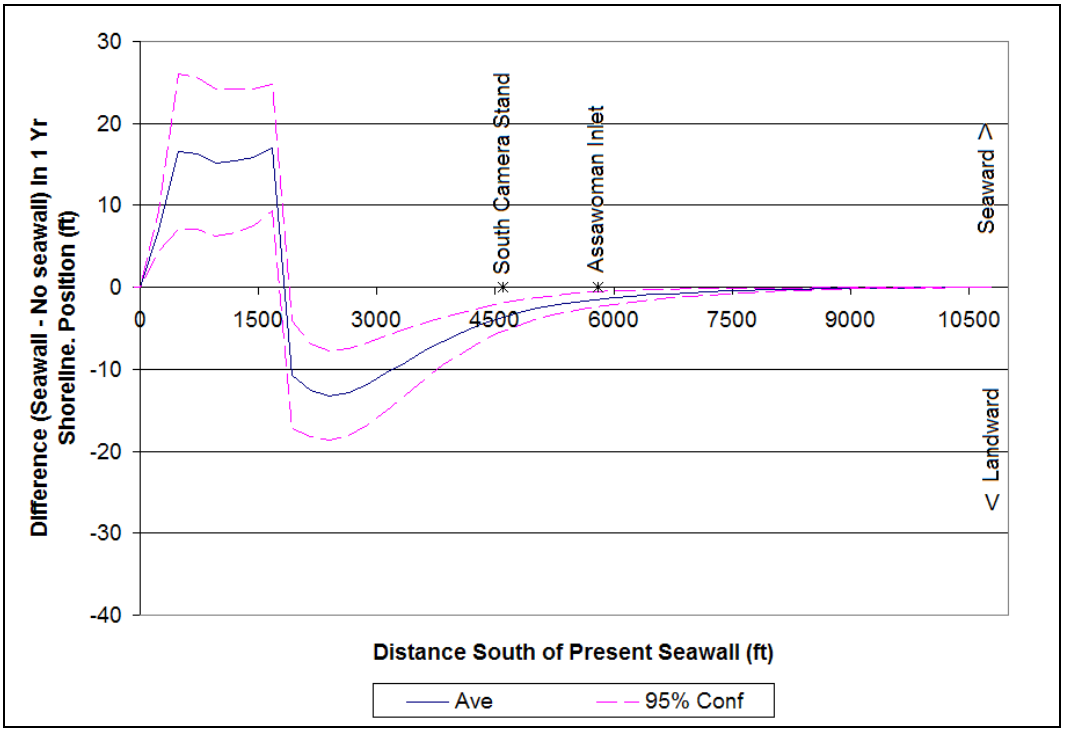

Figure 10 5. One year shoreline difference between 1500 ft seawall extension at the shoreline and no seawall extension.

Figure 10-6 shows the same results as Figure 10-5 except that the seawall is placed 10 yards landward of the shoreline. Placed at this location, the seawall causes substantially less negative impacts to the south of the extension (max about 2.4 ft (0.7 m)).

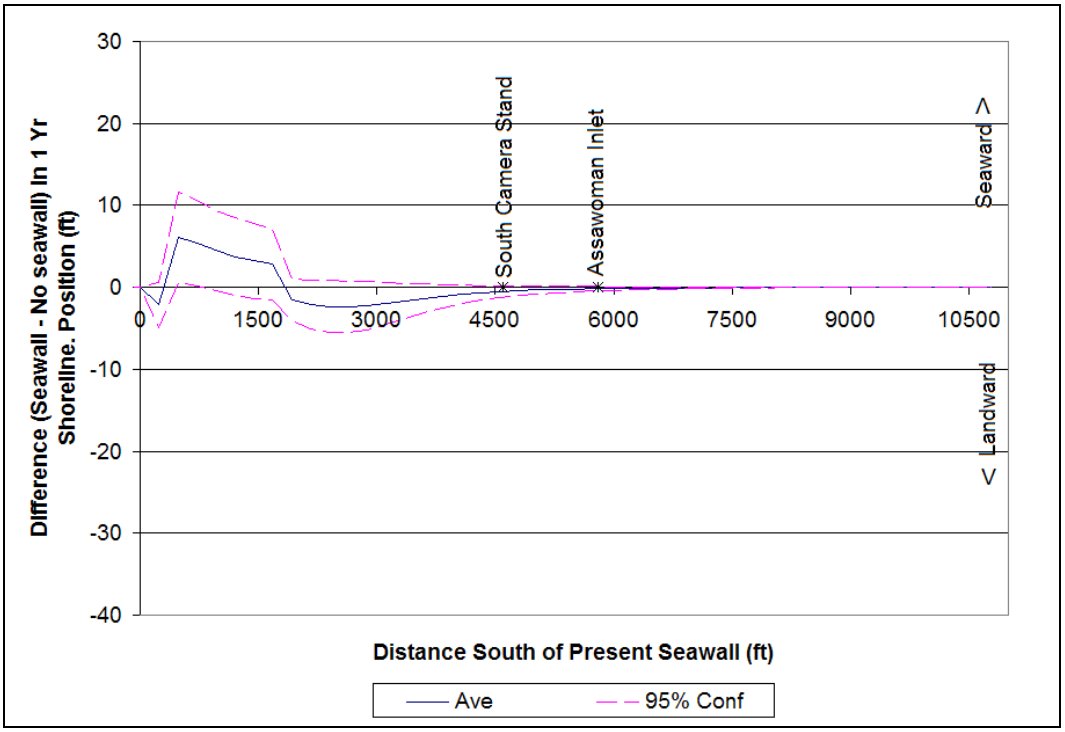

Figure 10 6. One year shoreline difference between 1500 ft seawall extension 10 yards landward and no seawall extension.

1-Year, 3000 ft Extension

Figures 10-7 and 10-8 show the same conditions as Figures 10-5 and 10-6, respectively, except that these are for a 3000 ft seawall extension. In Figure 10-7, the Average (blue) line shows the difference in the two blue lines in Figure 10-3. Again, there is much less impact from the seawall that is 10 yds inland from the shoreline. The maximum increase in erosion is 20.1 ft (6.1 m) in Figure 10-7, but only 3.7 ft (1.1 m) in Figure 10-8.

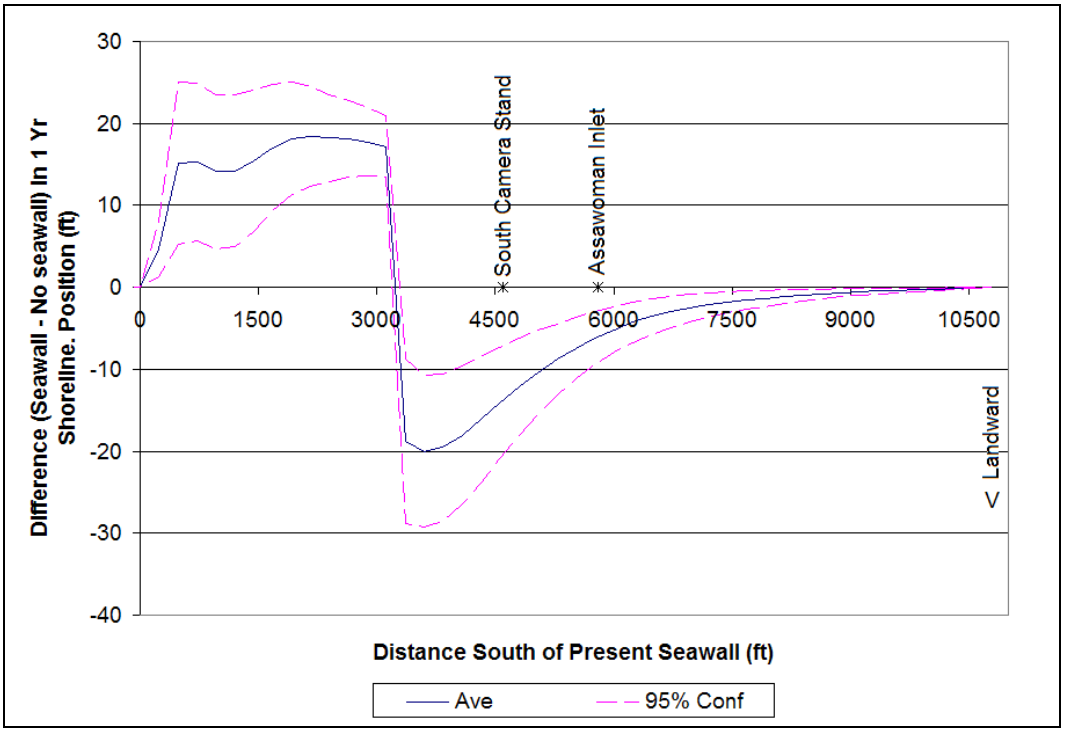

Figure 10-7. One year shoreline difference between 3000 ft seawall extension at the shoreline and no seawall extension.

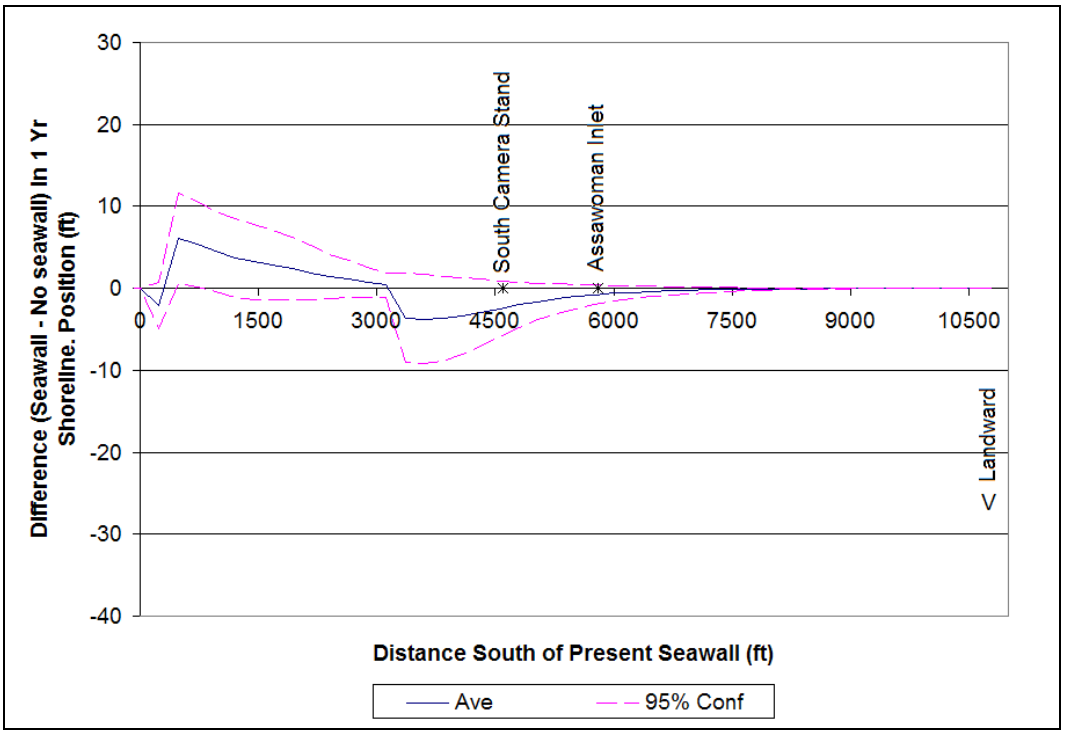

Figure 10-8. One year shoreline difference between 3000 ft seawall extension 10 yds landward and no seawall extension.

1-Year, 4600 ft Extension

Figures 10-9 and 10-10 show the same conditions as above, except that these are for a 4600 ft seawall extension. The seawall at the shoreline, Figure 10-9, shows a maximum erosion increase of 27.5 ft (8.4 m) while the 10 yd landward seawall has a more modest maximum erosion increase of 4.3 ft (1.3 m)

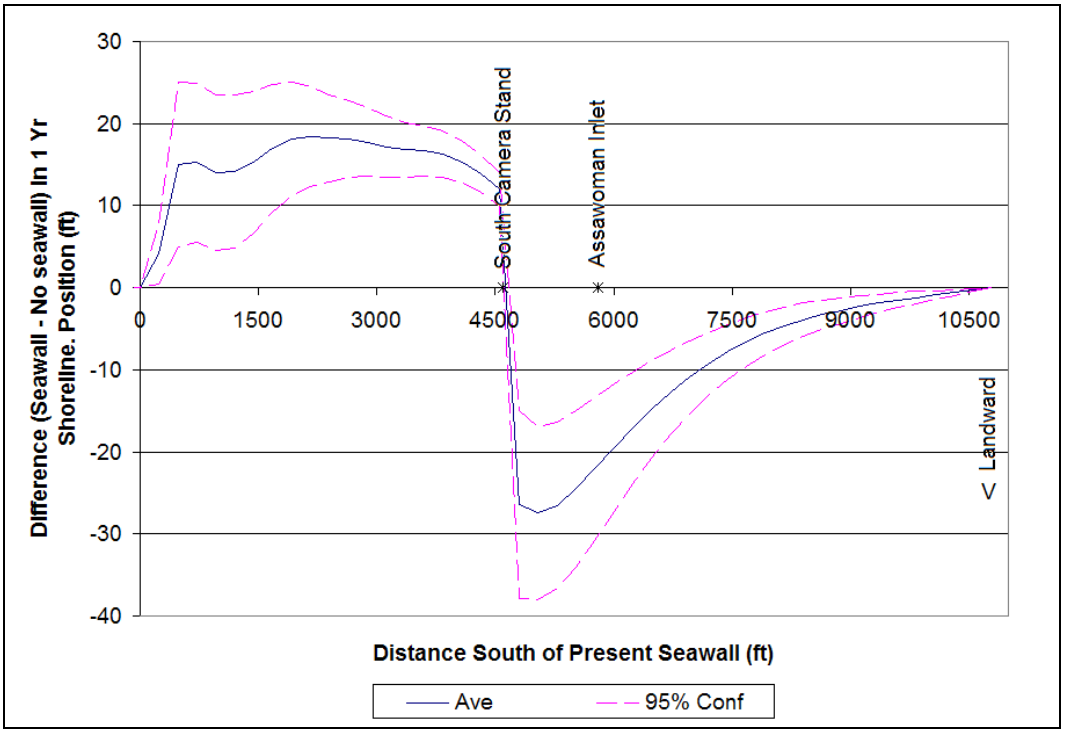

Figure 10-9. One year shoreline difference between 4600 ft seawall extension at the shoreline and no seawall extension.

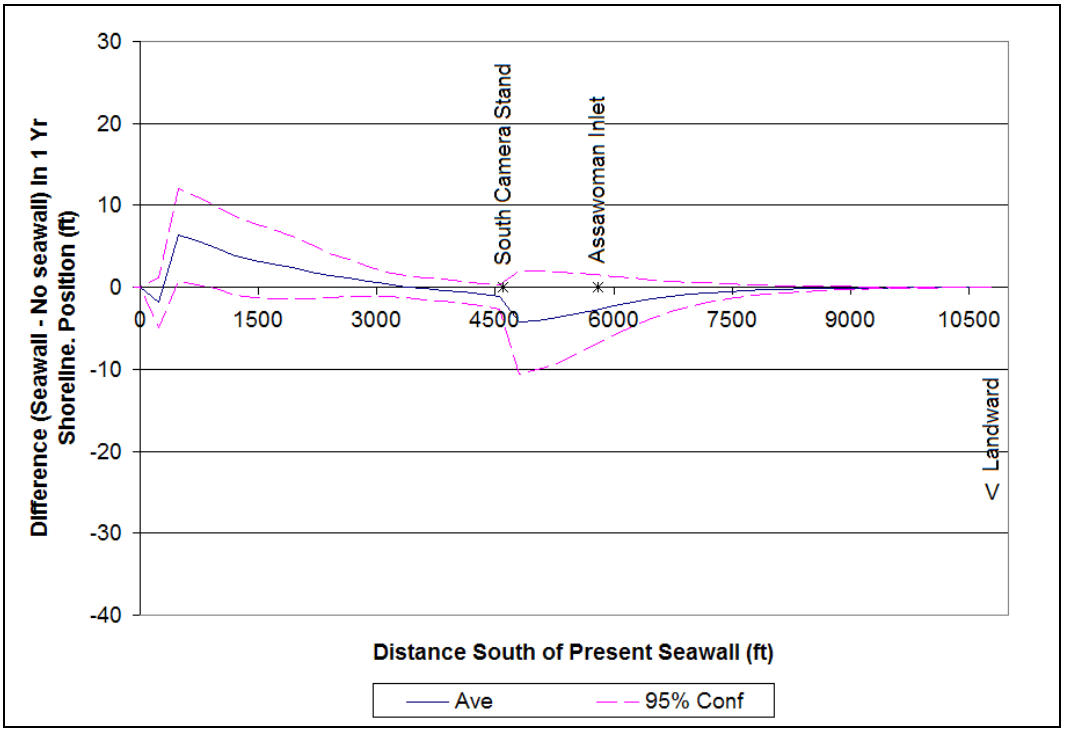

Figure 10-10. One year shoreline difference between 4600 ft seawall extension 10 yds landward and no seawall extension.

2-Year and 10-Year Shoreline Changes

The modeling results for the 2 year and 10 year ft shoreline differences show the same patterns as the 1 Year differences above. Impacts were largest immediately south of structure and the seawall placed 10 yards landward of the shoreline had significantly milder impacts than the seawall placed at the shoreline. The maximum erosion differences were not substantially larger than for the 1 year results. However, the impacts did extend further south as the longer time periods allowed the effects to diffuse down the coast. The 2 Year and 10 Year shoreline difference figures corresponding to Figures 10-5 through 10-10 are included in Appendix F.

It should be noted that the model requires that the shoreline change rate be specified at each end of the model. That has the effect of forcing the shoreline differences to zero at the 10,800 distance in these figures. For many of the figures shown above, the shoreline differences pinch out to zero well to the north of this point, and those are valid model predictions. However, some of the figures, particularly those for the 4600 ft seawall

extension and those for the longer time periods show the differences being forced to zero at the 10,800 ft distance. These should be considered model artifacts and not representative of the true distance that impacts could extend onto Assawoman Island.

Discussion

Table 10-1 shows the 1-year average deficit volumes. The column labeled "South of Extension" is equivalent to the areas in Figures 10-5 to 10-10 between the blue lines and the zero line that are between the end of the extensions and 10,800 ft. The areas are converted to volumes by multiplying by the vertical distance between the top of the berm and the depth of closure. The column labeled "South of Assawoman Inlet" is equivalent to the more restrictive area between the blue line and zero that is between the point labeled Assawoman Inlet and the 10,800 ft distance. The first column represents the total negative impacts while the second represents the negative impacts to Assawoman Island. These volumes can be compared to the total 1-year volume change within the 10,800 ft distance (equivalent to the "no action alternative") of 96,000 yds^3. This number is equivalent to the area between the orange line and the dashed blue line in Figures 10-2 through 10-4. Because of the caveat discussed in the preceding paragraph, these numbers should not be used for planning purposes. Rather they are meant for internal comparisons to show the relative magnitudes of the impacts for the different scenarios.

Table 10-1. 1-Year Seawall Extension Deficit Volumes (yd^3)

		South of Extension	South of Assawoman Inlet
1500 ft Extension	Seawall at Shoreline	22,000	1,000
	Seawall 10 yds Inland	4,000	0
3000 ft Extension	Seawall at Shoreline	32,000	5,000
	Seawall 10 yds Inland	5,000	0
4600 ft Extension	Seawall at Shoreline	45,000	22,000
	Seawall 10 yds Inland	16,000	6,000

Table 10-2 shows the relative magnitude of the shoreline impacts in a different way. It shows the average shoreline change rate at Assawoman Inlet. These values were calculated by dividing the 10-year shoreline changes at Assawoman Inlet by 10. The "Ave" column under "Total

Shoreline Change Rate" is equivalent to the distance between the orange line and the various green lines in Figures 10-2 through 10-4 at Assawoman Inlet divided by 10. The columns under "Shoreline Change Rate Attributed to Construction" are equivalent to the distance between the zero line and the various colored lines in Figures F-7 through F12 at Assawoman Inlet divided by 10.

Table 10-2. Average Shoreline Change Rate (ft/yr) at Assawoman Inlet.

	Total Shoreline Change Rate			Shoreline Change Rate Attributed to Construction		
	Min	Ave	Max	Min	Ave	Max
No Seawall Extension	-9.3	-10.3	-11.3			
1500 ft Extension at Shoreline	-9.8	-10.9	-12.0	-0.4	-0.6	-0.7
1500 ft Extension 10 yds Landward	-9.4	-10.5	-11.7	0.0	-0.2	-0.4
3000 ft Extension at Shoreline	-9.4	-10.9	-12.4	0.1	-0.5	-1.2
3000 ft Extension 10 yds Landward	-9.1	-10.5	-12.0	0.4	-0.2	-0.8
4600 ft Extension at Shoreline	-9.7	-11.7	-13.7	-0.1	-1.4	-2.7
4600 ft Extension 10 yds Landward	-9.4	-11.4	-13.5	0.2	-1.1	-2.4

The most important result of this analysis is that construction of a seawall extension will have only modest negative impacts of the adjacent shoreline, particularly if the seawall is set back at least 10 yards from the shoreline. As seen in Table 10-2, the average shoreline change rate at Assawoman Inlet attributed to the construction will be less than the variability in the change rate caused by yearly changes in the wave climate. That is, stormy years are expected to cause greater shoreline change than the seawall extension will in years of normal waves.

Not surprisingly, the smallest impacts are caused by the shortest seawall extension and the shortest time interval between extension construction and beach fill placement. It is expected that any negative impacts can be redressed at the time of placement and that following beach fill placement, this area will accrete rather than erode.

11 Conclusions and Recommendations

The most important conclusion from the analysis described in this document is that it is feasible to design a project that provides a significant level of storm damage reduction to the facilities on Wallops Island, while at the same time does not negatively impact Assawoman Island to the south.

The storm damage reduction project is designed as a three tiered defense, including a beachfill, the rock seawall, and flood protecton. The beachfill is expected to provide the majority of the defense against smaller, more frequent storms. The rock seawall is intended to provide damage reduction against the largest storms expected over the lifetime of the project. While the seawall is expected to reduce wave heights in its lee, flooding can still be an issue. To provide a high level of protection, NASA personnel need to continue to address flooding concerns for each structure on the island.

Modeling of the beach's response to storms (SBEACH modeling in Chapter 4) has indicated that the beach fill should provide a minimum 70 ft wide berm with a 14 ft high dune. This defense should run from the end of the seawall at the north to the south camera stand, a distance of 19,000 ft.

The rock seawall is in need of maintenance, as discussed in Chapter 3. It is recommended that repairs be made at low elevation locations to raise the seawall to +12 or optimally +14 ft and at steep seaward-facing slopes to create a 1:2 slope. Repairs should be made by keying armor stones into the existing matrix or by rebuilding the wall where necessary. These repairs are similar to those recommended in Moffat and Nichol (1998) and Morang, Williams, and Swean (2006). Any future storm damage will need to be addressed as appropriate.

Due to the porosity of the seawall, the continued development of scour holes behind the seawall is expected until the beachfill is in place. It appears that placing rubble in the scour holes has been effective at halting the scour.

The seawall should be extended south as far as the South Camera Stand, if possible.

The components of the initial fill (Chapter 6) should include a seawall deficit volume, a berm volume, a dune volume, an overfill volume and an advanced nourishment volume. The components of the renourishment fill should include the advanced fill volume and a sea-level rise volume.

From a large initial list, three final alternatives are presented in this report that have gone through an extensive optimization process. These all have similar performance characteristics, and any of the three are expected to satisfy the project requirements. As discussed in Chapter 7, concerns about unintended consequences has led to the selection of Alternative 1, the no sand retention structure alternative as the recommended alternative.

The offshore borrow sites are analyzed in Chapter 8. It is recommended that the Blackfish Bank site be removed from further consideration as a source of project fill material because of the potential to negatively impact the Assateague Island shoreline in the vicinity of Tom's Cove. MMS guidelines indicate that the other two sites are equally acceptable alternatives. However, because of the location of the shoreline impacts, distance to the project, borrow site grain size, and other considerations, Site A is the recommended alternative, though Site B is still acceptable if needed. Anything that can be done to reduce the amount of total fill taken from these sites will lessen their shoreline impacts.

Chapter 9 discusses the potential of the north end of Wallops Island as an alternative borrow site. It is recommended that the initial fill be obtained from an offshore site, but that as much of the renourishment fill as practical be obtained from the onshore site.

As discussed in Chapter 10, the seawall extension should be constructed a minimum of 10 yards landward of the shoreline.

A monitoring program should be initiated as soon as practical. Analysis of the data collected will be the primary tool to monitor the behavior of the project and identify any problems. These data will also be used to determine when renourishment should take place and the amount of

material needed. They will also be used to determine the amount of material available from the north end of Wallops Island.

References

Ahrens, J.P. 2000. A fall-velocity equation. Journal of Waterway, Port, Coastal, and Ocean Engineering. ASCE. 126 (2) 99-102.

Alpine Ocean Seismic Survey. 2007. Vibracore Sampling, Wallops Island Flight Facility, Part A. Report 1552, Prepared for U.S. Army Corps of Engineers, Norfolk, VA. Prepared by Alpine Ocean Seismic Survey, Inc., 70 Oak St, Norwood, NJ, July 20.

Alpine Ocean Seismic Survey. 2008. Vibracore Sampling, Wallops Island Flight Facility, Part B. Report 1558, Prepared for U.S. Army Corps of Engineers, Norfolk, VA. Prepared by Alpine Ocean Seismic Survey, Inc., 70 Oak St, Norwood, NJ, January 17.

ASBPA Science and Technology Committee. 2008. Terminal Groins at Coastal Inlets. ASBPA Position Paper. American Shore and Beach Preservation Association. Available at: http://www.asbpa.org/pdfs/ASBPATerminalGroinsatCoastalInletsPositionPaperFinal.pdf

Basco, D.R. 2002. Chapter 3, Shore Protection Projects. Coastal Engineering Manual, Part V, Coastal Project Planning and Design, Chapter V-3, Engineer Manual 1110-2-1100. Washington, DC: U.S. Army Corps of Engineers (available online: http://chl.erdc.usace.army.mil/chl.aspx?p=s&a=ARTICLES;104

Borgman, L.E., Miller, M.C., Butler, H.L., and Resinhard, R.D. 1992. Empirical simulation of future hurricane storm histories as a tool in engineering and economic analysis. Proc., Civ. Engrg. in the Oceans, V, ASCE, New York, N.Y., 42-45.

Bruun, P., 1962. Sea level rise as cause of shore erosion. Am. Soc. Civ. Eng. Proc., J. Waterways Harbors Div., 88: 117-130.

Chasen, M.A., Rosati, J.D., McCormick, J.W., and Randall, R.E. 1993. Engineering Design Guidance for Detached Breakwaters as Shoreline Stabilization Structures. Technical Report CERC-93-19,

U.S. Army Engineer Waterways Experiment Station, Coastal Engineering Research Center, Vicksburg, MS.

Combe, A. and Soileau, C. 1987. Behavior of man-made beach and dune, Grand Isle, Louisiana. Coastal Sediments '87. 1232 –1233.

Dean, Robert G. 2002. Beach Nourishment, Theory and Practice. Advanced Series on Ocean Engineering - Vol 18. World Scientific Publishing Co. Singapore.

Dean, R. G. and R. A. Dalrymple (2002) "Coastal Processes with Engineering Applications," Cambridge University Press, Cambridge, England, 475 Pages.

Dean R.G. and T.L. Walton Jr., 1975, Sediment Transport Processes in the Vicinity of Inlets with Special Reference to Sand Trapping, Estuarine Research, Vol II, Academic Press, pp129 149.

Gravens, M. 1989. "Estimating potential longshore sand transport rates using WIS data," Coastal Engineering Technical Note CETN-II-19, U.S. Army Engineer Waterways Experiment Station, Coastal Engineering Research Center, Vicksburg, MS.

Gravens, M. B., Ebersole, B.A., Walton. T.L., and Wise, R.A. 2006. Beach-fill design. Coastal Engineering Manual, Part V, Coastal Project Planning and Design, Chapter V-4, Engineer Manual 1110-2-1100. Washington, DC: U.S. Army Corps of Engineers (available online: http://chl.erdc.usace.army.mil/chl.aspx?p=s&a=ARTICLES;104 (accessed 3 May 2006).

Gravens, M.B., Kraus, N.C., and Hanson, H. 1991. GENESIS: Generalized model for simulating shoreline change, Report 2, Workbook and system user's manual, Technical Report CERC-89-19, U.S. Army Engineer Waterways Experiment Station, Coastal Engineering Research Center, Vicksburg, MS.

Hallermeier, R. J. 1981. Terminal settling velocity of commonly occurring sand grains, Sedimentology (28).

Hanson, H. (1987). GENESIS - A generalized shoreline change numerical model for engineering , Report No. 1007, University of Lund, Department of Water Resources Engineering, Lund, Sweden.

Hanson, H. and Kraus, N.C. (1989). GENESIS: Generalized model for simulating shoreline change, Report 1, Technical reference, Technical Report CERC-89-19, U.S. Army Engineer Waterways Experiment Station, Coastal Engineering Research Center, Vicksburg, MS.

Jonsson, I. G. (1990). "Wave-current interactions," The sea. Vol. 9, Part A, B. LeMehaute and D. M. Hanes, ed., John Wiley & Sons, Inc., New York.

Kelley, S.W., Ramsey, J.S., and Byrnes, M.R. 2001. Numerical Modeling Evaluation of the Cumulative Physical Effects of Offshore Sand Dredging for Beach Nourishment. U.S. Department of the Interior, Minerals Management Service, International Activities and Marine Minerals Division (INTERMAR), Herndon, VA. OCS Report MMS 2001-098, 95 pp. + 106 pp. appendices. Available on the web at: http://www.mms.gov/itd/pubs/2001/2001-098.pdf

Kraus, N. C., H. Hanson, H., and Blomgren, S. 1994. Modern functional design of groins. In: Proceedings of the 24th Coastal Engineering Conference, ASCE, pp1327-1342.

Knuuti, K. 2002. "Planning for sea-level rise: U.S. Army Corps of Engineers policy." Proceedings Solutions to Coastal Disasters '02, ASCE, 549 - 560.

Larson, M. and Kraus, N. C. (1989). "SBEACH: Numerical model for simulating storm-induced beach change; Report 1: Empirical foundation and model development," Technical Report CERC-89-9, U.S. Army Engineer Waterways Experiment Station, Coastal Engineering Research Center, Vicksburg, MS.

Larson, M. and Kraus, N. C. (1991). "Mathematical modeling of the fate of beach fill," Artificial beach nourishments, H. D. Niemayer, J. van Overeem, and J. van de Graaff, eds, (special issue of) Coastal Engineering, 16, 83-114.

Larson, M. and Kraus, N. C. (1995). "Representation of non-erodible bottoms in SBEACH," TAMU-CC-CBI-95-11, Conrad Blucher Institute for Surveying and Science, Texas A&M University-Corpus Christi, Corpus Christi, TX.

Larson, M., Kraus, N. C., and Byrnes, M. R. (1990). "SBEACH: Numerical model for simulating storm-induced beach change; Report 2: Numerical formulation and model test," Technical Report CERC-89-9, U.S. Army Engineer Waterways Experiment Station, Coastal Engineering Research Center, Vicksburg, MS.

Leadon, M. Gates, E., Watters, T. 2004. Monitoring Standards for Beach Erosion Control Projects. Bureau of Beaches and Coastal Systems, Dept of Environmental Protection, State of Florida. Available at: http://www.floridadep.org/beaches/publications/pdf/standard.pdf

Lee, G. and Birkemeier, W.A. 1993. Beach and Nearshore Survey Data: 1985-1991 CERC Field Research Facility. Technical Report CERC-93-3, U.S. Army Corps of Engineers, Engineer Research and Development Center, Vicksburg, MS. Available at: http://chl.erdc.usace.army.mil/Media/8/2/1/CERC-TR-93-3.pdf

Melby, J.A., Thompson, E.F., Cialone, M.A., Smith, J.M., Borgman, L.E., Demirbilek, Z., Hanson, J.L., and Lin, L. 2005. Life-Cycle Analysis of Mid Bay and Poplar Island Projects, Chesapeake Bay, Maryland. Technical Report ERDC/CHL TR-05-12, U.S. Army Corps of Engineers, Engineer Research and Development Center, Vicksburg, MS.

Moffatt & Nichol, Engineers. 1986. Wallops Island shore protection study. Prepared for NASA/Goddard Space Flight Facility, Wallops Island, VA.

Moffatt & Nichol, Engineers. 1987. Shore protection alternatives, Goddard Space Flight Facility, Wallops Island, Virginia: Phase A report. Prepared for NASA/Goddard Space Flight Facility, Wallops Island, VA.

Moffatt & Nichol, Engineers. 1989. Study of Wallops Island seawall repair alternatives: Phase B. Presented to National Aeronautics and Space

Administration, Goddard Space Flight Center, Wallops Flight Facility.

Moffatt & Nichol, Engineers. 1992. Wallops Island shoreline evolution modeling study. Prepared for NASA/Goddard Space Flight Facility, Wallops Island, VA.

Moffatt & Nichol, Engineers. 1998. Wallops Island seawall study, final report. Prepared for National Aeronautics and Space Administration, Goddard Space Flight Center, Wallops Flight Facility.

Morang, A., Williams, G.G., and Swean, J.W. 2006. Beach Erosion Mitigation and Sediment Management Alternatives at Wallops Island, VA. Technical Report ERDC/CHL TR-06-21, U.S. Army Corps of Engineers, Engineer Research and Development Center, Vicksburg, MS.

National Research Council (1987). Responding to Changes in Sea Level: Engineering Implications, National Academy Press, 148 p. available on the web at: http://www.nap.edu/catalog/1006.html

National Research Council (1995). Beach Nourishment and Protection. National Academy Press, Washington.

Resio, D. T. (1987). "Shallow-water waves. I: Theory," J. Waterway., Port, Coast., and Oc. Engrg., ASCE, 113(3), 264-281.

Resio, D. T. (1988a). "Shallow-water waves. II: Data comparisons," J. Waterway., Port, Coast., and Oc. Engrg., ASCE, 114(1), 50-65.

Resio, D. T. (1988b). "A steady-state wave model for coastal applications," Proc. 21st Coast. Engrg. Conf., ASCE, 929-940.

Richardson, T.M. and McBride, R.A. 2007. Historical Shoreline Changes and Morphodynamics of Parramore Island, Virginia (1852-2006). Proceedings, Coastal Sediments '07, American Society of Civil Engineers, New Orleans, Louisiana.

Rosati, J.D., and Kraus, N.C. 2009. Sea Level Rise and Consequences for Navigable Coastal Inlets. Submitted to *Shore and Beach*.

Rosati, J.D., Walton, T.L., and Bodge, K. 2006. Longshore Sediment Transport. Coastal Engineering Manual, Part III, Coastal Sediment Processes, Chapter III-2, Engineer Manual 1110-2-1100. Washington, DC: U.S. Army Corps of Engineers (available online: http://chl.erdc.usace.army.mil/chl.aspx?p=s&a=ARTICLES;104

Scheffner, N.W., Borgman, L.E., and Mark, D.J. 1996. Journal of Waterway, Port, Coastal, and Ocean Engineering. Vol 122, No.2. ASCE, New York, N.Y., 93-101.

Scheffner, N.W., Clausner, J.E., Militello, A., and Borgman, L.E. 1999. Use and Application of the Empirical Simulation Technique: User's Guide. Technical Report CHL-99-10, U.S. Army Corps of Engineers, Engineer Research and Development Center, Vicksburg, MS.

Shortal, J.A. 1978. A New Dimension - Wallops Island Flight Test Range: The First Fifteen Years. NASA Reference Publication 1028. Available at: http://ntrs.nasa.gov/archive/nasa/casi.ntrs.nasa.gov/19790011995_1979011995.pdf

Slingerland, R. 1983. "Systematic Monthly Morphologic Variation of Assawoman Inlet: Nature and Causes," Earth Surface Processes and Landforms, Vol 8, pp 161-169.

Smith, J. M. (2001). "Modeling nearshore transformation with STWAVE," Coastal and Hydraulics Engineering Technical Note CHETN I-64, U.S. Army Engineer Research and Development Center, Coastal and Hydraulics Laboratory, Vicksburg, MS.

Tracy, B. A., 2002. Directional characteristics of the 1990-1999 Wave Information Studies Gulf of Mexico hindcast. 7th International Workshop on Wave Hindcasting and Forecasting October 21-25, 2002, Banff, Alberta, Canada.

Tracy, B. A., and A.C. Cialone, 2004. Comparison of Gulf of Mexico Wave Information Studies (WIS) 2-G Hindcast with 3-G Hindcasting. 8th International Workshop on Wave Hindcasting and Forecasting November 11-19, 2004, North Shore, Hawaii.

U.S. Army Corps of Engineers. 1993. Coastal Project Monitoring. Engineer Manual 1100-2-1004, U.S. Army Corps of Engineers, Washington, D.C.

U.S. Army Corps of Engineers. 2000. "Planning guidance notebook." Engineering Regulation ER 1105-2-100 Headquarters, USACE, Washington, DC, 639 p.

U.S. Army Corps of Engineers. 2002. Coastal Engineering Manual. Engineer Manual 1110-2-1100, U.S. Army Corps of Engineers, Washington, D.C. (in 6 volumes). Available at: http://140.194.76.129/publications/eng-manuals/

U.S. Army Corps of Engineers. 2009a. "Incorporating sea-level change considerations in civil works programs." Engineering Circular 1165-2-211. Headquarters, USACE, Washington, DC.

U.S. Army Corps of Engineers. 2009b. "North End Sand Borrow Site, NASA Wallops Flight Facility, Wallops Island, Virginia; Report of Subsurface Exploration and Laboratory Testing." Geo Environmental Section, Norfolk District, U.S. Army Corps of Engineers.

Wikel, G.L. 2008. Variability in Geologic Framework and Shoreline Change: Assateague and Wallops Islands, Eastern Shore of Virginia. M.S. Thesis. The College of William and Mary in Virginia. 210 pp.

Wise, R. A., and Kraus, N. C. (1993). "Simulation of beach fill response to multiple storms, Ocean City, Maryland," in Beach Nourishment Engineering and Management Considerations, Proceedings Coastal Zone '93, ASCE, D. K. Stauble, and N. C. Kraus (Volume Editors), 133-147.

Wise, R. A., Smith, S. J., and Larson, M. (1996). "SBEACH: Numerical model for simulating storm-induced beach change, Report 4, Cross-

shore transport under random waves and model validation with SUPERTANK and field data," Technical Report CERC-89-9 , U.S. Army Engineer Waterways Experiment Station, Coastal Engineering Research Center, Vicksburg, MS.

Zervas, C., 2001: Sea Level Variations of the United States 1854-1999. NOAA Technical Report NOS CO-OPS 36, 201 p. http://tidesandcurrents.noaa.gov/publications/techrpt36doc.pdf

Appendix A: Vibracore Sediment Data

Table A1. Grain Size Data from Borrow Site A

Core #	Position	Depth (ft)	Mean (mm)	Median (mm)	ϕ St Dev
WIVC-29	Upper	0-3.7	0.382	0.342	0.69
	Mid	3.7-7.2	0.382	0.344	0.63
	Lower	7.2-11.3	0.46	0.406	0.82
	Composite	0-11.3	0.39	0.339	0.77
WIVC-30	Upper	0-4.1	0.599	0.49	0.93
	Mid	4.1-9.5	0.493	0.457	0.76
	Lower	9.5-15.6	0.423	0.403	0.67
	Composite	0-20.2	0.503	0.454	0.85
WIVC-54	Upper	0-5	0.695	0.616	1.225
	Mid				
	Lower	5-11.4	0.785	0.616	1.25
	Composite	0-11.4	0.901	0.683	1.55
WIVC-55	Upper	0-5.6	0.366	0.342	0.5
	Mid	5.6-9	0.451	0.366	0.675
	Lower	9-13.4	0.347	0.342	0.425
	Composite	0-13.4	0.392	0.342	0.55
WIVC-56	Upper	0-6.1	0.354	0.33	0.48
	Mid				
	Lower	6.1-10	0.254	0.259	0.425
	Composite	0-10	0.308	0.287	0.5
WIVC-57	Upper	0-4	0.243	0.241	0.44
	Mid	4-8	0.246	0.241	0.425
	Lower	8-12.5	0.231	0.233	0.365
	Composite	0-12.5	0.243	0.241	0.44
WIVC-58	Upper	0-4	0.302	0.297	0.425
	Mid	4-8	0.282	0.287	0.275
	Lower	8-13	0.273	0.277	0.325
	Composite	0-13	0.279	0.287	0.36
WIVC-61	Upper	0-5	0.218	0.218	0.45
	Mid				
	Lower	5-9.5	0.221	0.233	0.475
	Composite	0-9.5	0.218	0.218	0.45
WIVC-65	Upper	0-2	0.399	0.349	0.575
	Mid	2-5	0.342	0.33	0.4
	Lower	5-8	0.354	0.33	0.45
	Composite	0-8	0.372	0.342	0.475
WIVC-66	Upper	0-1.8	0.47	0.349	0.89
	Mid	1.8-5	0.241	0.241	0.5
	Lower	5-9.2	0.27	0.259	0.59
	Composite	0-9.2	0.386	0.287	1.075

Table A2. Grain Size Data from Borrow Site B

Core #	Position	Depth (ft)	Mean (mm)	Median (mm)	ϕ St Dev
WIVC-67	Upper	0-5	0.324	0.33	0.325
	Mid	5-10	0.475	0.406	0.775
	Lower	10-15.5	0.416	0.366	0.715
	Composite	0-15.5	0.394	0.354	0.645
WIVC-68	Upper	0-5	0.366	0.342	0.5
	Mid	5-9.3	0.428	0.392	0.625
	Lower	9.3-13	0.308	0.301	0.45
	Composite	0-13	0.379	0.5	0.55
WIVC-69	Upper	0-5	0.423	0.379	0.74
	Mid	5-10	0.268	0.259	0.6
	Lower	10-14.1	0.297	0.287	0.7
	Composite	0-14.1	0.342	0.319	0.85
WIVC-70	Upper	0-5	0.268	0.277	0.45
	Mid				
	Lower	5-9.2	0.287	0.241	0.65
	Composite	0-9.2	0.273	0.268	0.525
WIVC-71	Upper	0-1.3	0.313	0.241	1.075
	Mid	1.3-5	0.171	0.165	0.5
	Lower	5-9.8	0.132	0.139	0.375
	Composite	0-9.8	0.171	0.165	0.5
WIVC-72	Upper	0-2.6	0.354	0.297	0.9
	Mid	2.6-5	0.25	0.25	0.45
	Lower	5-9.9	0.224	0.218	0.36
	Composite	0-9.9	0.256	0.25	0.485

Table A3. Offshore Borrow Site Core Locations

Borrow Site A				
Core #	**Collection Date**	**Latitude N**	**Longitude W**	**Water Depth (ft)**
WIVC-29	5/26/2007	37º 50.8256’	75º 12.6719’	33.8
WIVC-30	5/26/2007	37º 50.4283’	75º 13.2921’	30.9
WIVC-54	12/19/2007	37º 50.6815'	75º 13.1323'	39.1
WIVC-55	12/19/2007	37º 50.5173'	75º 12.8844'	31.5
WIVC-56	12/19/2007	37º 51.1555'	75º 12.3637'	37.9
WIVC-57	12/19/2007	37º 51.0571'	75º 12.0077'	45.9
WIVC-58	12/19/2007	37º 50.8522'	75º 12.3458'	38.7
WIVC-61	12/9/2007	37º 51.6176'	75º 10.5438'	53.4
WIVC-65	12/19/2007	37º 51.5180'	75º 11.9769'	46.7
WIVC-66	12/19/2007	37º 51.4734'	75º 11.6215'	48.5
Borrow Site B				
Core #	**Collection Date**	**Latitude N**	**Longitude W**	**Water Depth (ft)**
WIVC-67	12/18/2007	37º 51.7890'	75º 08.0322'	48.9
WIVC-68	12/18/2007	37º 51.4230'	75º 07.6073'	41.3
WIVC-69	12/18/2007	37º 52.3717'	75º 07.0961'	54.6
WIVC-70	12/18/2007	37º 52.0486'	75º 06.2773'	41.8
WIVC-71	12/18/2007	37º 52.7470'	75º 06.1573'	63.4
WIVC-72	12/18/2007	37º 52.4896'	75º 05.4791'	55.9

Figure A-1. Example Core, WIVC-65, top 5 feet.

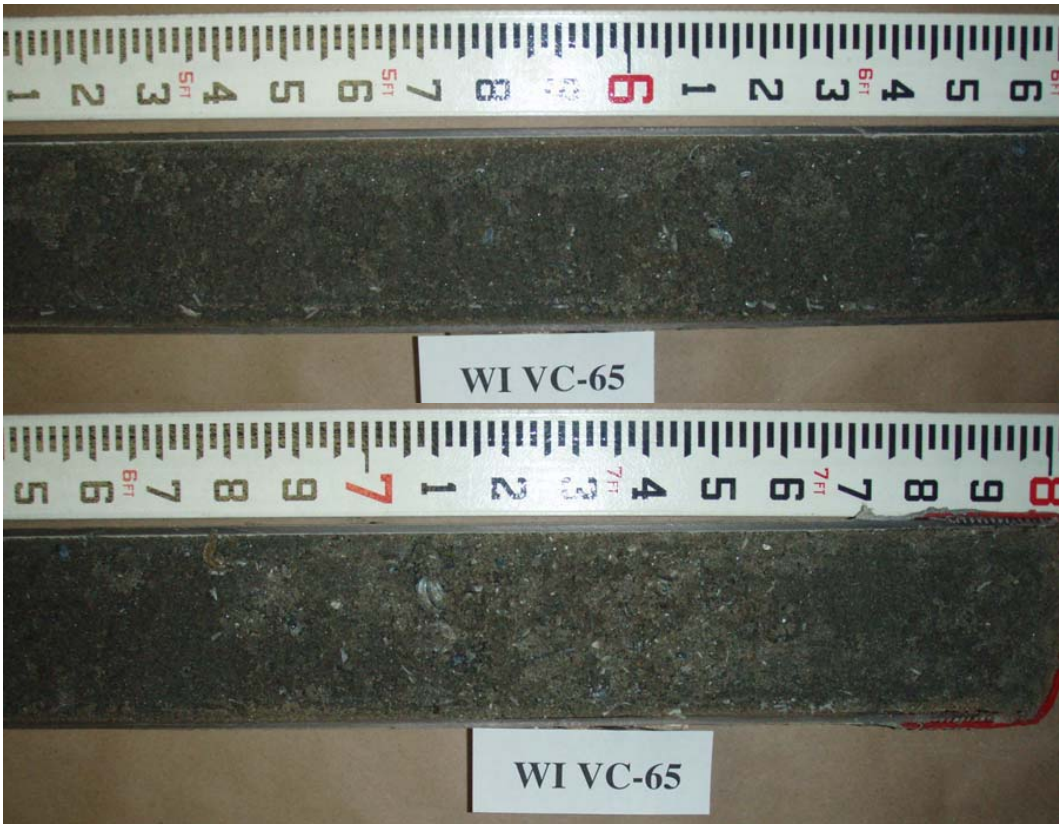

Figure A-2. Example Core, WIVC-65, depth: 5 8 feet.

Appendix B: Wallops Island Site Visit Report of 07 September 1999

This appendix provides the USACE site visit report of 07 September 1999 to Wallops Island, VA.

Wallops Island, VA Site Visit
September 07, 1999

Attendees

Verizon

Mr. Sam McGee
CENAO

Mr. Mark Hudgins
CENAO

Ms. Joan Pope
CEERD

Mr. William R. Curtis
CEERD

Mr. William (Bill) D. Phillips
Head, Facilities Management Branch
National Aeronautics and Space Administration
Goddard Space Flight Center
Wallops Flight Facility
Bldg. N-161 Room 126
Wallops Island, VA 23337
Voice: (757) 824-1209
Fax: (757) 824-1831
William.D.Phillips.1@gsfc.nasa.gov

Mr. Thomas Arceneaux
National Aeronautics and Space Administration
Goddard Space Flight Center
Wallops Flight Facility
Bldg. N-161
Wallops Island, VA 23337

Mr. Peter N. Turlington
Civil Engineer, facilities Engineering/Planning Group
National Aeronautics and Space Administration
Goddard Space Flight Center
Wallops Flight Facility
Bldg. N-161 Room 124
Wallops Island, VA 23337
Voice: (757) 824-1748
Fax: (757) 824-1831
Peter.N.Turlington.1@gsfc.nasa.gov

Mr. William B. Bott
Environmental Group Leader, Code 205.W Wallops Environmental Office
National Aeronautics and Space Administration
Goddard Space Flight Center
Wallops Flight Facility

Bldg. N-161 Room 127
Wallops Island, VA 23337
Voice: (757) 824-1103
Fax: (757) 824-1876
William.B.Bott.1@gsfc.nasa.gov

Mr. David Morris
Private Environmental Contractor
Goddard Space Flight Center
Wallops Flight Facility

Meeting Notes

- Complex coastal project due to proximity if inlet to location of site on barrier island. Therefore CHL involvement.
- Not a recreational beach. Need not consider aesthetics, but only functionality.
- No erosion at north end of island.
- Important facilities above 100-year water level.
- 10-ft structure elevation would prevent nuisance flooding if impermeable structure.

- WRDA'99: Wallops authorized as Corps project. Authorization only, not funds received yet.
- Unusual funding avenue, may need political involvement to execute funding.
- Authorized as emergency project and for plans and specifications and construction, rather than as a study.
- WRDA written as beach restoration with language for recovery of funds from other federal agencies. Language leaves avenue for open inter-governmental exchange of funds.
- $8 million FY00, $8 million FY01, $4 million FY02 appropriated.
- May not be able to spend $8 million in FY00 due to environmental permitting issues and site investigations (borrow site identification, etc). May be able to get permitting from State in a year if project is non-controversial. Large constituency/proponency for project, and NASA may be able to round up political pressure to expedite permitting.

- Seawall constructed by NASA in-house labor to save on cost.
- Seawall 3-mi long and 12-ft MSL high. Crest elevation currently being raised to 15 ft MSL at cost of $5 million for additional stone (NASA funding).
- Seawall to be extended at southern end to protect Virginia Commercial Space Flight Center in FY00 at cost of $3 million.
- Launch range operations expansions documentation will allow for extension of seawall without NEPA document.
- 60% of stone specified as 2-3 ton granite. Stone shipped via rail from Lawrenceville, VA.
- $35/ton delivered plus $10/ton placed.
- Stone to arrive in November and will be placed over 1.5 years.

- Seawall too permeable and has experienced loss of material on landward side.

- Voids, no toe protection, no core, narrow crest, steep slopes (nearly vertical at some locations).
- May consider pre-cast units and setting up batch plant.

- Hog Creek dredged every three years. Fine-grained material placed at southern end of facility and vegetated.
- May be able to re-dredge existing Navy birthing sites in backside of island to create infrastructure for construction of shore protect project. Highly encouraged by Turlington.

- May be able to spend some Corps FY00 dollars for armor stone placement at end of FY00 is permitting moves quickly.
- Beach nourishment will go out for bid in FY01.
- Can only dredge between 150-250 mcy from Chin. Inlet annually without modifying hydrodynamics of inlet.
- Inlet material may be too fine. Therefore may need to identify borrow areas.
- Perhaps there are MMS surveys of sand resources in the area. VIMS will also be a good resource for sand.

- GIS model of site available. Need to specify what format is preferred to Turlington. Need to get model quickly, as GIS person is leaving facility.
- Topo based on GPS survey. Have own GPS base station.

- Possibility of some historical wave data. No historical tide data for inlet and sound.

- Demo project will span 3500 ft of shoreline centered on nodal point.

- How can structure be retrofitted without removing stone?

CEERD-HC-S (1110-2-1403b) 19 October 1999

MEMORANDUM FOR Commander, U.S. Army Engineer District, Norfolk ATTN: CENAO-EN-C (Mr. Samuel E. McGee) and CENAO-EN-H (Mr. Mark Hudgins), 803 Front Street Norfolk, VA 23510-1096

SUBJECT: Transmittal of Trip Report for Site Visit to Goddard Space Flight Center, Wallops Island, Virginia

1. Please find enclosed two copies of the trip report requested by your office. If you have any questions pertaining to the material contained herein, my technical point of contacts are Ms. Joan Pope (601/634-3034) or Mr. William R. Curtis (601/634-3040).

Encls

JAMES R. HOUSTON, PhD
Director
Coastal and Hydraulics Laboratory

Copy Furnished w/enclosures:

Mr. Thomas Arceneaux
National Acronautics and Space Administration
Goddard Space Flight Center
Wallops Flight Facility
Building N-161
Wallops Island, VA 23337

SUBJECT: Site visit and general recommendations for shore protection options at Goddard Space Flight Center, Wallops Island, Virginia.

1. U.S. Army Engineer District, Norfolk (CENAO) requested that the US Army Engineer Research and Development Center's Coastal and Hydraulics laboratory (CHL) provide technical assistance in evaluating the shore protection features and developing strategies for improving the shore protection system at the Goddard Space Flight Center (GSFC) on Wallops Island, Virginia. Existing works, including a rubblemound seawall, degraded timber groins, and various relict structures do not provide adequate protection during coastal storm events nor from long-term erosion trends. Critical Federal (i.e., NASA and Navy) and non-Federal (Virginia Commercial Space Flight Center (VCSFC)) facilities are at risk.

2. Personnel from CHL, CENAO and GSFC visited the site and held a project review meeting on September 7, 1999. At the time of the site visit, as-built structure drawings, design wave and water level information, survey data, and project history data were not yet available to CHL personnel. Wallops Island is a low relief, approximately 6-mile long barrier island along the Delmarva (i.e., Delaware-Maryland-Virginia Peninsula). It is located immediately southwest of Chincoteague Inlet and Assateague Island. Assateague Island protects the northern one-third of Wallops Island from open-coast waves. This portion of the island is wide, backed by dunes, has a broad flat beach, and is dominated by the tide processes associated with Chincoteague Inlet, while the southern one mile section of the island is unstructured, narrow, and prone to overwash. The central 3-4 miles is faced by a rubblemound seawall and assorted relict structures. During the site visit, the seaward face of the seawall was partially submerged and being impacted by breaking waves. Thus it was only possible to closely examine the subaerial structure from the landward side. Even from this limited perspective and with the assistance of the GSFC and CENAO representatives familiar with this project, it is possible to make an initial field summary of the project status and provide some general recommendations for improving structure functionality. These field observations and recommendations are provided in this Trip Report. The discussion of field observations references several figures, which are included as an enclosure to this report.

3. General field observations pertaining to the current shore protection condition are:

a. The rubblemound seawall is a linear structure that demarcates a structured shoreline fronting GSFC launch facilities and infrastructure. At the southern end, the seawall extends landward behind the natural shoreline to provide protection to the Virginia Commercial Space Flight Center (VCSFC). (Figure 1).

b. The seawall is constructed of 60% 2 to 3 ton granite stones. These large stones function effectively as armor units (Figure 2).

c. The seawall has a narrow crest width of 1 or two stone widths.

d. Crest elevation ranges from less than 12 ft to 15 ft NGVD. Maximum crest elevation is limited by the necessity for observation of spacecraft launches from various camera platforms located landward of the seawall. According to GSFC, personnel the crest elevation for the entire seawall will be raised to 15 ft NGVD over the next 1.5 years.

e. Seaward and landward cross sectional slopes are 1:1.5 to 1:2. In areas where it is assumed that loss of stone or subsidence has occurred on the seaward face of the structure, the seaward slope is nearly vertical.

f. It is assumed that the structure has no toe protection or bedding layer, although this could not be confirmed during the site visit.

g. The seawall has no graded core material to reduce structure permeability and wave transmission. However, the large stone was placed over a pre-existing sheet pile and timber pile wall (Figures 3 and 4). The crest elevation of the pile wall was not available during the site visit. The pile wall is not continuous. It is assumed where the pile wall is non-existent, that either the wall failed or was removed prior to seawall construction, or the timber pile wall rotted and failed following construction. Where the pile wall did not exist, or where the water elevation was higher than the pile wall elevation, swash was observed to rapidly permeate the seawall with the extent of runup located landward of the structure.

h. On the landward side of the seawall, a narrow-crested dune was constructed to provide protection from coastal flooding. The crest elevation of the dune was not available during the site visit. However, it was observed that the dune crest was equivalent to or exceeded the seawall crest elevation. Significant dune erosion occurred at discrete locations behind the seawall during Hurricane Dennis, which occurred recently before the site visit. Figures 5 and 6 show examples of dune erosion. It is speculated that the eroded dune material was lost to the nearshore area through the highly permeable seawall as overtopped and transmitted waves drained seaward through the structure.

i. Near the southern end of the seawall a cement ramp extends from the dune crest to the top of the pile wall (Figure 4). Armor stone does not protect the ramp. Foundation material (sand) has eroded from beneath the cement (Figure 7). Consequently the ramp is in a state of disrepair. It is speculated that the ramp facilitates wave overtopping of the dune during storm events.

j. GSFC infrastructure landward of the seawall is at an elevation of at least 10-ft NGVD. According to GSFC personnel, a design elevation of 10 ft NGVD is sufficient to avoid damage caused by nuisance flooding that may occur during normal extratropical storms.

k. Relic timber groins are located intermittently along the length of the seawall and beyond the southern extent of the seawall (Figures 3, 4, and 8). Groin structures extending from the seawall do not extend far enough into the surf zone to impede alongshore sediment transport and are ineffective in accreting beach material.

4. Based on these observations, the seawall and dune provide limited functional shore and flood protection during large coastal storms and are likely to require significant maintenance as their foundation and shoreward base material are under continuous long-term erosion. To summarize:

a. The seawall is highly permeable and allows wave transmission and loss of sediment from landward of the seawall to the nearshore during interior drainage of wave runup and overtopping.

b. Pile walls located below and immediately landward of the permeable seawall cause wave reflection that may enhance scour of foundation material and subsidence of stone. Additionally, timber pile walls will eventually degrade which will increase wave

transmission to areas landward of the seawall, erosion of foundation material and subsequent subsidence of stone.

c. If the seawall has no bedding layer and toe protection, continued loss of foundation material and subsidence of stone at the base of the structure is likely.

d. Existing groin structures are ineffective at accreting sediment to provide a protective beach.

e. Site evidence including the shoreward propagation of non-breaking waves suggests that the bottom seaward of the seawall is fairly flat, deep and sand deficient.

5. Shore protection alternatives that may be applied at GSFC are briefly discussed in this report. Alternatives are identified as immediate activities designed to improve the integrity and performance of the seawall and as longer-term shore protection strategies. The "do nothing" option would expose the facility launch pads and infrastructure to potential risk from damaging waves, flooding, and erosion. All alternatives should be evaluated from environmental, engineering, economic, and societal perspectives and require study beyond this cursory discussion prior to implementation. It is important to note that the seaward shoreline of Wallops Island is part of a complex littoral system. The complexity of this system arises from the presence of nearby established and intermittent coastal inlets. Keeping this complex system in mind, alternatives considered for coastal protection at Wallops Islands should be evaluated within the regional context. A regional understanding of coastal processes is necessary to ensure a functional long-term shore protection project with minimal negative impact on adjacent shorelines.

6. To provide sound engineering recommendations for a long-term shoreline management plan at Wallops Island, both short-term and long-term trends in hydrodynamic conditions, sediment transport, geomorphology evolution, and land use must be examined. An list of elements to be investigated before specific shoreline protection alternatives can be designed includes:

a. Identification of key Federal and non-Federal facilities and prioritization for protection

b. History of coastal damage to Federal and non-Federal facilities

   i. When and what damage occurred

   ii. Cause of damage (waves, flooding, wind)

c. Historic shore protection activities at Wallops Island

   i. Pre-construction and as-built designs

   ii. Date of construction and /or removal

   iii. Performance evaluation

   iv. Regulatory history

d. Previous technical documentation of coastal processes (regional and local)

e. Sediment transport (regional and local)

i. Recent and historic aerial shoreline surveys (regional and local)

ii. Historic shoreline change maps (regional and local)

iii. Recent and historic wading surveys (local)

iv. Recent and historic nearshore bathymetry (regional and local)

v. Predicted shoreline change based on geologic assessment and numerical modeling

f. Waves, currents and water levels (regional and local)

i. Measured

ii. Numerically modeled

g. Design storm event and other design criteria

h. Chincoteague Inlet maintenance history and plans for continued maintenance

i. Frequency of dredging (maintenance and emergency operations)

ii. Volume per dredge cycle

iii. Present method of dredging and disposal

iv. Cost per dredge cycle

v. Regulatory history

vi. Sediment analysis (physical and chemical)

i. Environmental considerations

j. Local land use (both ocean-side and bay side of island)

7. Immediate and long-term actions may be taken to improve the degree of protection provided by the existing rubblemound seawall. These alternatives are outlined below and the advantages and disadvantages of each alternative are summarized in Table 1. Potential alternatives for immediate action include:

a. Develop and implement emergency response plan. The plan should focus on the repair and construction of a continuous dune landward of the seawall. The dune should have a crest elevation sufficient to provide flood protection from a selected design storm. The dune should be wide enough to sacrifice material during the design storm, yet maintain crest elevation.

b. Remove existing seawall and construct new seawall. New seawall design should be based upon a sound and stable cross-section including a bedding layer, toe protection and core. Seawall design should be based on a selected design storm event.

c. Identify seriously deficient sections of existing protection and retrofit existing seawall. Retrofit design may vary along the length of the seawall depending on the present condition of the structure and the nature/value of the protected facilities. General retrofit recommendations include:

i. Place fill between the dune and seawall with large gravel and cobble material. During periods of elevated water levels and storms, waves will permeate the structure and move the fill material into the voids of the seawall creating a self-sealing mechanism. As the fill is lost from behind the seawall, it should be replaced until loss of fill material abated.

ii. Construct a splash apron on the landward side of the seawall to reduce fluid velocities during wave overtopping.

iii. Remove cement ramp. The cement may be broken up *in situ* to gravel or cobble sized pieces and used as fill material between the dune and seawall.

iv. Design and construct the seaward slope of the seawall based on an engineering evaluation of the local wave climate and existing stone size.

v. If seawall toe protection does not exist, construct a bedding layer of stone material and a structure toe to minimize scour of foundation material at the base of the structure.

vi. If a bedding layer of stone material does not exist below the seawall, place fill material at the seaward base of the structure. Wave action will work the fill material through the structure voids and fill scour holes. Fill should continue to be placed at the base of the structure until voids are filled to a desired elevation.

vii. The crest elevation of the dune should be raised and maintained to an elevation sufficient to provide flood protection from a design water level and wave event.

viii. Prior to retrofitting, it is recommended that CENAO and CHL personnel conduct a detailed engineering inspection of the seawall structure (including pile walls, groins and dune). It is also recommended that CENAO personnel collect cross sectional surveys of the seawall including a wading survey to identify existence of toe protection and the presence of scour at the base of the seawall.

d. Initiate activities to collect data and conduct analysis required to develop a longer-term shoreline management plan.

e. Design, implement and monitor proposed beach nourishment pilot project.

8. A longer-term shore protection strategy may include the proper design, construction and maintenance of a protective beach nourishment project potentially in combination with beach erosion control structures to reduce erosion rates. Beach nourishment is the placement of large quantities of sand into the littoral zone. The objective of the nourishment is to build the shoreline

seaward so that the beach may provide protection to landward areas from wave attack and coastal flooding. Elements of this strategy include:

a. Evaluation of sediment source areas and construction methods.

b. Development of cross-sectional design for an integrated beach, seawall, dune system. The integrated design may include limited retrofit of existing seawall.

c. Beach nourishment performance modeling that includes consideration of beach fill alone and beach fill with sediment retaining structures (i.e., detached breakwaters, submerged sills, groins, etc).

d. Development of beach nourishment maintenance and monitoring plan.

Table 1. Summary of Shore Protection Alternatives

Alternative	Advantage	Disadvantage
Emergency dune repair and construction	• Low construction and maintenance cost • Limited degree of flood protection • Immediate construction without regulatory considerations	• Temporary structure without adequate wave protection • Continued maintenance
Removal and reconstruction of existing seawall	• Highly functional shore protection • Low/no maintenance	• High material and labor costs • Deepening of beach profile immediately seaward of structure allowing larger waves to impact shoreline • Regulatory considerations
Retrofit of existing seawall and dune	• Functional shore protection, though to a lesser degree than reconstruction • Low construction and maintenance costs • Immediate construction without regulatory considerations	• Continued maintenance • Deepening of beach profile immediately seaward of structure allowing larger waves to impact shoreline • Difficult to obtain design crest elevation of impermeable core
Construction of beach nourishment pilot project	• Will provide localized shore protection • Environmentally favorable • Low construction costs • Opportunity for evaluation of design and construction techniques to be applied to larger beach nourishment project	• Limited area of protection due to placement of small volume of sediment • Rapid loss of sediment from project area due to placement of material in a sediment starved system, potential lack of beach-grade material, and lack of sediment retaining structures • Limited protection (temporal and spatial)
Construction of beach nourishment shore protection project	• Highly functional shore protection if maintained • Environmentally favorable • Potential beneficial use of dredged material	• Potentially high construction costs if distance from borrow site to project is great • Regulatory considerations • Continued maintenance
Construction of beach nourishment shore protection project with erosion control structures	• Highly functional shore protection • Reduction in maintenance over non-structural alternative • Environmentally favorable • Potential beneficial use of dredged material	• Potentially high construction costs • Regulatory considerations • Continued maintenance

9. A roundtable discussion at GSFC of existing shore protection structures was conducted on September 7, 1999. Present were:

Mr. Thomas Arceneaux (GSFC)
Mr. William B. Bott (GSFC)
Mr. William R. Curtis (CHL)
Mr. Mark Hudgins (CENAO)
Mr. Sam McGee (CENAO)
Mr. David Morris (GSFC)
Mr. William D. Phillips (GSFC)
Ms. Joan Pope (CHL)
Mr. Peter N. Turlington (GSFC)

Each of the individuals present at the roundtable discussion (with the exception of Messrs. Arceneaux, Bott and Phillips) participated in the site visit to the seawall on the same day.

10. Questions regarding this trip Report may be addressed to Ms Joan Pope (601/634-3034) or Mr. William R. Curtis (601/634-3040).

Ms. Joan Pope
Acting Chief/ Coastal Sediments and Engineering Division

Mr. William R. Curtis
Research Oceanographer

Appendix C: Seawall Condition Survey of 29 October 2008 - Calculations

Example calculations are based on equations in the Coastal Engineering Manual (CEM) available online at http://chl.erdc.usace.army.mil/cem

Structure Stability

Equations: CEM VI-5-67 (Hudson Equation)

$$\frac{H}{\Delta Dn_{50}} = \left(K_D \cot \alpha \right)^{1/3}$$

where

H = incident wave height
K_D = stability coefficient
α = structure slope with the horizontal
Dn_{50} = nominal cubic dimension of the median stone size

$$\Delta = \frac{\gamma_r}{\gamma_w} - 1$$

where

Δ = relative density of stone
γ_r = unit weight of rock
γ_w = unit weight of water

Definition: $W_{50} = Dn_{50}^3 \, \gamma_r$

where

W_{50} = weight of median stone

Assumptions: the unit weight of stone (γ_r) is 165 pcf, unit weight of water (γ_w) is 64 pcf, the stability coefficient (K_D) for breaking waves is 2.0 (CEM Table VI-5-22), and structure slope is 1:2 ($\cot\alpha = 2.0$).

From the above equations, a 2.5-ton stone (W_{50}) has a nominal cubic dimension (Dn_{50}) of 3.1 ft. For a 1:2 slope, this stone will be stable against a wave height (H) of 7.8 ft.

Wave Runup

Equations: Coastal Engineering Manual (CEM) VI-5-2

$$\xi_{op} = \frac{\tan\alpha}{\sqrt{s_{op}}}$$

where

ξ_{op} = surf similarity parameter based on deepwater wavelength and wave period of
peak energy density
α = structure slope with the horizontal

$$s_{op} = \frac{2\pi H_s}{g T_p^2}$$

where

s_{op} = wave steepness based on deepwater wavelength and wave period of peak
energy density
H_s = significant wave height
g = acceleration of gravity
T_p = wave period of peak energy density

CEM VI-5-6

$$\frac{Ru_{2\%}}{H_s} = 1.5\,\xi_{op} \quad for\ 0.5 \prec \xi_{op} \prec 2.0$$

$$3.0 \quad for\ 2.0 \prec \xi_{op}\ 3-4$$

where

$Ru_{2\%}$ = vertical elevation of runup exceeded by 2% of the waves

From the above equations, an 8 ft wave height (H_s) with 8 sec peak period (T_p) will have a wave steepness (s_{op}) of 0.0244. With a structure slope of 1:2 (tanα = ½ = 0.5), the surf similarity parameter (ξ_{op}) is 3.2. The $Ru_{2\%}$ is therefore three times the wave height, or 24 ft for an 8 ft wave height. This is for runup on a smooth slope.

From CEM Table VI-5-3, the runup reduction factor for 2 or more layers of rock is 0.55 – 0.60. Using 0.55, the calculated runup for an 8 ft, 8 sec wave is therefore (0.55 * 24 ft) 13.2 ft above the swl.

Appendix D: Datums

Horizontal Datums

The horizontal datum used for coordinate data input into the models was NAD83, State Plane Virginia South, 4502, meters. Where necessary, coordinates in other datums were converted to this datum using the conversion program Corpscon, ver 6.0.1, available at: <http://www.tec.army.mil/>.

Several figures presented in this report are based upon the GENESIS grid set up on Wallops Island. These figures generally show along shore distances along the X axis and offshore distances along the Y axis (and frequently the offshore scales are distorted relatively to the along shore scales). the origin of this coordinate system is at: 3768396.5200 Easting, 1174969.9500 Northing in the Virginia State Plane system listed above. This origin is located in the front yard of building V50, the NASA Dynamic Balance Facility, Center Bldg. The grid is rotated 129^{o} clockwise from North, which is the equivalent of a counter-clockwise rotation of 231^{o} from East. This allows the GENESIS x-axis (horizontal) to run in a SSW direction generally parallel to the beach.

Vertical Datums

The vertical datum used in this study was MSL (mean sea level), meters. The difference in MLLW (mean lower low water) elevations and MSL elevations is 0.58 m (1.9 ft). This is the NOAA value for half the tide range (between MLLW and MHHW) on the open coast at Wallops Island as shown in Table D-1. The data in this table were obtained from the website: <http://tidesandcurrents.noaa.gov/tides07/tab2ec2b.html#44>. These relationships were derived from a temporary tide station deployed on the open coast offshore of Wallops Island during 1983.

Since NOAA does not provide a full suite of tidal relationships for this location, when necessary Chincoteague Harbor of Refuge relationships, supplied by NAO were used. These are shown in Figure D-1. For example,

MLW (mean low water) elevations were first converted to MLLW by adding (subtracting a negative) 0.04 m (1.4 ft), the value given in Figure D-1. Most GEODAS depths were referenced to Mean Low Water.

LIDAR elevations were generally given in NAVD88. NAVD88 is 0.05 ft above MSL (1.95-1.90 ref to MLLW). Note, this is equivalent to 1.5 cm of elevation. This small difference is less than the accuracy of some measurement systems, and thus, for practical purposes, at Wallops Island NAVD88 and MSL elevations can be used interchangeably.

Table D-1: Elevation data for the open coast at Wallops Island, VA

Outer Coast Station	Latitude	Longi-tude	Mean Range (ft)	Spring Range (ft)	Mean Tide Level (ft) (relative to MLLW)
Wallops Island	37° 50.5'	75° 28.7'	3.6	4.4	1.9

Chincoteague Harbor of Refuge

Elevations of datums referred to NOS MLLW, 1960-1978 tidal epoch, in feet

NOS MHW	2.63
NAVD 1988	1.95
NGVD 1929	1.14
NOS MLW	0.14
NOS MLLW	0.00

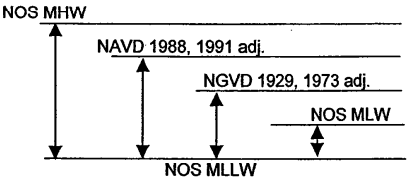

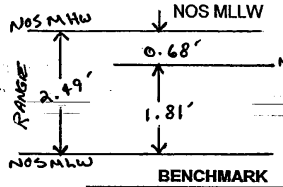

BENCHMARK ELEVATIONS IN FEET

BENCHMARK	NOS MLLW	NOS MLW	NOS MHW	NGVD 1929, 1973 adj	NAVD 1988, 1991 adj
NOS "NO 2, 1962"	5.32	5.18	2.69	4.17	3.36
NOS "NO 3, 1962"	4.74	4.60	2.11	3.61	2.80
NOS "863 0316 A 1977"	4.99	4.85	2.36	3.85	3.04
NOS "863 0316 B 1977"	6.45	6.31	3.82	5.31	4.50
NOS "863 0316 C 1977"	5.90	5.76	3.27	4.76	3.95
CE "HARBOR RESET, 1984"	6.47	6.33	3.84	5.33	4.52
CE "BASIN-1, 1984"	6.75	6.61	4.12	5.61	4.80

NOTE: NOS MLLW, 1960-1978 tidal epoch, elevations for CE "HARBOR RESET, 1984" and CE "BASIN-1, 1984" were established by USACE Norfolk District. The established elevations being utilized since 14 December 1998. (No backup exists for how the elevations were established.) NGS Published elevations (NGVD and NAVD) utilized for NOS "NO 2, 1962" and NOS "NO 3, 1962".

STATEMENT OF TECHNICAL REVIEW

Notice is hereby given that an independent technical review, has been conducted for the datum diagram /vertical control monuments for Chincoteague Harbor of Refuge as defined in the Norfolk District, Operating Branch, 'Standard Operating Procedure (SOP) for Quality Control and Quality Assurance Associated with Survey Datum Diagram/Vertical Control Monuments Determinations', dated 2, June 2003. The following signatories attest to this fact.

Survey Manager (E. Legaspi) Date: 02 July 2003

Independent Technical Review (D. Linn) Date: 02 July 2003

Independent Technical Review Date: _____

Chief, Navigation and Survey Section (T. Woodward) Date: 02 July 2003

Created by E. Legaspi
02 July 2003

Figure D-1: Harbor of Refuge Tidal Datums obtained from NAO.

Appendix E: Model Configuration Parameters

The SBEACH / EST and the STWAVE / GENESIS modeling systems that are available within CEDAS (version 4.03) were used in this study. The CEDAS package is available to USACE employees at:

<http://chl.erdc.usace.army.mil/cedas>,

or to the general public at:

<http://www.veritechinc.com>.

SBEACH Configuration Parameters

The description of the SBEACH modeling effort is given in Chapter 4. The SBEACH model configuration parameters that were used are listed in Table E-1.

Table E-1. SBEACH Configuration Parameters

Reach Configuration		
Grid Data		
	Grid Type	Variable
	Position of Landward boundary	-50
Beach		
	Landward surf zone depth limit:	0.30
	Effective grain size (mm)	0.29
	Maximum slope	30
Sediment Transport Parameters		
	Transport rate coefficient	1.5E-06
	Overwash transport parameter	0.005
	Coefficient for slope-dependent term	0.002
	Transport rate decay coefficient multiplier	0.5
	Water temperature	16
Storm Configuration		
Storm Information		
	Time step (min)	1
	Wave type	Irregular
	Input wave water depth	6

	Wave Height Randomization	Yes
	Seed Value	8186
	% variability	5
Wave Height and Period		
	Input	Variable
	Time step (min)	60
Wave Angle		
	Input	Constant
	Wave Angle	0
Water Elevation		
	Input	Variable
	Time step (min)	60
Wind Speed		
	Input	Constant
	Wind Speed	0
	Wind Angle	0

EST Configuration Parameters

The description of the EST modeling effort is given in Chapter 4. EST configuration parameters are listed in Table E-2.

Table E-2. EST Configuration Parameters

Case Properties	**Value**
Units	English
Vertical Datum	0
Tropical Event Input	**Value**
Number of Input Parameters	9
Event Frequency	0.277
Number of Response Parameters	8
Life Cycles	500
Duration of Life-Cycles in years	100
Probability Assignment	Read from file
Random number seed	123456
Extra-tropical Event Input	**Value**
Number of Input Parameters	9

Event Frequency	0.78
Number of Response Parameters	8
Life Cycles	500
Duration of Life-Cycles in years	100
Probability Assignment	Read from file
Random number seed	123456

Wallops Island STWAVE Grid Parameters

The description of the STWAVE modeling effort for the Wallops Island domain is given in Chapter 5. The parameters used to set up the Wallops Island STWAVE bathymetry grid within CEDAS (Version 4.03) are listed in Table E-3.

Table E-3: Wallops Island STWAVE Grid Parameters

Project Name	Wallops Island Storm Damage Reduction Project	
Domain Name	Wallops Island	
Domain Number	1 of 3	
Domain Descriptive Shoreline Boundaries	Mid Tom's Cove to Mid Assawoman Island	
USGS Reference Charts	12210, 12211	
Data Horizontal Coordinate System	Virginia State Plane South, 4502, NAD 83, meters	
Data Vertical Coordinate System	MSL, meters	
Set up date	20-Jul-07	
STWAVE Origin Coordinates	1167524.1515 N	3787122.9661 E
Approximate Offshore Boundary Depth	20 m	
X_Azimuth (Onshore Direction)	309°, clockwise from N	N51W
Grid cell size cross-shore Δ_x	73.152 m	240 ft
Grid cell size along-shore Δ_y	73.152 m	240 ft
Number of Grid Cells	265 cross-shore	221 along-shore
Grid Distance Cross-shore, R_x	19312.128 m	63360 ft
Grid Distance Along-shore, R_y	16093.440 m	52800 ft
Near-shore Save Station Target Depth	6 m	

Wallops Island STWAVE Wave Parameters

The description of the STWAVE modeling effort for the Wallops Island Domain is given in Chapter 5. The Wallops Island STWAVE wave parameters used in the modeling effort are listed in Table E-4.

Table E-4: Wallops Island STWAVE Wave Parameters		
Project Name	Wallops Island Storm Damage Reduction Project	
Domain Name	Wallops Island	
Domain Number	1 of 3	
Set up date	20-Jul-07	
Wave Config Number	1 of 1	
WIS Station Number	178, Atlantic	
WIS Station Location	37.75° N	75.25° W
WIS Station Depth	20 m	
Shore_Ref 1 Wave Angle	129°, clockwise from N	
Wave Bin Boundaries		
Height	**Period**	**Angle**
mean	mean	mean
0	3	90
0.4	4	65
0.6	5	45
0.8	6	30
1	7	20
1.2	9	10
1.6	11	0
2	13	-10
3	20.5	-20
6		-30
		-45
		-65
		-90

GENESIS Configuration and Calibration Parameters

The GENESIS module within CEDAS (version 4.03) was used in this study. The GENESIS grid was set up using the configuration parameters listed in Table E-5.

Table E-5: GENESIS Configuration Parameters		
GENESIS Origin Coordinates	3768396.5200 Easting	1174969.9500 Northing
Offset from STWAVE X-Axis	6071.616 m	19920 ft
X_Azimuth Alongshore Orientation	219°, clockwise from N	S39W
Grid cell size along-shore	73.152 m	240 ft
Number of Grid Cells	121	
Grid Distance Along-shore	8851.392 m	29040 ft
Model Time step	1 hour	
Ratio GEN to STW cells	1:1	

It was necessary to modify the GENESIS grid when detached breakwaters were being modeled, because of the finer shoreline resolution needed in the lee of the breakwaters. Modified parameters are shown in Table E-6. For these runs, the other parameters remained as shown in Table E-5.

Table E-6: GENESIS Configuration Parameters for Detached Breakwater Runs

Grid cell size along-shore	18.288 m	60 ft
Number of Cells	484	
Model Time Step	0.15 hour	
Ratio GEN to STW cells	4:1	

The GENESIS calibration parameters used in this study are listed in table E-7.

Table E-7. GENESIS calibration parameters.

Parameter	Value
K_1	0.39
K_2	0.195
Median Grain Size	0.2 mm
Berm Height	2 m
Depth of Closure	4 m
Initial calibration shoreline	1996 LIDAR shoreline
Final calibration shoreline	2005 LIDAR shoreline
Initial verification shoreline	2005 LIDAR shoreline
Final verification shoreline	2007 Profile shoreline
Model wave climate	Average years
Calibration duration	9 years
Verification duration	2 years
Left lateral boundary condition	Moving @ +0.011 m/day
Right lateral boundary condition	Moving @ -0.015 m/day
Regional Contour Trend	As shown in Figure 5-9
Hard Structures	Seawall and Geotextile Tube
Soft Structures	No beachfill or Bypassing

When the alternatives were being modeled, beach fills were added, sand retention structures were added as appropriate, and the median grain size was changed from 0.2 to 0.29 mm.

Fishing Point STWAVE Coarse Grid Parameters

The description of the STWAVE modeling effort for the Fishing Point Coarse Grid domain is given in Chapter 8. The parameters used to set up the Fishing Point Coarse Grid STWAVE bathymetry grid within CEDAS (Version 4.03) are listed in Table E-8.

Table E-8: Fishing Point STWAVE Coarse Grid Parameters

Project Name	Wallops Island Storm Damage Reduction Project	
Domain Name	Fishing Point Coarse	
Domain Number	2 of 3	
Domain Descriptive Shoreline Boundaries	Wachapreague Inlet to Tingles Island camping area	
USGS Reference Charts	12210, 12211	
Data Horizontal Coordinate System	Virginia State Plane South, 4502, NAD 83, meters	
Data Vertical Coordinate System	MSL, meters	
Set up date	15/5/2009	
STWAVE Origin Coordinates	1197436.0162 N	3812183.8413 E
Approximate Offshore Boundary Depth	20 m	
X_Azimuth (Onshore Direction)	300^{o}, clockwise from N	N60W
Grid cell size cross-shore Δ_x	200 m	656.168 ft
Grid cell size along-shore Δ_y	200 m	656.168 ft
Number of Grid Cells	151 cross-shore	376 along-shore
Grid Distance Cross-shore, R_x	30000 m	98425.197 ft
Grid Distance Along-shore, R_y	75000 m	246062.992 ft
Near-shore Save Station Target Depth	6 m	19.685 ft

Fishing Point STWAVE Fine Grid Parameters

The description of the STWAVE modeling effort for the Fishing Point Fine Grid domain is given in Chapter 8. The parameters used to set up the Fishing Point Fine Grid STWAVE bathymetry grid within CEDAS (Version 4.03) are listed in Table E-9.

Table E-9: Fishing Point STWAVE Fine Grid Parameters

Project Name	Wallops Island Storm Damage Reduction Project
Domain Name	Wallops Island
Domain Number	3 of 3

Domain Descriptive Shoreline Boundaries	Fishing Point northward to 2 miles south of VA/MD State Line	
USGS Reference Charts	12211	
Data Horizontal Coordinate System	Virginia State Plane South, 4502, NAD 83, meters	
Data Vertical Coordinate System	MSL, meters	
Set up date	15/5/2009	
STWAVE Origin Coordinates	1180115.5081 N	3802183.8413 E
Approximate Offshore Boundary Depth	20 m	
X_Azimuth (Onshore Direction)	300°, clockwise from N	N60W
Grid cell size cross-shore Δ_x	40 m	131.234 ft
Grid cell size along-shore Δ_y	40 m	131.234 ft
Number of Grid Cells	514 cross-shore	501 along-shore
Grid Distance Cross-shore, R_x	20520 m	67322.835 ft
Grid Distance Along-shore, R_y	20000 m	65616.800 ft
Near-shore Save Station Target Depth	6 m	19.685 ft

Fishing Point STWAVE Wave Parameters

The description of the STWAVE modeling effort for Fishing is given in Chapter 8. The STWAVE wave parameters used in the modeling effort for both the coarse grid and the fine grid are listed in Table E-10.

Table E-10: Fishing Point STWAVE Wave Parameters

Project Name	Wallops Island Storm Damage Reduction Project	
Domain Names	Fishing Point Coarse and Fine Grids	
Domain Numbers	2 of 3 and 3 of 3	
Set up date	15/05/2009	
Wave Config Number	1 of 1	
WIS Station Number	177, Atlantic	
WIS Station Location	37.75° N	75.083° W
WIS Station Depth	25 m	
Shore_Ref 1 Wave Angle	120°, clockwise from N	
Wave Bin Boundaries		
Height	**Period**	**Angle**
mean	mean	mean
0	3	90
10	5	65
	7	45
	9	30
	20.5	20
		10
		0
		-10
		-20

		-30
		-45
		-65
		-90

Appendix F: Seawall Extension Shoreline Difference Figures

These figures are discussed in Chapter 10.

2 Year Shoreline Differences

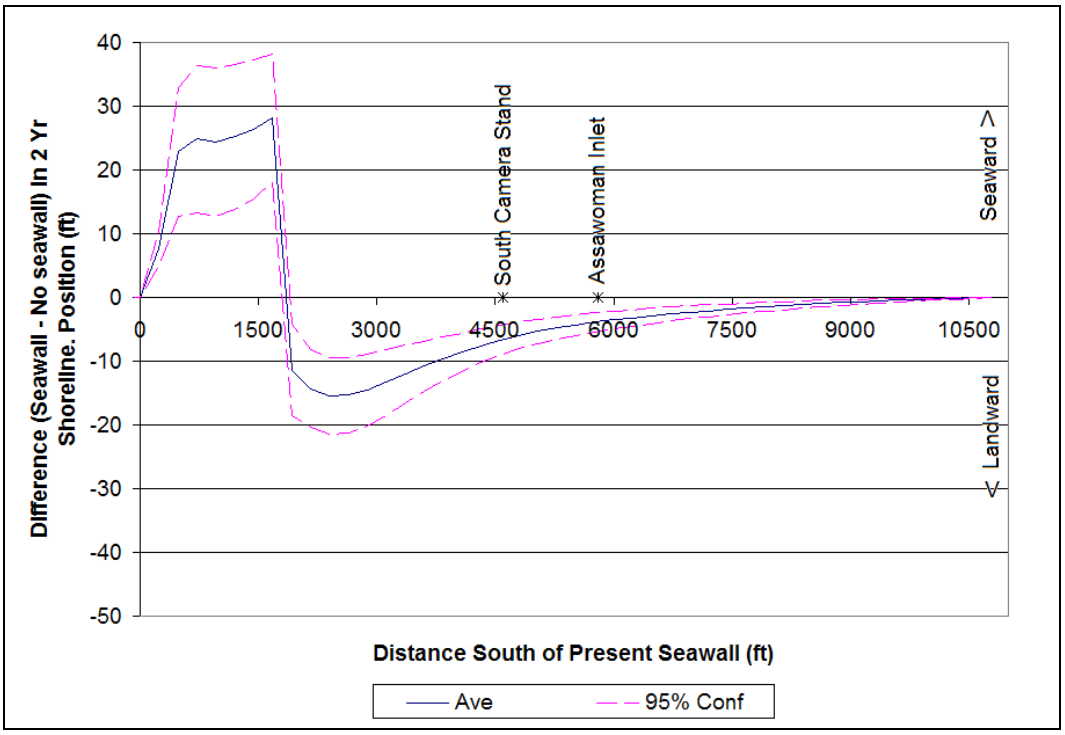

Figure F-1. Two year shoreline difference between 1500 ft seawall extension at the shoreline and no seawall extension.

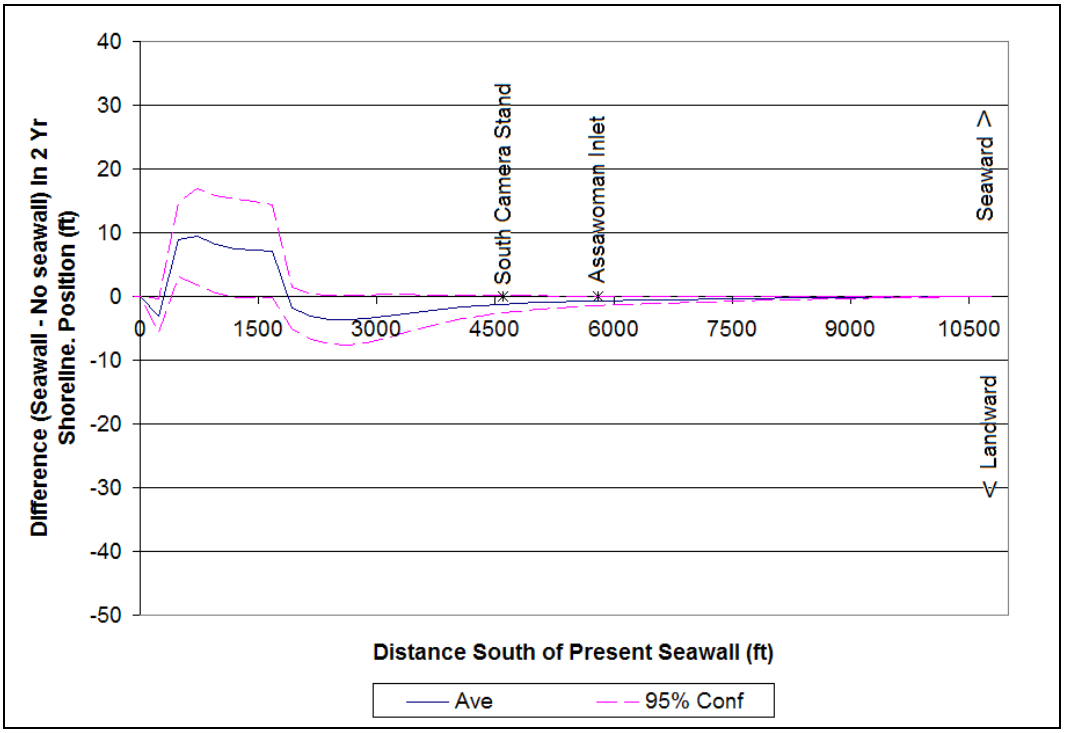

Figure F-2. Two year shoreline difference between 1500 ft seawall extension 10 yds landward and no seawall extension.

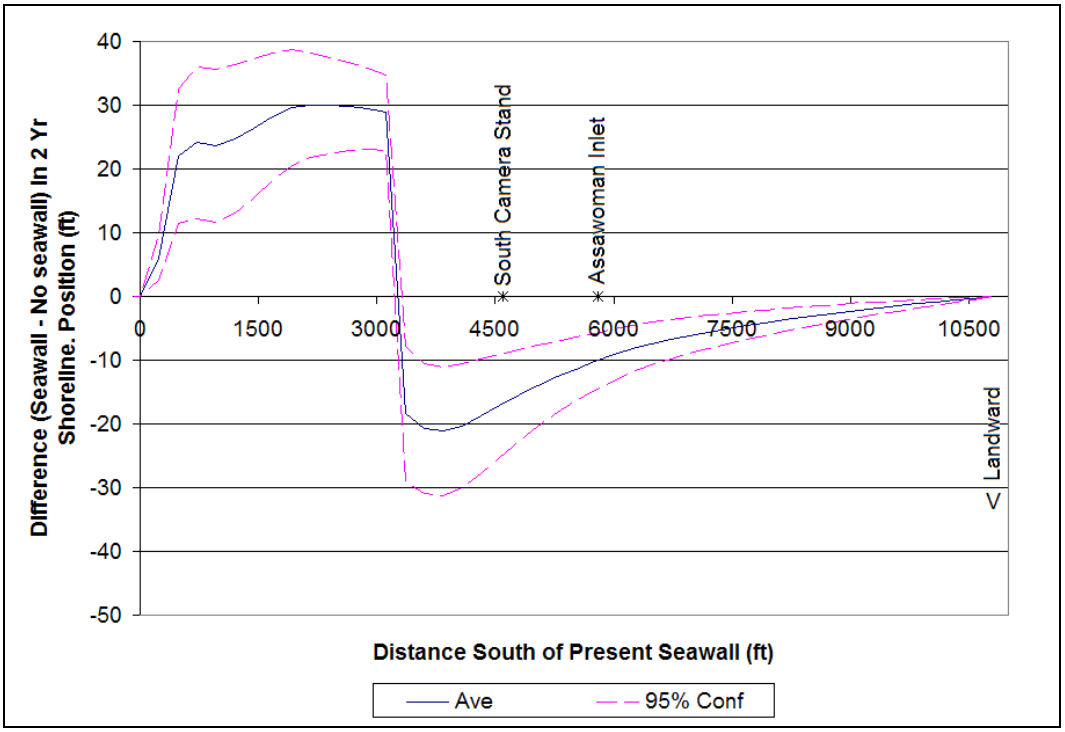

Figure F-3. Two year shoreline difference between 3000 ft seawall extension at the shoreline and no seawall extension.

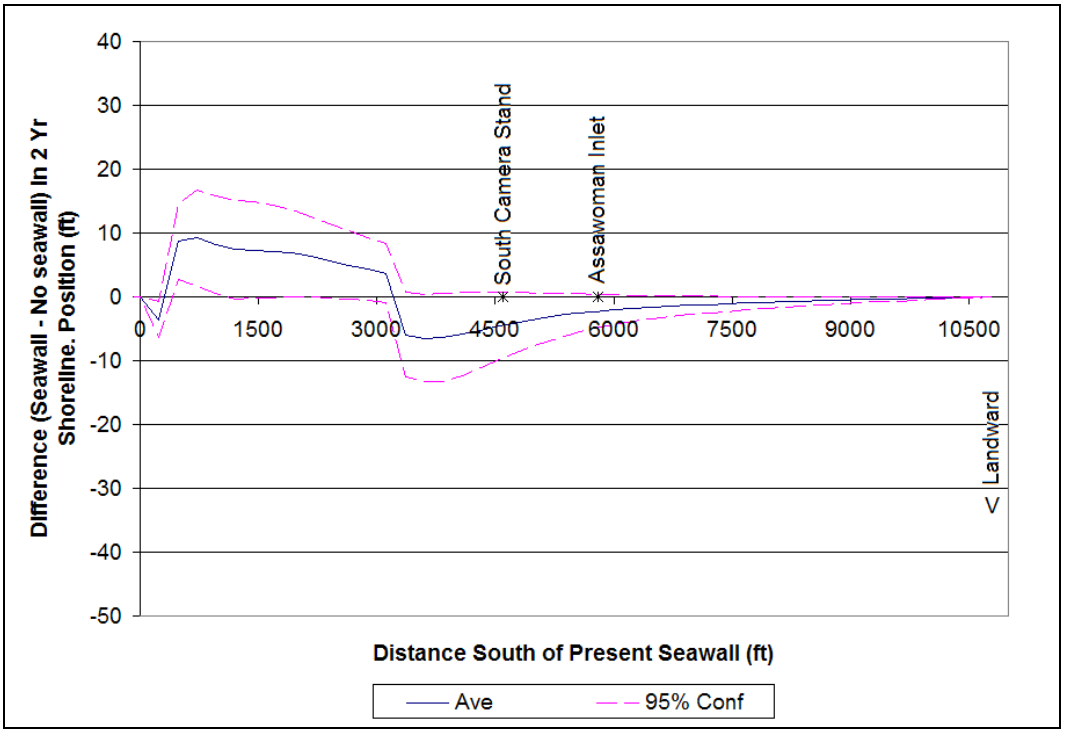

Figure F-4. Two year shoreline difference between 3000 ft seawall extension 10 yds landward and no seawall extension.

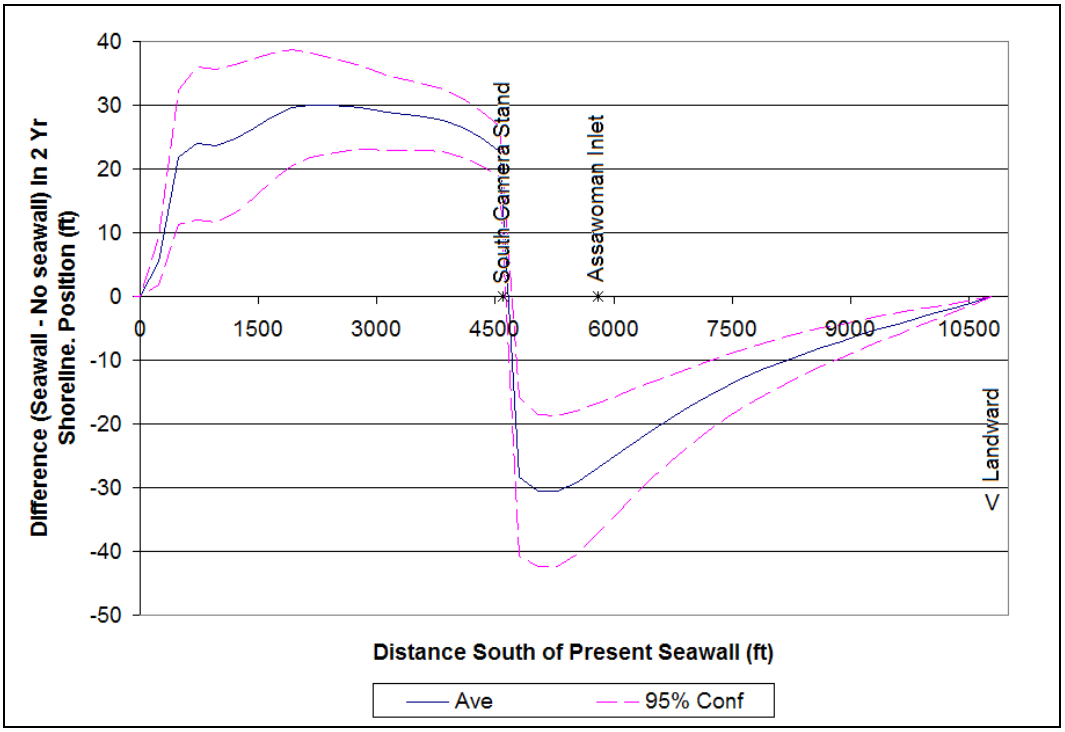

Figure F-5. Two year shoreline difference between 4600 ft seawall extension at the shoreline and no seawall extension.

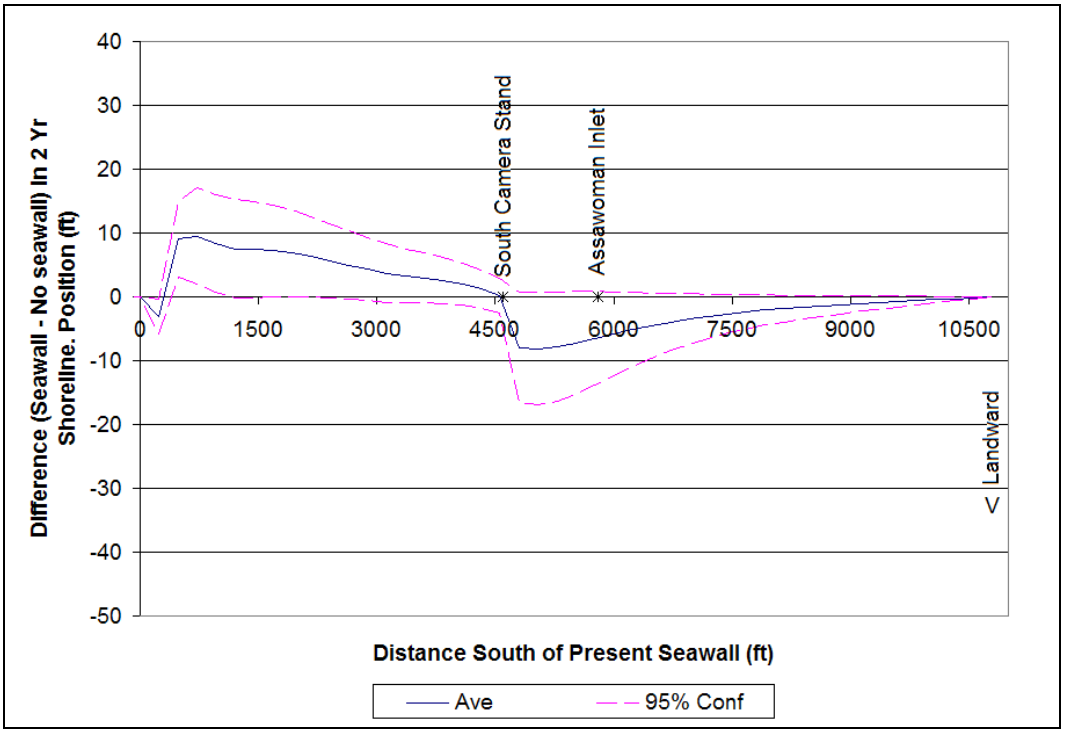

Figure F-6. Two year shoreline difference between 4600 ft seawall extension 10 yds landward and no seawall extension.

10 Year Shoreline Differences

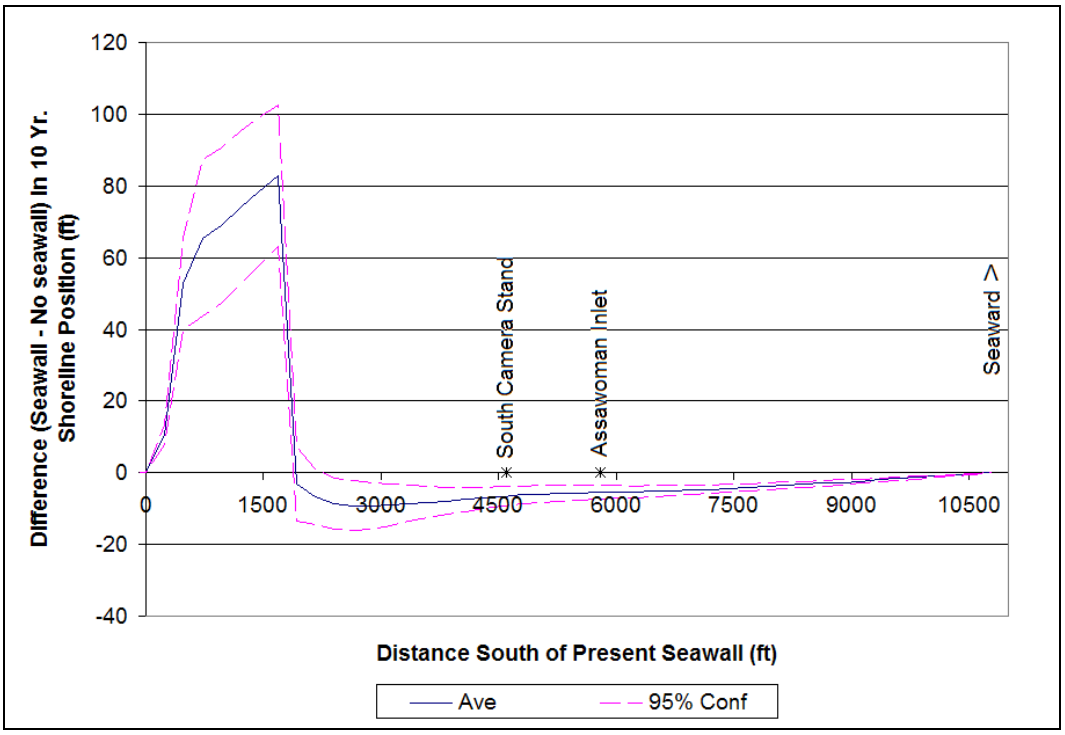

Figure F-7. Ten year shoreline difference between 1500 ft seawall extension at the shoreline and no seawall extension.

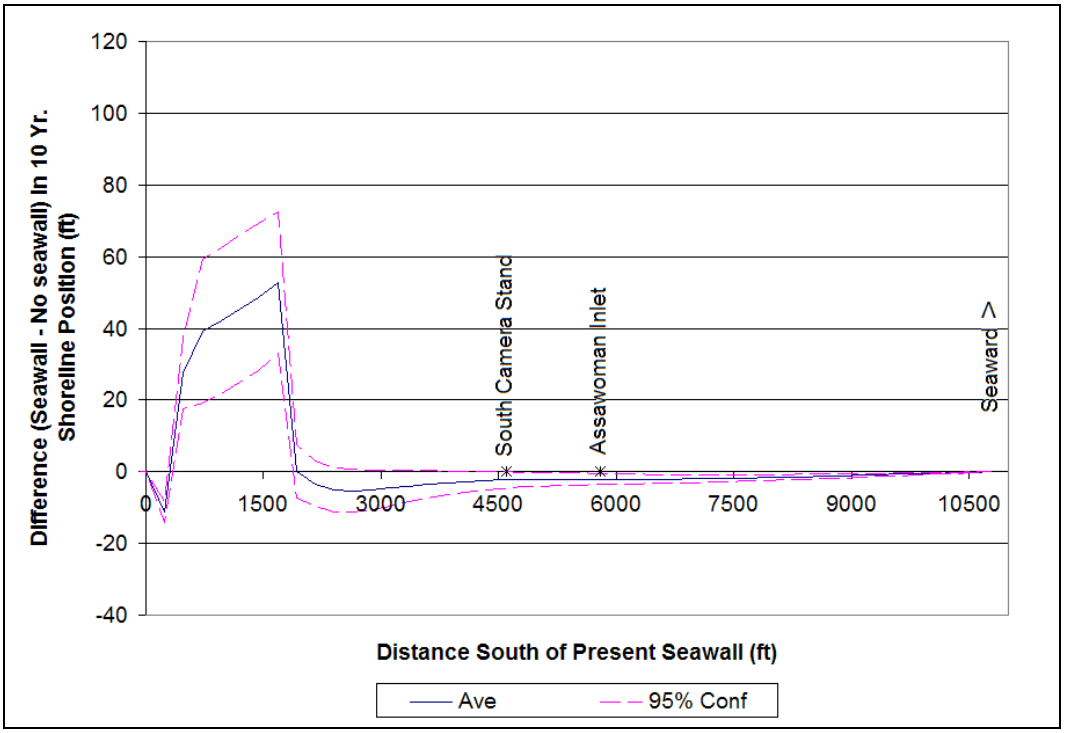

Figure F-8. Ten year shoreline difference between 1500 ft seawall extension 10 yds landward and no seawall extension.

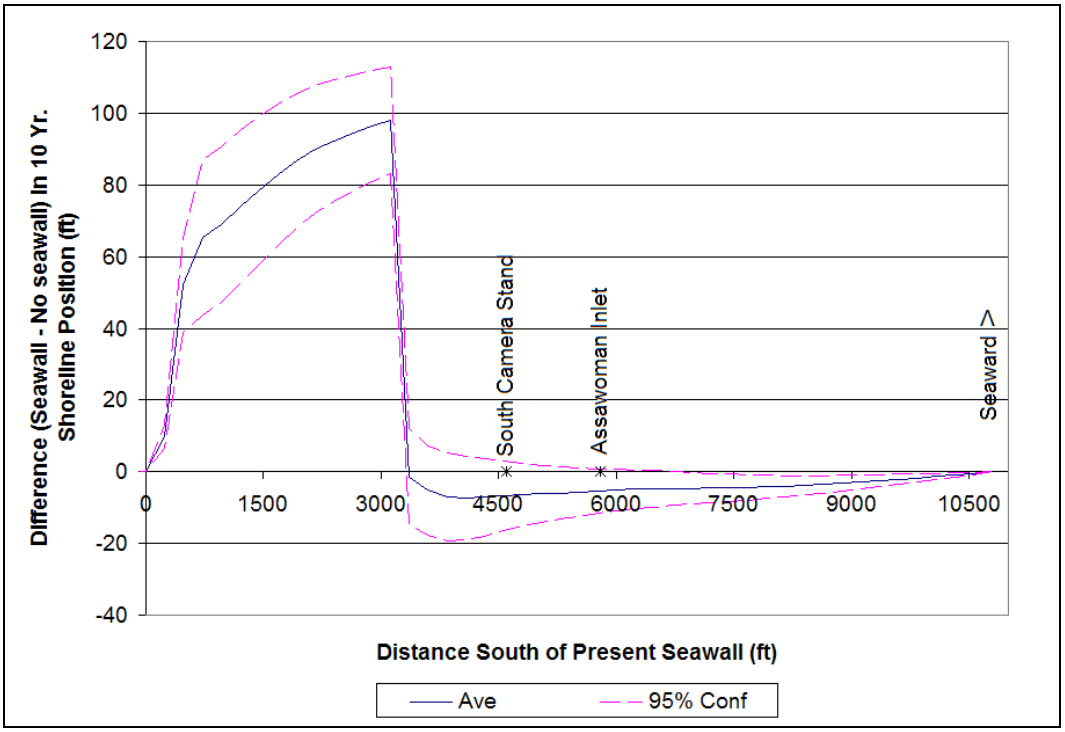

Figure F-9. Ten year shoreline difference between 3000 ft seawall extension at the shoreline and no seawall extension.

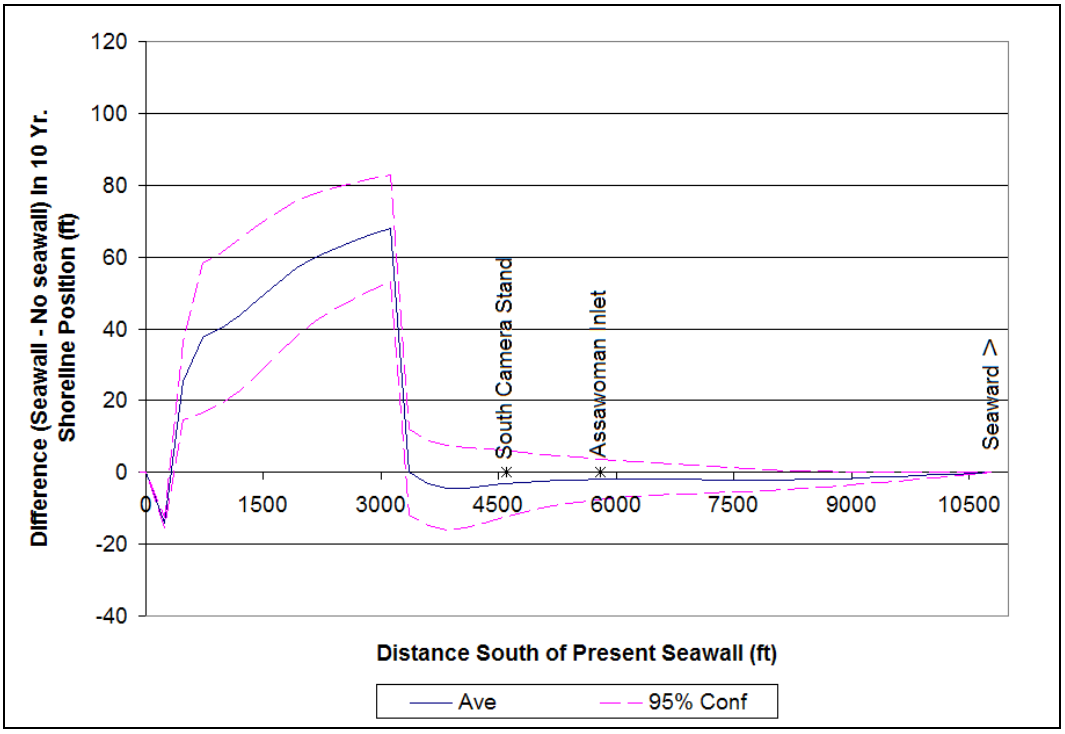

Figure F-10. Ten year shoreline difference between 3000 ft seawall extension 10 yds landward and no seawall extension.

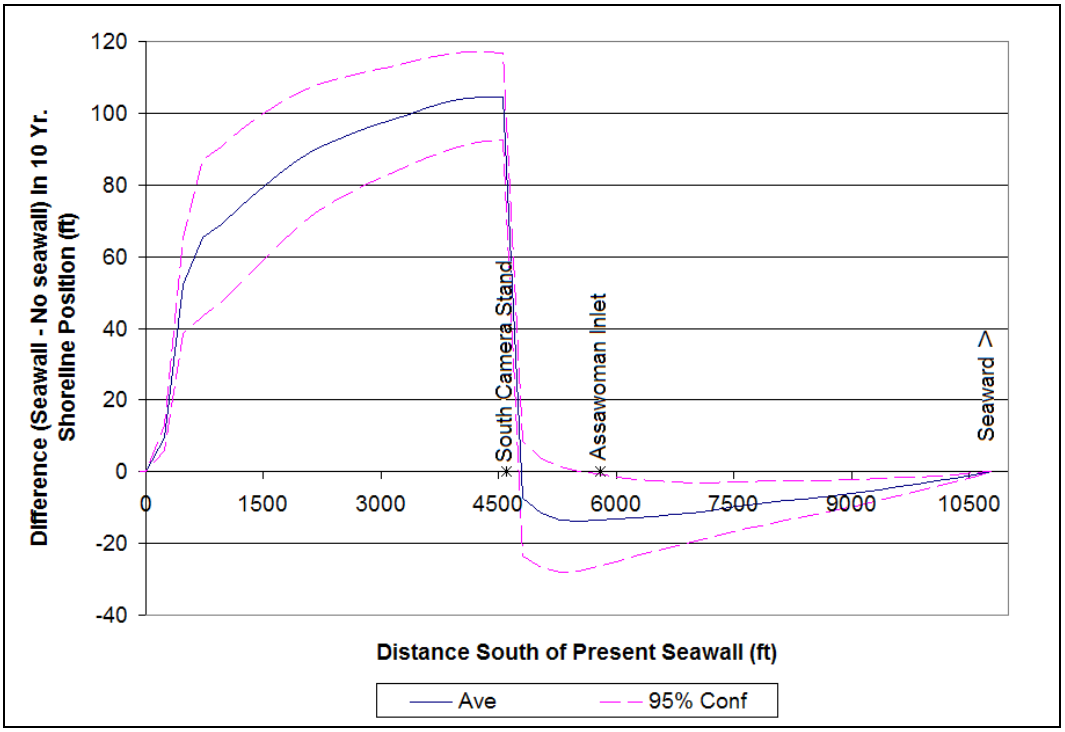

Figure F-11. Ten year shoreline difference between 4600 ft seawall extension at the shoreline and no seawall extension.

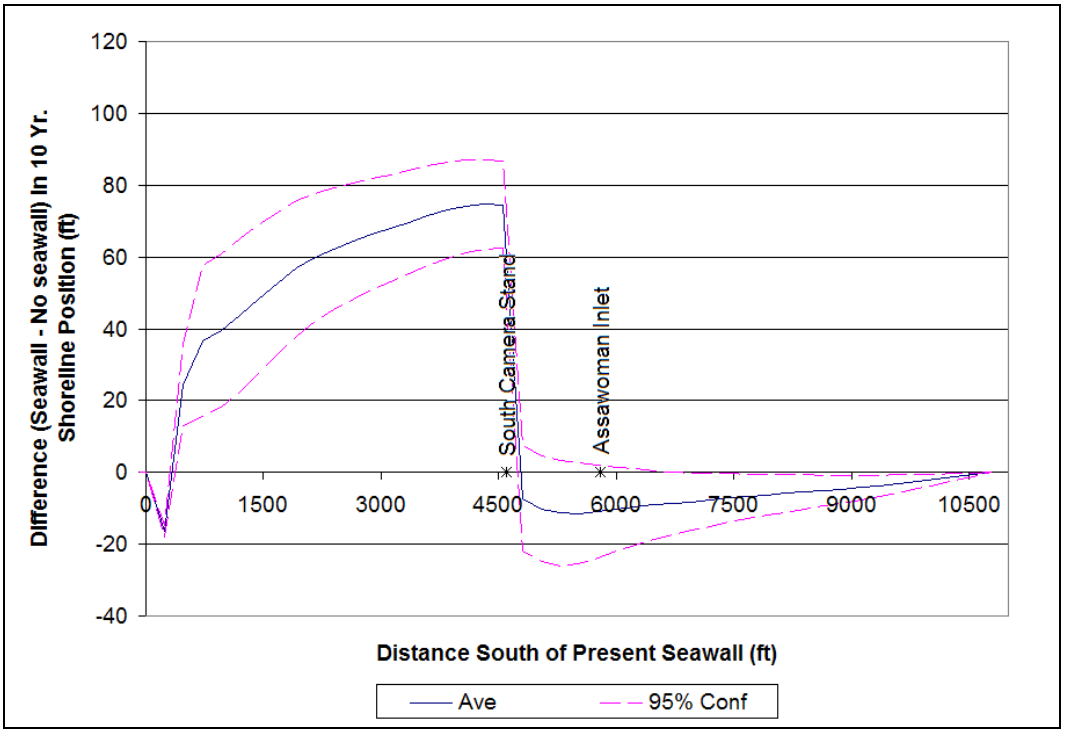

Figure F-12. Ten year shoreline difference between 4600 ft seawall extension 10 yds landward and no seawall extension.